MAYFLOWER WIND

Appendix F2. Scour Potential Impacts from Operational Phase and Post-Construction Infrastructure

Document Revision	A
Issue Date	February 2021

Final Scour Potential Impacts from Operational Phase and Post-Construction Infrastructure

Mayflower Wind Energy LLC

C170693-01 (07) | 22 January 2020
Final Report
AECOM

Document Control

Document Information

Project Title	Mayflower Wind Energy LLC
Document Title	Final Scour Potential Impacts from Operational Phase and Post-Construction Infrastructure
Fugro Project No.	C170693C170693
Fugro Document No.	C170693-01
Issue Number	(07)
Issue Status	Final Report
Fugro Legal Entity	Fugro USA Marine Inc.
Issuing Office Address	6100 Hillcroft Ave, Houston, TX 77081, USA

Client Information

Client	AECOM
Client Address	9 Jonathan Bourne Dr., Pocasset, MA 02559
Client Contact	Nancy Palmstrom
Client Document No.	F2

Document History

Revision	Date	Status	Comments on Content	Prepared By	Checked By	Approved By
0	14 February 2021		Final Report	SBL/BSP/RVS	BSP	RVS

Project Team

Initials	Name	Role
BSP	Benoit Spinewine, PhD	Principal Engineer, Project Manager
SBL	Sébastien Blaise, PhD	Senior Engineer
RVS	Rafael V. Schiller, PhD	Metocean Consultancy Manager, Americas

Executive Summary

Mayflower Wind Energy LLC (Mayflower Wind) proposes an offshore wind renewable energy generation project (the Project) located in federal waters off the southern coast of Massachusetts in the Outer Continental Shelf (OCS) Lease Area OCS-A 0521 (Lease Area). The Project will deliver electricity to the regionally administered transmission system via export cables with a sea-to-shore transition in Falmouth, Massachusetts and onshore transmission system extending to the anticipated point of interconnection (POI) in Bourne, Massachusetts.

Mayflower Wind's construction and installation concept includes Wind Turbine Generators (WTGs), Offshore Substation Platform(s) (OSP(s)), inter-array cables, and offshore export cables. The effect of scour associated with the construction and operation of the planned infrastructure is a fundamental assessment and part of the development of the Construction and Operation Plan (COP). In alignment with the Bureau of Ocean Energy Management (BOEM) guidelines, this study addresses the following objectives in support of the COP:

- Quantify the effect of scour during the operational phase associated with installed infrastructure in the lease and export cable areas;
- Quantify sediment mobility potential and implications to the Project; and
- Discuss implications of scour to the asset integrity and potential needs for scour protection.

Analytical modelling and qualitative assessment are employed to investigate the scour potential for four types of foundations: monopile, piled jacked, suction bucket jacket, and gravity-based. In addition to design specifications provided by Mayflower Wind, the study employs geotechnical data from two grab sample surveys over the Project Area, bathymetric data from site-specific surveys and publicly available sources, and site-specific metocean conditions from a high-resolution model developed specifically for this Project.

The sediment mobility potential analysis revealed a very limited potential for background sediment transport activity across the Lease Area and along the southern part of the export cable routes (KP 50.0 – 88.0). Bed shear stresses resulting from currents and waves are only exceeding critical shear stresses for initiation of sediment movement during a very low percentage of the time, and no significant bedform or other presently active geomorphological feature is observed from the review of the currently available data. In the vicinity of the Vineyard and Nantucket Sounds and Muskeget Channel, much stronger currents and waves occur along the shallower sections of the export cable routes (Kilometer Point [KP] 0.0 – 50.0). These are associated with widespread evidence of sediment transport activity and bedforms such as megaripples and sand waves, with height locally reaching up to 4 meters (m).

The potential for scour development around the wind turbine foundations is evaluated for the various foundation types considered. Clear-water conditions prevail for an overwhelmingly large fraction of the time, with live-bed conditions expected for only 1 to 2 percent of the time associated with episodic storms. Under live-bed conditions in areas of shallower water and strong currents, the literature often reports potential equilibrium scour depths of up to ~1.3 times the foundation

diameter (Sumer and Fredsøe, 2002). The potential scour depth at the Mayflower Wind Project site is expected to be less than this upper bound, owing to the water depth range, and the very small percentage of time over which live-bed conditions are expected to prevail. Practical scour estimates for monopiles, piled jacket foundations, suction-bucket jacket foundations and gravity-based foundations are provided in Section 5, along with similar estimates at the foundations of the Offshore Substation Platform(s). In addition, estimates for the timescale for scour development are in the order of several years, such that scour is unlikely to fully develop over the course of one or several storms.

Sediment mobility along the export cable routes varies over a wide range, with significant mobility associated with sand waves and shoals where strong tidal currents occur, especially in the vicinity of the Vineyard and Nantucket Sounds and Muskeget Channel. Scour is more likely to be associated with natural processes than caused by the cables themselves, provided the latter is buried such that it is not exposed to seabed currents. The burial depth will have to be determined to prevent the potential re-exposure of the cables in areas of migrating sand waves.

Contents

Attachments

Figures

Tables

Abbreviations

ASB	Above Seabed
BERR	Business, Enterprise and Regulatory Reform
BOEM	Bureau of Ocean Energy Management
COP	Construction and Operation Plan
CFR	Code of Federal Regulation
CPS	Cable Protection Systems
ft	feet/foot
GBS	Gravity-Based Structure
HDD	Horizontal Directional Drilling
KC	Keulegan-Carpenter
km	kilometer(s)
KP	Kilometer Point
m	meter (s)
m^2	square meter(s)
Mayflower Wind	Mayflower Wind Energy LLC
MLLW	Mean Lower Low Water
mm	millimeter(s)
NOAA	National Oceanic and Atmospheric Administration
nm	nautical mile(s)
OCS	Outer Continental Shelf
OSP	Offshore Substation Platform
Pa	Pascal(s)
POI	Point of Interconnection
PSD	Particles Size Distribution
ROV	Remotely Operated Vehicle
USGS	United States Geological Survey
WTG	Wind Turbine Generator

1 Introduction

Mayflower Wind Energy LLC (Mayflower Wind) proposes an offshore wind renewable energy generation project (the Project) located in federal waters off the southern coast of Massachusetts in the Outer Continental Shelf (OCS) Lease Area OCS-A 0521 (Lease Area). The Project will deliver electricity to the regionally administered transmission system via export cables with a sea-to-shore transition in Falmouth, Massachusetts.

This report presents an assessment of the potential for scour during the operational phase of the Project at installed infrastructure (cables and foundations) to inform Project design. Scour, the removal of sediment around the base of the installed structures due to current-wave-structure interactions, can be a major hazard to foundations that must be addressed during Project design. Seabed mobility, which could present a hazard for inter-array and export cables installed below the seabed surface, is also evaluated.

The remainder of this section articulates the assessment objectives, provides a Project overview, describes the report organization, and summarizes units and conventions used throughout the balance of the report.

1.1 Assessment Objectives

The overarching objective of this study is to determine the potential scour hazard for installed Wind Turbine Generator (WTG)/Offshore Substation Platform (OSP) foundations as well as the hazards associated with seabed mobility for installed inter-array and export cables.

The Bureau of Ocean Energy Management (BOEM) has produced regulations and guidelines for preparing a COP as well as conducting specific technical studies to support COP development. Consistent with BOEM's Information Guidelines for a Renewable Energy Construction and Operation Plan (COP) (BOEM, 2020) and 30 Code of Federal Regulations (CFR) 585.627(a)(1), this assessment was completed to support the following objectives:

- Characterize the stability of seafloor morphology (i.e., seabed mobility);
- Model the effect of waves and currents on the offshore structures;
- Quantify the potential of scour effect on WTG/ OSP foundations;
- Quantify the seabed mobility potential along the offshore export/inter-array cable routes;
- Assess the implications of scour to the design and asset integrity during operations; and
- Assess the potential needs for scour protection.

Results from the scour and seabed mobility assessment provide quantitative and qualitative information to support the Mayflower Wind COP.

1.2 Project Overview

The Lease Area is located offshore of the southern coast of Massachusetts, approximately 26 nautical miles (nm) (49 kilometers [km]) south of Martha's Vineyard and 20 nm (37 km) south of Nantucket (Figure 1.1). The closest location (WTG/OSP position on the 1 x 1 nm grid layout) within the Lease Area to the mainland is 52 nm (96.5 km).

The Project layout will align to a 1 nm x 1 nm grid with an east-west and north-south orientation, across the entire Massachusetts/Rhode Island (MA/RI) Wind Energy Areas. The Project will consist of up to 149 positions within the Lease Area, to be occupied by WTGs, OSP(s), and inter-array cables.

For purposes of this modelling effort, water depths were estimated based on preliminary information. The water depths within the Lease Area range from 122 feet (ft) (37.2 meters [m]) to 211 ft (64.4 m), with deeper waters located in the southwestern portion. The average depth is 167.9 ft (51.2 m).

The submarine offshore export cables will travel from one or more OSP(s) within the Lease Area through Muskeget Channel into Nantucket Sound and make landfall in Falmouth, Massachusetts. Landfall locations under consideration, are, from west to east: at the end of Mill Road, Shore Street, or Worcester Avenue.

Additional details regarding the Project description and construction and installation method are available in Section 3 of the COP. Specific details regarding Project design used in this assessment are provided in Section 2 of this report.

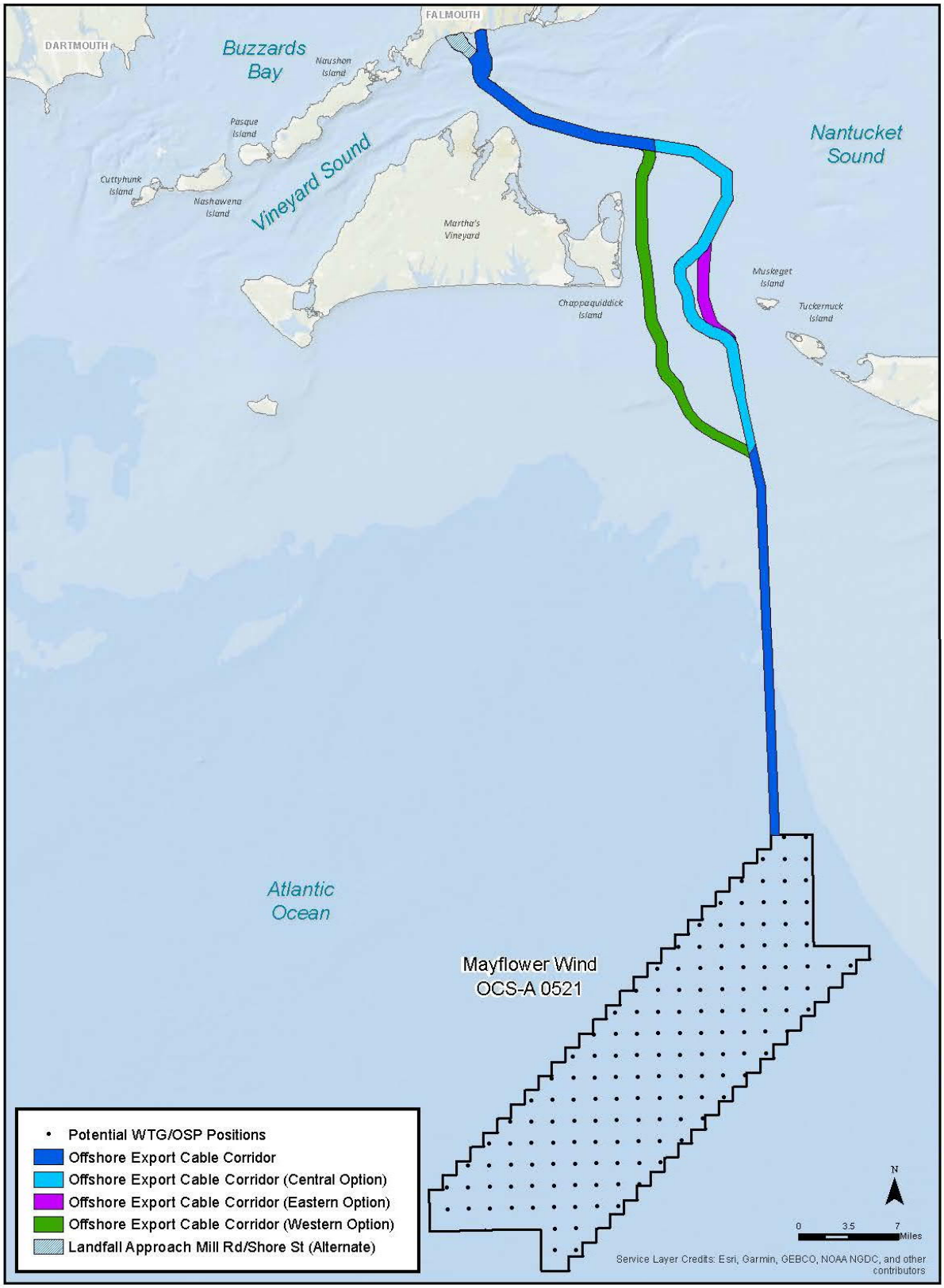

Figure 1.1. Location of Mayflower Wind Project.

1.3 Report Organization

This report is organized to include:

- A presentation of the design and construction scenarios to be evaluated (Section 2);
- An outline of the scour modelling approach (Section 3);
- A summary of the sediment mobility assessment in the Lease Area and along the export cable routes (Section 4);
- A presentation and discussion of the scour potential effects within the Lease Area (WTGs, OSP(s), and inter-array cables – Section 5);
- A presentation and discussion of the scour potential effects along the export cable routes (Section 6);
- Conclusions (Section 7);
- References (Section 8);
- Details on the data sources and result tables (Attachment A);
- Details on the modelling methodology (Attachment B);
- Details on the sediment mobility assessment (Attachment C); and
- Profiles of elevation and bedform height along the export cable routes (Attachment D).

1.4 Units and Conventions

The following list describes the units and conventions used in this report, expressed using the SI convention.

- Water level is expressed in meters (m);
- Vertical elevations in the water column are expressed in meters. Depths are quoted below Mean Lower Low Water (MLLW) and heights are quoted Above Seabed (ASB);
- Shear stresses are expressed in pascals (Pa);
- Sediment grain sizes are expressed in millimeters (mm); and
- Positions are quoted relative to WGS84 except where stated.

2 Construction and Design Scenarios

This section describes the design and construction scenarios that were evaluated as part of this assessment. The effect of scour was assessed at the Lease Area (WTGs/OSP foundations and inter-array cables) and along the export cable corridors.

2.1 Turbines and Inter-Array Cable Layout

The WTG/OSP layout is illustrated in Figure 2.1, with a total of 149 WTG/OSP positions. The complete list of positions with coordinates and seabed elevations is provided in Attachment A. Inter-array cables connect the WTGs to the OSP(s).

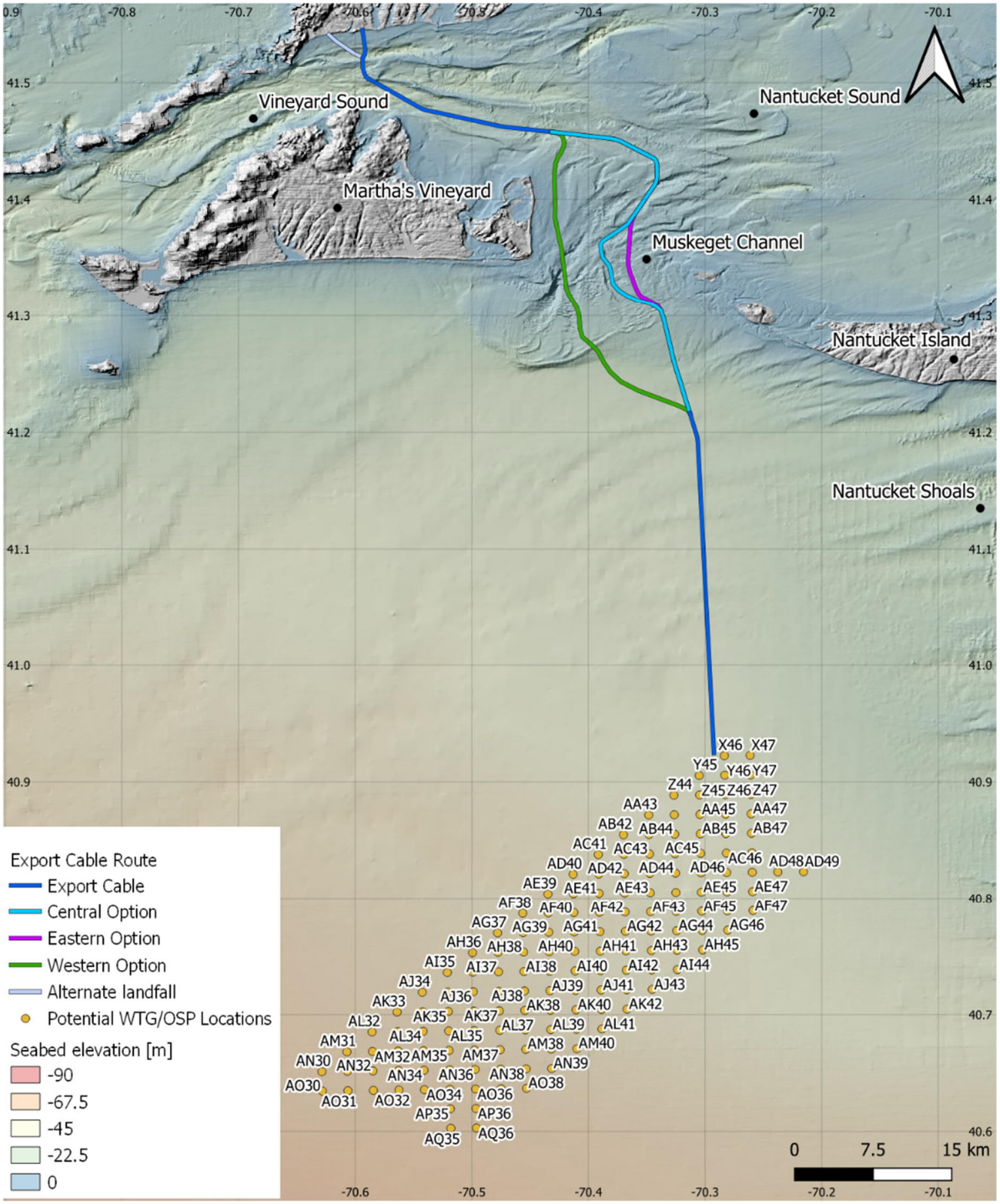

Figure 2.1. Project WTG/OSP layout.

2.2 Offshore Substation Platforms

The Project may install up to five OSP units of varying sizes, foundation types, and combinations. These types and sizes are described further in COP Section 3, Description of Proposed Activities. Foundations could be monopiles, piled jackets (with 3 - 27 piles per OSP), suction bucket jacket and/or a Gravity-Based Structure (GBS). The final location(s) of the OSP unit(s) are not yet finalized but OSP(s) will sit on grid positions within the 1 nm by 1 nm grid layout.

2.3 WTG Foundations

Four different types of WTG foundations are considered for the scour assessment study, with the following characteristics:

- Monopiles with a seabed diameter of up to 16 m (maximum diameter currently under consideration);
- Piled jackets with three or four legs on piles with a diameter of up to 4.5 m, equally spaced on a horizontal circle of 50 m diameter;
- Suction bucket jackets with three or four legs and buckets with a diameter up to 20 m and penetration of up to 20 m, equally spaced on a horizontal circle of 55 m diameter; and
- Gravity-based structure present as either up to 70 m diameter fixed structure (concrete) or an alternative structure with a seabed footing of 3 x 40 m diameter pads or 4 x 35 m diameter pads, with maximum footprint area of 3,850 square meters (m^2).

2.4 Export Cable Routes

Three export cable route options are considered through Muskeget Channel, namely the Western, the Central, and the Eastern options as shown on Figure 1.1. Their approximate lengths (as defined between the edge of the Lease Area and landfall) vary between 80 km and 90 km. The Kilometer Point (KP) system adopted herein follows the Central Route Option, with KP 0 at the landfall, as shown on Figure 2.2.

Three landfall options are considered. Horizontal Directional Drilling (HDD) will be used at the landing(s) to bring the cables ashore below the shoreline, with an HDD exit pit located in the nearshore. The cables are planned to be buried from the HDD exit pits.

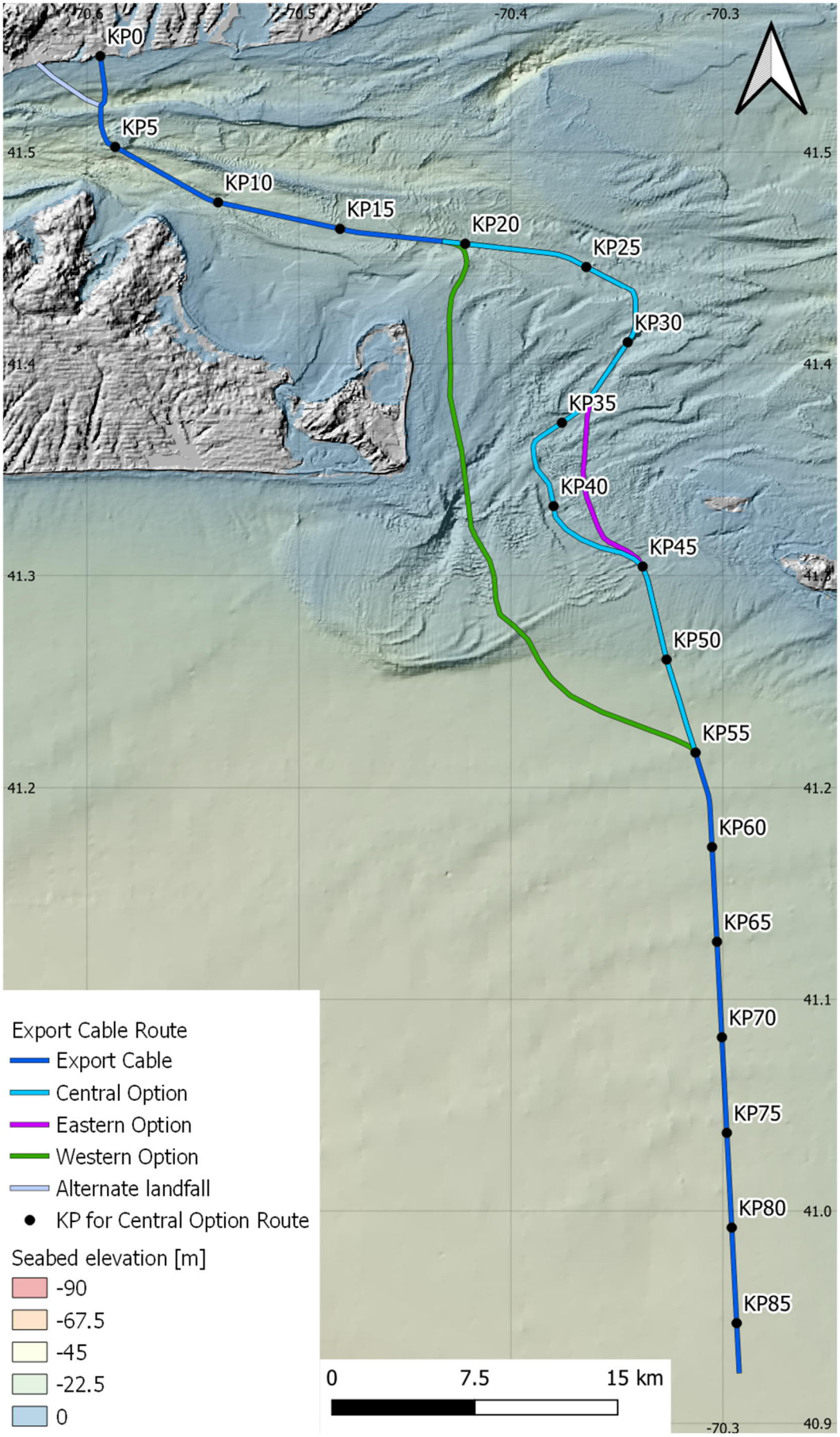

Figure 2.2. Adopted KP system for offshore export cable route along Central Option.

2.5 Input Geotechnical, Bathymetric, and Metocean Data

The study makes use of a variety of input data specific to the Project:

- Geotechnical (i.e., grain size distribution) data from grab samples collected during two benthic survey campaigns (May 2020 and August 2020) in the Lease Area and export cable corridors; and
- Bathymetric data from site-specific surveys and publicly available sources.

In addition, metocean conditions, which are a key driver to the scour assessment, were evaluated from two years of time series of site-specific waves and currents derived from a high-resolution metocean model that was specifically developed for this Project.

Details are provided in Attachment A.

3 Scour Modelling Approach

The scour assessment includes two primary elements, including:

- Evaluation of sediment mobility; and
- Characterization of scour effects of built/installed infrastructure.

The assessment approach for each of the above elements of the assessment are summarized below and are detailed in Attachment B. A metocean numerical model was developed to support this assessment. Additional details on the modelling are included in COP Appendix F1, Sediment Plume Impacts from Construction Activities.

3.1 Evaluation of Sediment Mobility

The potential for background sediment mobility was assessed across the Lease Area and along the export cable routes. This assessment will identify whether the seabed is expected to be mobile or immobile under the action of waves and currents, and for what percentage of the time. This will determine the degree to which clear water conditions or live bed conditions will constrain the potential for local scour development at the infrastructure.

Four lines of evidence were used to characterize the background sediment mobility:

- Literature review;
- Bathymetric and geomorphological data review;
- Sediment grain size data from two rounds of benthic sampling; and
- Bed shear stress and sediment transport analysis.

3.2 Effect of Scour at Built/Installed Infrastructure

Local scour at the structures (WTGs and OSP[s]) may result from bed shear stress amplification due to fluid-structure interactions. Background bed shear stresses associated with waves/currents are sourced from the metocean modelling exercise reported separately (COP Appendix F1, Sediment Plume Impacts from Construction Activities) and used to assess clear water or live bed scour conditions.

Local scour predictions presented in the report are established using analytical means following the methodology proposed by Sumer and Fredsøe (2002). The predictions are provided assuming no scour protection layer in place at the structures.

The analytical modelling approach is described in detail in Attachment B and is applied to the following foundation types:

- Monopile;
- Piled Jacket;
- Suction Bucket Jacket; and
- Gravity-Based Structure (GBS).

Results are presented in terms of local scour depth, time scales for scour development, and group effect (for the piled jacket case). More detailed modelling will be performed at later stages of the design to investigate the effects of design optimisations, such as for example the use of multiple thin piles per jacket leg.

4 Sediment Mobility Potential and Implications for the Project

Sediment mobility potential was assessed based on four primary lines of evidence:

- Literature review;
- Review of bathymetric and geomorphological data;
- Sediment grain size data from two rounds of benthic sampling; and
- Bed shear stress and sediment transport analysis.

Details of the assessment are provided in Attachment A and are briefly summarized below.

Figure 4.1 and Figure 4.2 illustrate the distribution of the soil particle size at different locations, based on the sample data collected during two benthic surveys conducted by Mayflower Wind in May and August 2020. Sediment in the Lease Area largely consists of fine sand, very fine sand, and silt. The southwestern portion of the Lease Area contains larger amounts of silt, and non-negligible amounts of clay are observed. This increase of finer material is related to the presence of a Mud Patch described in the literature (Attachment C).

The current seabed mobility assessment is based on bed shear stresses as evaluated from a dedicated metocean numerical modelling performed as part of the study, and covering a two-year period from July 1, 2018 to June 26, 2020 (see Attachment A). Figure 4.3 shows a mapping of maximum bed shear stress induced by currents and waves during the simulation period. While the bed shear stress is relatively limited in the Lease Area, it quickly increases in shallower areas, with maximum values approaching 2.5 Pa at the Muskeget Channel separating Martha's Vineyard and Nantucket, as well as along Vineyard Sound north of Martha's Vineyard.

The dimensionless form of the shear stress, also known as the Shields parameter, is a useful indicator to characterize the susceptibility to sediment mobility. It incorporates the interdependence of sediment mobility to sediment particle size and density. The values of the Shields parameter need to be compared with a critical Shields threshold, which itself is dependent on the particle grain size and density. When the Shields parameter is above the critical Shields threshold, particle movement is initiated, and sediment transport may occur.

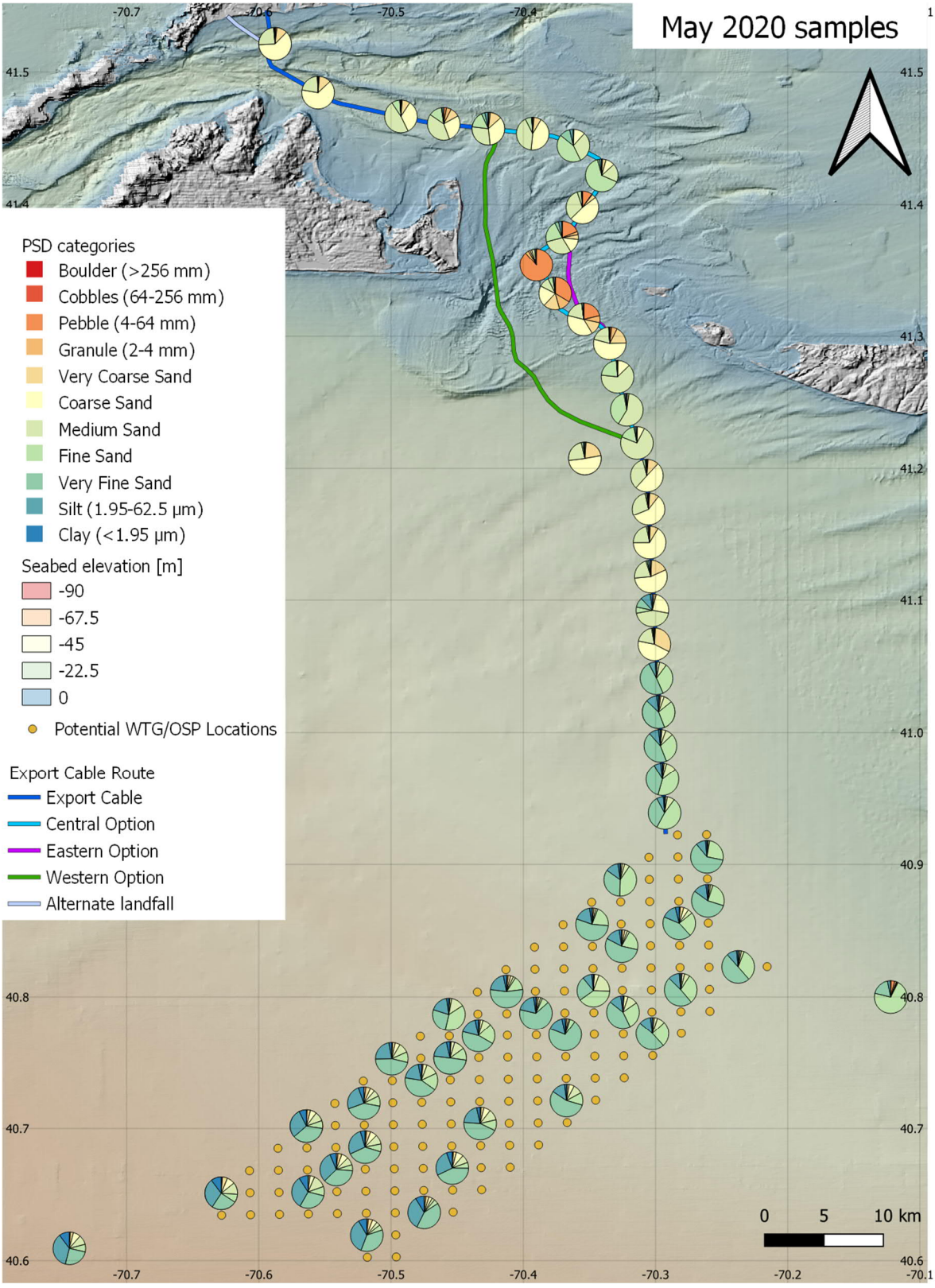

Figure 4.1. Pie charts of the particles size distribution at the grab locations for the May 2020 survey.

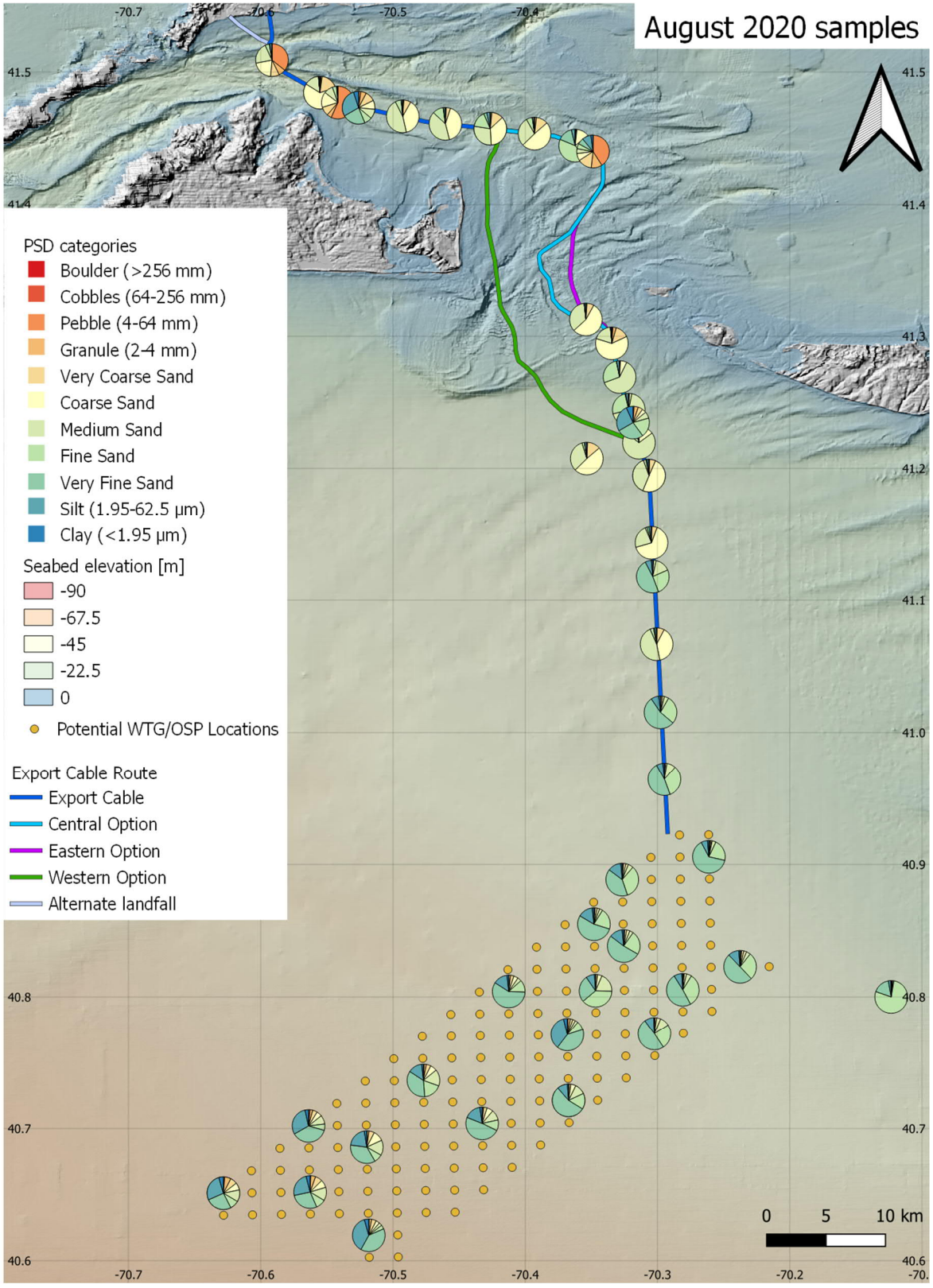

Figure 4.2. Particles size distribution pie charts at the grab locations for the August 2020 survey.

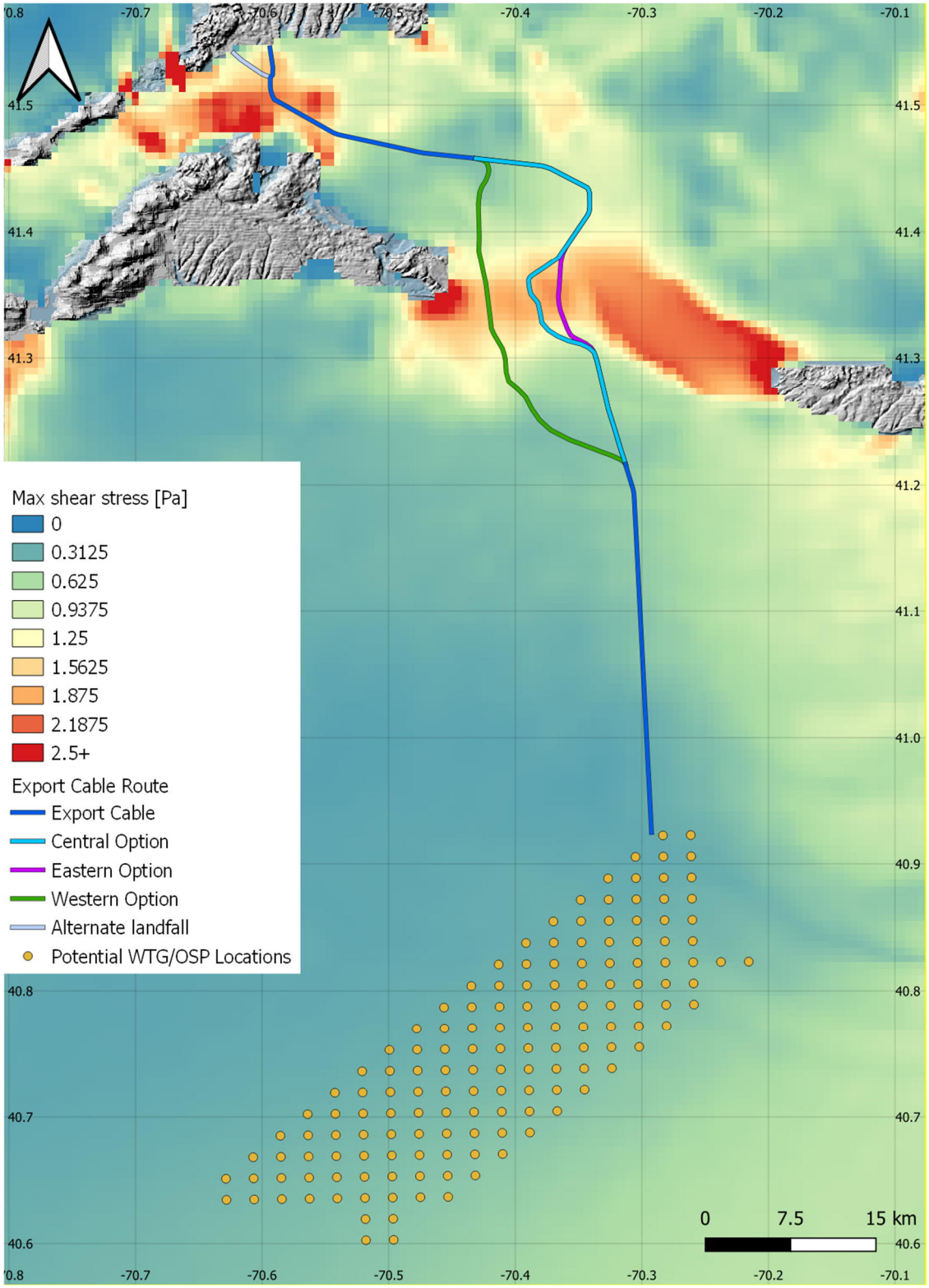

Figure 4.3. Mapping of maximum bed shear stress.

Figure 4.4 shows the percentages of time during which the critical Shields threshold is exceeded during the metocean simulation period. The critical Shields parameter is computed using the formula of Soulsby and Whitehouse (1997). These percentages of exceedance are computed at the grab sample locations where particle size data are available, for the May 2020 survey (left) and the August 2020 survey (right) and indicate the percentage of time during which surface sediment is expected to be mobile.

The data illustrated in Figure 4.4 reveal a very limited potential for background sediment transport in the Lease Area and southern part of the export cable routes (KP ~50.0 – 88.0, see Figure 2.2) and, by contrast, a very dynamic background sediment mobility for some of the shallower areas along the export cable corridors, especially in the vicinity of the Muskeget Channel and Vineyard Sound. This is consistent with literature reports and the review of the bathymetry as discussed in Attachment C.

The conditions across the Lease Area are such that the threshold for sediment movement initiation would be exceeded for no more than 1 to 2 percent of the time (i.e., in the order of 5 to 10 days per year). Clear water conditions prevail overwhelmingly over live bed conditions. However, localized sediment transport may occur due to shear stress amplification in the vicinity of infrastructure, associated with short-lived episodes of more intense metocean conditions. For that reason, a degree of local scour development around the WTG and OSP foundations cannot be excluded. The extent and timescale over which local scour may develop is elaborated in Section 5.

The northern, shallower part of the export cable routes is significantly more exposed, with high bed shear stresses and percentages of exceedance of the critical Shields parameter. This is a sign of active seabed mobility, with potential implications on the export cables, such as risk of exposure resulting from the migration of bedforms. This risk will be discussed in Section 6 on the scour potential effects along the export cable routes.

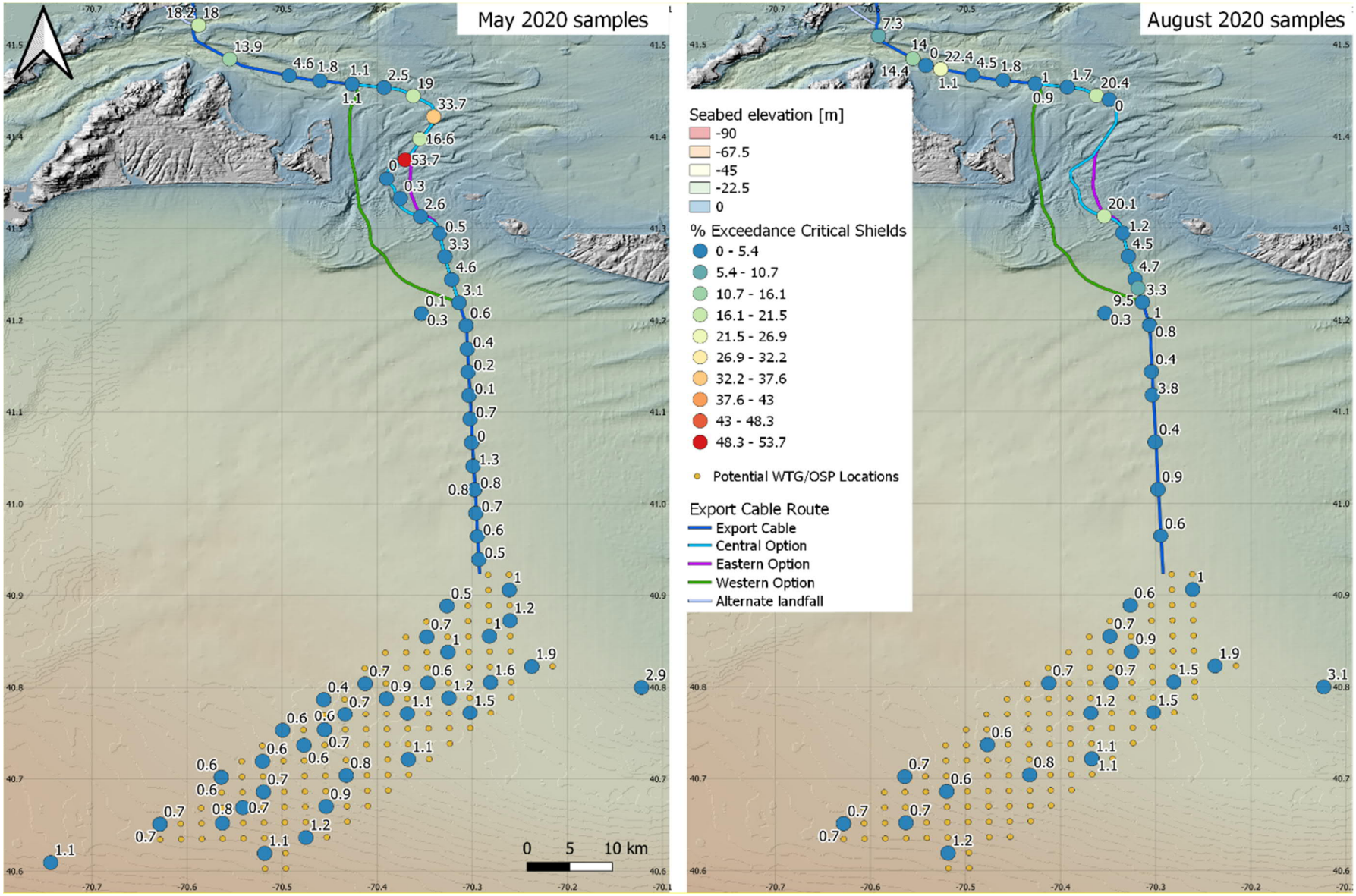

Note: See Attachment C, Figure C.14

Figure 4.4: Percentage of exceedance of the critical Shields threshold at the grab sample locations.

5 Scour Potential Effects within the Lease Area

Scour results from an increase in sediment entrainment from the bed in the vicinity of an object or infrastructure, as compared to background sediment transport away from it. The increase is due to the interaction of current or wave-induced flows with the said infrastructure. Scour is intrinsically related to the interactions between the flows and the "perturbation" (infrastructure or seabed object) and, as such it differentiates from a generalized seabed erosion process associated with natural processes.

If a structure is susceptible to scour development, distinct pathways to a safe design can be adopted, depending on whether scour is allowed to develop without jeopardizing the structure, or whether scour protection measures are taken to prevent or minimize its development.

One may further differentiate different types of scour, namely:

- Local scour, which occurs in the immediate vicinity of the individual members of a composite structure (e.g., a monopile or a single pile of a multiple leg jacket);
- Global scour, which may occur at the scale of the structure itself in case of a composite structure (e.g., at the scale of a jacket with multiple legs grounded on piles or suction buckets);
- Edge scour, which may occur at interfaces between areas with distinct scour susceptibility, such as at the seabed immediately adjoining a scour protected area; and
- Far-field or regional scour, which may occur over even larger distances such as an entire wind farm and caused for example by interactions between the various WTGs or by natural geomorphological processes active in the area.

Three interrelated drivers to scour development are identified by: (i) the nature of the seabed and subsurface and the background mobility of sediment and sedimentary bedforms in the area; (ii) the regime of waves and currents representative of the area; (iii) the configuration of the infrastructure and the restriction it creates for the background flows.

Edge scour is not considered in the present study. Should a scour protection around the foundations be implemented, the potential edge scour would be less than the predicted foundation scour without scour protection, which is discussed in this study. The regional conditions of seabed sediment and their expected mobility is discussed extensively in Section 4 and Attachment C. Building upon this description of the natural conditions, the following sections aim to establish the potential for scour development around the WTG and OSP foundations within the Mayflower Wind Lease Area, following the methodology described in Attachment B. The various foundation options (monopile, piled jacket, suction bucket jacket or gravity-based foundation) are discussed in sequence.

5.1 WTG Foundations

5.1.1 Monopile

Modelling was conducted in accordance with the methods described in Section 3. Local scour around a monopile foundation stems from the amplification of sediment entrainment action due to waves and currents interacting with the infrastructure. For live bed conditions and with currents only (absence of waves), the potential scour (S) may typically reach a depth of up to $S = 1.3\ D$, where D is the pile diameter (Sumer and Fredsøe, 2002; Attachment B). For a monopile diameter D =16 m, this would result in a scour depth of 20.8 m and estimated scour diameter of 122.5 m.

However, for the Mayflower Wind Lease Area, this appears as an overly conservative estimate for several reasons: (i) sediment transport across the Lease Area is only expected to occur during a very small fraction of the time, associated with a few episodic periods of intense metocean activity during the year; (ii) even during those events, the conditions for sediment transport only slightly exceed the conditions for initiation of motion; (iii) the timescales for scour development, even when considering the highest bottom currents, are in the range of years, largely exceeding the duration of potential storm events (days); (iv) thanks to the redistribution effect associated with the waves, the combined action of currents and waves during storm conditions would result in a lesser degree of scour development than estimated for currents alone.

Figure 4.4 shows that, during the metocean simulation period, live bed conditions are expected to be met during less than 2 percent of the time (i.e., in the order of 5 to 10 days per year). In clear water conditions the formula from Whitehouse (1998) can be used to estimate the reduced scour depth (Attachment B). When the ratio of Shields parameter over critical Shields parameter lies below 0.25, no scour is expected. When relying on the median (50^{th} percentile) Shields parameter, this ratio is always below 0.25 in the Lease Area, with a maximum of 0.15 (Attachment C, Figure C.16), hence no scour is expected to develop under median conditions. When considering the 90^{th} percentile of the Shields parameter (Attachment C, Figure C.17), the same ratio does slightly exceed 0.25, with a maximum value in the Lease Area of 0.49 on the eastern side. Local scour may therefore develop under these more extreme conditions. Applying the formula from Whitehouse (1998) with a ratio of 0.49 (see Attachment B) results in a predicted maximum scour depth of 8.3 m, with an estimated scour diameter of 58 m. This is considered as the worst-case scour susceptible to develop around the monopiles (Table 5.1).

The effect of waves can be assessed through the Keulegan-Carpenter (KC) number. Based on the metocean modelling, the maximum value of the KC number encountered during the simulation ranges in the Lease Area from 0.03 to 0.96, a value largely below 6 and, therefore, excluding the formation of vortex-shedding and horseshoe vortex at the pile face. In this case, local scour, if any, rather results from steady-streaming acceleration of flowlines around

the pile. The maximal local scour due to waves only is estimated from Figure B.2 (Attachment B), dependent on KC values and the diffraction parameter D/L, where L is the wave length. Under those circumstances, a conservative upper-bound for the maximum wave-induced scour depth would be $S \sim 0.04D = 0.64$ m and scour diameter 19 m (i.e., a width of 1.5 m around the pile contour).

Table 5.1: Estimated potential scour depth for monopile foundations.

Scour driver	Scour depth (m)	Scour diameter (m) (*)	Timescale for scour development
Normal currents (P50)	None	-	-
Normal waves (P50)	None	-	
Extreme currents (max) (**)	8.30	58	> 6 years
Extreme waves (max) (**)	0.64	19	
Global scour	Not relevant		
(*) Scour diameter includes the pile diameter of 16 m (**) Max scour for combinations of waves/currents is max of either of two scour drivers (not the sum of the two)			

To put these potential equilibrium scour depths in context, it is important to assess the typical timescales over which scour is expected to develop to an equilibrium and compare them with typical durations of the associated metocean drivers (normal and extreme conditions). The timescale to scour development is estimated at each location following the method described in Attachment B. Figure 5.1 shows an estimation of the timescale to scour development, associated with the greatest simulated bottom currents, which would be representative of conditions for the strongest storm captured over the simulation period. This estimated timescale is in excess of 6 years everywhere in the Lease Area. This suggests that even during storms, scour would proceed at a slow pace. It is therefore considered extremely unlikely that scour may develop toward its full potential over a single storm event or even a number of storms. Besides, partial backfilling of the developing scour holes is also expected in between periods of extreme conditions.

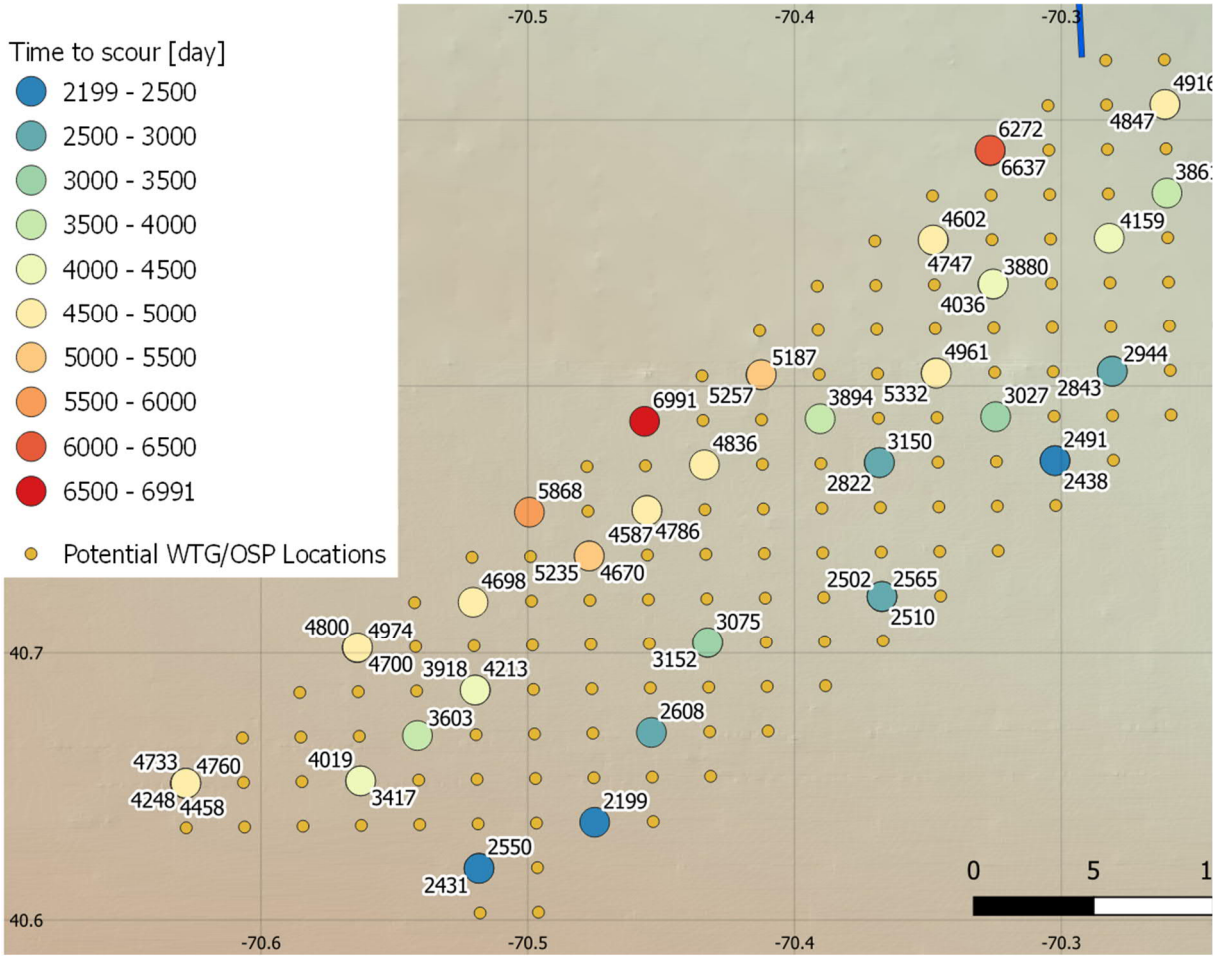

Figure 5.1. Estimation of timescale to scour for monopiles, based on the greatest modelled bottom currents.

5.1.2 Piled Jacket

For live bed conditions in the absence of waves (i.e., currents only) the scour depth is computed similarly as for the monopile. The upper bound scour depth amounts to 5.9 m with an estimated scour diameter of 34.7 m. This assessment considers live bed conditions, expected to be met during less than 2 percent of the time (i.e., in the order of 5 to 10 days per year). As discussed for monopiles, however, such a scour depth is considered overly conservative, as it does not account for several convincing elements reducing the scour potential, such as the very low percentage of time during which live bed conditions are expected, and the redistribution effect of waves.

Applying the formula from Whitehouse (1998) to account for predominantly clear water conditions, and conservatively considering the 90th percentile of Shields parameter over the area, which would be representative of the strongest storm captured over the simulation period, the maximum scour depth for currents would reduce to only 2.16 m, with estimated scour diameter of 15.6 m (Table 5.2).

Table 5.2. Estimated potential scour depth and associated timescales for piled jacket per pile.

Scour driver	Scour depth (m)	Scour diameter (m) (*)	Timescale for scour development
Normal currents (P50)	None	-	-
Normal waves (P50)	None	-	
Extreme currents (max)	2.16	15.6	> 1.6 years
Extreme combined waves/currents (max)	0.51 – 0.83	7.1 – 8.7	
Global scour (pile group)	Insignificant		
(*) Scour diameter includes the pile diameter of 4.5 m			

Potential scour estimates for the combined action of currents and waves is illustrated in Figure 5.2. These estimates were computed at each location where sediment sample data are available, at the simulation time for which the bottom current is the greatest at this location. The piled jacket foundation differs from the monopile by the significantly smaller pile diameter (i.e., 4.5 m instead of 16 m). In this case, the "large pile" hypothesis cannot be retained, as the assessment needs to include the intensity of potential vortex-shedding and horseshoe vortex. The predicted scour depth is below 0.85 m in the Lease Area, with scour diameters below 9 m. The southeastern region shows larger scour holes while the northern region is relatively more preserved.

Figure 5.3 shows the estimated minimal timescales for scour development at each location, based on the highest bottom currents encountered during the simulation. These estimates are everywhere above 600 days (1.6 years). It is again extremely unlikely that scour would fully develop over the course of a single storm.

The above estimates consider scour around an individual leg. The piled jackets have three or four legs, modelled here as four piles equally spaced on a horizontal circle of 50 m diameter (i.e., the legs lie on the corners of a square of size G = 35 m). It is possible that additional global scour will occur due to the interaction between the legs. The non-dimensional gap (G/D) is then 7.8 (see Attachment B).

For a side-by-side arrangement of the piles and G/D > 2, Sumer and Fredsøe (2002) showed that the interference effect between the piles practically disappears; therefore, each individual pile acts as a single pile. Likewise, for a tandem arrangement and for G/D > 1, the piles act like two individual piles with practically no interference.

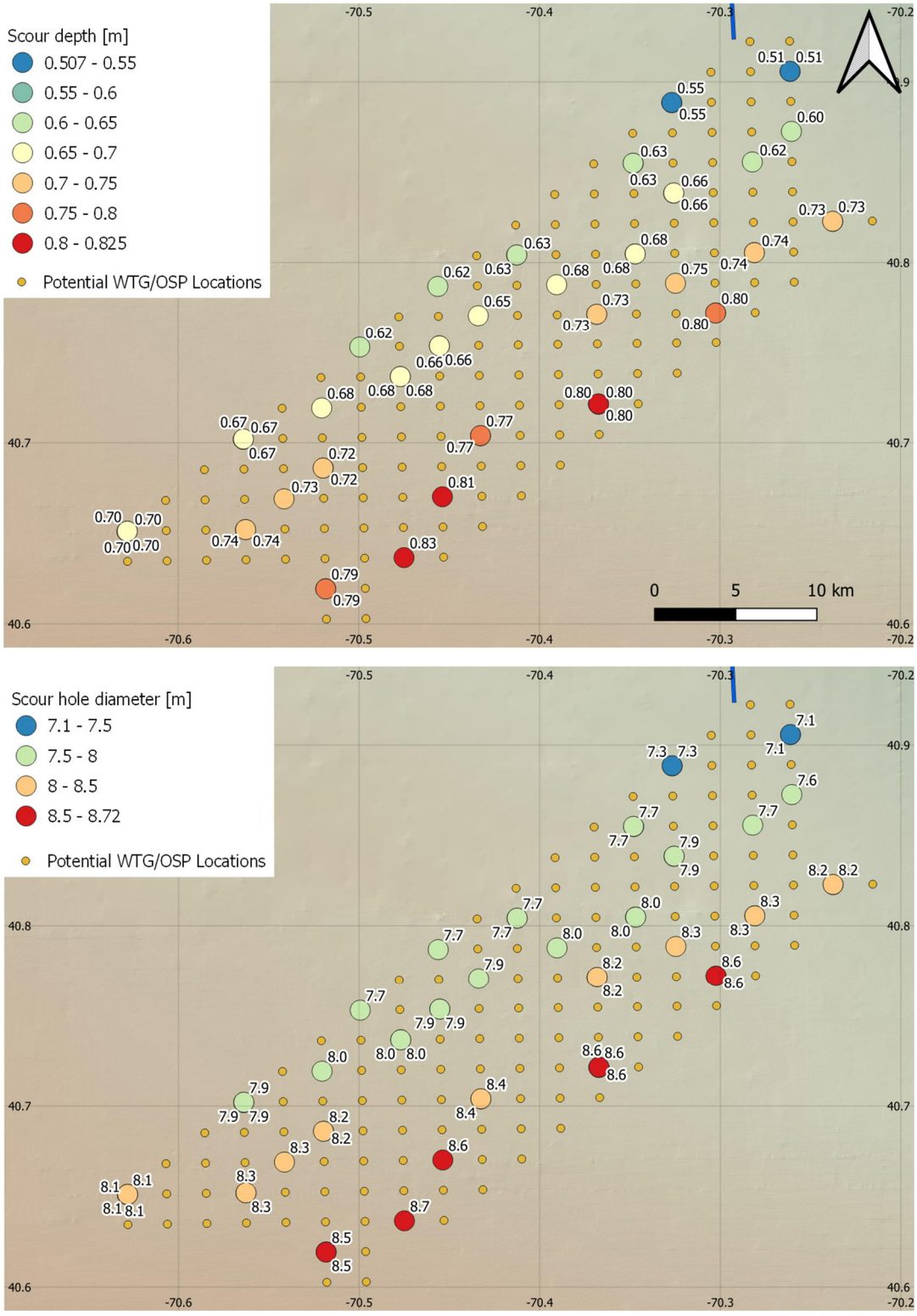

Figure 5.2. Estimation of scour hole dimensions for jacket piles under the combined action of waves and currents (estimate less than 0.85 m deep).

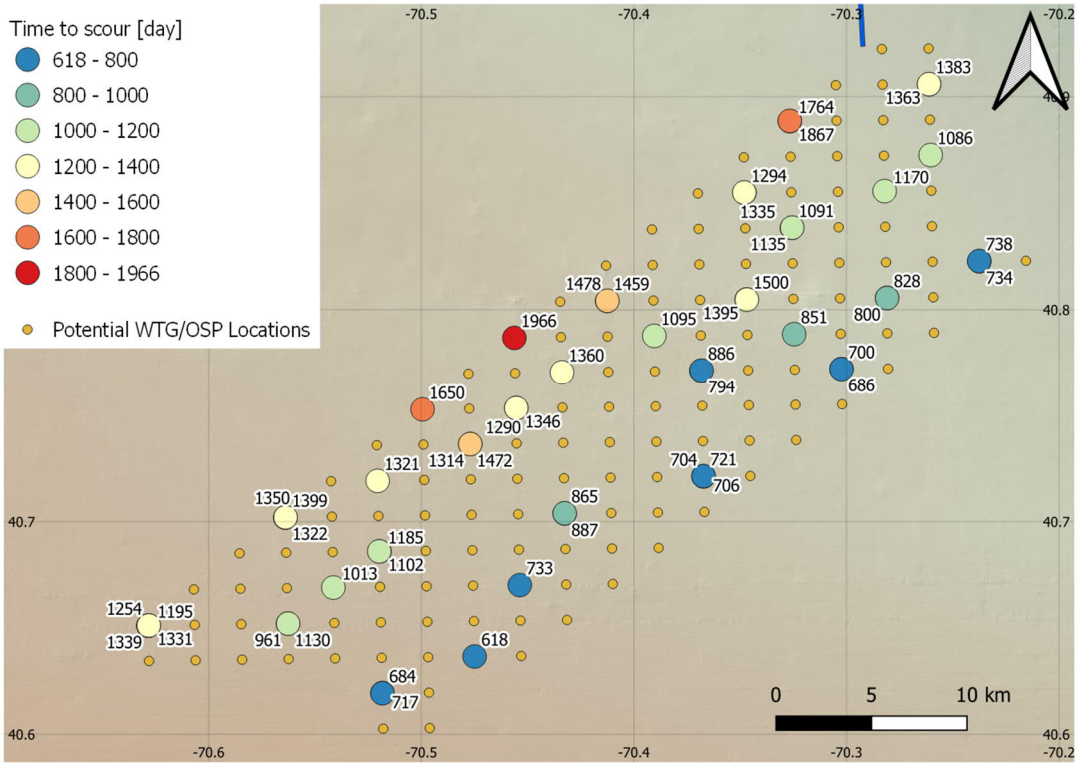

Figure 5.3. Estimation of timescale to scour for jacket piles, based on the highest modelled bottom currents.

5.1.3 Suction Bucket Jacket

The diameter of suction bucket jacket is D =20 m per bucket (i.e., larger than the 16 m diameter of the monopiles). However, the suction bucket diameter is not representative of the actual obstruction to the flow, as it would not cover the entire water depth, and instead would stick up only a small elevation above the seabed before connecting with the jacket leg, which itself will have a much smaller diameter and represent a milder obstruction to flow. However, the stick-up of the suction bucket and the diameter of the connecting jacket piles are unknown at this stage and are to be refined during detailed design; therefore, a very conservative assessment of the potential scour at the suction bucket can be obtained by considering that the buckets occupy the entire water depth. Doing so, using the formula from Whitehouse (1998) based on the 90th percentile of the Shields parameter, the potential scour depth for currents alone amounts to 10.4 m with an estimated diameter of 73 m. The effect of waves can be assessed through the KC number, with a range during the simulation in the Lease Area from 0.02 to 0.77. A "large pile" situation prevails as the intensity of potential vortex-shedding and horseshoe vortex at the pile face is low. Using the same methodology as for the monopile, a maximum wave-induced scour depth of $S \sim 0.03D = 0.6$ m and scour diameter 23 m (i.e., a width of 1.5 m) around the caisson contour can be expected (Table 5.3).

As discussed previously, the stick-up of the suction bucket above the seabed is currently unknown, and the estimates above consider that the suction bucket height occupies the whole water depth. Figure B.7 (Attachment B) shows that the above estimates of scour depth

and diameter are likely to be very significantly reduced for a suction bucket of limited height above the seabed (order of 1 to a few meters maximum).

Table 5.3. Estimated potential scour depth for suction bucket jacket foundations.

Scour driver	Scour depth (m) (*)	Scour diameter (m) (**)	Timescale for scour development
Normal currents (P50)	None	-	-
Normal waves (P50)	None	-	
Extreme currents (max) (***)	10.4	73	> 6 years
Extreme waves (max) (***)	0.6	23	
Global scour (bucket group)	insignificant		

(*) Conservatively considering suction buckets stick up over the entire water depth. Actual scour for small bucket stick-up expected to be very significantly lower and shall be estimated at later stage of design if applicable.

(**) Scour diameter includes the bucket diameter of 20 m

(***) Max scour for combinations of waves/currents is max of either of two scour drivers (not the sum of the two)

Figure 5.4 shows estimates for the associated timescale to scour development, which is greater than 6 years everywhere in the Lease Area. It is again extremely unlikely that scour would fully develop over the course of a single storm.

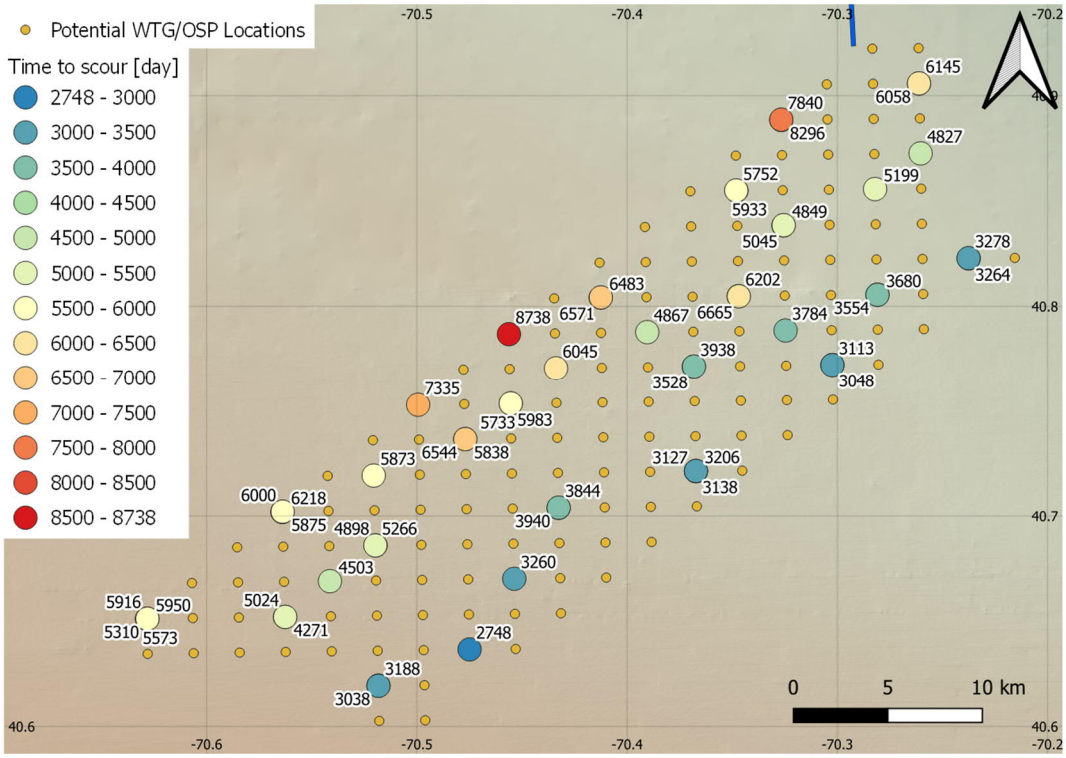

Figure 5.4. Estimation of timescale to scour for suction caissons, based on highest modelled bottom currents.

For purposes of this analysis, the suction bucket jackets were assumed to have three or four legs, modelled here as four piles equally spaced on a horizontal circle of 55 m diameter (i.e.,

the legs lie on the corners of a square of size G = 39 m). With a caisson separation to diameter ratio G/D of 1.95, the potential for global scour due to the group effect of the four suction caissons is expected to be minimal as explained above in Section 5.1.2 (see Sumer and Fredsøe, 2002). The potential for global scour will be further evaluated in final design.

5.1.4 Gravity-Based Structure

Gravity-based structures (GBS) present a much larger footprint at seabed than the other foundation options considered. Such structures are less susceptible to scour; however, they are highly sensitive to scour as they would only marginally penetrate on the seabed. Therefore, seabed preparation typically takes place ahead of the placement of gravity-based foundations to remove the surficial layer of sediment, level the seabed over the target footprint, and/or place a filter layer in the form or gravel or stone bed to prevent occurrence of scour at its base.

Therefore, no significant scour is expected to develop around the infrastructure based on the assumption of seabed preparation within the Lease Area if gravity-based foundations are adopted.

5.2 Offshore Substation Platforms

At this stage, the assessments performed for the monopile foundations presented in Section 5.1.1, piled jacket foundations in Section 5.1.2, suction bucket jacket in Section 5.1.3 and gravity-based foundations in Section 5.1.4 can be considered as representative of the potential scour development at the foundations for the OSP types that would rely on these foundation options.

6 Potential Scour Effects Along the Offshore Cable Routes

Cable routes under consideration include the offshore export cable routes as well as the inter-array cable routes. The inter-array cable routes are undefined at this stage. However, the sediment mobility potential across the Lease Area is very small, with no significant bedform observed (see Section 3 and Attachment C). The cables will be buried and no significant scour effect is expected for the inter-array cables.

The offshore export cables are planned to be buried along their entire length, with possible exclusion of crossing points or sections where burial is not achieved due to field conditions. Alternative protection methods, such as mattresses or rock installation, would be implemented along those localised areas.

In areas where the export cables are buried within a backfilled trench, background scour conditions would not be affected by the presence of the cables. However, seabed mobility due to natural causes can potentially expose the buried cables in areas of sand waves. To mitigate this risk, cables are planned to be buried below the mobile sand layer in order to minimize the risk of exposure at the surface.

Section 4 and Attachment D show that the potential for seabed mobility can be significant along the shallower northern area of the offshore export cable routes, and this poses a potential risk of exposure over the Project life cycle. Figure 4.4 shows that the critical Shields threshold in the less favourable areas of this northern area is exceeded 10 – 30 percent of the time, with an extreme value of 53.7 percent. The review of the bathymetry along the offshore cable routes, including observed bedforms, confirms the conclusions from the seabed mobility potential analysis. While the southern part of the cable routes is rather preserved, Figure 6.1 shows several visible bedforms affecting the Muskeget Channel, Vineyard Sound, and Nantucket Sound areas.

A quantitative evaluation of potential sand wave migration rates is beyond the scope of this study. However, an evaluation of the thickness of potentially mobile sediment from the movement of these bedforms is obtained by quantifying the variability of sediment wave heights along the export cable routes.

Attachment D shows seabed elevation profiles along the different export cable route options. From these profiles, an envelope of lower/higher expected values of local bedform elevation was determined. Bedform heights were calculated based on this envelope, also visible in Attachment D. These bedforms heights are then used to define a morphological zonation along the export cable routes, which is visible on both the profile plots of Attachment D and the maps of Figure 6.1.

Significant bedforms with heights locally up to 4 m are expected in the Muskeget Channel, especially on the eastward side (Central and Eastern Route Options), while less prominent bedforms are observed along the Western Route Option. High bedforms of similar heights are also observed at Vineyard Sound and Nantucket Sound in the section common to the three route options. The presence of the bedforms is correlated with the high percentage of exceedance for the critical Shields threshold seen in Figure 4.4, confirming that the southern part of the export cable routes (KP 50.0 – 88.0) is not subject to significant mobility.

As mentioned above, the offshore export cables are planned to be buried below the mobile sediment layer in order for the cables to remain buried during the lifetime of the infrastructure. If this is not achieved, alternative mitigation measures for cable protection in the critical areas may be considered, (Business, Enterprise and Regulatory Reform [BERR), 2008) to include but not limited to:

- Prefabricated concrete mattresses, consisting of several concrete block sections connected by polypropylene;
- Frond mattresses specifically designed to promote sedimentation and mitigate scour;
- Rock installation by means of a shaped berm profile or rock bags;
- Cable Protection Systems (CPS), typical example comprising two cylindrical half-shells of polyurethane or similar material, which overlap and interlock to form close-fitting protection around the cables; and
- Grout or sand bags, which can be installed by divers or Remotely Operated Vehicles (ROVs) to stabilise or fix in place cables over short distances.

Pre-sweeping of the bedforms, especially around the crestlines of the most prominent sand waves, may also be considered as a measure to see that burial below the mobile sediment layer is achieved, in place of or in association with the above-mentioned measures.

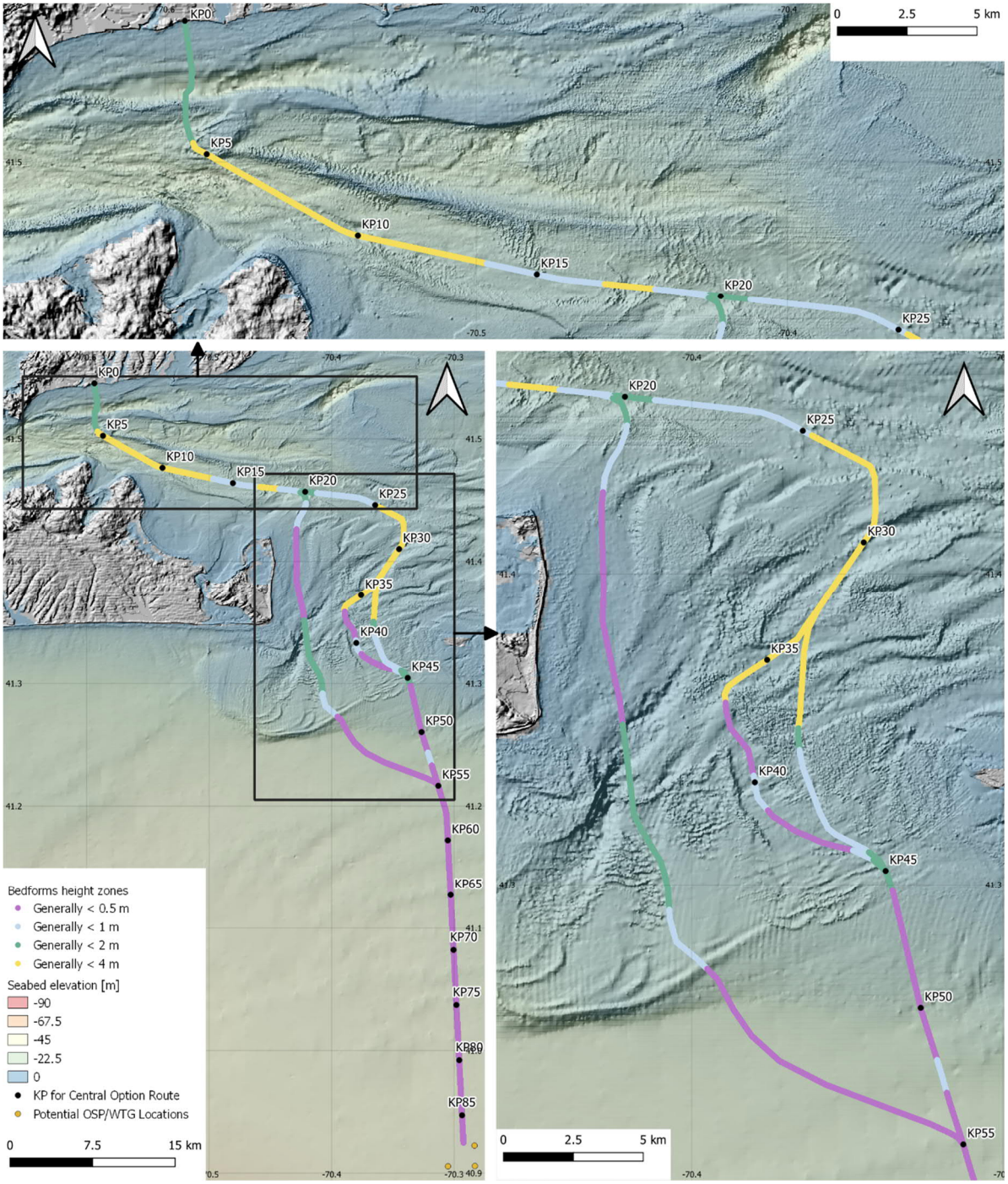

Figure 6.1. Morphological zonation for the export cable route options, based on the estimated bedform heights described in Attachment D.

7 Conclusions on Potential Scour Effect

A combined assessment of background seabed mobility potential and local scour at the planned infrastructure was performed for the Mayflower Wind Lease Area and export cable routes.

The Lease Area is characterized by a very low background sediment mobility, with very low percentage of critical Shields threshold exceedance and no observation of significant bedform or other markers of active sediment transport processes. As a result, clear-water conditions prevail for an overwhelmingly large fraction of the time, with live-bed conditions expected for only 1 to 2 percent of the time associated with episodic storms. The potential scour depth at the foundations is expected to be significantly less than the classical equilibrium value of ~1.3 times the foundation diameter. Practical estimates for monopiles, piled jacket foundations, or suction-bucket jacket foundations are provided in Section 5. Estimates for the timescale for scour development are in the order of several years, such that scour is unlikely to fully develop over the course of one or several storms. The results of this assessment indicate that given the seabed preparation required prior to installation, scour is not expected at gravity-based foundations.

Similar conditions prevail along the southern sections of the export cable routes (KP ~50.0 – 88.0), where sediment mobility potential is equally low and no significant bedforms are observed. No effect of scour is anticipated in this area if the cables are buried below seabed.

By contrast, the shallower water sections of the export cable routes (KP 0.0 – 50.0) feature a very active seabed with frequent sediment transport and active bedforms, especially in the region of Muskeget Channel, Vineyard Sound, and Nantucket Sound. A zonation of representative bedform height was performed, with heights locally reaching 4 m, but decreasing to less than 0.5 m in areas less exposed to strong tidal currents. The crests of the higher bedforms may need to be pre-swept with seabed preparation prior to cable installation and burial, to facilitate sufficient burial and limit the risk of cable re-exposure due to migrating bedforms.

The present assessment of potential effects from scour for operational phase and post-construction infrastructure is based on the metocean data resulting from a 2-year model simulation, considered as representative of the regional conditions. It should not be used for detailed design, for which site-specific design metocean criteria should be established.

8 References

Alpha analytical, 2020a. Analytical report: MAYFLOWER SUMMER 2020. Project number 124560, lab number L2036591, serial number 9252017:01.

Alpha analytical, 2020b. Analytical report: MAYFLOWER SUMMER 2020. Project number 124560, lab number L2036615, serial number 09292009:35.

Alpha analytical, 2020c. Analytical report: MAYFLOWER SUMMER 2020. Project number 124560, lab number L2036622, serial number 09252017:36.

Alpha analytical, 2020d. Analytical report: MAYFLOWER SUMMER 2020. Project number 124560, lab number L2036657, serial number 09252017:36.

Business, Enterprise and Regulatory Reform (BERR), 2008. Review of cabling techniques and environmental effects applicable to the offshore wind farm industry. Technical report, UK Department of Business, Enterprise & Regulatory Reform.

Bureau of Ocean Energy Management (BOEM) 2020. Information Guidelines for a Renewable Energy Construction and Operations Plan (COP). Version 4.0: May 27, 2020. United States Department of the Interior. Sterling, VA

Dalyander, P.S., Butman, B., Sherwood, C.R., Signell, R.P., Wilki, J.L., 2013. Characterizing wave- and current- induced bottom shear stress: U.S. middle Atlantic continental shelf. Continental Shelf Research, 52.

Guo, J., 2020. Empirical Model for Shields Diagram and Its Applications. Journal of Hydraulic Engineering, 146(6).

Hathaway, J.C., 1972. Data file, Continental Margin Program, Atlantic Coast of the United States: vol. 2 sample collection and analytical data. Technical report, Woods Hole Oceanographic Inst., DOI:10.1575/1912/1035.

Limeburner, R., 1968. Hydrography and Circulation about Nantucket Shoals. Massachusetts Institute of Technology.

Soulsby, R.L. and Whitehouse, R., 1997. Threshold of Sediment Motion in Coastal Environments. Proceedings of the Pacific coasts and ports 1997 conference.

Staudt, F., 2016. The influence of sediment texture on the mobility of mixed beds: Annular flume experiments and numerical modelling. PhD dissertation, Danish Hydraulic Institute (DHI).

Sumer, M. and Fredsøe, J. 2002. The Mechanics of Scour in the Marine Environment. World Scientific, Advanced Series on Ocean Engineering, 17.

Twichell, D.C., McCle, C.E., Butman, B., 1981. Morphology and Processes Associated with the Accumulation of the Fine-Grained Sediment Deposit on the Southern New England Shelf. Journal of Sedimentary Petrology, 51(1).

Whitehouse, R., 1998. Scour at Marine Structures – A manual for practical applications. Thomas Telford.

Attachment A

Data Sources and Tables

A.1 Bathymetry

In this study, several bathymetric datasets were considered.

For the regional background, the public bathymetry from NCEI U.S. Coastal Relief Model, with a 3 arc-seconds resolution (~70-90 m) is used (reference 1 below). Two other public datasets are also considered. A dataset from the National Oceanic and Atmospheric Administration's (NOAA) National Geophysical Data Center covers the cable routes, its surroundings and the northern part of the Lease Area with a resolution up to 10 m. A 10 m resolution dataset built from data collected by the United States Geological Survey (USGS), the NOAA, and the U.S. Army Corps of Engineers covers Vineyard Sound and western Nantucket Sound. Information on these datasets is accessible through the following links:

- https://www.ngdc.noaa.gov/mgg/coastal/crm.html;
- https://data.noaa.gov/metaview/page?xml=NOAA/NESDIS/NGDC/MGG/DEM//iso/xml/385.xml&view=getDataView&header=none#; and
- https://catalog.data.gov/dataset/10-m-bathymetry-grid-of-vineyard-and-western-nantucket-sounds-produced-from-lead-line-and-singl.

In addition, this study makes use of two bathymetry datasets surveyed by Fugro. The first one of 0.5 m resolution covers gridded corridors aligned with the turbine locations. The other dataset is available from the partially processed 2020 survey for the integrated geotechnical/geophysical interpretative study. It has a resolution of 0.25 m. This dataset partially covers the export cable corridors and some South-North oriented corridors aligned with the turbine locations.

Modelling was based on best available bathymetric data at the time of modelling.

A.2 Geotechnical data

The current study is based on Particles Size Distribution (PSD) of surface or shallow sub-surface as collected from the grab samples. Two grab sampling surveys were considered: May 2020 (68 samples) and August 2020 (48 samples). These samples mostly cover the Lease Area as well as the export cable routes (Central Option).

For the August 2020 benthic survey, reports by Alpha analytical (2020a, 2020b, 2020c, 2020d) were available, providing values for the median particle diameters used in this study.

A.3 Metocean conditions

The metocean conditions used in this study including the description of currents and waves covering a period from July 1, 2018 to June 26, 2020 were extracted from time series of the dataset resulting from the coupled metocean modelling task reported separately (COP Appendix F1, Sediment Plume Impacts from Construction Activities). No metocean criteria associated with specific return periods have yet been established for the Project.

A.4 WTG layout

Table A.1. WTG layout, including seabed elevation in MLLW and coordinates in the WGS 84/UTM Zone 19N coordinates system (EPSG: 32619).

Name	Easting (m)	Northing (m)	Seabed elevation (m)
X47	393806	4530924	-37.75
Y47	393806	4529072	-38.86
X46	391954	4530924	-39.53
Z47	393806	4527220	-40.26
Y46	391954	4529072	-40.62
AD49	397510	4519812	-40.82
AA47	393806	4525368	-41.44
Y45	390102	4529072	-41.81
Z46	391954	4527220	-41.86
AD48	395658	4519812	-42.33
AB47	393806	4523516	-42.95
AA46	391954	4525368	-43.01
Z45	390102	4527220	-43.19
AC47	393806	4521664	-43.28
AD47	393806	4519812	-43.53
AB46	391954	4523516	-43.90
AF47	393806	4516108	-43.93
AA45	390102	4525368	-43.99
AC46	391954	4521664	-44.05
AE47	393806	4517960	-44.05
Z44	388250	4527220	-44.12
AF46	391954	4516108	-44.29
AB45	390102	4523516	-44.52
AC45	390102	4521664	-44.60
AA44	388250	4525368	-44.74
AF45	390102	4516108	-44.75
AE46	391954	4517960	-44.76
AD46	391954	4519812	-44.82
AG46	391954	4514256	-44.87
AE45	390102	4517960	-45.09
AB44	388250	4523516	-45.72
AE44	388250	4517960	-45.73
AA43	386398	4525368	-45.84
AD45	390102	4519812	-45.85

Name	Easting (m)	Northing (m)	Seabed elevation (m)
AG45	390102	4514256	-46.30
AE43	386398	4517960	-46.31
AF44	388250	4516108	-46.61
AC44	388250	4521664	-46.79
AH45	390102	4512404	-47.28
AB43	386398	4523516	-47.39
AD44	388250	4519812	-47.46
AF43	386398	4516108	-47.51
AI43	386398	4510552	-47.57
AG44	388250	4514256	-47.73
AD43	386398	4519812	-47.86
AI44	388250	4510552	-47.86
AC43	386398	4521664	-48.01
AD42	384546	4519812	-48.28
AI42	384546	4510552	-48.37
AJ43	386398	4508700	-48.45
AH44	388250	4512404	-48.45
AE42	384546	4517960	-48.48
AB42	384546	4523516	-48.61
AG43	386398	4514256	-48.77
AF42	384546	4516108	-48.78
AH42	384546	4512404	-48.88
AJ42	384546	4508700	-48.88
AC42	384546	4521664	-48.93
AH43	386398	4512404	-49.00
AD40	380842	4519812	-49.10
AE41	382694	4517960	-49.37
AC41	382694	4521664	-49.42
AI41	382694	4510552	-49.44
AD41	382694	4519812	-49.60
AH41	382694	4512404	-49.68
AG42	384546	4514256	-50.01
AH40	380842	4512404	-50.08
AI40	380842	4510552	-50.20
AJ41	382694	4508700	-50.29
AG40	380842	4514256	-50.38
AG41	382694	4514256	-50.52

Name	Easting (m)	Northing (m)	Seabed elevation (m)
AK42	384546	4506848	-50.53
AF41	382694	4516108	-50.57
AG39	378990	4514256	-50.67
AF39	378990	4516108	-50.71
AH39	378990	4512404	-50.93
AF38	377138	4516108	-50.95
AE40	380842	4517960	-51.17
AJ40	380842	4508700	-51.20
AK41	382694	4506848	-51.21
AG38	377138	4514256	-51.37
AI39	378990	4510552	-51.42
AG37	375286	4514256	-51.52
AH38	377138	4512404	-51.53
AF40	380842	4516108	-51.57
AI38	377138	4510552	-51.78
AK40	380842	4506848	-51.93
AJ39	378990	4508700	-52.09
AL41	382694	4504996	-52.20
AJ38	377138	4508700	-52.48
AH37	375286	4512404	-52.59
AE39	378990	4517960	-52.62
AL40	380842	4504996	-52.81
AI37	375286	4510552	-52.86
AK39	378990	4506848	-52.89
AI36	373434	4510552	-53.21
AJ37	375286	4508700	-53.33
AK38	377138	4506848	-53.57
AL39	378990	4504996	-53.62
AH36	373434	4512404	-53.91
AM40	380842	4503144	-53.93
AM39	378990	4503144	-54.28
AL38	377138	4504996	-54.41
AK37	375286	4506848	-54.41
AJ36	373434	4508700	-54.52
AI35	371582	4510552	-54.98
AL37	375286	4504996	-55.02
AK36	373434	4506848	-55.07

Name	Easting (m)	Northing (m)	Seabed elevation (m)
AM38	377138	4503144	-55.19
AJ35	371582	4508700	-55.42
AL36	373434	4504996	-55.69
AK35	371582	4506848	-55.88
AM35	371582	4503144	-56.25
AM37	375286	4503144	-56.36
AL35	371582	4504996	-56.50
AN39	378990	4501292	-56.73
AM36	373434	4503144	-56.75
AJ34	369730	4508700	-56.80
AK34	369730	4506848	-56.88
AN38	377138	4501292	-57.06
AK33	367878	4506848	-57.15
AL34	369730	4504996	-57.40
AL33	367878	4504996	-57.75
AN37	375286	4501292	-57.97
AM33	367878	4503144	-58.53
AM34	369730	4503144	-58.54
AN35	371582	4501292	-58.75
AO38	377138	4499440	-58.78
AN34	369730	4501292	-58.80
AN36	373434	4501292	-58.83
AL32	366026	4504996	-58.89
AN33	367878	4501292	-58.96
AO37	375286	4499440	-59.10
AO36	373434	4499440	-59.41
AM32	366026	4503144	-59.59
AN31	364174	4501292	-60.01
AN32	366026	4501292	-60.12
AO35	371582	4499440	-60.48
AO33	367878	4499440	-60.50
AO34	369730	4499440	-60.50
AO32	366026	4499440	-60.62
AM31	364174	4503144	-60.65
AO31	364174	4499440	-60.94
AP36	373434	4497588	-61.00
AN30	362322	4501292	-61.08

Name	Easting (m)	Northing (m)	Seabed elevation (m)
AP35	371582	4497588	-61.21
AO30	362322	4499440	-61.43
AQ36	373434	4495736	-62.47
AQ35	371582	4495736	-62.70

A.5 Collected and computed data at grab sample locations

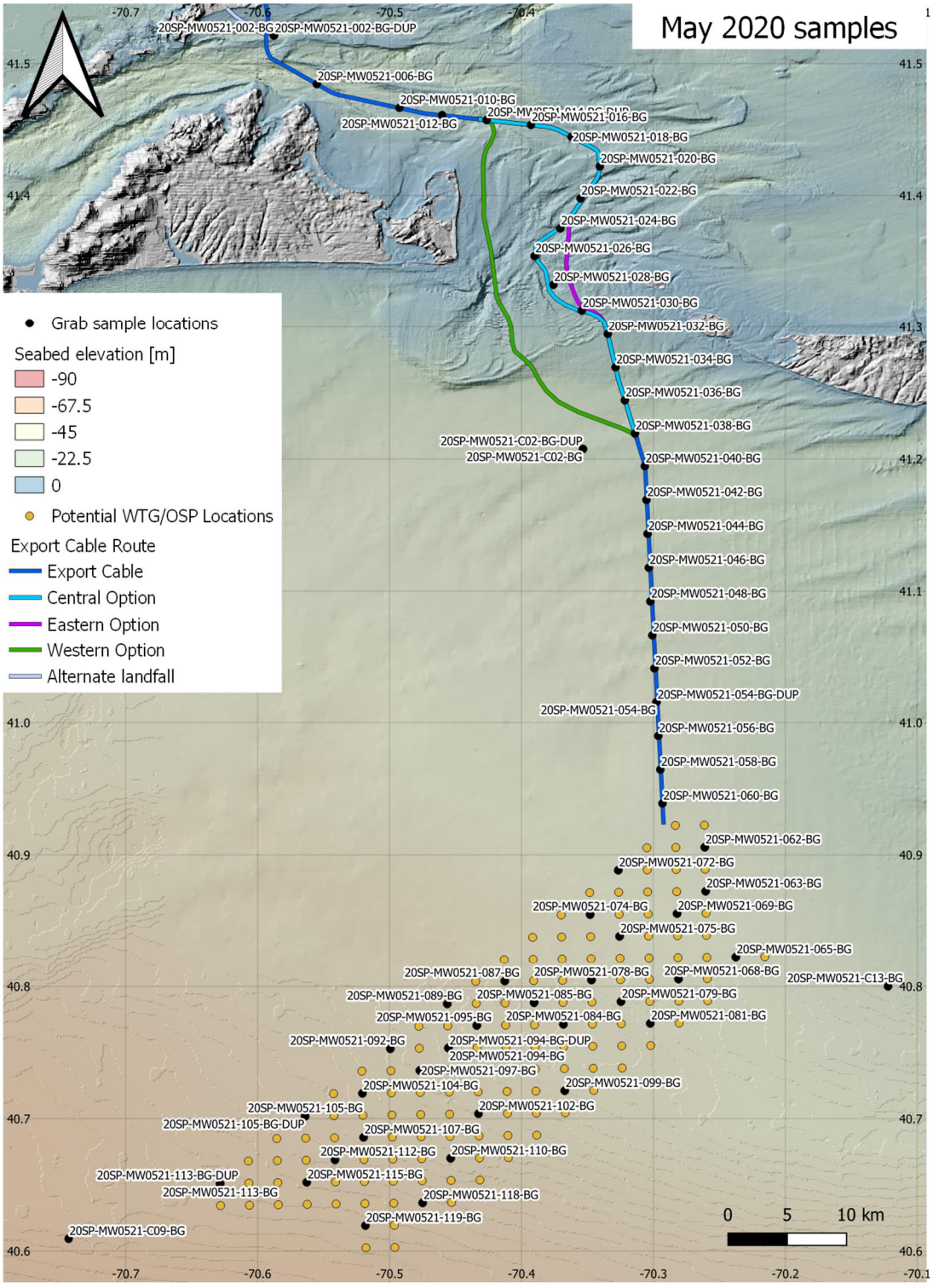

Figure A.1. Location of the grab samples corresponding to Table A.2 (May 2020 samples).

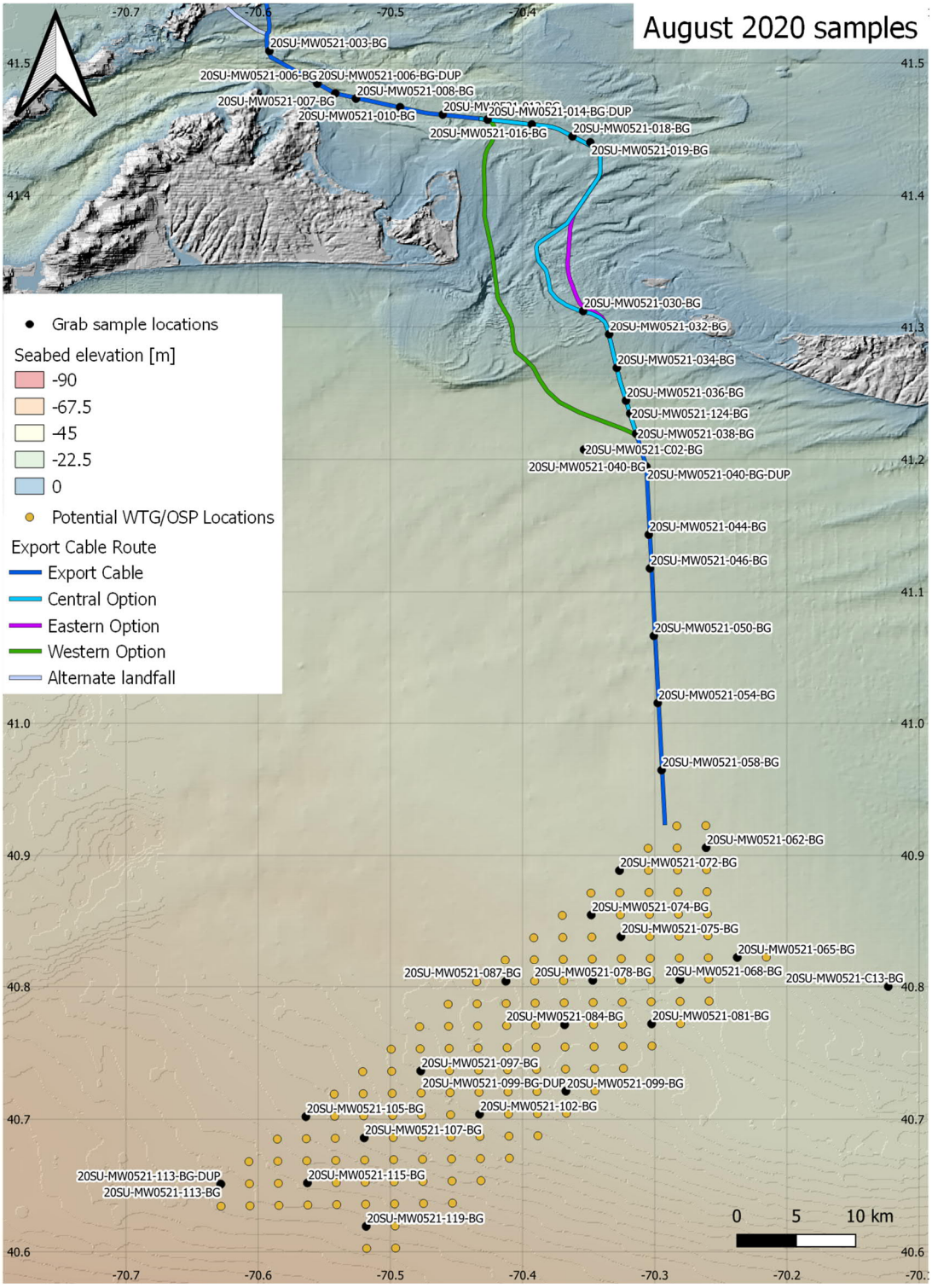

Figure A.2. Location of the grab samples corresponding to Table A.3 (August 2020 samples).

Table A.2. Collected and computed data at grab sample locations for May 2020 benthic survey.

Sample ID	Easting (m)	Northing (m)	d50 (mm)	Maximum shear stress (Pa)	Mean shear stress (-)	Maximum Shields parameter (-)	Time T of maximum Shear stress / Shields parameter	Mean Shields parameter (-)	Shields parameter percentile 50 (-])	Shields parameter percentile 90 (-)	Critical Shhields (Soulsby and Whitehouse, 1997)	Percentage of exceedance for critical Shields (Soulsby and Whitehouse, 1997)
20SP-MW0521-002-BG	367534	4597861	0.703	1.664	0.196	0.149	1/31/2019 17:00	0.017	0.012	0.04	0.03	18
20SP-MW0521-006-BG	370177	4593729	0.715	1.736	0.169	0.152	1/31/2019 17:00	0.015	0.01	0.035	0.03	13.9
20SP-MW0521-010-BG	375374	4591645	0.463	0.686	0.068	0.093	3/18/2020 22:00	0.009	0.006	0.021	0.032	4.6
20SP-MW0521-012-BG	378066	4590977	0.465	0.468	0.05	0.063	4/19/2019 14:00	0.007	0.004	0.016	0.032	1.8
20SP-MW0521-014-BG	380881	4590524	0.486	0.435	0.046	0.056	4/19/2019 14:00	0.006	0.004	0.013	0.031	1.1
20SP-MW0521-016-BG	383675	4590060	0.521	0.616	0.068	0.074	1/31/2019 17:00	0.008	0.006	0.017	0.031	2.5
20SP-MW0521-018-BG	386229	4589016	0.229	0.899	0.109	0.246	1/31/2019 17:00	0.03	0.022	0.06	0.045	19
20SP-MW0521-020-BG	387985	4586492	0.214	1.053	0.14	0.308	1/31/2019 16:00	0.041	0.033	0.082	0.047	33.7
20SP-MW0521-022-BG	386720	4583826	0.634	1.126	0.179	0.111	1/31/2019 16:00	0.018	0.015	0.035	0.03	16.6
20SP-MW0521-024-BG	385398	4581320	0.427	1.54	0.271	0.226	1/31/2019 3:00	0.04	0.036	0.08	0.033	53.7
20SP-MW0521-026-BG	383728	4579019	30.237	1.719	0.307	0.004	1/31/2019 3:00	0.001	0.001	0.001	0.055	0
20SP-MW0521-028-BG	384883	4576582	1.742	1.676	0.277	0.06	1/31/2019 3:00	0.01	0.009	0.02	0.037	0.3
20SP-MW0521-030-BG	386653	4574372	0.886	0.934	0.178	0.066	1/25/2019 10:00	0.013	0.012	0.023	0.03	2.6
20SP-MW0521-032-BG	388274	4572331	0.768	0.667	0.125	0.055	1/31/2019 16:00	0.01	0.01	0.017	0.03	0.5
20SP-MW0521-034-BG	388721	4569515	0.355	0.566	0.071	0.1	1/31/2019 4:00	0.013	0.011	0.023	0.035	3.3
20SP-MW0521-036-BG	389268	4566735	0.289	0.507	0.054	0.11	1/31/2019 18:00	0.012	0.008	0.027	0.039	4.6
20SP-MW0521-038-BG	389867	4563940	0.356	0.484	0.05	0.085	4/4/2020 18:00	0.009	0.005	0.022	0.035	3.1

Sample ID	Easting (m)	Northing (m)	d50 (mm)	Maximum shear stress (Pa)	Mean shear stress (-)	Maximum Shields parameter (-)	Time T of maximum Shear stress / Shields parameter	Mean Shields parameter (-)	Shields parameter percentile 50 (-])	Shields parameter percentile 90 (-)	Critical Shhields (Soulsby and Whitehouse, 1997)	Percentage of exceedance for critical Shields (Soulsby and Whitehouse, 1997)
20SP-MW0521-040-BG	390454	4561182	0.619	0.53	0.046	0.054	4/4/2020 18:00	0.005	0.003	0.012	0.03	0.6
20SP-MW0521-042-BG	390517	4558349	0.662	0.508	0.043	0.048	4/4/2020 18:00	0.004	0.002	0.01	0.03	0.4
20SP-MW0521-044-BG	390544	4555502	0.689	0.498	0.039	0.045	4/4/2020 18:00	0.004	0.002	0.009	0.03	0.2
20SP-MW0521-046-BG	390580	4552652	0.714	0.488	0.035	0.043	4/4/2020 18:00	0.003	0.002	0.007	0.03	0.1
20SP-MW0521-048-BG	390636	4549824	0.376	0.427	0.032	0.071	4/4/2020 18:00	0.005	0.003	0.012	0.034	0.7
20SP-MW0521-050-BG	390720	4546977	0.81	0.447	0.031	0.035	4/4/2020 18:00	0.002	0.002	0.005	0.03	0
20SP-MW0521-052-BG	390810	4544130	0.117	0.378	0.027	0.203	4/4/2020 18:00	0.014	0.01	0.029	0.071	1.3
20SP-MW0521-054-BG	390903	4541293	0.117	0.304	0.024	0.162	4/4/2020 19:00	0.013	0.009	0.025	0.071	0.8
20SP-MW0521-056-BG	390975	4538457	0.117	0.299	0.023	0.16	4/4/2020 19:00	0.012	0.009	0.024	0.071	0.7
20SP-MW0521-058-BG	391061	4535626	0.139	0.288	0.023	0.13	4/4/2020 19:00	0.01	0.008	0.02	0.063	0.6
20SP-MW0521-060-BG	391157	4532782	0.146	0.291	0.023	0.125	4/4/2020 19:00	0.01	0.007	0.019	0.061	0.5
20SP-MW0521-062-BG	393800	4529062	0.103	0.295	0.026	0.18	4/4/2020 19:00	0.016	0.012	0.031	0.078	1
20SP-MW0521-063-BG	393808	4525375	0.102	0.334	0.026	0.205	4/4/2020 19:00	0.016	0.011	0.033	0.078	1.2
20SP-MW0521-065-BG	395658	4519813	0.111	0.414	0.029	0.234	4/4/2020 19:00	0.016	0.011	0.036	0.074	1.9
20SP-MW0521-068-BG	391968	4517955	0.111	0.41	0.026	0.232	4/4/2020 20:00	0.015	0.01	0.033	0.074	1.6
20SP-MW0521-069-BG	391955	4523523	0.108	0.337	0.024	0.196	4/4/2020 19:00	0.014	0.01	0.03	0.075	1
20SP-MW0521-072-BG	388248	4527218	0.127	0.289	0.021	0.143	4/4/2020 19:00	0.01	0.007	0.021	0.067	0.5
20SP-MW0521-074-BG	386395	4523519	0.098	0.324	0.02	0.208	4/4/2020 19:00	0.013	0.009	0.028	0.08	0.7

Sample ID	Easting (m)	Northing (m)	d50 (mm)	Maximum shear stress (Pa)	Mean shear stress (-)	Maximum Shields parameter (-)	Time T of maximum Shear stress / Shields parameter	Mean Shields parameter (-)	Shields parameter percentile 50 (-])	Shields parameter percentile 90 (-)	Critical Shhields (Soulsby and Whitehouse, 1997)	Percentage of exceedance for critical Shields (Soulsby and Whitehouse, 1997)
20SP-MW0521-075-BG	388249	4521661	0.1	0.35	0.022	0.219	4/4/2020 20:00	0.014	0.009	0.03	0.079	1
20SP-MW0521-078-BG	386393	4517960	0.173	0.362	0.022	0.131	4/4/2020 20:00	0.008	0.005	0.018	0.054	0.6
20SP-MW0521-079-BG	388253	4516118	0.115	0.409	0.024	0.223	4/4/2020 20:00	0.013	0.008	0.028	0.072	1.2
20SP-MW0521-081-BG	390106	4514271	0.11	0.443	0.025	0.253	4/4/2020 20:00	0.014	0.009	0.031	0.074	1.5
20SP-MW0521-084-BG	384537	4514268	0.09	0.384	0.021	0.268	4/4/2020 20:00	0.014	0.009	0.031	0.085	1.1
20SP-MW0521-085-BG	382697	4516118	0.09	0.35	0.019	0.243	4/4/2020 20:00	0.013	0.008	0.03	0.085	0.9
20SP-MW0521-087-BG	380855	4517969	0.094	0.314	0.018	0.21	4/4/2020 20:00	0.012	0.007	0.027	0.083	0.7
20SP-MW0521-089-BG	377140	4516102	0.138	0.31	0.017	0.141	4/4/2020 20:00	0.008	0.005	0.017	0.063	0.4
20SP-MW0521-092-BG	373430	4512393	0.096	0.306	0.015	0.199	4/4/2020 20:00	0.01	0.006	0.022	0.081	0.6
20SP-MW0521-094-BG	377153	4512399	0.103	0.335	0.017	0.205	4/4/2020 20:00	0.01	0.006	0.023	0.078	0.6
20SP-MW0521-095-BG	379003	4514267	0.102	0.332	0.018	0.203	4/4/2020 20:00	0.011	0.007	0.024	0.078	0.7
20SP-MW0521-097-BG	375293	4510546	0.103	0.343	0.017	0.209	4/4/2020 20:00	0.01	0.006	0.022	0.078	0.6
20SP-MW0521-099-BG	384537	4508699	0.102	0.439	0.021	0.271	4/4/2020 20:00	0.013	0.008	0.028	0.078	1.1
20SP-MW0521-102-BG	378986	4506855	0.1	0.407	0.018	0.255	4/4/2020 20:00	0.011	0.007	0.025	0.079	0.8
20SP-MW0521-104-BG	371582	4508686	0.092	0.337	0.015	0.23	4/4/2020 20:00	0.01	0.006	0.023	0.084	0.6
20SP-MW0521-105-BG	367878	4506831	0.082	0.329	0.014	0.251	4/4/2020 20:00	0.011	0.006	0.025	0.091	0.6
20SP-MW0521-107-BG	371593	4504999	0.092	0.372	0.015	0.253	4/4/2020 20:00	0.01	0.006	0.023	0.084	0.7
20SP-MW0521-110-BG	377142	4503144	0.089	0.438	0.018	0.309	4/4/2020 20:00	0.013	0.007	0.027	0.086	0.9

Sample ID	Easting (m)	Northing (m)	d50 (mm)	Maximum shear stress (Pa)	Mean shear stress (-)	Maximum Shields parameter (-)	Time T of maximum Shear stress / Shields parameter	Mean Shields parameter (-)	Shields parameter percentile 50 (-])	Shields parameter percentile 90 (-)	Critical Shhields (Soulsby and Whitehouse, 1997)	Percentage of exceedance for critical Shields (Soulsby and Whitehouse, 1997)
20SP-MW0521-112-BG	369724	4503143	0.085	0.38	0.015	0.282	4/4/2020 20:00	0.011	0.006	0.025	0.089	0.7
20SP-MW0521-113-BG	362329	4501282	0.095	0.354	0.014	0.235	4/4/2020 20:00	0.01	0.005	0.022	0.082	0.7
20SP-MW0521-115-BG	367883	4501292	0.08	0.387	0.015	0.303	4/4/2020 20:00	0.012	0.006	0.027	0.092	0.8
20SP-MW0521-118-BG	375281	4499444	0.074	0.459	0.018	0.389	4/4/2020 20:00	0.015	0.008	0.033	0.097	1.2
20SP-MW0521-119-BG	371580	4497600	0.073	0.436	0.017	0.375	4/4/2020 20:00	0.014	0.007	0.032	0.098	1.1
20SP-MW0521-002-BG-DUP	367534	4597861	0.698	1.664	0.196	0.15	1/31/2019 17:00	0.018	0.012	0.041	0.03	18.2
20SP-MW0521-014-BG-DUP	380881	4590524	0.487	0.435	0.046	0.056	4/19/2019 14:00	0.006	0.004	0.013	0.031	1.1
20SP-MW0521-054-BG-DUP	390903	4541293	0.117	0.304	0.024	0.163	4/4/2020 19:00	0.013	0.009	0.025	0.071	0.8
20SP-MW0521-094-BG-DUP	377153	4512399	0.097	0.335	0.017	0.218	4/4/2020 20:00	0.011	0.007	0.025	0.081	0.7
20SP-MW0521-105-BG-DUP	367878	4506831	0.086	0.329	0.014	0.239	4/4/2020 20:00	0.01	0.006	0.023	0.087	0.6
20SP-MW0521-113-BG-DUP	362329	4501282	0.086	0.354	0.014	0.258	4/4/2020 20:00	0.01	0.005	0.024	0.088	0.7
20SP-MW0521-C02-BG	386544	4562685	0.616	0.431	0.04	0.044	4/4/2020 18:00	0.004	0.002	0.01	0.03	0.3
20SP-MW0521-C02-BG-DUP	386544	4562685	0.728	0.431	0.04	0.037	4/4/2020 18:00	0.003	0.002	0.009	0.03	0.1
20SP-MW0521-C09-BG	352523	4496842	0.073	0.334	0.015	0.288	4/4/2020 20:00	0.013	0.006	0.031	0.098	1.1
20SP-MW0521-C13-BG	405360	4517157	0.176	0.606	0.042	0.216	4/4/2020 19:00	0.015	0.011	0.029	0.053	2.9

Table A.3: Collected and computed data at grab sample locations for August 2020 survey.

Sample ID	Easting [m]	Northing [m]	d50 [mm]	Maximum shear stress [Pa]	Mean shear stress [-]	Maximum Shields parameter [-]	Time T of maximum Shear stress / Shields parameter	Mean Shields parameter [-]	Shields parameter percentile 50 [-]	Shields parameter percentile 90 [-]	Critical Shhields (Soulsby and Whitehouse, 1997)	Percentage of exceedance for critical Shields (Soulsby and Whitehouse, 1997)
20SU-MW0521-003-BG	367191	4596510	1.066	1.954	0.187	0.115	3/18/2020 22:00	0.011	0.007	0.027	0.032	7.3
20SU-MW0521-006-BG	370168	4593728	0.7	1.737	0.169	0.156	1/31/2019 17:00	0.015	0.01	0.036	0.03	14.4
20SU-MW0521-006-BG-DUP	370168	4593728	0.712	1.737	0.169	0.153	1/31/2019 17:00	0.015	0.01	0.035	0.03	14
20SU-MW0521-007-BG	371287	4592880	6.465	1.366	0.12	0.013	1/31/2019 17:00	0.001	0.001	0.003	0.054	0
20SU-MW0521-008-BG	372587	4592423	0.872	0.855	0.081	0.062	1/31/2019 17:00	0.006	0.004	0.014	0.03	1.1
20SU-MW0521-009-BG	372587	4592423	0.092	0.855	0.081	0.582	1/31/2019 17:00	0.055	0.036	0.132	0.084	22.4
20SU-MW0521-010-BG	375362	4591650	0.473	0.687	0.068	0.091	3/18/2020 22:00	0.009	0.006	0.021	0.032	4.5
20SU-MW0521-012-BG	378047	4590980	0.471	0.469	0.05	0.062	4/19/2019 14:00	0.007	0.004	0.016	0.032	1.8
20SU-MW0521-014-BG	380875	4590522	0.505	0.435	0.046	0.054	4/19/2019 14:00	0.006	0.004	0.013	0.031	0.9
20SU-MW0521-014-BG-DUP	380875	4590522	0.489	0.435	0.046	0.056	4/19/2019 14:00	0.006	0.004	0.013	0.031	1
20SU-MW0521-016-BG	383664	4590062	0.599	0.615	0.068	0.064	1/31/2019 17:00	0.007	0.005	0.015	0.03	1.7
20SU-MW0521-018-BG	386216	4589019	0.206	0.898	0.108	0.273	1/31/2019 17:00	0.033	0.025	0.067	0.048	20.4
20SU-MW0521-019-BG	387335	4588506	2.184	0.997	0.124	0.029	1/31/2019 17:00	0.004	0.003	0.007	0.041	0
20SU-MW0521-030-BG	386664	4574363	0.566	0.931	0.178	0.103	1/25/2019 10:00	0.02	0.018	0.037	0.03	20.1
20SU-MW0521-032-BG	388277	4572332	0.672	0.667	0.125	0.062	1/31/2019 16:00	0.012	0.011	0.019	0.03	1.2
20SU-MW0521-034-BG	388723	4569501	0.296	0.565	0.071	0.12	1/31/2019 4:00	0.015	0.013	0.028	0.038	4.5
20SU-MW0521-036-BG	389263	4566744	0.286	0.507	0.054	0.111	1/31/2019 18:00	0.012	0.008	0.028	0.039	4.7

Sample ID	Easting [m]	Northing [m]	d50 [mm]	Maximum shear stress [Pa]	Mean shear stress [-]	Maximum Shields parameter [-]	Time T of maximum Shear stress / Shields parameter	Mean Shields parameter [-]	Shields parameter percentile 50 [-]	Shields parameter percentile 90 [-]	Critical Shhields (Soulsby and Whitehouse, 1997)	Percentage of exceedance for critical Shields (Soulsby and Whitehouse, 1997)
20SU-MW0521-038-BG	389865	4563956	0.349	0.484	0.05	0.087	4/4/2020 18:00	0.009	0.005	0.022	0.035	3.3
20SU-MW0521-040-BG	390463	4561185	0.573	0.53	0.046	0.058	4/4/2020 18:00	0.005	0.003	0.012	0.03	0.8
20SU-MW0521-040-BG-DUP	390463	4561185	0.538	0.53	0.046	0.062	4/4/2020 18:00	0.005	0.003	0.013	0.031	1
20SU-MW0521-044-BG	390538	4555483	0.619	0.497	0.039	0.05	4/4/2020 18:00	0.004	0.002	0.009	0.03	0.4
20SU-MW0521-046-BG	390572	4552653	0.117	0.488	0.035	0.261	4/4/2020 18:00	0.018	0.011	0.043	0.071	3.8
20SU-MW0521-050-BG	390733	4546989	0.473	0.448	0.031	0.059	4/4/2020 18:00	0.004	0.003	0.009	0.032	0.4
20SU-MW0521-054-BG	390895	4541274	0.111	0.303	0.024	0.172	4/4/2020 19:00	0.013	0.01	0.026	0.074	0.9
20SU-MW0521-058-BG	391058	4535627	0.118	0.288	0.023	0.154	4/4/2020 19:00	0.012	0.009	0.024	0.071	0.6
20SU-MW0521-062-BG	393796	4529067	0.105	0.295	0.026	0.177	4/4/2020 19:00	0.015	0.012	0.03	0.077	1
20SU-MW0521-065-BG	395654	4519824	0.111	0.414	0.029	0.233	4/4/2020 19:00	0.016	0.011	0.036	0.074	1.9
20SU-MW0521-068-BG	391972	4517948	0.116	0.41	0.026	0.221	4/4/2020 20:00	0.014	0.009	0.031	0.071	1.5
20SU-MW0521-072-BG	388247	4527238	0.117	0.289	0.021	0.154	4/4/2020 19:00	0.011	0.008	0.023	0.071	0.6
20SU-MW0521-074-BG	386386	4523533	0.102	0.324	0.02	0.199	4/4/2020 19:00	0.012	0.008	0.027	0.078	0.7
20SU-MW0521-075-BG	388259	4521673	0.106	0.35	0.022	0.207	4/4/2020 20:00	0.013	0.009	0.028	0.076	0.9
20SU-MW0521-078-BG	386402	4517952	0.157	0.362	0.022	0.145	4/4/2020 20:00	0.009	0.006	0.019	0.058	0.7
20SU-MW0521-081-BG	390104	4514264	0.114	0.444	0.025	0.245	4/4/2020 20:00	0.014	0.009	0.03	0.073	1.5
20SU-MW0521-084-BG	384546	4514273	0.077	0.384	0.021	0.313	4/4/2020 20:00	0.017	0.01	0.036	0.094	1.2
20SU-MW0521-087-BG	380865	4517979	0.096	0.314	0.018	0.205	4/4/2020 20:00	0.012	0.007	0.026	0.082	0.7

Sample ID	Easting [m]	Northing [m]	d50 [mm]	Maximum shear stress [Pa]	Mean shear stress [-]	Maximum Shields parameter [-]	Time T of maximum Shear stress / Shields parameter	Mean Shields parameter [-]	Shields parameter percentile 50 [-]	Shields parameter percentile 90 [-]	Critical Shhields (Soulsby and Whitehouse, 1997)	Percentage of exceedance for critical Shields (Soulsby and Whitehouse, 1997)
20SU-MW0521-097-BG	375294	4510544	0.121	0.343	0.017	0.177	4/4/2020 20:00	0.009	0.005	0.019	0.069	0.6
20SU-MW0521-099-BG	384539	4508716	0.102	0.439	0.021	0.269	4/4/2020 20:00	0.013	0.008	0.028	0.078	1.1
20SU-MW0521-099-BG-DUP	384539	4508716	0.105	0.439	0.021	0.261	4/4/2020 20:00	0.013	0.008	0.027	0.076	1.1
20SU-MW0521-102-BG	378987	4506867	0.096	0.406	0.018	0.265	4/4/2020 20:00	0.012	0.007	0.025	0.081	0.8
20SU-MW0521-105-BG	367888	4506846	0.08	0.329	0.014	0.259	4/4/2020 20:00	0.011	0.006	0.025	0.092	0.7
20SU-MW0521-107-BG	371582	4505000	0.102	0.372	0.015	0.228	4/4/2020 20:00	0.009	0.005	0.021	0.078	0.6
20SU-MW0521-113-BG	362345	4501293	0.08	0.354	0.014	0.276	4/4/2020 20:00	0.011	0.006	0.026	0.092	0.7
20SU-MW0521-113-BG-DUP	362345	4501293	0.094	0.354	0.014	0.237	4/4/2020 20:00	0.01	0.005	0.022	0.083	0.7
20SU-MW0521-115-BG	367891	4501290	0.101	0.387	0.015	0.24	4/4/2020 20:00	0.009	0.005	0.021	0.078	0.7
20SU-MW0521-119-BG	371580	4497587	0.068	0.436	0.017	0.401	4/4/2020 20:00	0.015	0.008	0.035	0.102	1.2
20SU-MW0521-124-BG	389515	4565658	0.101	0.471	0.051	0.294	1/31/2019 18:00	0.032	0.019	0.076	0.079	9.5
20SU-MW0521-C02-BG	386538	4562681	0.605	0.431	0.04	0.045	4/4/2020 18:00	0.004	0.002	0.01	0.03	0.3
20SU-MW0521-C13-BG	405258	4517172	0.153	0.603	0.041	0.247	4/4/2020 19:00	0.017	0.012	0.034	0.059	3.1

Attachment B

Methodology

B.1 Background Sediment Mobility Potential

The potential for background sediment mobility across the Project Area site and along the export cable routes was assessed. The importance is related to whether the seabed is expected to be mobile or immobile under the action of waves and currents, and for what percentage of the time. This determines whether clear water conditions or live bed conditions will constrain the potential for local scour development at the infrastructure.

The potential for background sediment mobility is established from the three following principles:

- Literature review;
- Bathymetric and geomorphological review; and
- Bed shear stress and sediment transport analysis.

B.1.1 Literature review

The literature review summarizes the current understanding of the expected sediment transport and geomorphological processes active within the study area, as established from public data sources and relevant references of the scientific literature. It sets the regional context of the study area for the study purposes and allows to place the site-specific study assessments in regard of this regional context.

B.1.2 Bathymetric and geomorphological review

The site-specific bathymetric datasets that were made available at the time the present study is performed, are reviewed, especially with respect to the identification of potential scour-related features that would pinpoint to sediment transport activity. As the high-resolution bathymetric dataset is currently limited to narrow corridors across the Lease Area and portions of the export cable routes, the review is not comprehensive.

Special attention is paid to identification and illustration of morphological features such as depressions, bedforms, scour marks, and preserved man-made features such as seabed scars from anchoring or fishing activity.

B.1.3 Bed shear stress and sediment transport analysis

Sediment mobility at the seabed is mainly driven by the combination of two factors: soil characteristics allowing for the sediment particles to be carried away (e.g., particles size, cohesion) and a bed shear stress sufficiently high to erode and transport these particles.

Several attempts have been made to relate the erodibility of a soil with the bed shear stress or flow velocity, with examples illustrated in Figure B.1. These show that for the largest particle sizes, the bed shear stress required to erode the soil increases with the grain size due to their increasing weight. In contrast, for the smallest particle sizes, the critical bed shear stress decreases with the grain size because of the reduced bed roughness implying less turbulence generation and erosion. For very fine particles such as in fine silt and clay, the

critical bed shear stress increases again, as the boundary layer evolves from turbulent to laminar. Cohesive forces between clay particles lead to an increased stability of a mixed bed with a threshold clay or mud content. At this threshold, the behaviour of the bed traverses from non-cohesive, sand-dominated to cohesive, mud-dominated behaviour (Staudt, 2016).

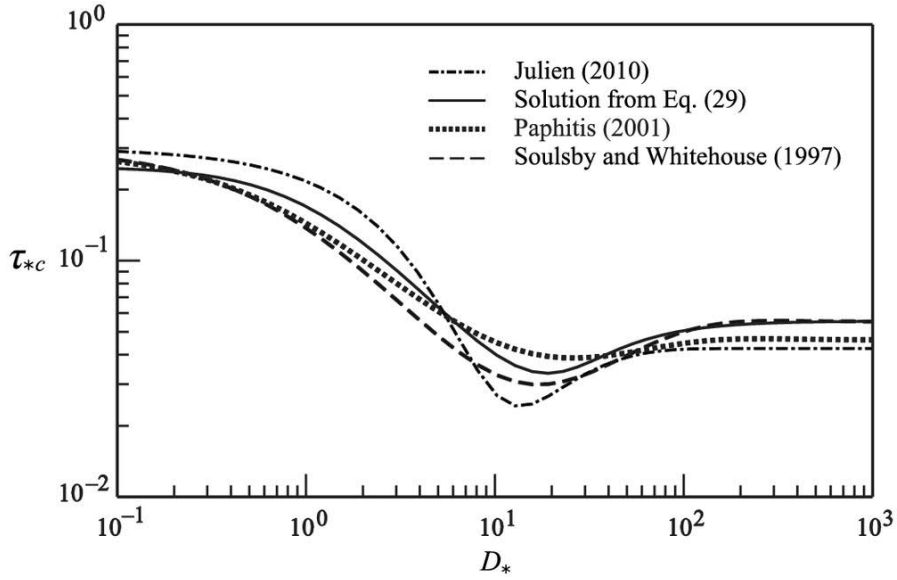

Figure B.1. Empirical curves defining the relationship between dimensionless sediment size D_* and the critical dimensionless shear stress τ_{*c} above which the soil can be eroded (critical Shields parameter). From Guo (2020).

For a more quantitative analysis of background sediment mobility assessment across the Lease Area and export cable routes, time series from the metocean modelling exercise reported separately (COP Appendix F1, Sediment Plume Impacts from Construction Activities) are analysed in details, along with correlations with the sediment particle size data. Combined wave/current bed shear stresses are calculated, and statistically meaningful values such as P50 (average) and P90 (90th percentile) are derived.

The dimensionless shear stress, also known as the Shields parameter, is calculated and compared with its critical values based on the sediment particle size. Conditions are considered to be live bed when the Shields parameter is greater than its critical value. Otherwise the morphological state is referred to as clear water conditions. Percentiles and percentages of Shields time exceedance are calculated in order to assess the severity of the potential seabed mobility. Their calculation requires data on sediment grain sizes. To assess the variability of the sediment mobility potential, the calculations are therefore performed at each location where grab sampling was performed from either of the May 2020 and August 2020 surveys. D_{50} median grain sizes are calculated at each location and used to convert bed shear stresses into Shields parameter values. A typical sediment particle density of 2,650 kg/m^3 is assumed in the conversion, which is conservatively taken toward the lower bound of the range based on site-specific data available for shallow soil units (~2,650-2,700 kg/m^3) .

The calculations allow to derive percentage of times that the seabed sediment are expected to be mobile under wave/current action at each location, which will inform the local scour assessment.

B.2 Local Scour Assessment

Local scour at the structures (wind turbine foundations or Offshore Substation Platform location) may result from bed shear stress amplification due to fluid-structure interactions. Background bed shear stresses associated with waves/currents are sourced from the metocean modelling exercise reported separately (COP Appendix F1, Sediment Plume Impacts from Construction Activities) and used to assess clear water or live bed scour conditions.

Local scour predictions presented in the report are established using analytical means following the methodology proposed by Sumer and Fredsøe (2002). The predictions are provided assuming no sour protection layer in place at the structures.

B.2.1 Local scour at monopile foundations

Local scour under wave action

According to Sumer and Fredsøe (2002), local scour processes around piles differ whether the piles behave as large piles or slender piles. This is assessed from the calculation of the Keulegan-Carpenter (KC) number representative of the regime of wave/pile interaction:

$$KC = \frac{2\pi a}{D} = \frac{u_m T}{D}$$

where a is the amplitude of orbital wave motions at seabed, u_m is the wave orbital velocity at seabed, T is the wave period and D is the pile diameter.

Given the water depth range in the Lease Area, and the large pile diameter, it is expected that KC values will remain less than a value of 6, whereby a “large pile” situation would prevail. Under such circumstances scour the intensity of potential vortex-shedding and horseshoe vortex at the pile face is low, and local scour, if any, would rather result from steady-streaming acceleration of flowlines around the pile.

Maximal local scour due to waves only is estimated from the relation proposed by Sumer and Fredsøe (2002) and is presented in Figure B.2, dependent on KC values and the diffraction parameter D/L, where L is the wave length.

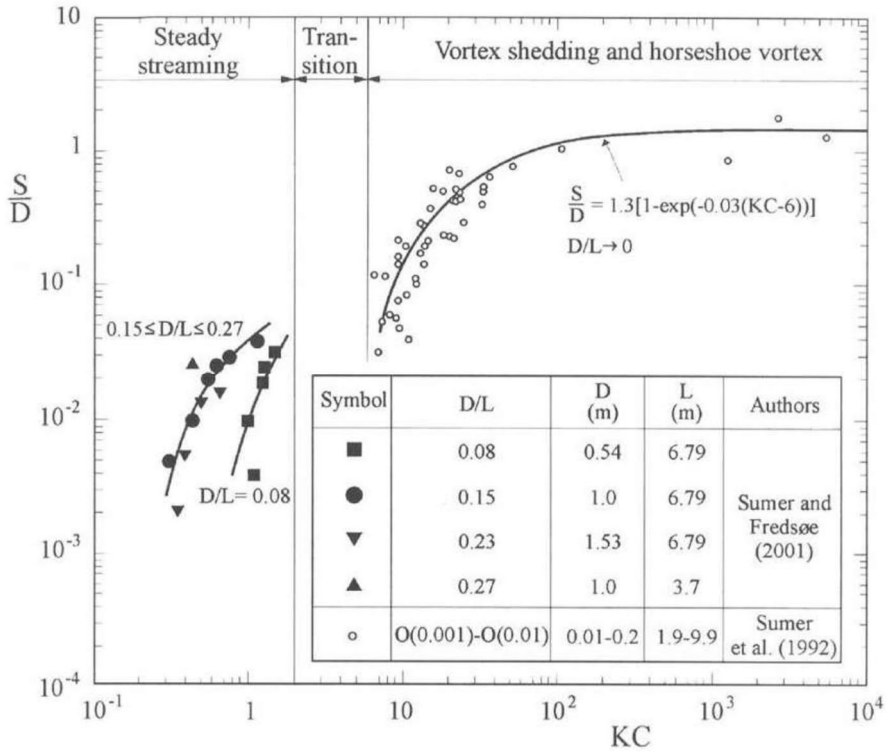

Figure B.2. Maximum scour depth at the pile periphery, live bed (Sumer and Fredsøe, 2002).

Local scour under current action

Maximal local scour depth due to currents alone is typically in the order of ~1.3 D (Soulsby and Whitehous, 1997; Sumer and Fredsøe, 2002). This is applicable to live bed conditions, which are expected in the present case within the Lease Area only for very small percentages of time associated with extreme conditions. Significantly lower values of scour depths are expected for clear water scour as a result, and will be evaluated from Whitehouse (1998), using P50 and P90 percentiles for Shields stress values:

$$S_{clear\ water} = S_{live\ bed}\left[2\sqrt{\frac{\theta}{\theta_{cr}}} - 1\right], \text{ when } 0.25 \leq \frac{\theta}{\theta_{cr}} \leq 1,$$

where θ is the Shields parameter and θ_{cr} its critical value, while $S_{clear\ water}$ and $S_{live\ bed}$ are the respective scour depths for clear water and live bed conditions.

Local scour under combined wave/current action

In case of combined waves and currents, the waves have the effect of reducing the potential scour that would be created in case of unidirectional currents only. That is a result of the waves causing additional stir and redistribution of sediment within the scour hole.

According to Sumer and Fredsøe (2002), the relative importance of wave and current action can be assessed by looking at the parameter U_{cw} as:

$$U_{cw} = \frac{U_c}{U_c + U_m}$$

where U_c is the current velocity estimated at a height of D/2 from the seabed, and U_m is the magnitude of near-bed orbital velocity due to waves. The parameter U_{cw} tends to a value of 1 in current-dominated regimes and 0 in wave-dominated regimes.

Figure B.3 shows expected reduction in normalised scour depth in combined co-directional waves and currents. Sumer and Fredsøe (2002) propose a quantitative relation to look at the effect of combined waves and current. The scour depth is related to U_{cw} and KC by the relation:

$$\frac{S}{D} = \frac{S_c}{D}\left[1 - \exp\left(-A(KC - B)\right)\right], \qquad \text{valid if} \qquad KC \geq B$$

with $A = 0.03 + 3/4\,U_{cw}^{2.6}$ and $B = 6\exp\left(-4.7U_{cw}\right)$

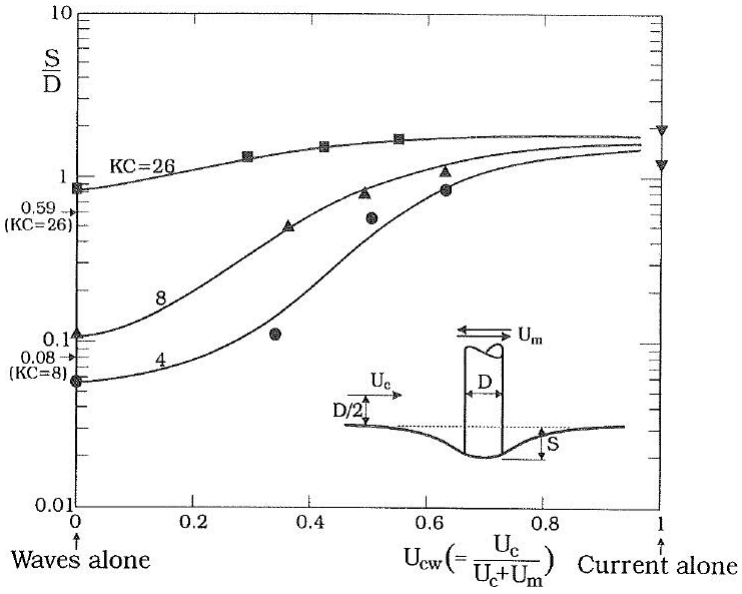

Figure B.3. Equilibrium scour depth for combined co-directional waves and currents. Live bed conditions assumed. (Sumer and Fredsøe, 2002).

The relative free scour potential at the periphery of the pile base under waves alone or under combined currents and waves is calculated from the empirical curves proposed by Sumer and Fredsøe (2002), as illustrated in Figure B.2 and Figure B.3.

Timescales for scour development

Sumer and Fredsøe (2002) also provide guidance into determination of expected time scale for equilibrium scour development around monopiles. A typical time development of scour is presented in Figure B.4 below. Scour develops as a gradual process. A representative time scale for scour, T, can be defined by calculating the slope of the line tangent to the curve S_t (t) at time t = 0.

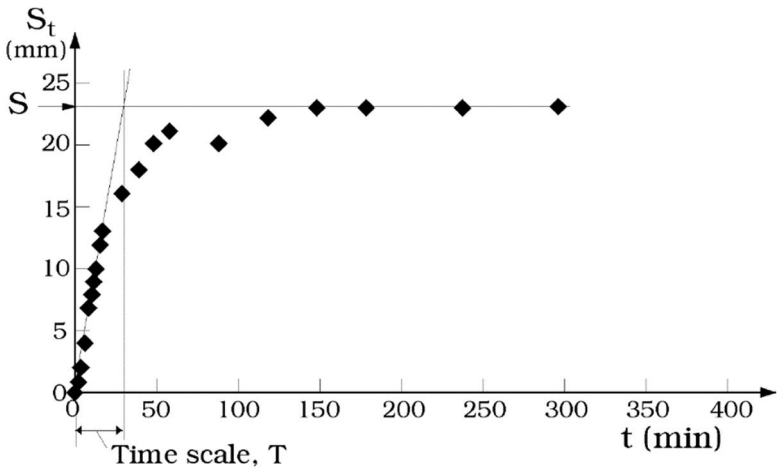

Figure B.4. Typical time development of maximum scour depth (Sumer and Fredsøe, 2002).

The time scale can be normalized as T* in the following way

$$T* = \frac{\sqrt{g(s-1)d^3}}{D^2}T$$

The normalized time scale is typically a function of wave regime (Keulegan-Carpenter number, KC, and diffraction parameter, D/L) and Shields parameter θ. In normalized terms, the time scale for scour decreases for large piles, and increases for small Shield stress values.

Estimates for scour development timescales are presented according to predictors proposed by Sumer and Fredsøe (2002).

Scour lateral extent

According to Sumer and Fredsøe (2002), the upstream slope of the scour hole around the pile is close to the angle of internal friction of the soil, while the downstream side is relatively less steep. Considering an internal angle of friction of 30°, which is an average for typical sands, laboratory experiments measured upstream and downstream slopes angles of respectively 32° and 23° (Figure B.5). The lowest value of 23°, will be used in this study to estimate the horizontal extent of the scour hole.

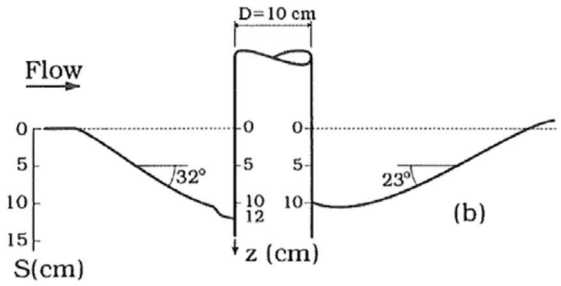

Figure B.5. Scour equilibrium profile measured in laboratory, for a soil with an internal angle of friction equal to 30°. From Sumer and Fredsøe (2002).

B.2.2 Local scour at pin-piled jacket foundation

Local scour estimates for a piled jacket foundation are calculated using the same methodology as for monopiles (see section above), the difference residing in the pile diameter.

In addition to the above, for jacket-type foundations, an assessment for the pile group effect and associated global scour, resulting from the short separation between jacket piles, is investigated in accordance with the methodology proposed by Sumer and Fredsøe (2002). The assessment depends on the non-dimensional gap G/D, where G is the separation distance between piles and on the arrangement of the piles (Figure B.6). Refer to Sumer and Fredsøe (2002) for calculation methods.

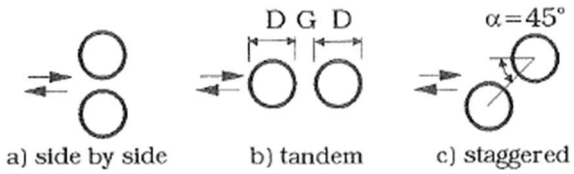

Figure B.6: Possible arrangements for two-piles groups.

Owing to the water depth range and relative gap to pile diameter ratio, pile group effect is expected to be very minor.

The assessment for pin-piled jacket foundations is made for turbine foundation jackets as well as OSP jacket.

B.2.3 Local scour at suction-bucket jacket foundation

Potential for local scour development around suction buckets is assessed, informed from the methodology adopted for monopiles, the difference residing in the suction bucket diameter and height.

Unlike the monopiles, the bucket caissons will not occupy the whole water depth but only a certain distance above the seafloor. They can be approximated as a pile of limited height, resulting in reduced scour (Figure B.7). Note that the stick-up of the suction bucket above seabed, and the configuration of the transition piece to turbine mast diameter, is currently unknown.

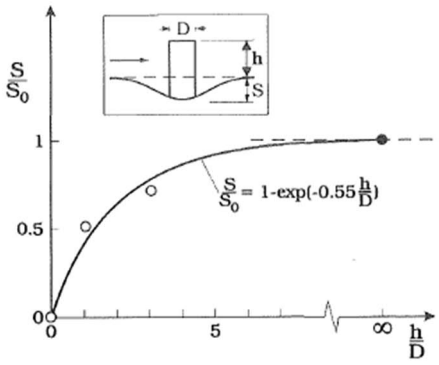

Figure B.7. Effect of pile height on scour. S_0 is the scour depth computed for a pile of infinite height. From Sumer and Fredsøe (2002).

B.2.4 Local scour at gravity-based foundation

Commentary on potential scour development around gravity-based foundations are made, informed from the maximum footprint area of the foundation. No calculations are proposed. Local scour around gravity-based structures (GBS) is expected to be significantly smaller than for monopiles, but on the other hand the design of GBS foundations themselves is much more sensitive to scour. Seabed preparation and scour protection is expected in case GBS foundations are adopted and the seabed is mobile.

Attachment C

Sediment Mobility Potential

C.1 Literature Review

C.1.1 Soil characteristics

Through high-resolution sub-bottom profiles and sonographs collected along 1,450 km and 1,220 km of ship tracks in 1978, Twichell et al. (1981) characterized the seabed sediments in the region encompassing the Lease Area.

A large part of the southern New England Continental Shelf is characterized by unusually smooth bathymetry. Within this area of smooth bathymetry, surface sediment consists primarily of fine sand to the east and silt plus clay to the west (Figure C.1). A gradual transition occurs between these extremes (Twichell et al., 1981). This fine sediment area was also described by Dalyander et al. (2013), who refers to it as a Mud Patch, defined by more than 25 percent mud (silt plus clay) and occupying an area in water depths between 55 and 65 m. The Mud Patch formed in the last 10,000 years during rising sea level, and is hypothesized to be fine-grained sediment winnowed from glacial deposits on Georges Bank, transported westward in the residual mean flow, and deposited where the tidal currents decrease sharply (Dalyander et al., 2013). Samples data from Hathaway (1972) show that medium sand plus coarser material constitutes more than 90 percent of the surface sediment on the surrounding shelf.

The Lease Area partly lies in the Mud Patch and is located ~20 km west of the Nantucket Shoals, a submerged sand and gravel shallow ridge that extends 33 km eastward and 80 km southeastward from Nantucket Island (Limeburner, 1968).

These studies suggest that a non-negligible amount of fine cohesive sediment is susceptible to be found at the Project site, especially the southwest area, which could potentially reduce sediment mobility in comparison with an entirely sandy seabed.

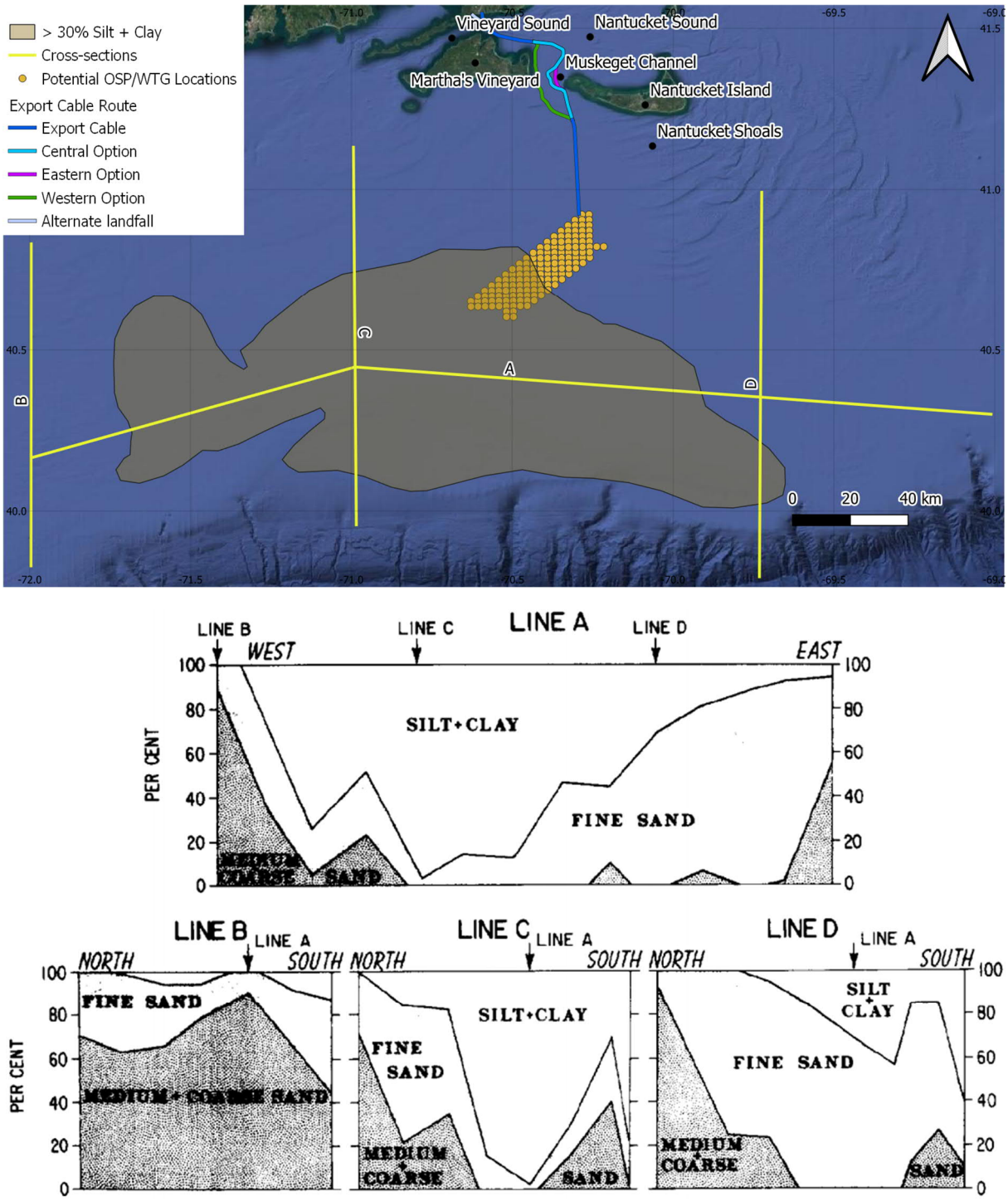

Figure C.1. Upper panel: map delimiting where the silt and clay fraction is above 30 percent, digitized from Twichell et al. (1981). The upper panel also show the sections along which contoured map of percent sediment types in surface samples are displayed on the lower panels (from Twichell et al. (1981), based on data from Hathaway, 1972).

C.1.2 Bed shear-stress and sediment mobility

Seabed disturbance occurs as a result of bottom shear stress resulting from the combined action of waves and currents on the sea floor. Dalyander et al. (2013) performed numerical modelling to characterize the wave- and current- induced bottom shear stress in the U.S. middle Atlantic continental shelf. The highest yearly median shear stresses were found over Nantucket Shoals east of the Lease Area, while the lowest stresses occurred in deeper regions including the outer continental shelf. Comparison of the stress distribution with surface sediment texture data showed that coarser sediments were typically found in regions of greater stress forcing. The critical stress threshold for mobility over locations of the Nantucket Shoals was exceeded greater than 75 percent of the year, while deeper areas and lower stress regions, such as over the fine-grained Mud Patch, were more quiescent, with <5 percent mobility throughout the year.

Over the Nantucket Shoals, tidal currents alone could induce bed mobility, but storm-induced bottom wave stress and non-tidal current-induced stress are also significant (Dalyander et al., 2013). Over the Mud Patch, the critical stress for resuspension was only exceeded by strong storm events occurring primarily in the winter, resulting in long gaps between resuspension events in the less energetic summer months and a virtually quiescent bed throughout most of the year.

These observations seem to suggest a low risk of sediment mobility for the southwestern area of the Project site (Mud Patch), but do not provide conclusions for the northeast area, in shallower waters and closer proximity with the Nantucket Shoals.

C.2 Bathymetric Review

Fugro performed a detailed observation of the bathymetry along corridors surveyed across the Project Area (Figure C.2), resulting in the identification of five different types of bathymetric features. Some specific examples were chosen to illustrate these features, with locations visible on Figure C.2.

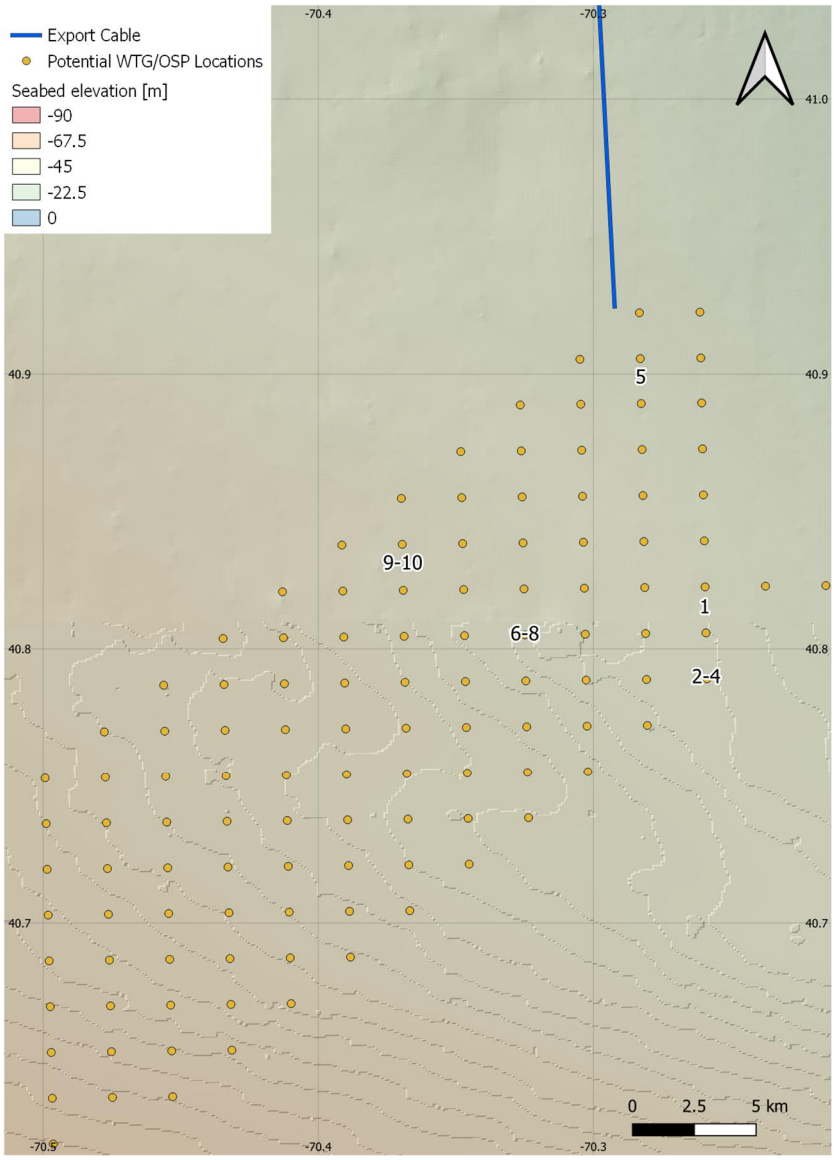

Figure C.2. Surveyed corridors (grey lines), and location of the observed features displayed in Figure C.3. These locations correspond to the displayed examples only. Features of the same types were observed at other locations.

For these examples, Figure C.3 shows an illustration of these features, while associated cross-section profiles are visible on Figure C.4 and Figure C.5. The following types of features were observed:

- Local sub-circular shallow depressions with central seabed feature (cross-section 1). These features are relatively limited in number and dimensions, with heights of ~0.2 m and horizontal extent below 10 m. They may correspond to boulders around which a

moderate scour hole would have formed under the action of currents and waves. However, there is no evidence to support that fact, and the bathymetric perturbation may also be caused by other phenomena (e.g., a fallen object that would have blown out the sediment in the vicinity of the effect). Less than 10 features of this type were observed along the surveyed corridors. No specific area of the Project site was found to be particularly affected.

- Patches of local shallow depressions were observed, of heights below 0.2 m (cross-sections 2-3-4). They affect a relatively large area in the eastern part of the Project Area, with a gradual transition from a smooth bed to a greater density of these depressions as seen in Figure C.3. The depressions may be circular or adopt a more irregular shape. It is possible that these depressions are associated with shallow gas expulsions or ancient scour marks.
- Irregular bed elevations of average heights ~0.1 m were observed at some areas (cross-section 5). Dominantly located at the northern and eastern areas of the site, these features may be sourced from the Nantucket shoals. There is no indication that the features are mobile.
- Larger-scale ridges of heights up to 0.6 m were observed. These features are distributed over the Project Area (cross-sections 6-7-8). They may be linked with paleobathymetric features such as remains of splays or terraces and are not anticipated to be widely mobile.
- Several anchor or fishing gear scars were observed over the Project Area, of height ~0.1 m (cross-sections 9-10).

The eastern portion of the Lease Area is more affected by the bathymetric features described above while the western, deeper part of the Project site is mostly smooth.

The observation of the bathymetry along the surveyed corridors did not reveal evidence of significant seabed mobility across the Project Area. No significant ripple or sand wave was observed. A few features may suggest the existence of moderate scour marks around boulders or objects. However, their number and severity are limited.

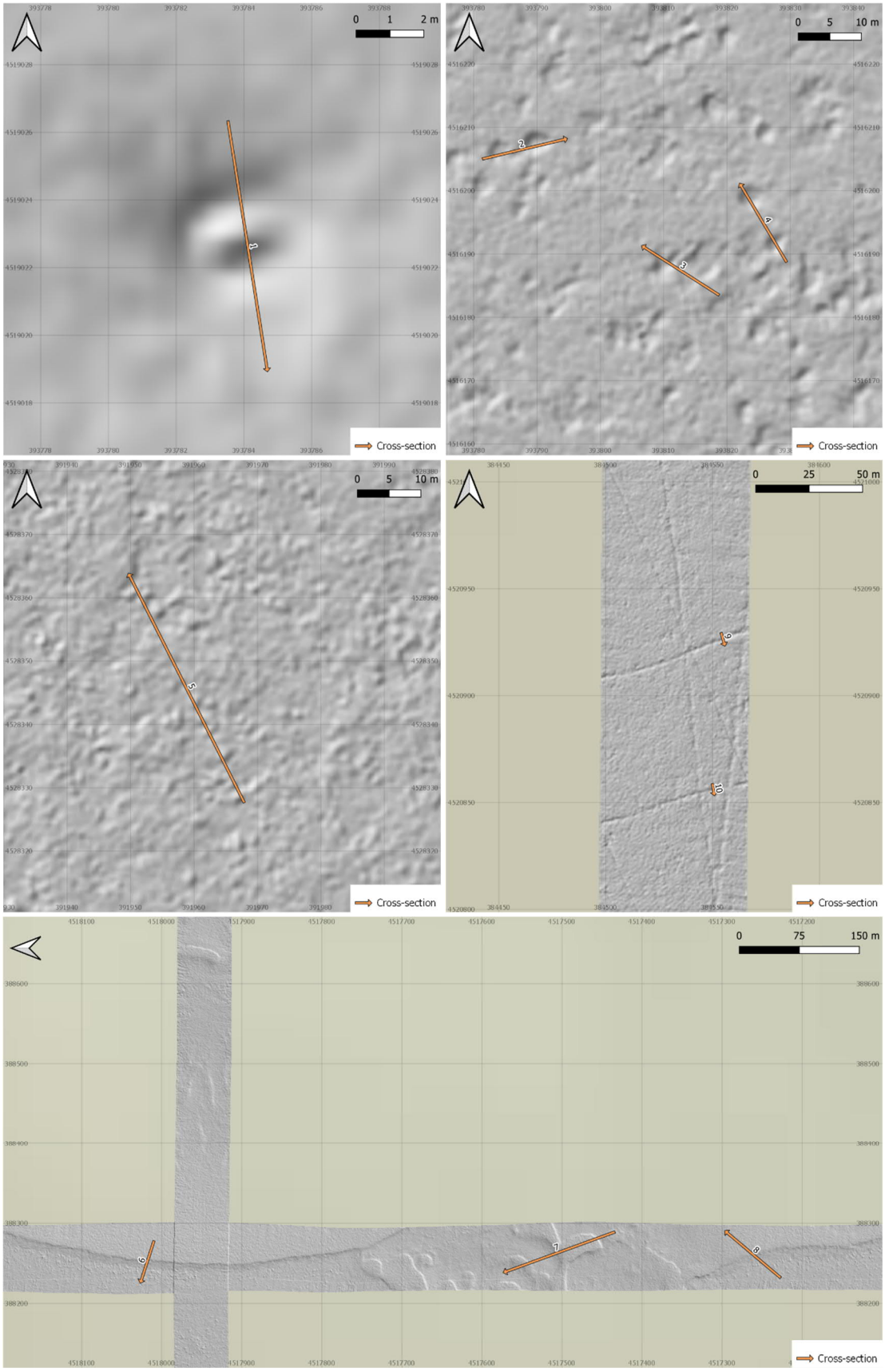

Figure C.3. Examples of observed features with location of the bathymetric cross-sections.

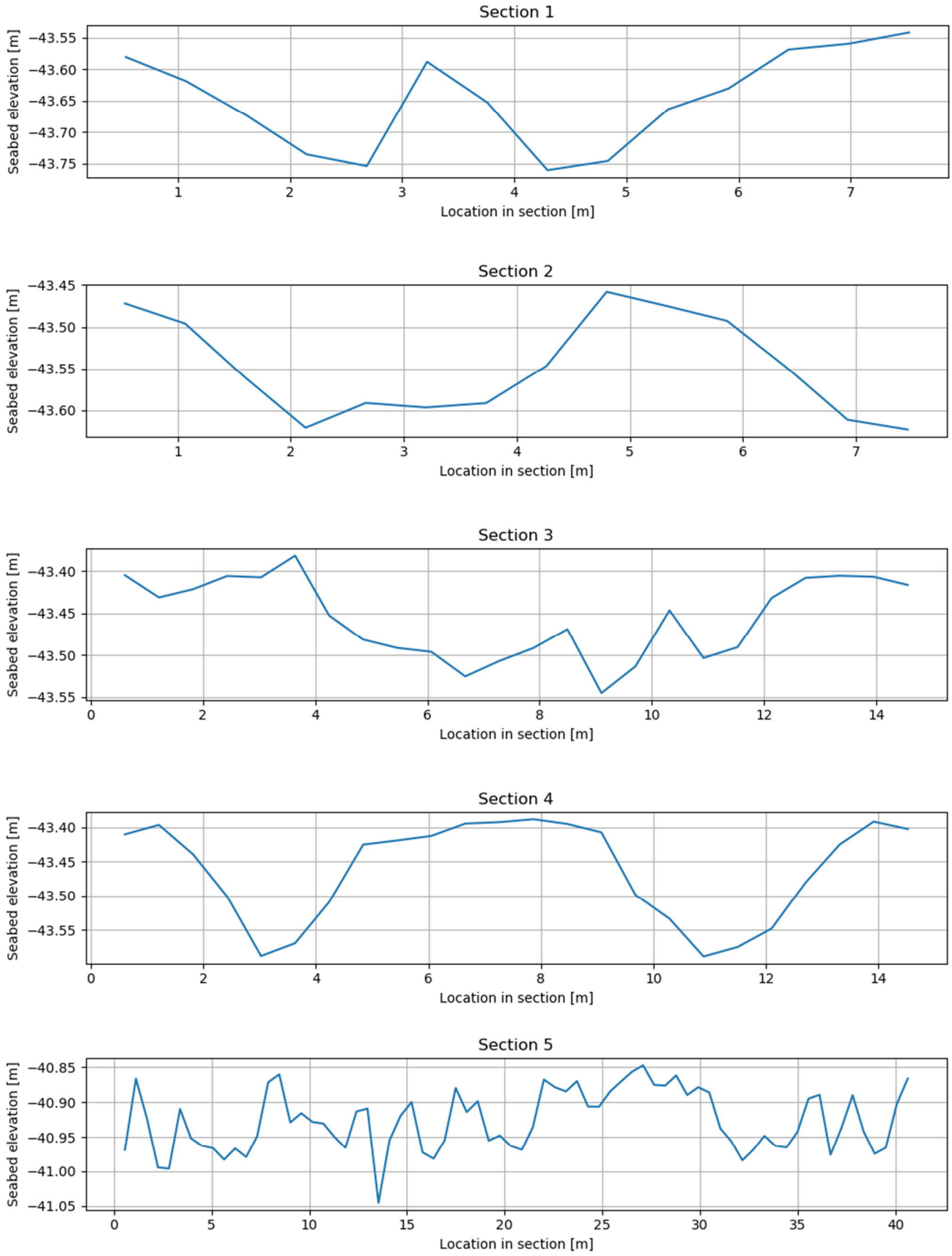

Figure C.4. Seabed elevation profiles across sections 1 to 5 of Figure C.3.

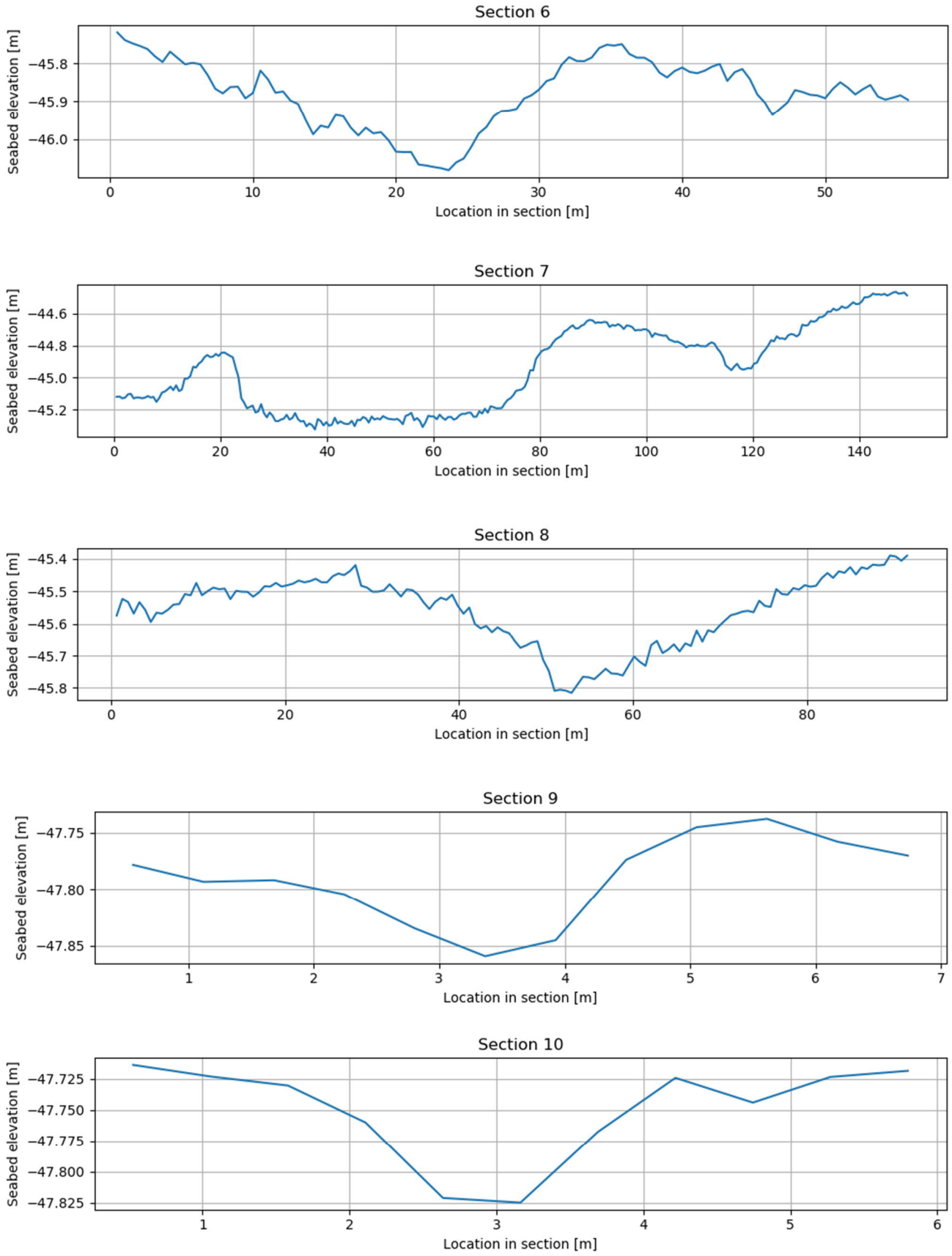

Figure C.5. Seabed elevation profiles across sections 6 to 10 of Figure C.3.

C.3 Assessment of Seabed Mobility Potential

C.3.1 Sediment mobility potential analysis

Figure C.6 illustrates the distribution of the soil particles size at different locations, based on the samples data corresponding to two survey periods: May and August 2020. Sediment in the Lease Area consists of a majority of fine sand, very fine sand, and silt. The southwestern part contains larger amounts of silt, and non-negligible amounts of clay are observed. This increase of finer material is related to the presence of the Mud Patch described in Section C.1.

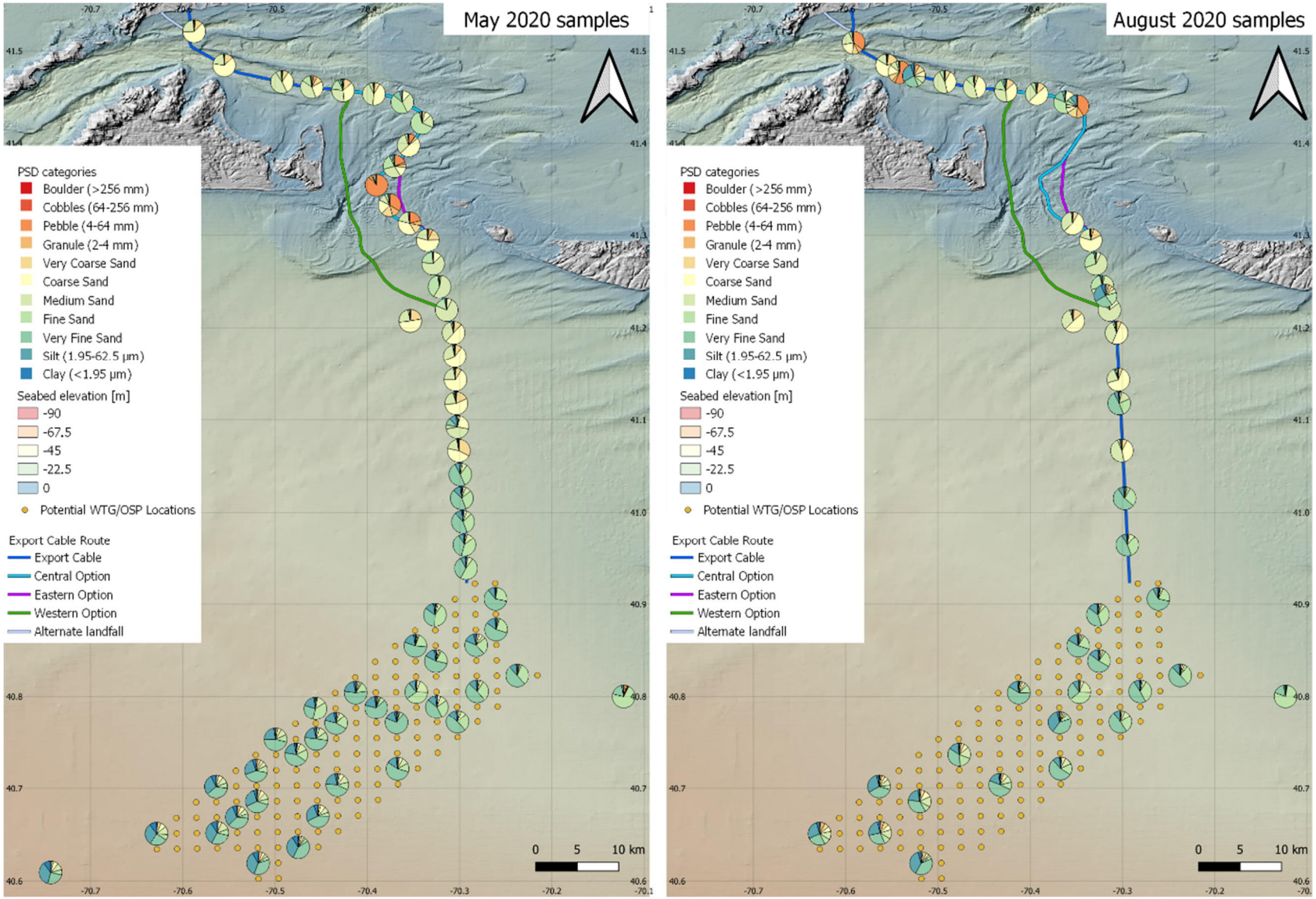

Figure C.6. Pie charts of the particles size distribution at the grab locations for the May 2020 survey (left) and the August 2020 survey (right).

The current seabed mobility assessment is based on bed shear stresses obtained from the metocean numerical modelling covering a period from July 1, 2018 to June 26, 2020. Figure C.7 shows a mapping of maximum bed shear stress induced by currents and waves during the simulation period, while Figure C.8 shows the time-averaged bed shear stress. While the bed shear stress is relatively limited in the Lease Area, it quickly increases in shallower areas, with maximum values approaching 2.5 Pa at the Muskeget Channel separating Martha's Vineyard and Nantucket Island, as well as along Vineyard Sound north of Martha's Vineyard.

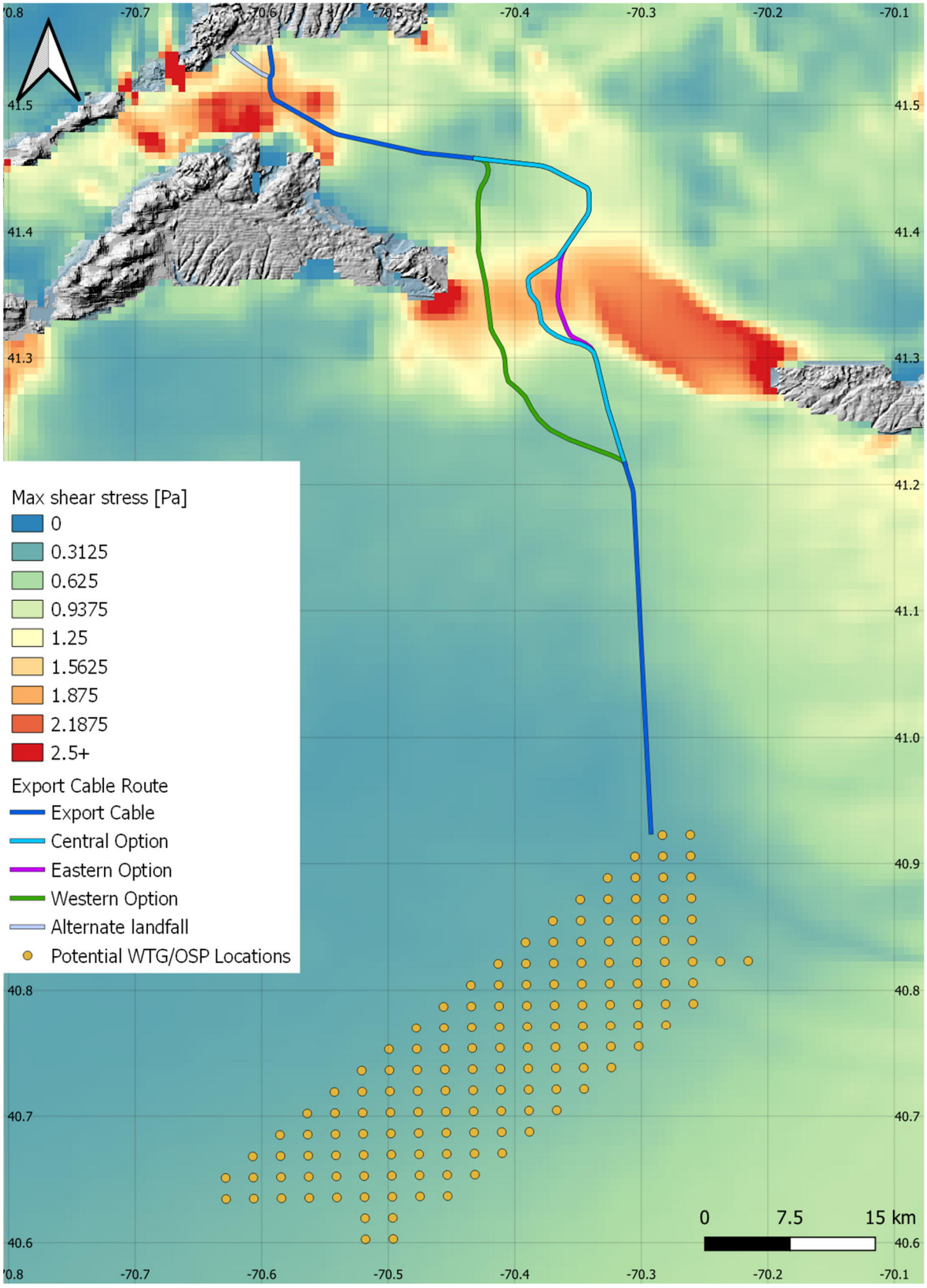

Figure C.7. Mapping of maximum bed shear stress.

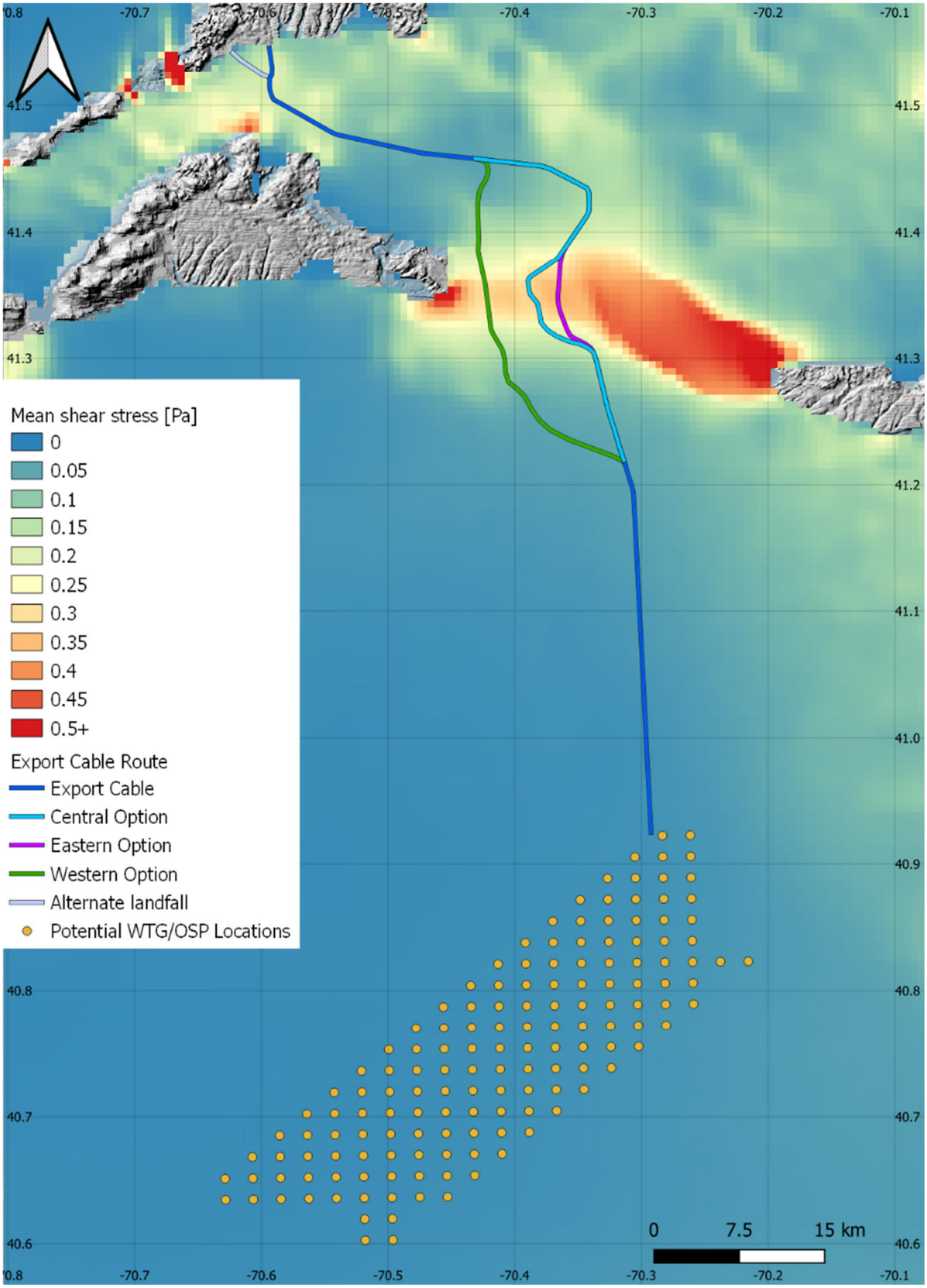

Figure C.8. Mapping of time-averaged bed shear stress.

While the bed shear stress is an indicator of the effect of currents and waves on the seabed, its dimensionless form, also known as the Shields parameter, is more appropriate to characterize the susceptibility to sediment mobility. It incorporates the interdependence of sediment mobility to sediment particle size and density. It is defined by

$$\theta = \frac{\tau}{(\rho_s - \rho) g d_{50}},$$

where τ is the bed shear stress while $\rho_s = 2650\ kg/m^3$ and $\rho = 1025\ kg/m^3$ are the respective sediment particles and seawater densities. The adopted sediment particle density ρ_s is aligned with site-specific data available for shallow soil units. The gravitational acceleration is $g = 9.81\ m/s^2$.

The median diameter d_{50} was derived from the particle size distributions of samples obtained during the May 2020 and August 2020 surveys. For the August 2020 survey, the d_{50} values were extracted from the pdf reports by Alpha analytical (2020a, 2020b, 2020c, 2020d). For the May 2020 survey, no such report was available. The d_{50} values were estimated from the provided particles distribution illustrated in Figure C.6, left panel. Figure C.9 shows the median diameters for both surveys. The two datasets are in relatively good agreement.

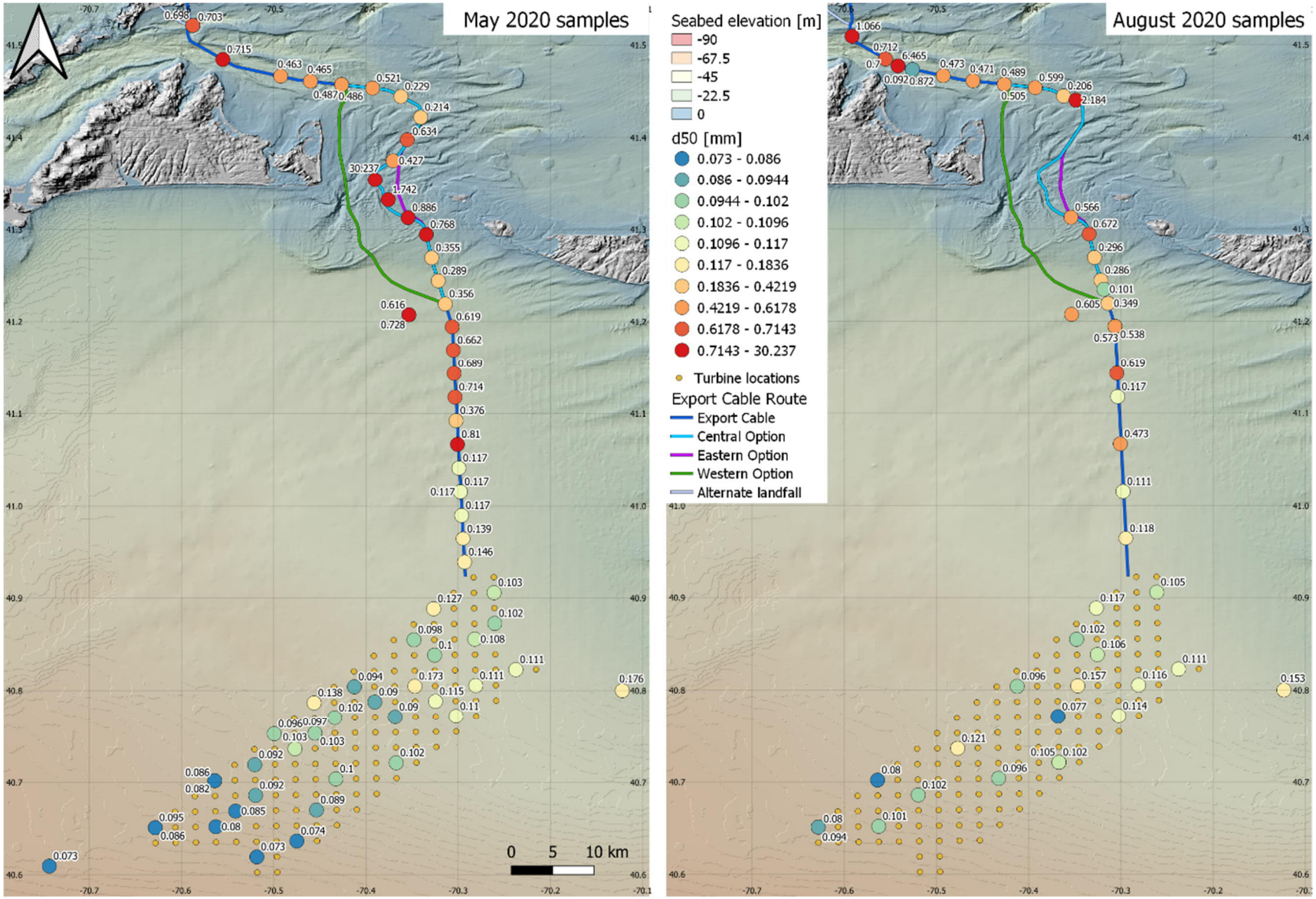

Figure C.9. Estimated d50 [mm] at grab locations.

The resulting maximum Shields parameters encountered during the simulation are displayed in Figure C.10, while Figure C.11 shows the average value for the simulation period. They are computed at the grab sample locations where particle size data are available. The maximum values are attained at the southern area of the Project site, as well as the northern part of the Muskeget Channel. However, time-averaged values have their highest values on the eastern part of the Lease Area, as well as in the Muskeget Channel and Vineyard Sound.

In addition to maximum and minimum values, percentiles are important to determine the maximum values of Shields parameters susceptible to be encountered during normal conditions and extreme conditions. Results are shown on Figure C.12 and Figure C.13 respectively for 50^{th} percentile (exceeded 50 percent of the time) and 90^{th} percentile (exceeded 10 percent of the time), again at the same grab sample locations where particle size data are available. Values of 50^{th} percentile show a spatial distribution similar to the mean values, with Shields parameters ranging from 0.001 to 0.036. Values of 90^{th} percentile range from 0.002 to 0.132.

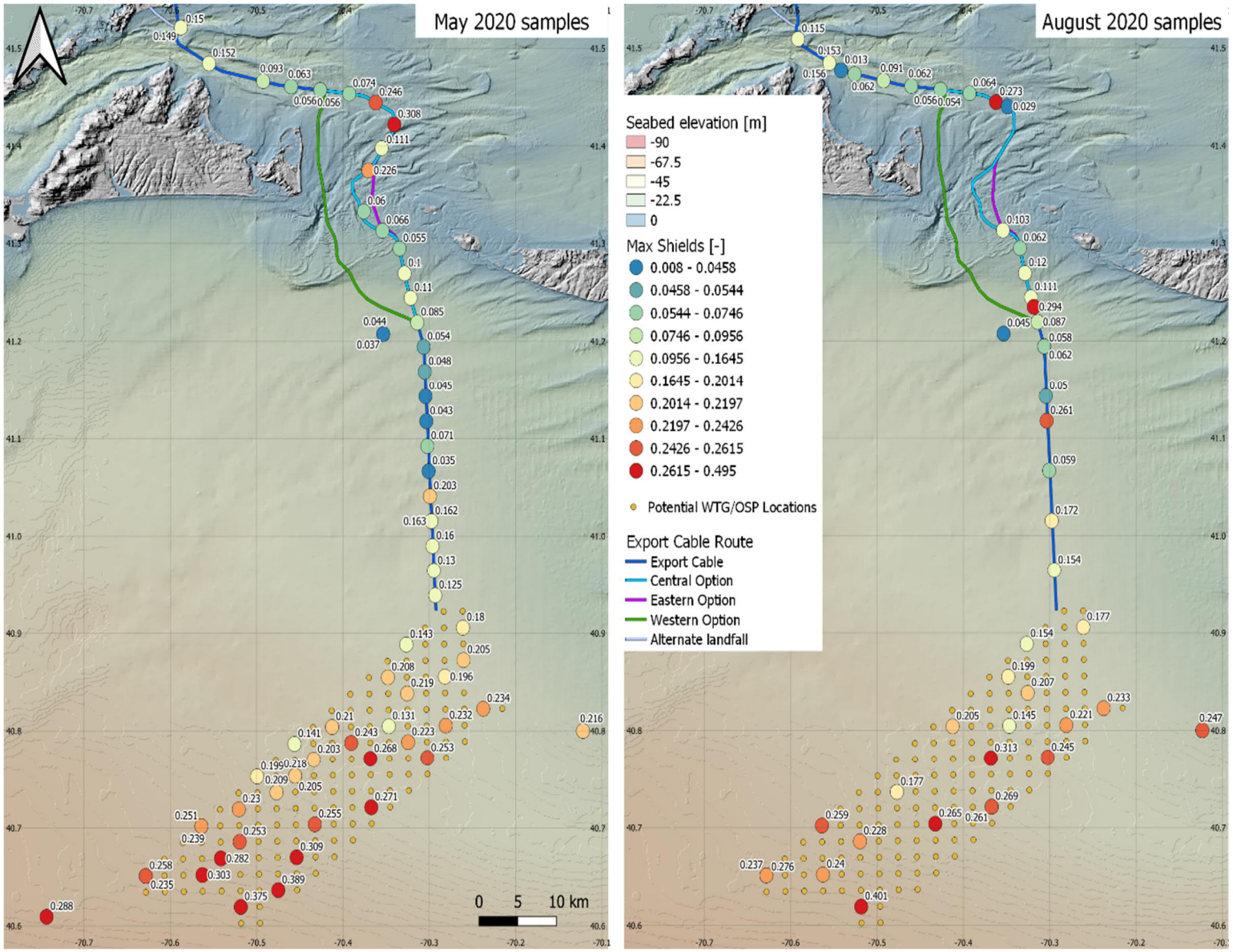

Figure C.10. Maximum Shields parameter computed at the grab sample locations for the May 2020 survey (left) and the August 2020 survey (right).

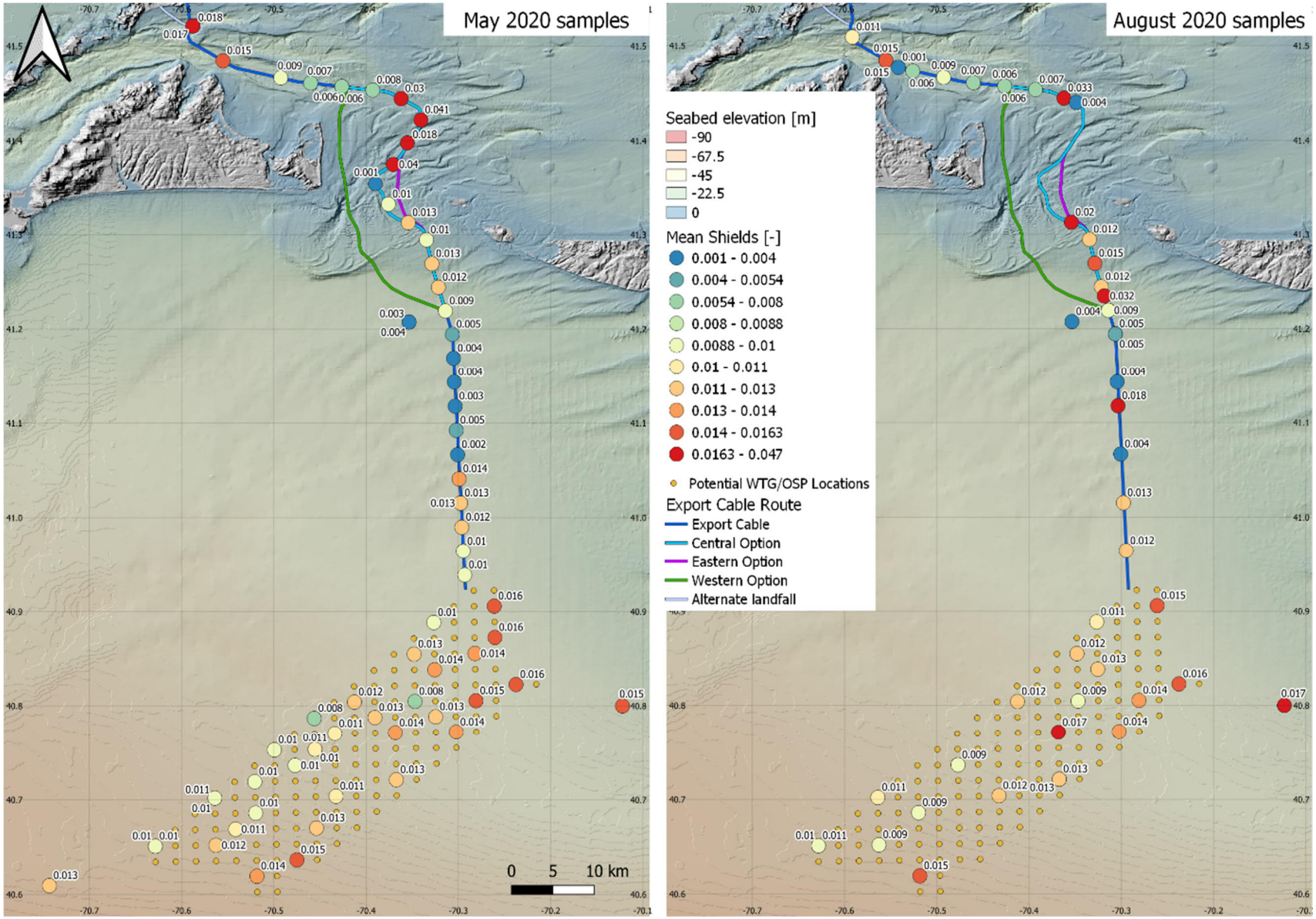

Figure C.11. Time-averaged Shields parameter computed at the grab sample locations for the May 2020 survey (left) and the August 2020 survey (right).

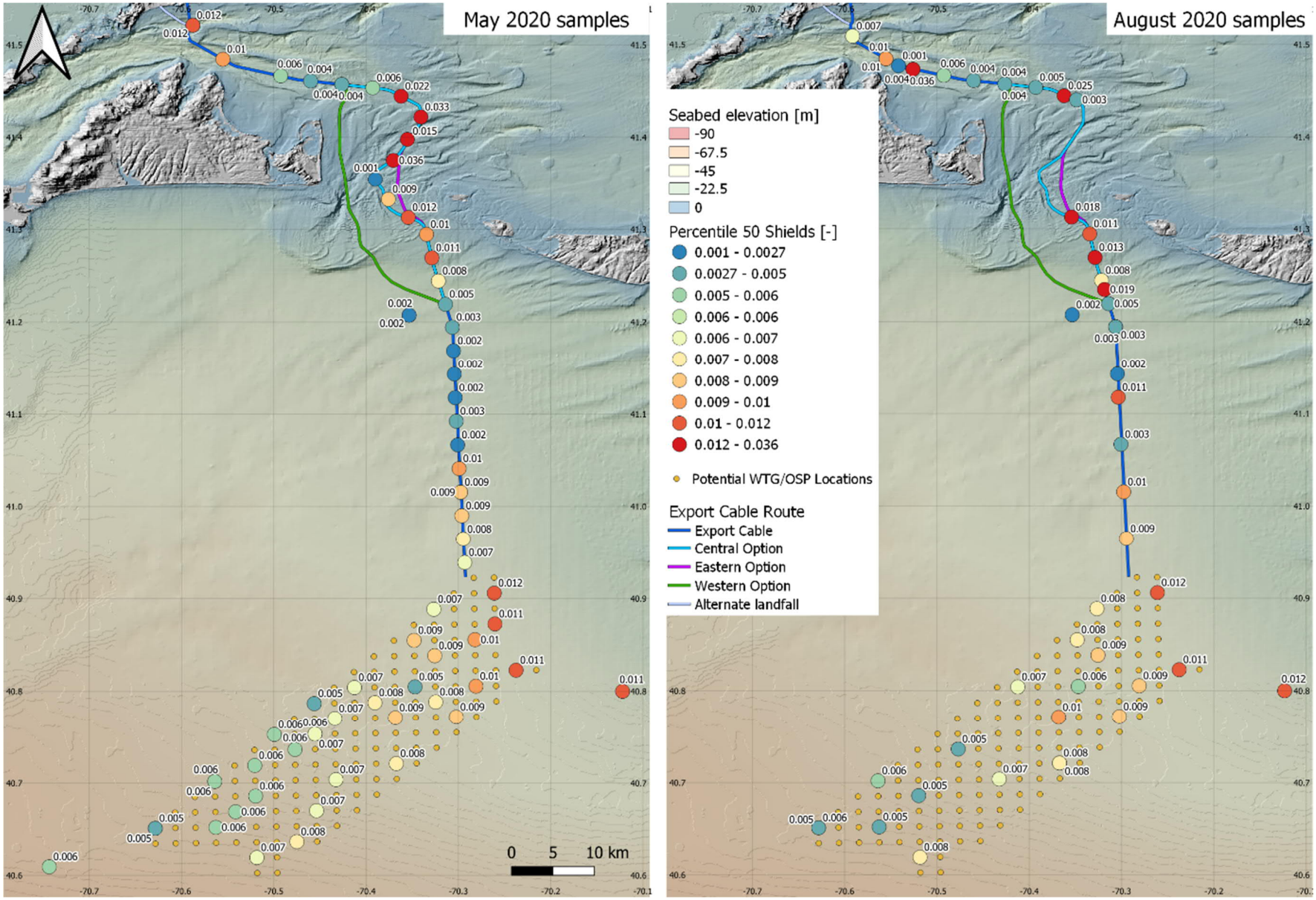

Figure C.12. Shields parameter percentile 50 computed at the grab sample locations for the May 2020 survey (left) and the August 2020 survey (right).

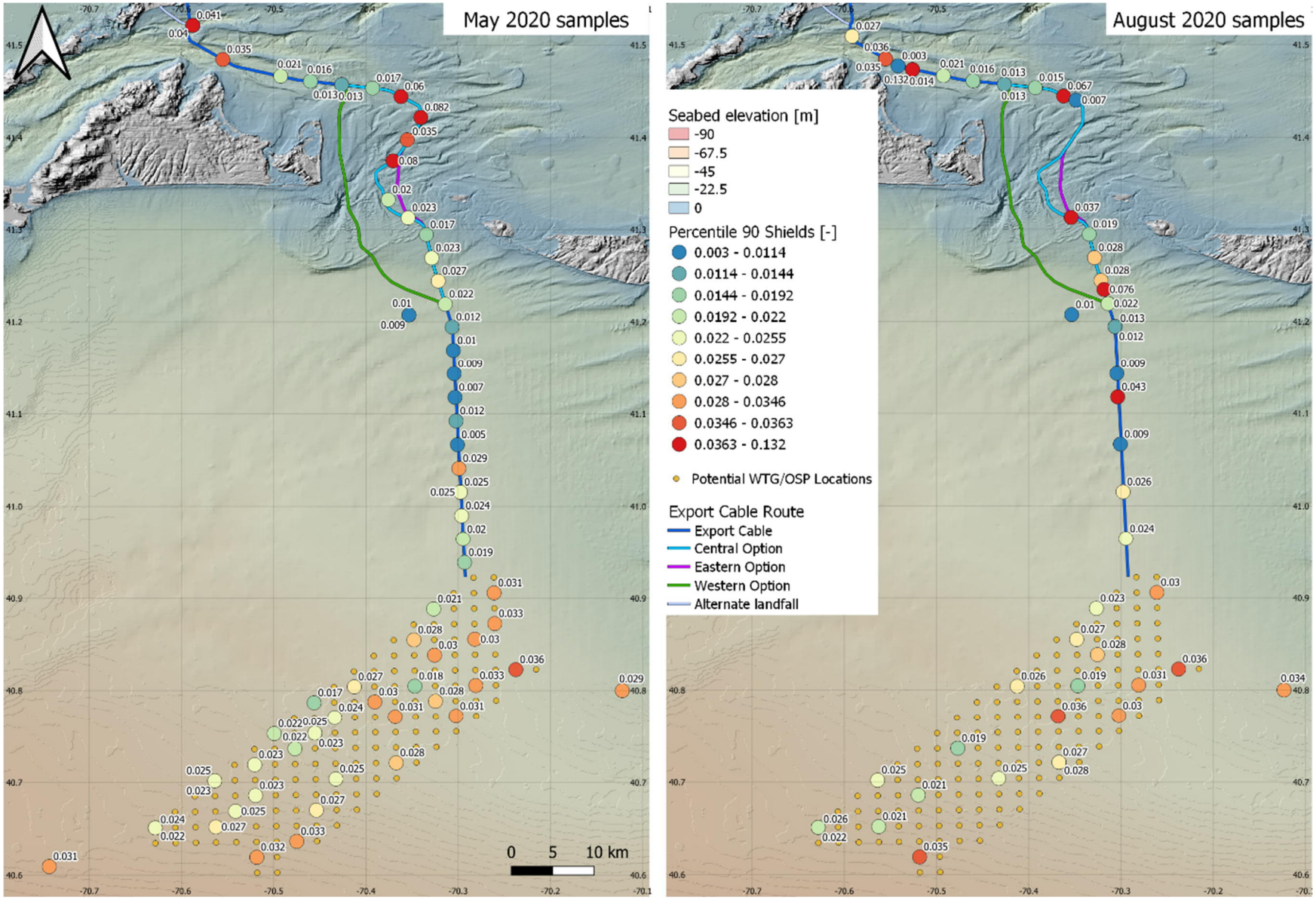

Figure C.13. Shields parameter percentile 90 computed at the grab sample locations for the May 2020 survey (left) and the August 2020 survey (right).

Shields parameter values need to be compared with a critical Shields threshold above which particle movement is initiated and sediment transport may occur. The critical Shields parameter itself is dependent on the actual particle grain size and density. While it is the lowest (in the range of ~0.03) for medium to coarse sand, it increases gradually to ~0.055 for gravel-size particles, as prevailing in some of the shallower areas with stronger tidal currents. It also increases significantly for fine to very fine sand and silt, as encountered across the Lease Area, as a result of the reduced bed roughness and the flow boundary condition becoming quasi-laminar at seabed. Extending from the classic work of Shields, Soulsby and Whitehouse (1997) have proposed a relation to estimate the critical Shields parameter corresponding to the initiation of sediment motion due to a combination of waves and currents in coastal and marine environments. Their proposed relation captures the variability for coarser and finer grain sizes expected along the Mayflower Wind Lease Area and export cable routes. The resulting critical Shields parameters are illustrated in Figure C.14. They are to be compared with the actual Shields values due to prevailing currents and waves obtained from the metocean simulation, with maximum, average, PC50 and PC90 values presented in Figure C.10 to Figure C.13.

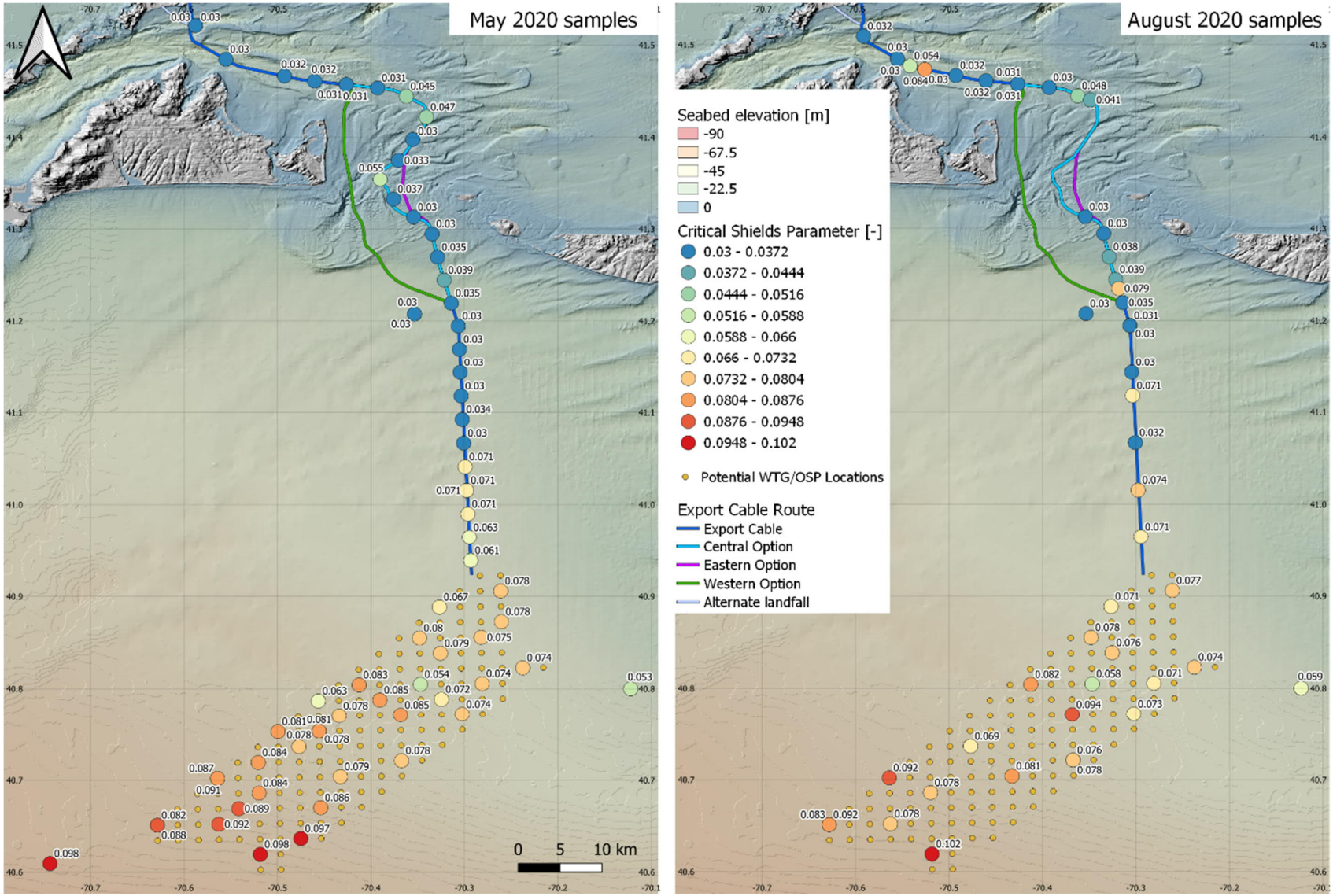

Figure C.14. Critical Shields parameter computed using the formula from Soulsby and Whitehouse (1997) based on the d_{50} values from the May 2020 survey (left) and the August 2020 survey (right).

Figure C.15 shows the associated percentages of time during which these critical Shields values are exceeded at each location during the metocean simulation period.

According to these criteria, background sediment mobility occurs within the Lease Area during less than 2 percent of the time, further reducing to less than 1 percent toward the western region of the Lease Area in deeper water. These percentages of exceedance remain less than ~2 percent for the deeper sections of the export cable routes (KP ~50.0 – 88.0), and only become greater along the northern part of the export cable routes, with percentages of exceedance locally up to 53.7 percent in the Muskeget channel and 18.2 percent in the Vineyard Sound.

Live bed conditions are met when the Shields parameter is greater than the critical Shields value, otherwise clear water conditions are said to prevail. On that basis it can be concluded that clear water conditions are met across the Lease Area for an overwhelmingly large percentage of the time.

The ratio between the Shields parameter and critical Shields is interesting to assess whether live-bed conditions or clear-water conditions would prevail at the Project site. This dictates the type of scour processes in direct vicinity of infrastructure such as foundations, which would result from an amplification of bed shear stresses due to current-structure interactions. Figure C.16 and Figure C.17 respectively show the ratio of 50^{th} percentile (PC50) and 90^{th} percentile (PC90) Shields parameter over the critical Shields computed using the method of Soulsby and Whitehouse (1997).

In the Lease Area, the ratio for PC50 Shields below 0.25, a threshold under which no sediment mobility and, therefore, no scour is expected even in the vicinity of infrastructure. The ratio for PC90 Shields is slightly in excess of 0.25, with a maximum of 0.49 in the Lease Area.

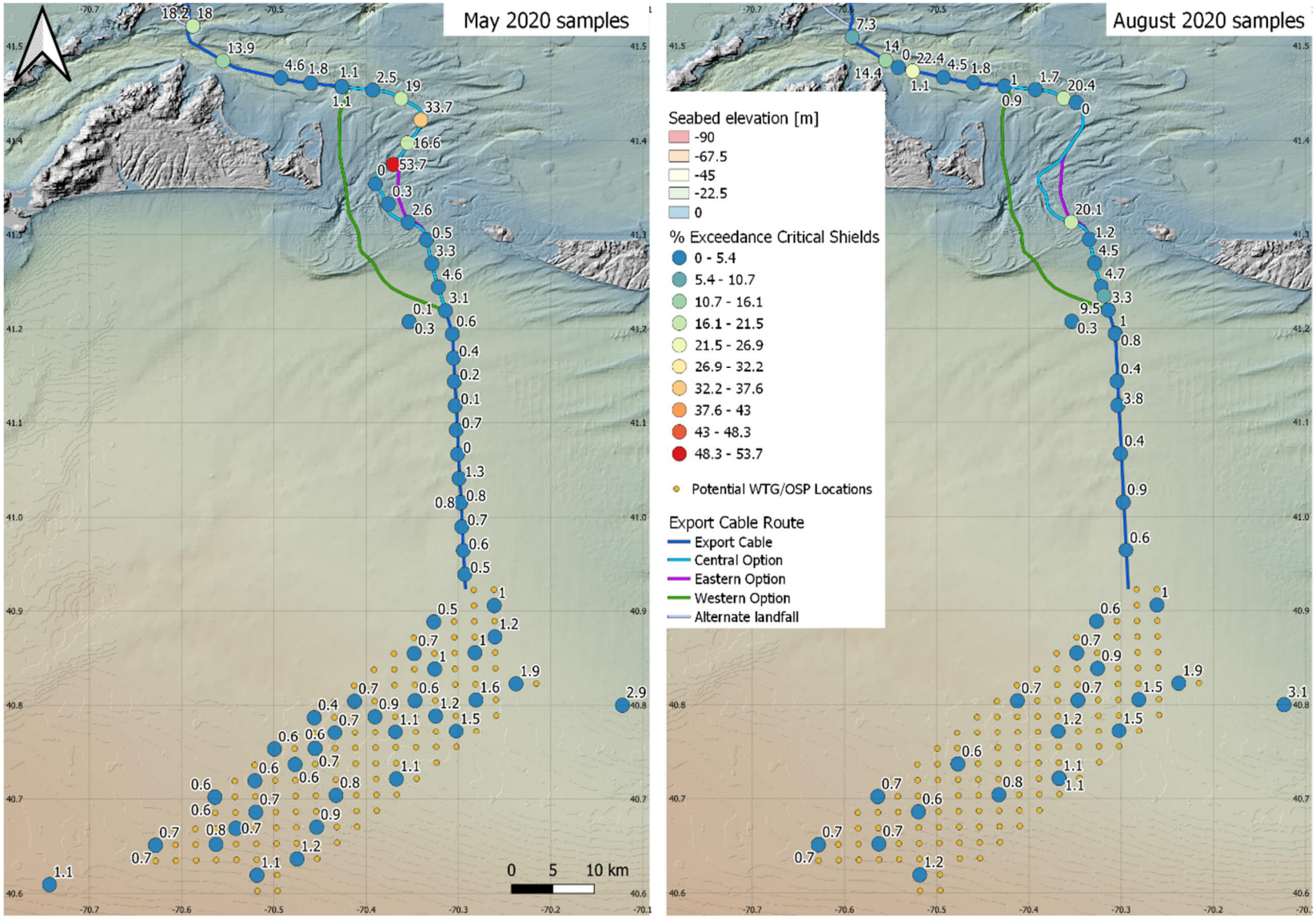

Figure C.15. Percentage of exceedance of the critical Shields parameter computed using the formula of Soulsby and Whitehouse (1997) and illustrated in Figure C.14 at the grab sample locations for the May 2020 survey (left) and the August 2020 survey (right).

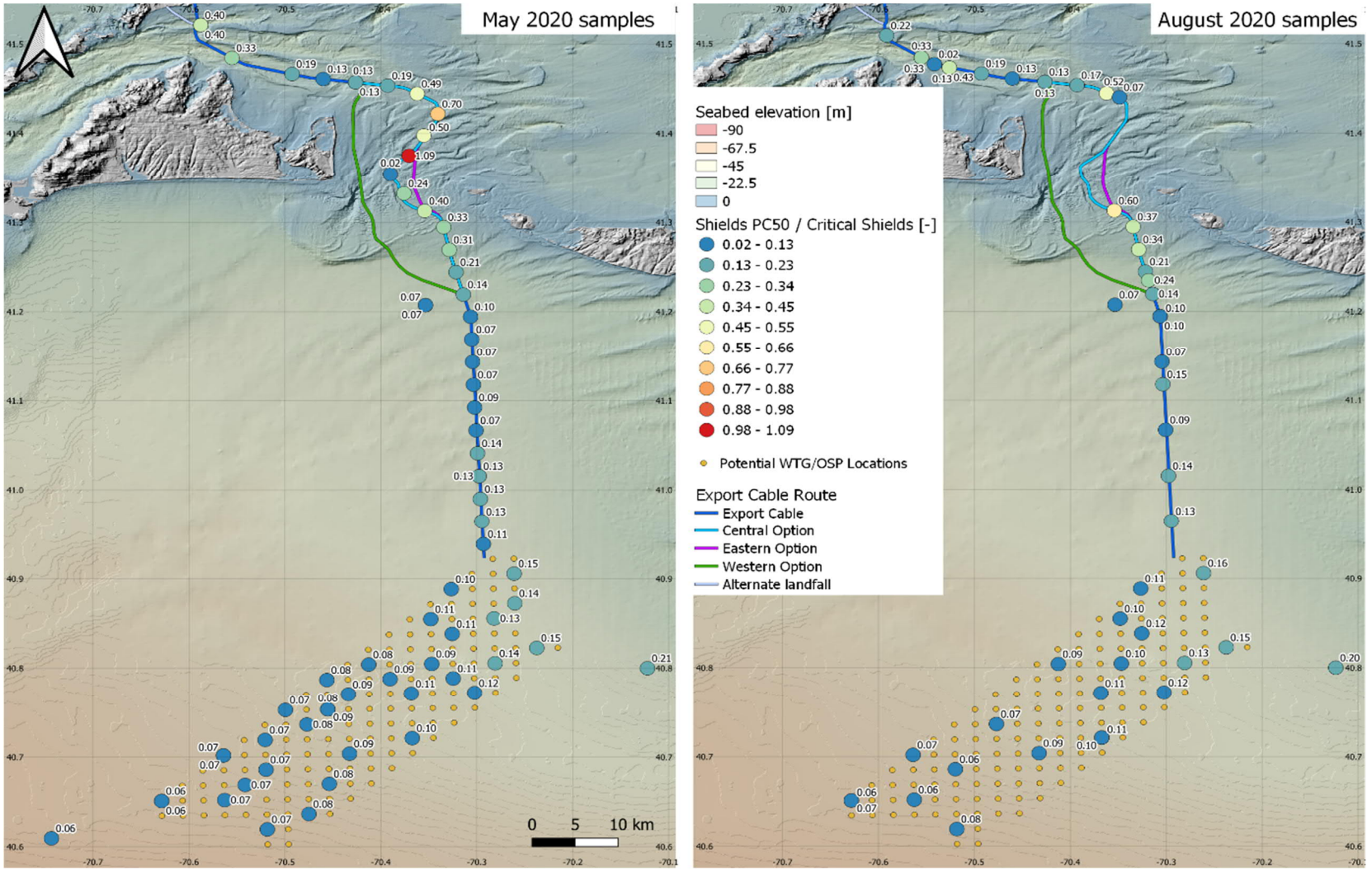

Figure C.16. Ratio of the percentile 50 Shields parameter over the critical Shields parameter computed using the formula of Soulsby and Whitehouse (1997) and illustrated in Figure C.14 at the grab sample locations for the May 2020 survey (left) and the August 2020 survey (right).

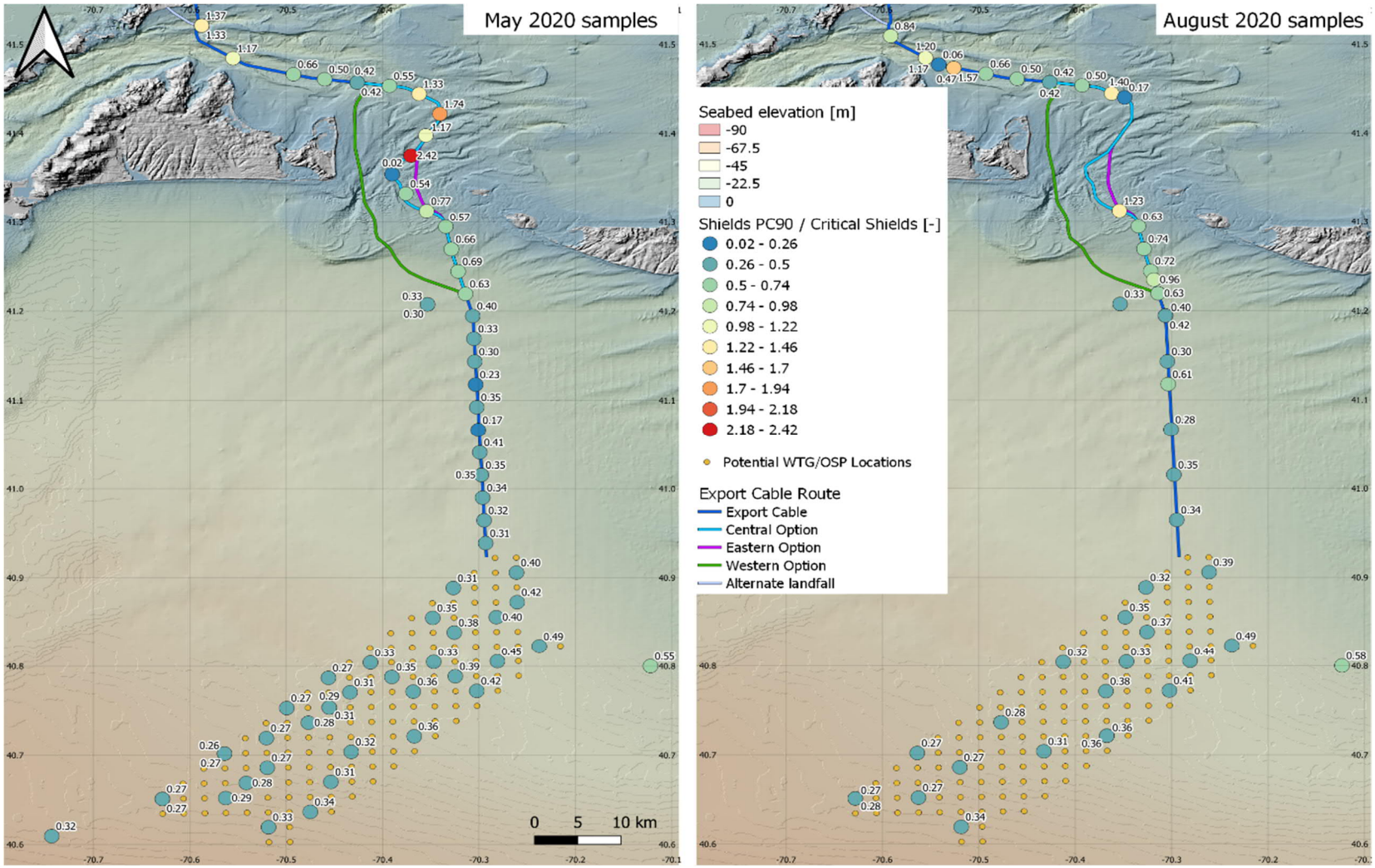

Figure C.17. Ratio of the percentile 90 Shields parameter over the critical Shields parameter computed using the formula of Soulsby and Whitehouse (1997) and illustrated in Figure C.14 at the grab sample locations for the May 2020 survey (left) and the August 2020 survey (right).

C.3.2 Discussion

The sediment mobility potential analysis revealed a very limited potential for background sediment transport in the Lease Area and southern part of the export cable routes (KP ~50.0 – 88.0), and by contrast a very dynamic background sediment mobility for some of the shallower areas along the export cable corridors, especially in vicinity of the Muskeget Channel and the Vineyard Sound. This is consistent with literature reports as discussed in the previous section.

The conditions across the Lease Area are such that the threshold for sediment movement initiation would be exceeded for no more than 1 to 2 percent of the time. Clear water conditions prevail overwhelmingly over live bed conditions. However, localized sediment transport may result due to shear stress amplification in vicinity of infrastructure, associated with short-lived episodes of more intense metocean conditions. For that reason, a degree of local scour development around the WTG and OSP foundations cannot be excluded. The extent to which, and timescale over which, local scour may develop is elaborated in the next section.

The northern, shallower part of the export cable routes is significantly more exposed, with high bed shear stresses and percentages of exceedance of the critical Shields parameter. This is a sign of active seabed mobility, with potential implications on the cables, such as risk of exposure resulting from the migration of bedforms. This risk is discussed in Section 6 on the scour potential effects along the export cable routes.

Attachment D

Profiles Along Export Cable Routes

D.1 Offshore Export Cable Route - Central Option

This section shows seabed elevation profiles along the Central Option export cable route, including an envelope of lower/higher expected values of local bedforms elevation. Bedform heights are estimated based on this envelope. A morphological zonation is then defined on the route based using the bedforms height. Figure D.1 shows the seabed elevation profile, bedforms height, and zonation along the whole route, while the following figures focus on 5-km long sections for improved readability.

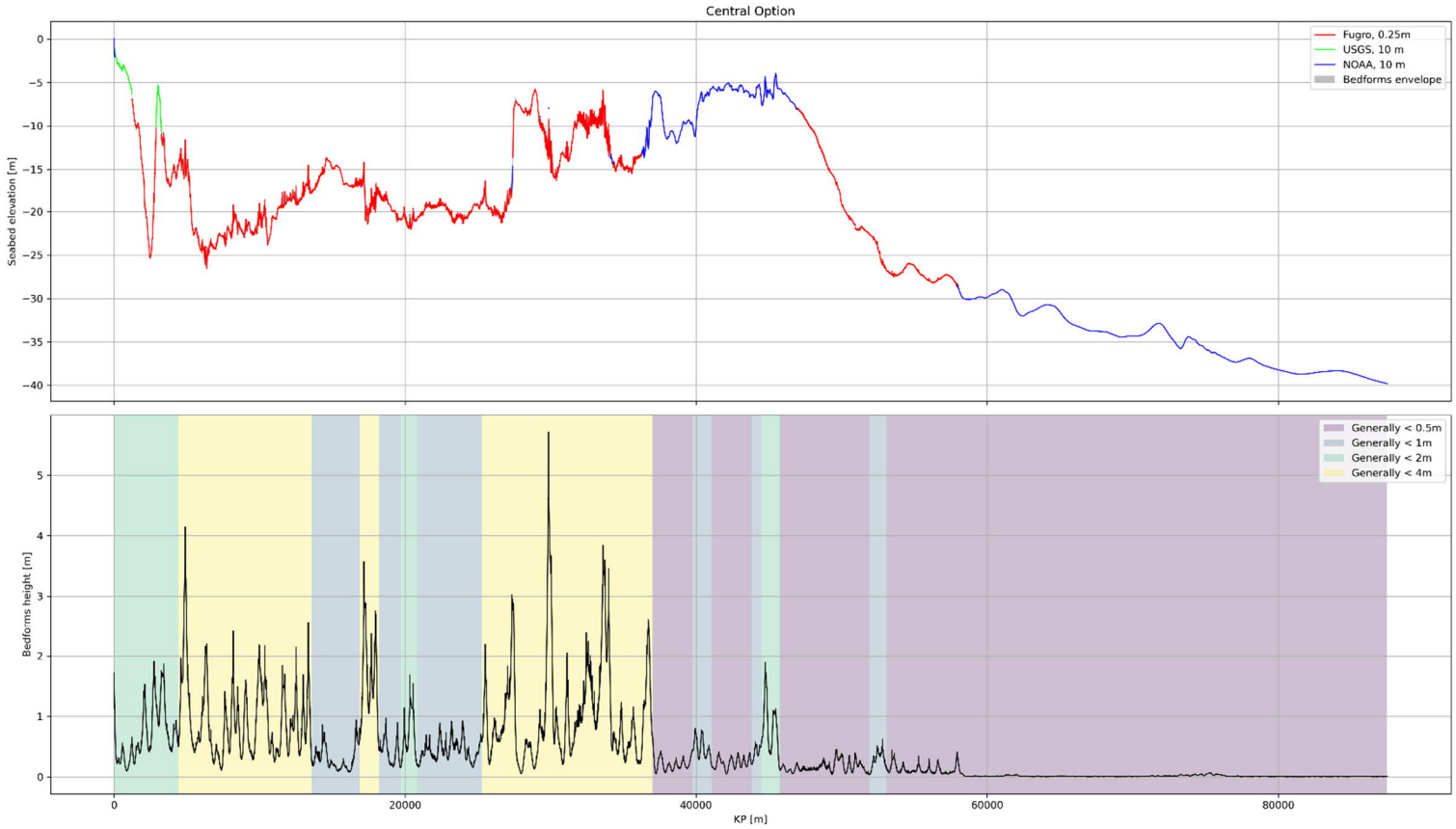

Figure D.1. Seabed elevation profile using the locally most accurate bathymetry (up). Computed bedforms heights and morphological zonation (down).

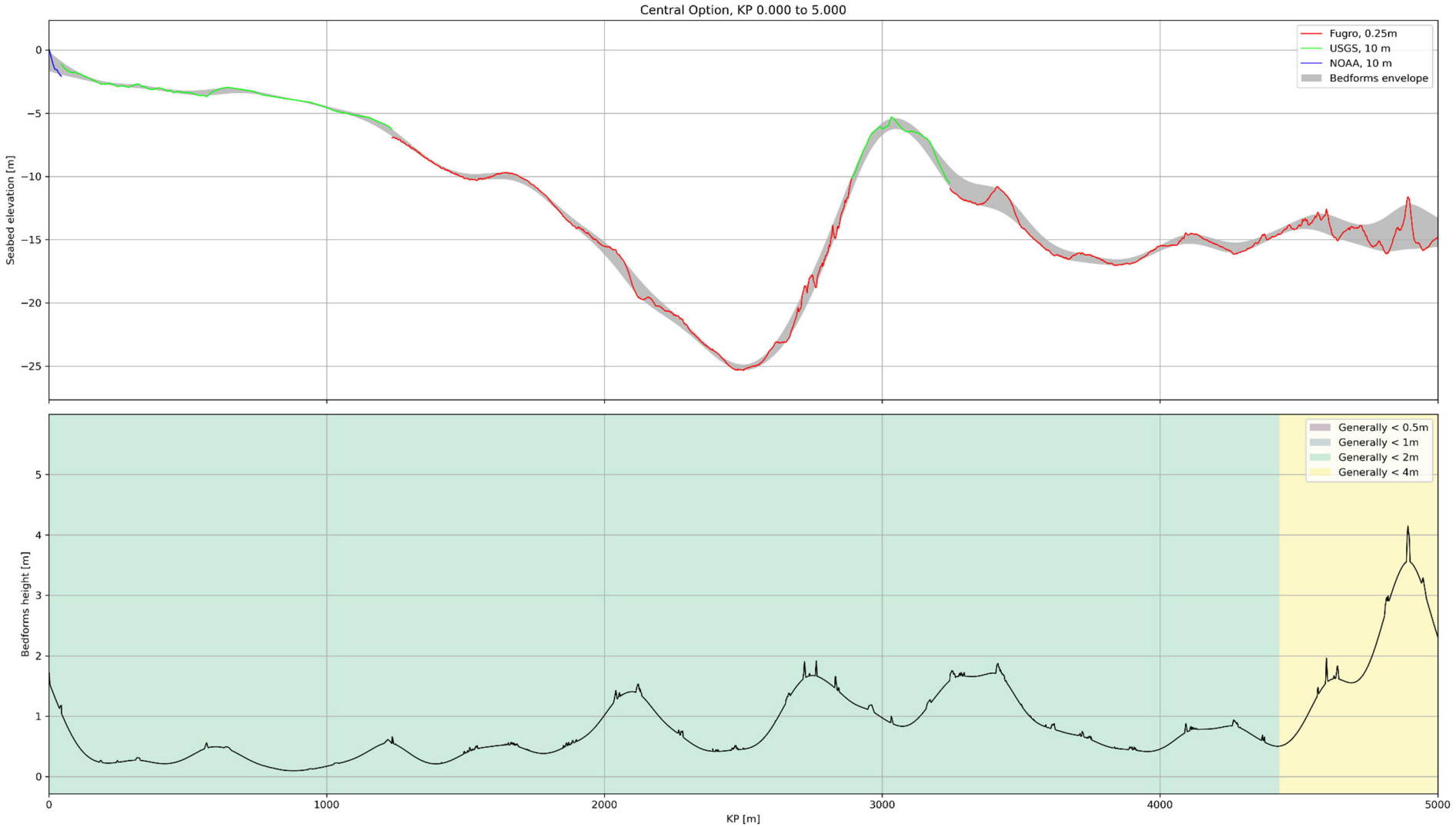
Central Option, KP 0.000 to 5.000
Fugro, 0.25m
USGS, 10 m
NOAA, 10 m
Bedforms envelope
Seabed elevation [m]
0
−5
−10
−15
−20
−25
Generally < 0.5m
Generally < 1m
Generally < 2m
Generally < 4m
Bedforms height [m]
0
1
2
3
4
5
0
1000
2000
3000
4000
5000
KP [m]

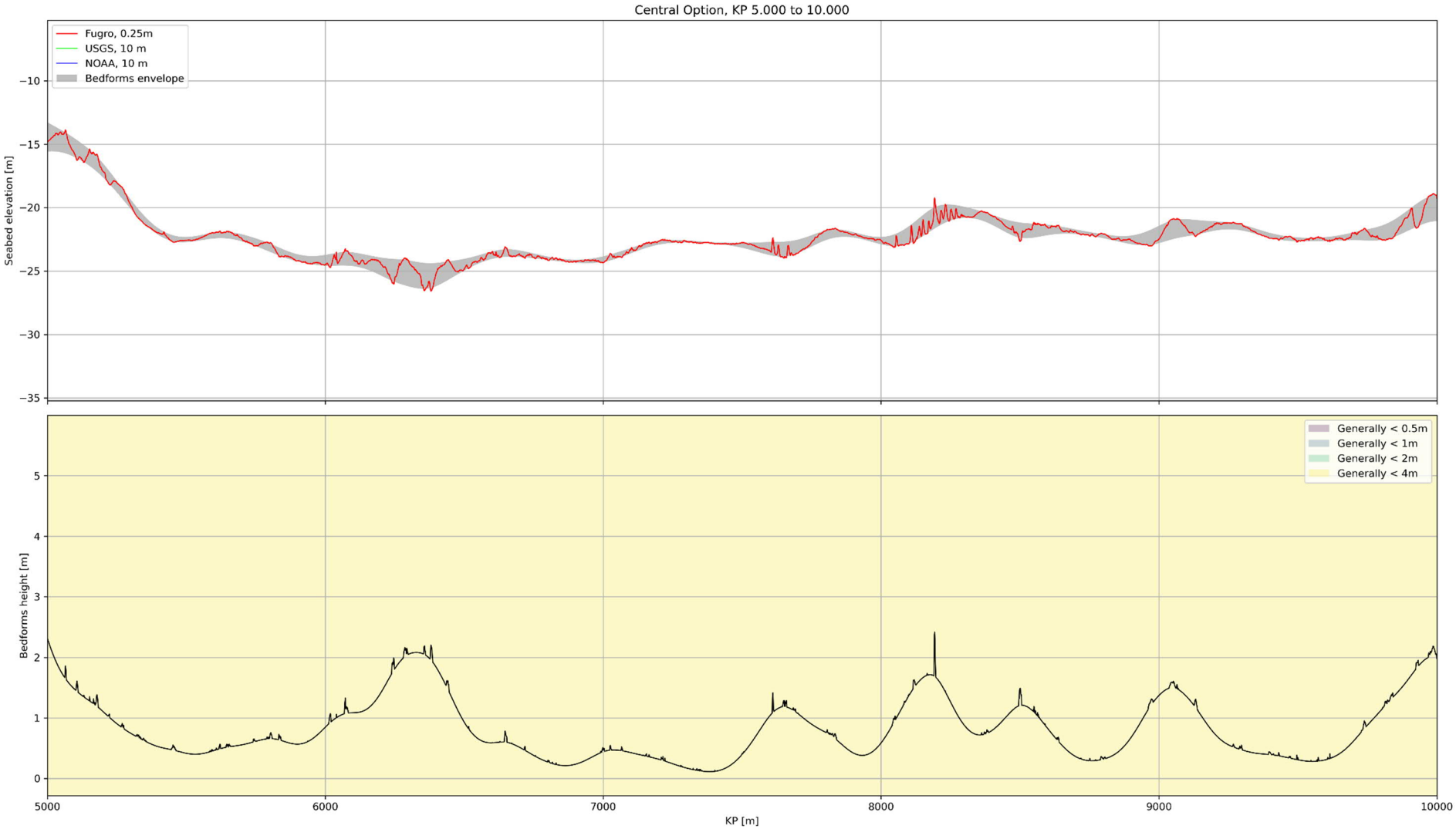
Central Option, KP 5.000 to 10.000
Fugro, 0.25m
USGS, 10 m
NOAA, 10 m
Bedforms envelope
Seabed elevation [m]
−10
−15
−20
−25
−30
−35
Generally < 0.5m
Generally < 1m
Generally < 2m
Generally < 4m
Bedforms height [m]
0
1
2
3
4
5
5000
6000
7000
8000
9000
10000
KP [m]

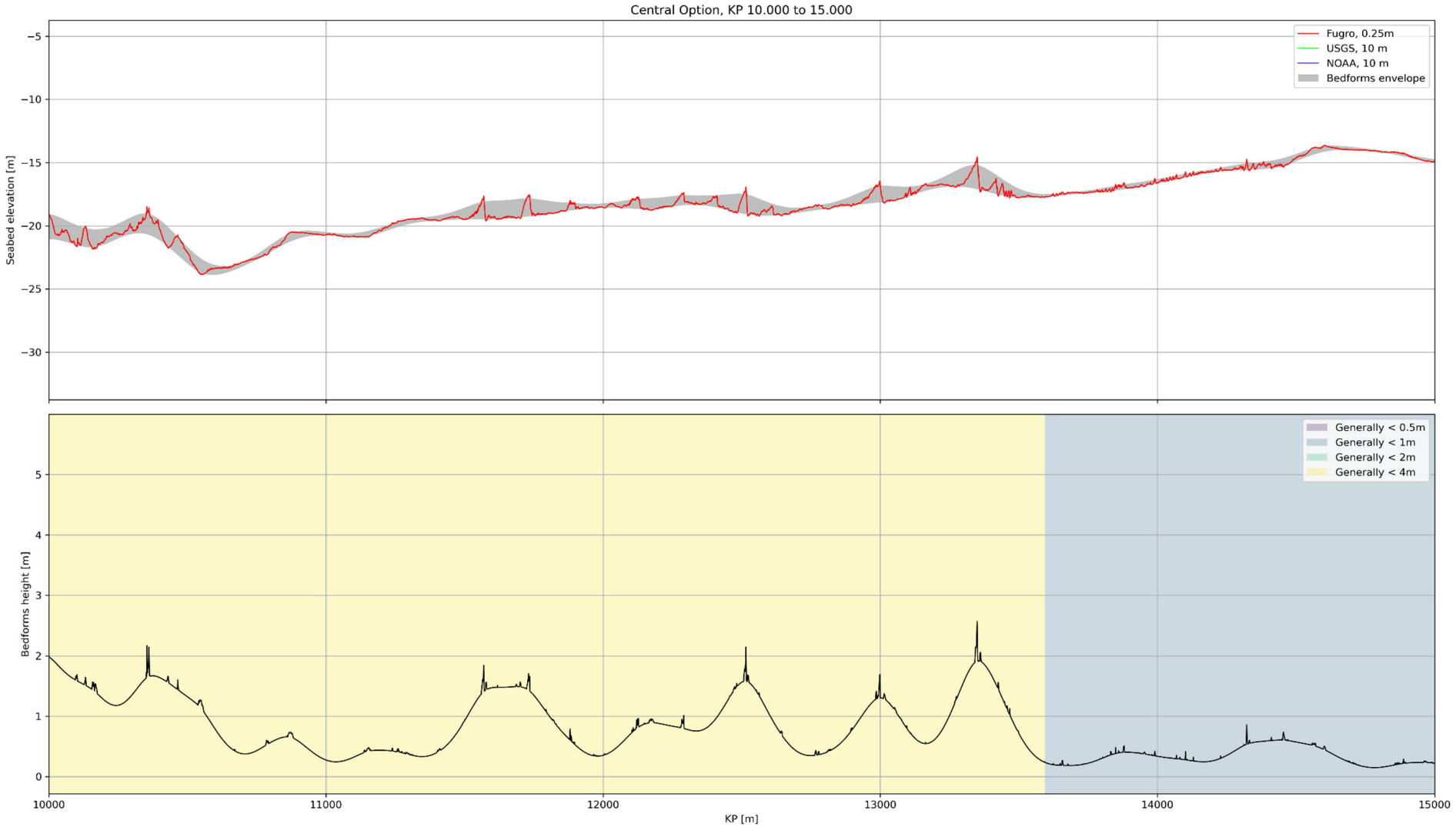
Central Option, KP 10.000 to 15.000
Fugro, 0.25m
USGS, 10 m
NOAA, 10 m
Bedforms envelope
Seabed elevation [m]
−5
−10
−15
−20
−25
−30
Generally < 0.5m
Generally < 1m
Generally < 2m
Generally < 4m
Bedforms height [m]
0
1
2
3
4
5
10000
11000
12000
13000
14000
15000
KP [m]

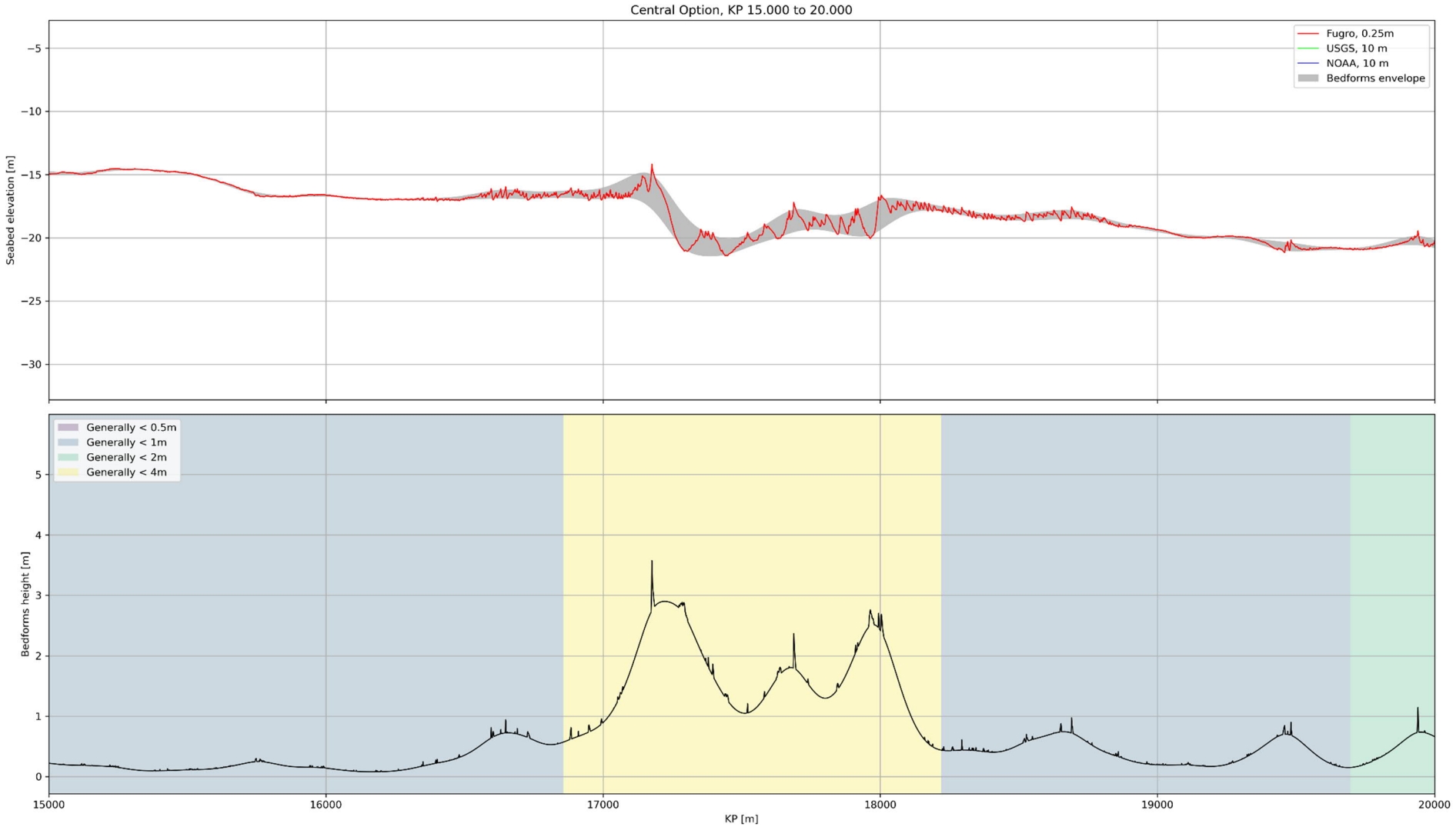
Central Option, KP 15.000 to 20.000
Fugro, 0.25m
USGS, 10 m
NOAA, 10 m
Bedforms envelope
Seabed elevation [m]
−5
−10
−15
−20
−25
−30
Generally < 0.5m
Generally < 1m
Generally < 2m
Generally < 4m
Bedforms height [m]
0
1
2
3
4
5
15000
16000
17000
18000
19000
20000
KP [m]

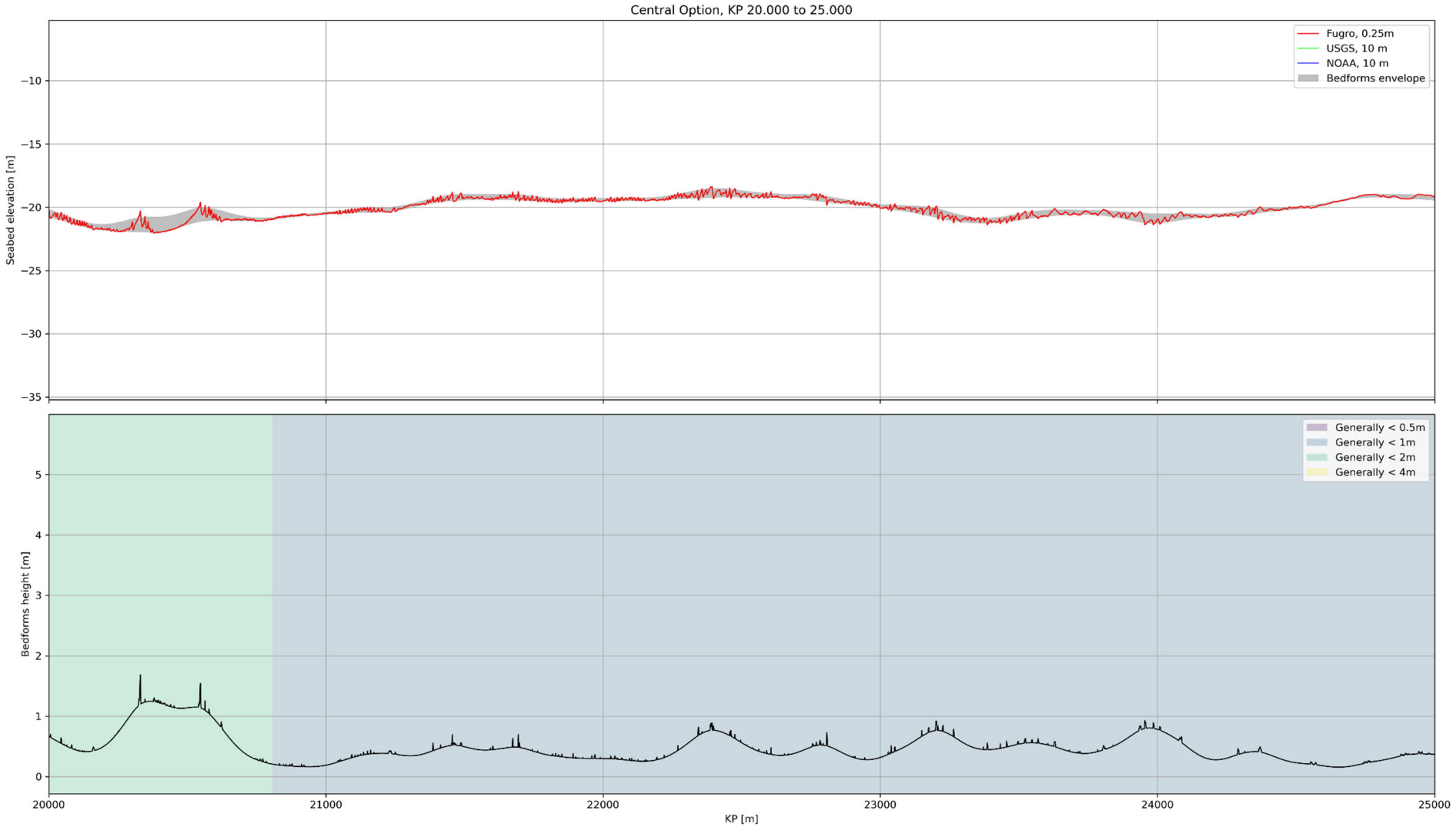
Central Option, KP 20.000 to 25.000
Fugro, 0.25m
USGS, 10 m
NOAA, 10 m
Bedforms envelope
Seabed elevation [m]
−10
−15
−20
−25
−30
−35
Generally < 0.5m
Generally < 1m
Generally < 2m
Generally < 4m
Bedforms height [m]
0
1
2
3
4
5
20000
21000
22000
23000
24000
25000
KP [m]

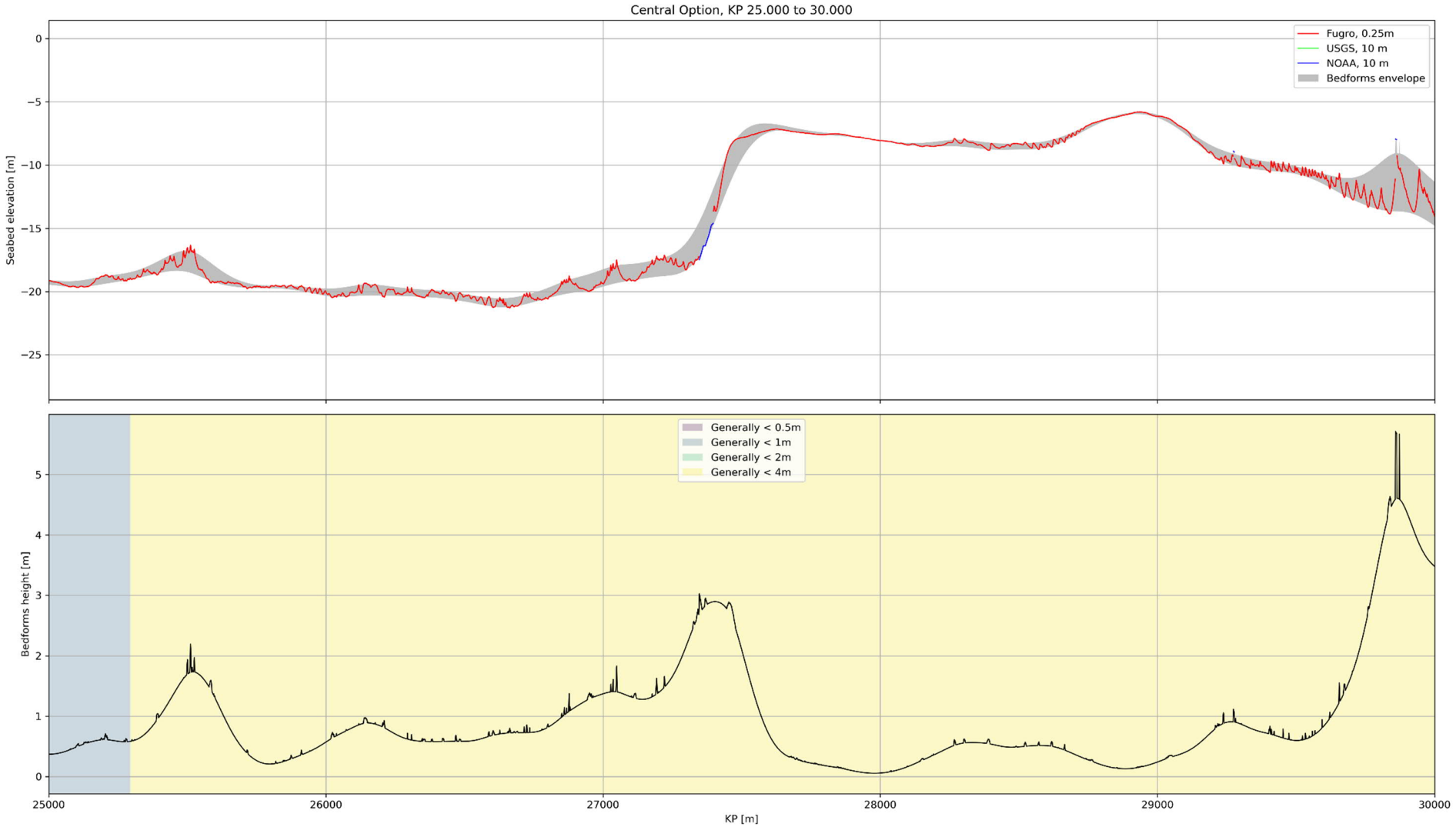
Central Option, KP 25.000 to 30.000
Fugro, 0.25m
USGS, 10 m
NOAA, 10 m
Bedforms envelope
Seabed elevation [m]
0
−5
−10
−15
−20
−25
Generally < 0.5m
Generally < 1m
Generally < 2m
Generally < 4m
Bedforms height [m]
0
1
2
3
4
5
25000
26000
27000
28000
29000
30000
KP [m]

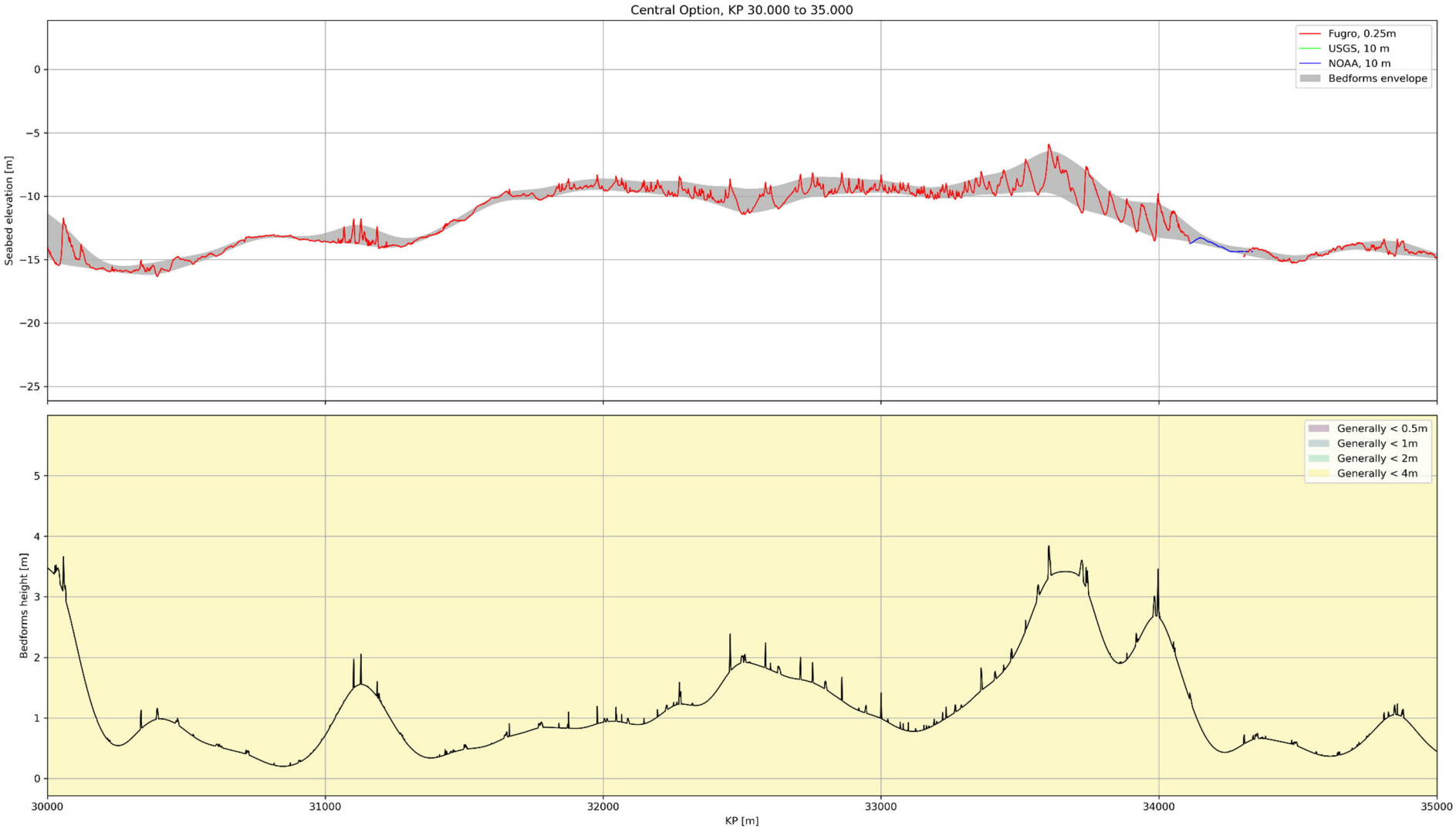
Central Option, KP 30.000 to 35.000
Fugro, 0.25m
USGS, 10 m
NOAA, 10 m
Bedforms envelope
Seabed elevation [m]
0
−5
−10
−15
−20
−25
Generally < 0.5m
Generally < 1m
Generally < 2m
Generally < 4m
Bedforms height [m]
0
1
2
3
4
5
30000
31000
32000
33000
34000
35000
KP [m]

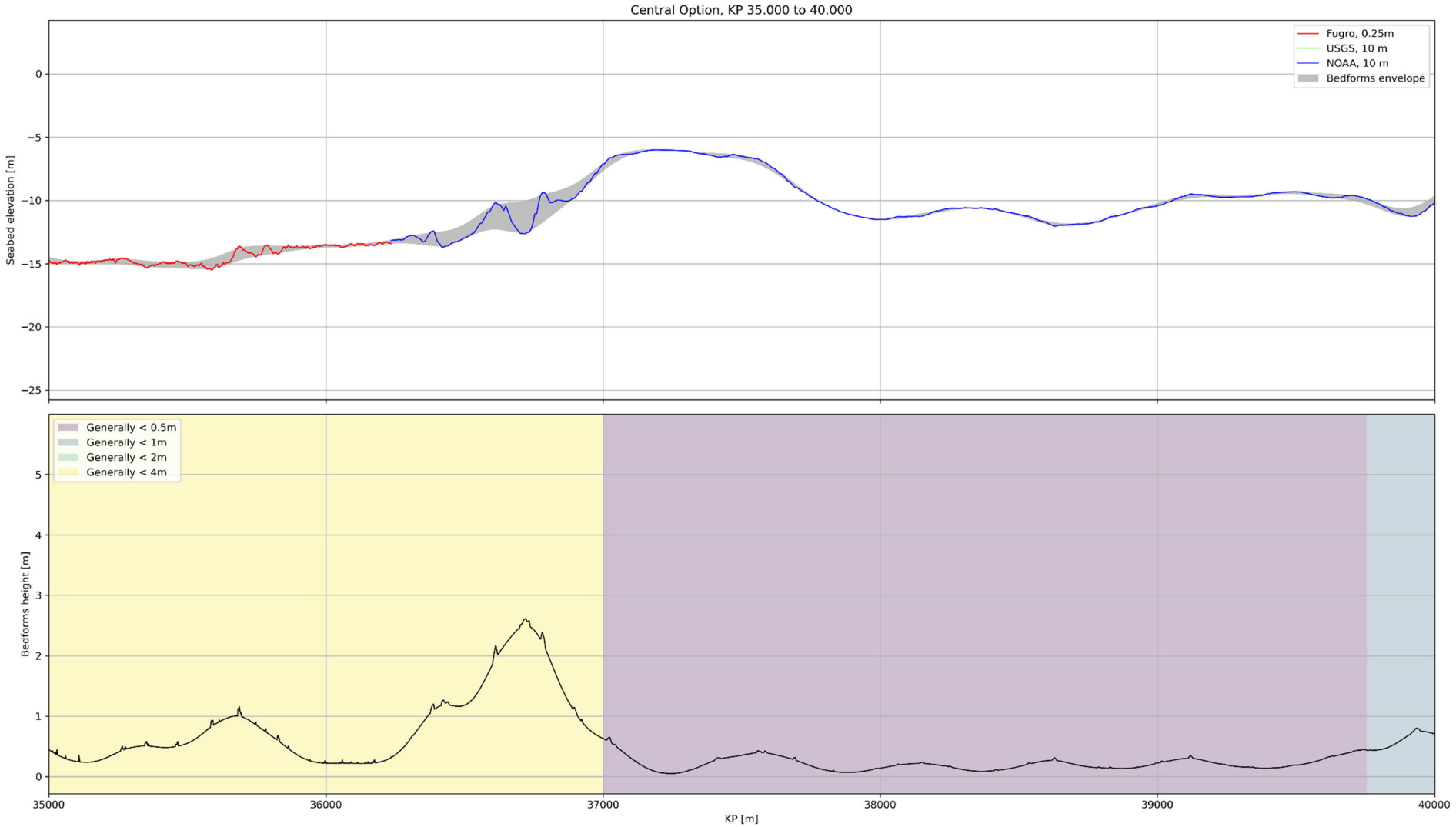
Central Option, KP 35.000 to 40.000
Fugro, 0.25m
USGS, 10 m
NOAA, 10 m
Bedforms envelope
Seabed elevation [m]
0
−5
−10
−15
−20
−25
Generally < 0.5m
Generally < 1m
Generally < 2m
Generally < 4m
Bedforms height [m]
0
1
2
3
4
5
35000
36000
37000
38000
39000
40000
KP [m]

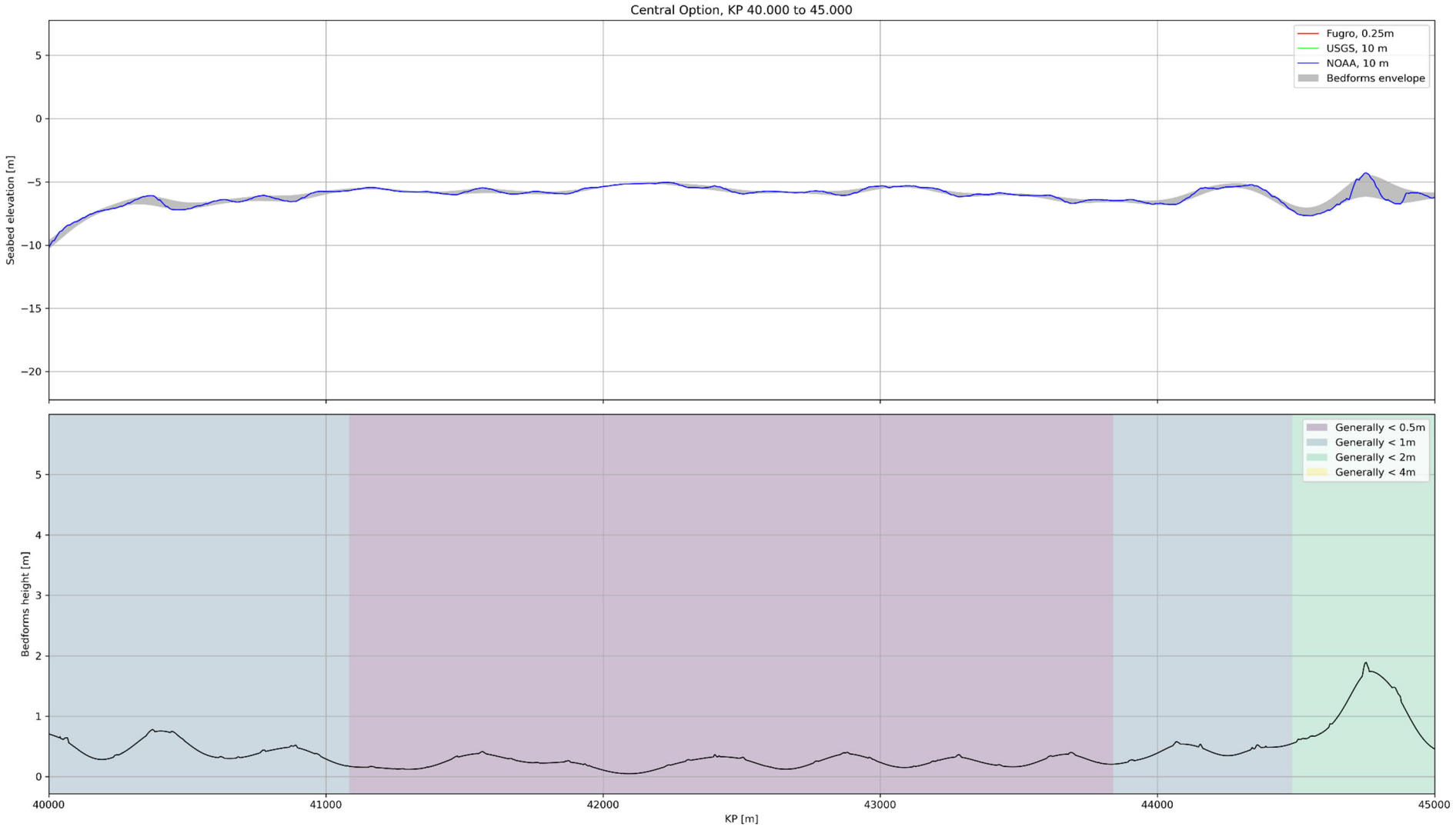
Central Option, KP 40.000 to 45.000
Fugro, 0.25m
USGS, 10 m
NOAA, 10 m
Bedforms envelope
Seabed elevation [m]
5
0
−5
−10
−15
−20
Generally < 0.5m
Generally < 1m
Generally < 2m
Generally < 4m
Bedforms height [m]
0
1
2
3
4
5
40000
41000
42000
43000
44000
45000
KP [m]

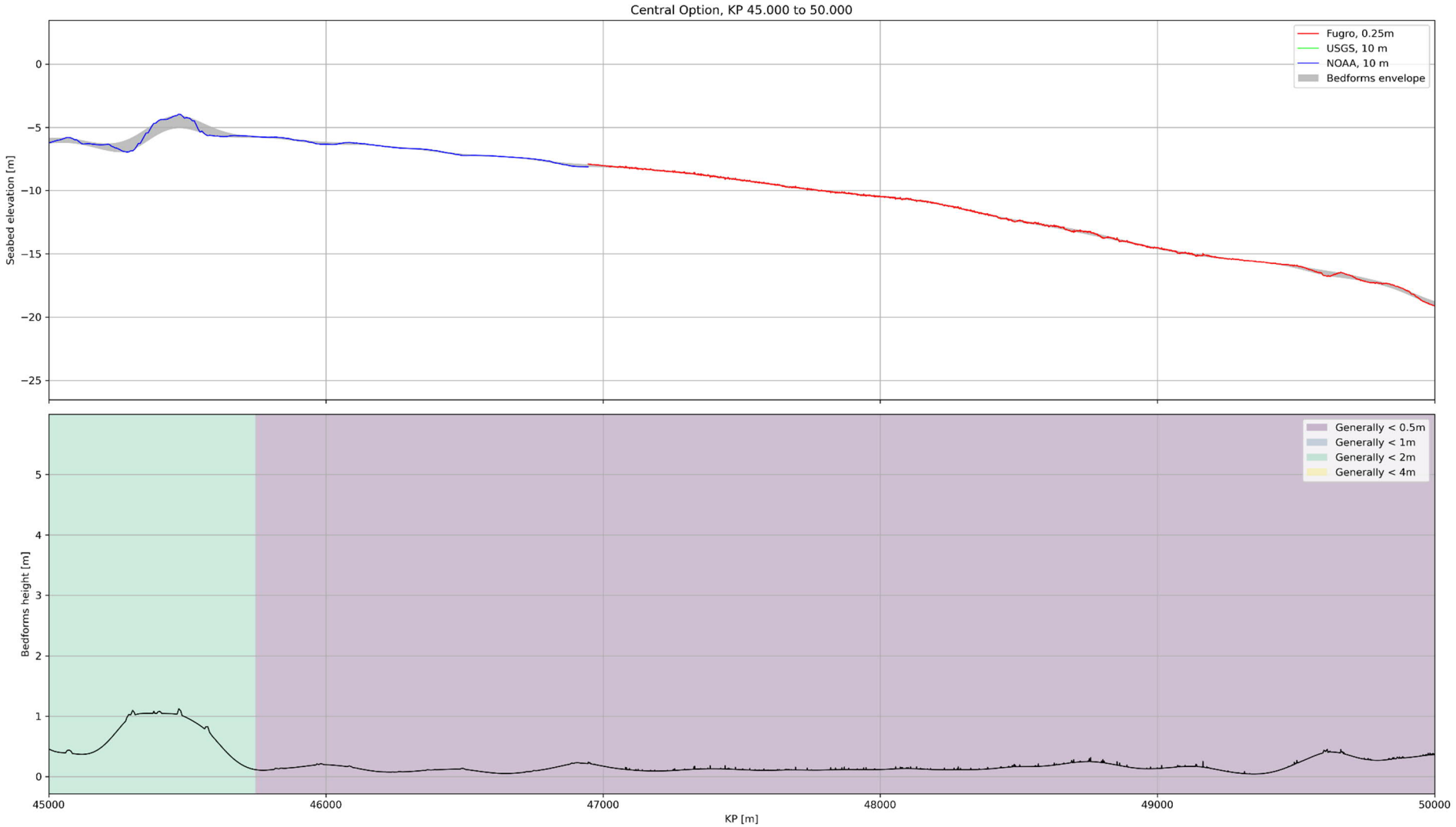
Central Option, KP 45.000 to 50.000
Fugro, 0.25m
USGS, 10 m
NOAA, 10 m
Bedforms envelope
Seabed elevation [m]
0
−5
−10
−15
−20
−25
Generally < 0.5m
Generally < 1m
Generally < 2m
Generally < 4m
Bedforms height [m]
0
1
2
3
4
5
45000
46000
47000
48000
49000
50000
KP [m]

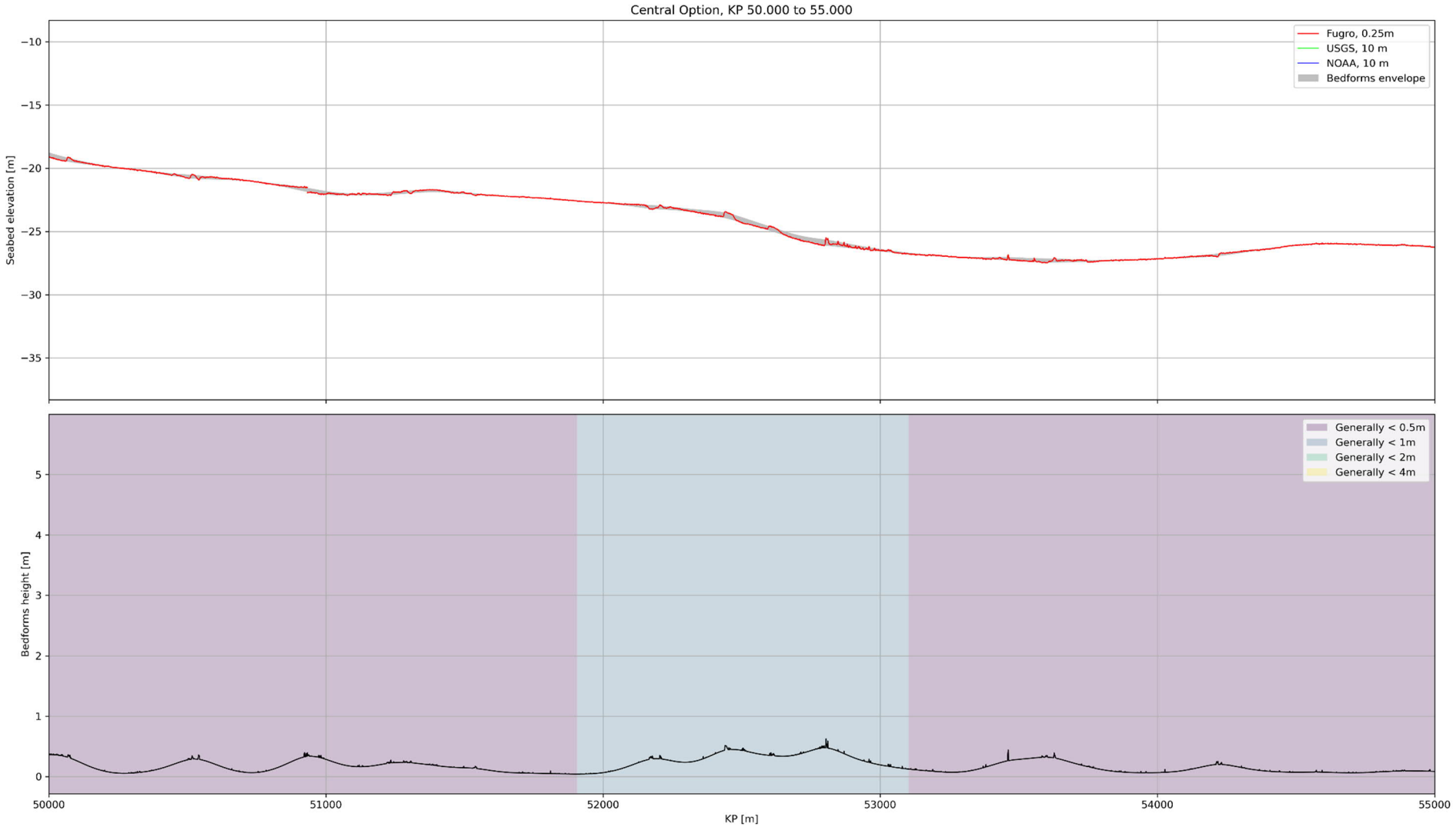
Central Option, KP 50.000 to 55.000
Fugro, 0.25m
USGS, 10 m
NOAA, 10 m
Bedforms envelope
Seabed elevation [m]
−10
−15
−20
−25
−30
−35
Generally < 0.5m
Generally < 1m
Generally < 2m
Generally < 4m
Bedforms height [m]
0
1
2
3
4
5
50000
51000
52000
53000
54000
55000
KP [m]

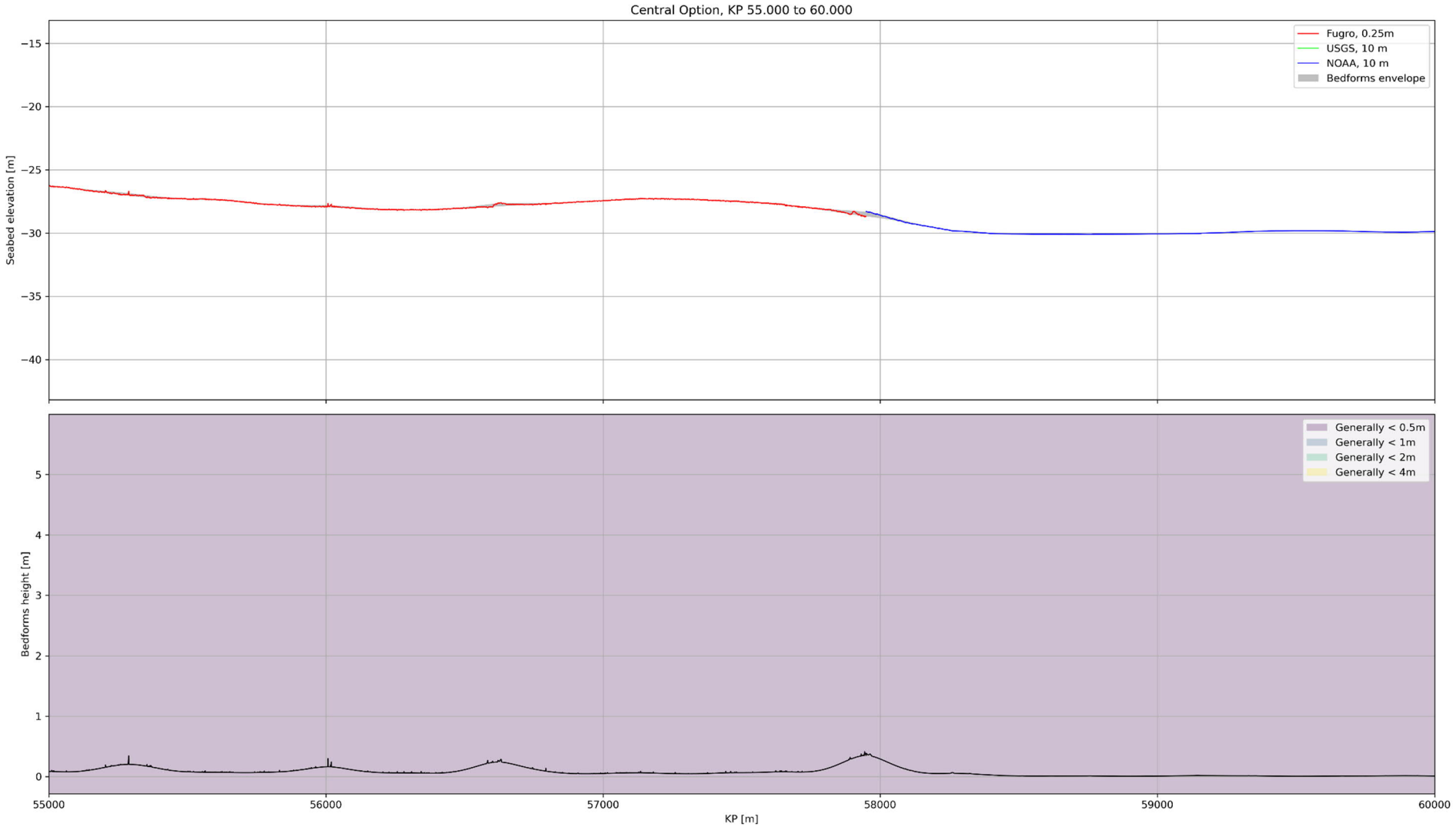
Central Option, KP 55.000 to 60.000
Fugro, 0.25m
USGS, 10 m
NOAA, 10 m
Bedforms envelope
Seabed elevation [m]
−15
−20
−25
−30
−35
−40
Generally < 0.5m
Generally < 1m
Generally < 2m
Generally < 4m
Bedforms height [m]
0
1
2
3
4
5
55000
56000
57000
58000
59000
60000
KP [m]

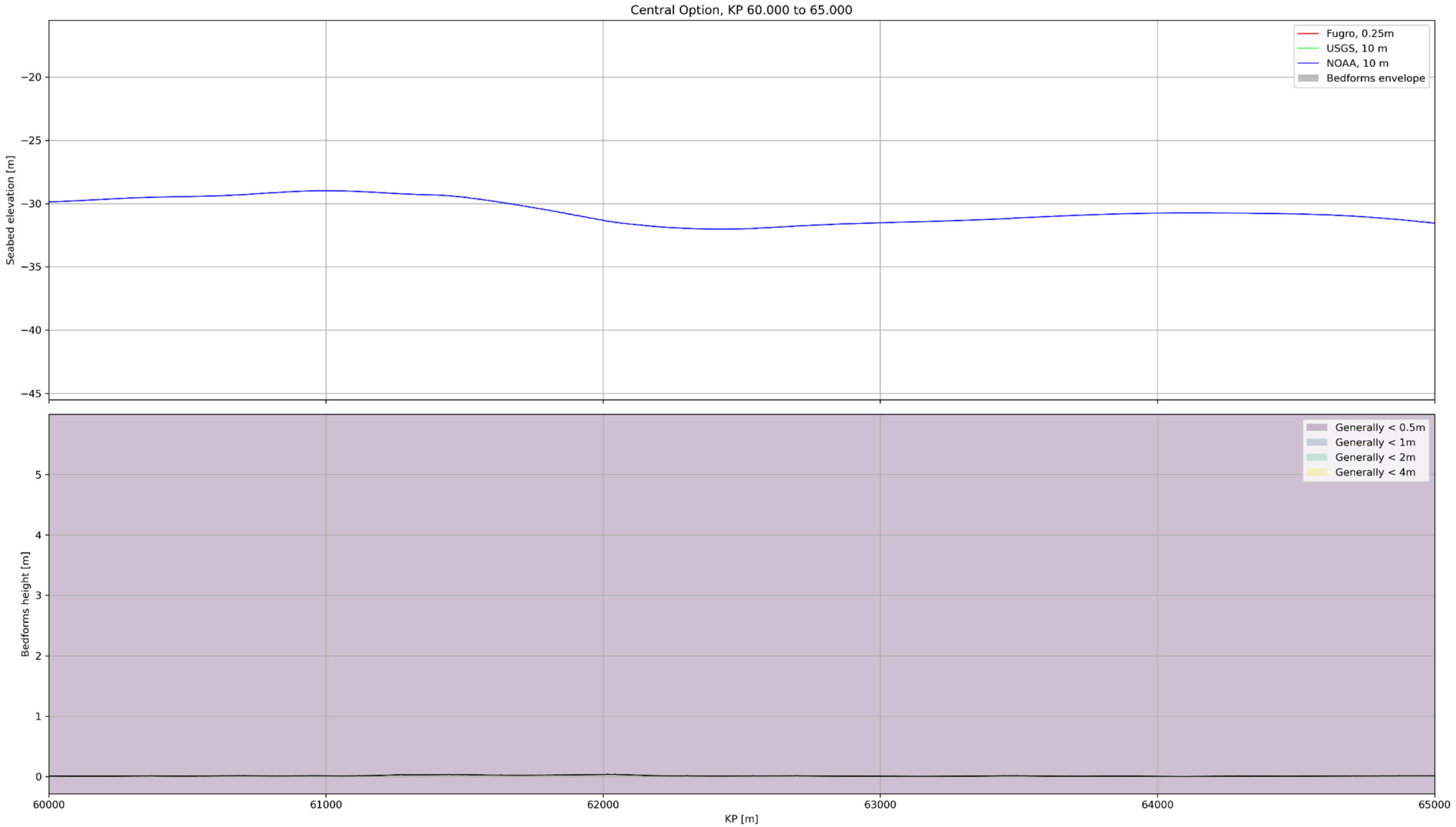
Central Option, KP 60.000 to 65.000
Fugro, 0.25m
USGS, 10 m
NOAA, 10 m
Bedforms envelope
Seabed elevation [m]
−20
−25
−30
−35
−40
−45
Generally < 0.5m
Generally < 1m
Generally < 2m
Generally < 4m
Bedforms height [m]
0
1
2
3
4
5
60000
61000
62000
63000
64000
65000
KP [m]

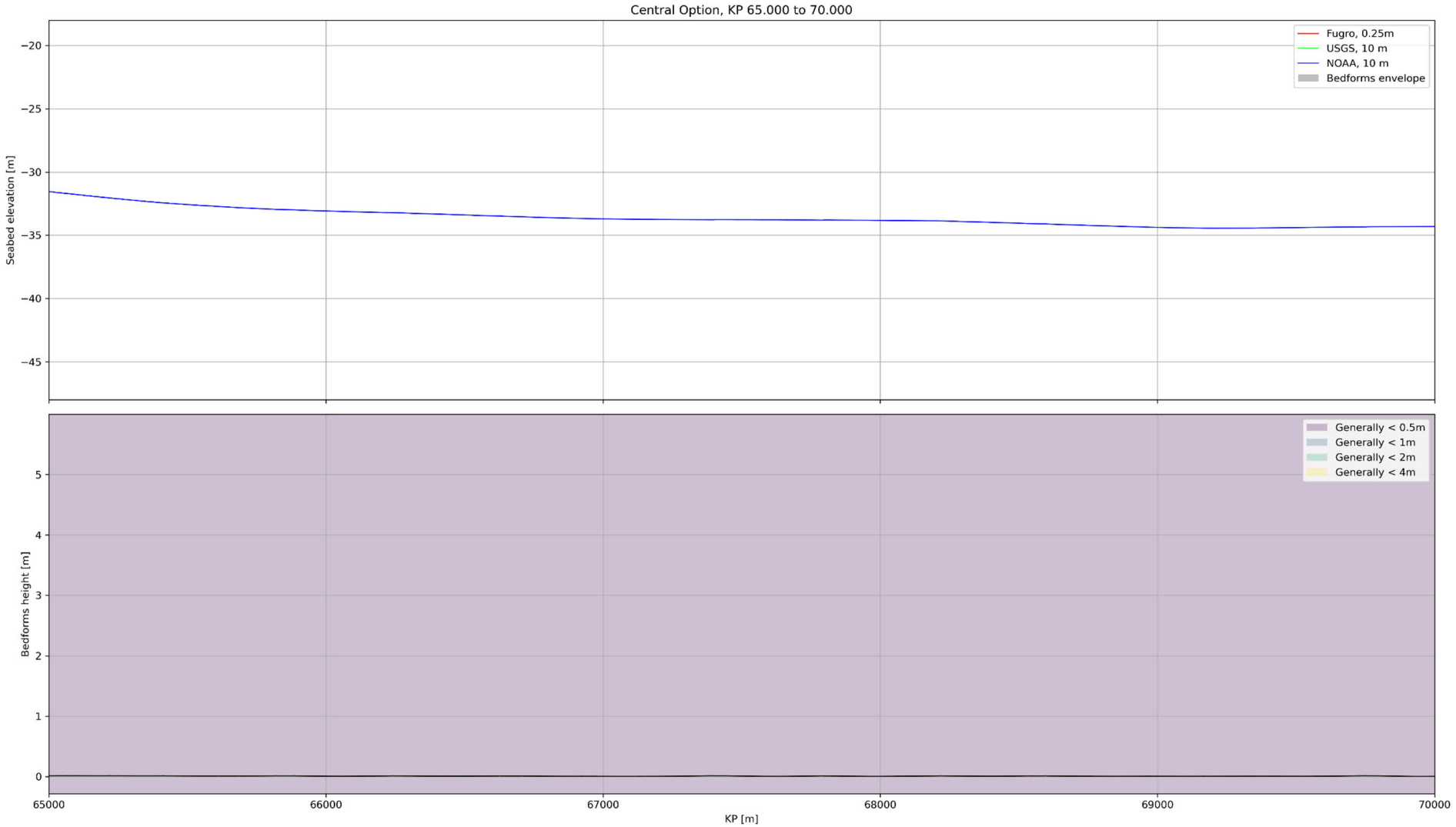
Central Option, KP 65.000 to 70.000
Fugro, 0.25m
USGS, 10 m
NOAA, 10 m
Bedforms envelope
Seabed elevation [m]
−20
−25
−30
−35
−40
−45
Generally < 0.5m
Generally < 1m
Generally < 2m
Generally < 4m
Bedforms height [m]
0
1
2
3
4
5
65000
66000
67000
68000
69000
70000
KP [m]

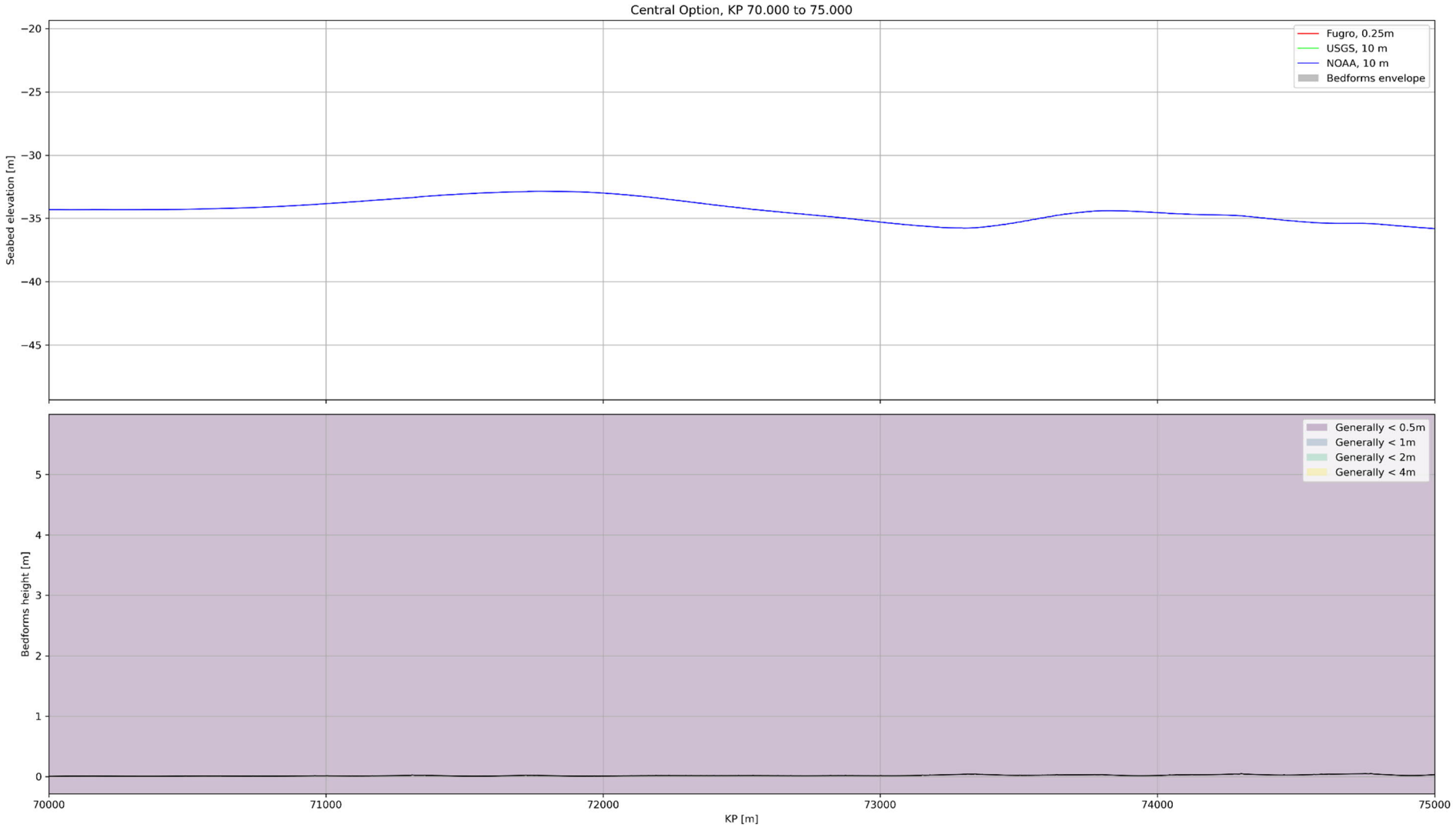
Central Option, KP 70.000 to 75.000
Fugro, 0.25m
USGS, 10 m
NOAA, 10 m
Bedforms envelope
Seabed elevation [m]
−20
−25
−30
−35
−40
−45
Generally < 0.5m
Generally < 1m
Generally < 2m
Generally < 4m
Bedforms height [m]
0
1
2
3
4
5
70000
71000
72000
73000
74000
75000
KP [m]

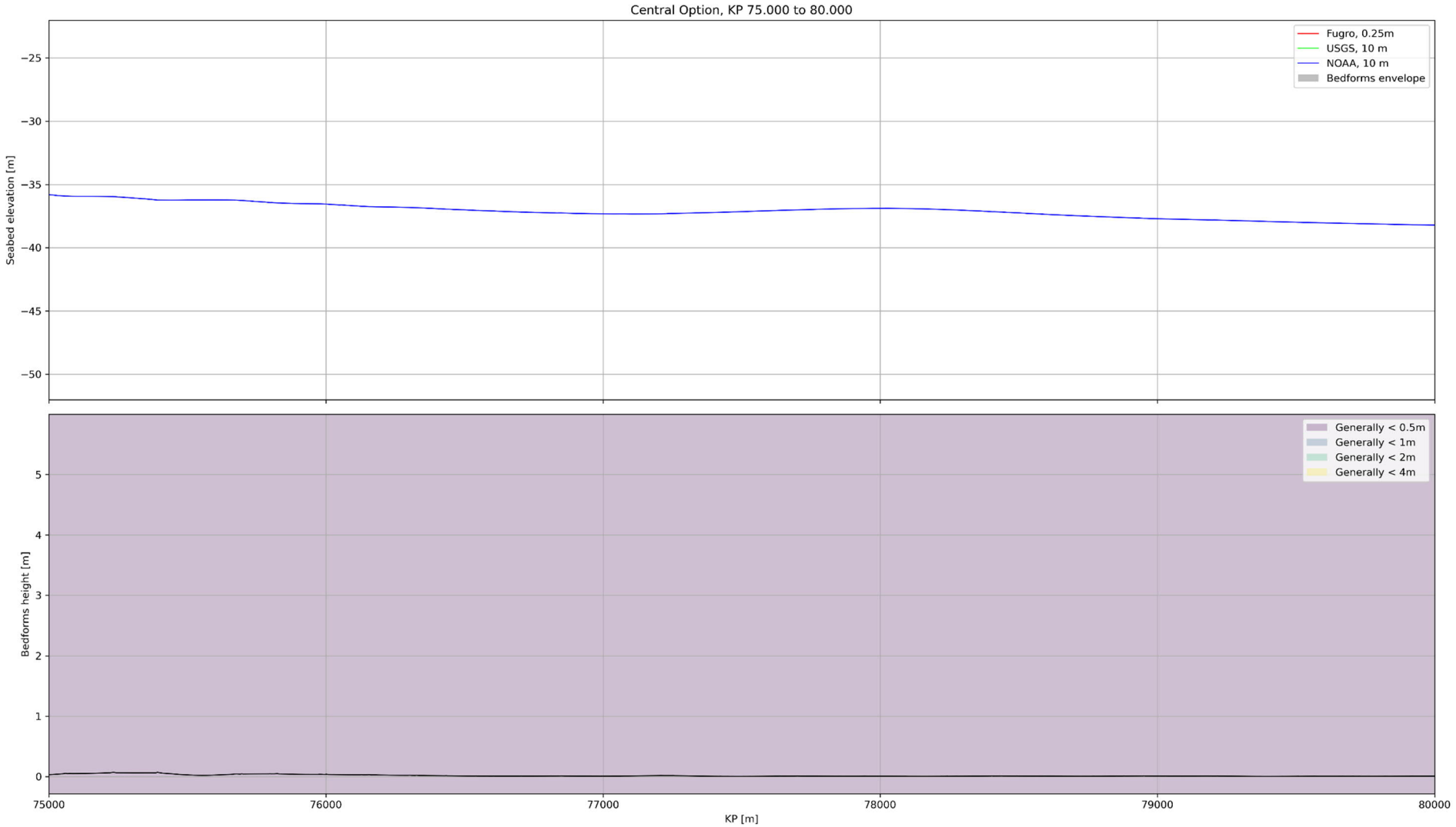
Central Option, KP 75.000 to 80.000
Fugro, 0.25m
USGS, 10 m
NOAA, 10 m
Bedforms envelope
Seabed elevation [m]
−25
−30
−35
−40
−45
−50
Generally < 0.5m
Generally < 1m
Generally < 2m
Generally < 4m
Bedforms height [m]
0
1
2
3
4
5
75000
76000
77000
78000
79000
80000
KP [m]

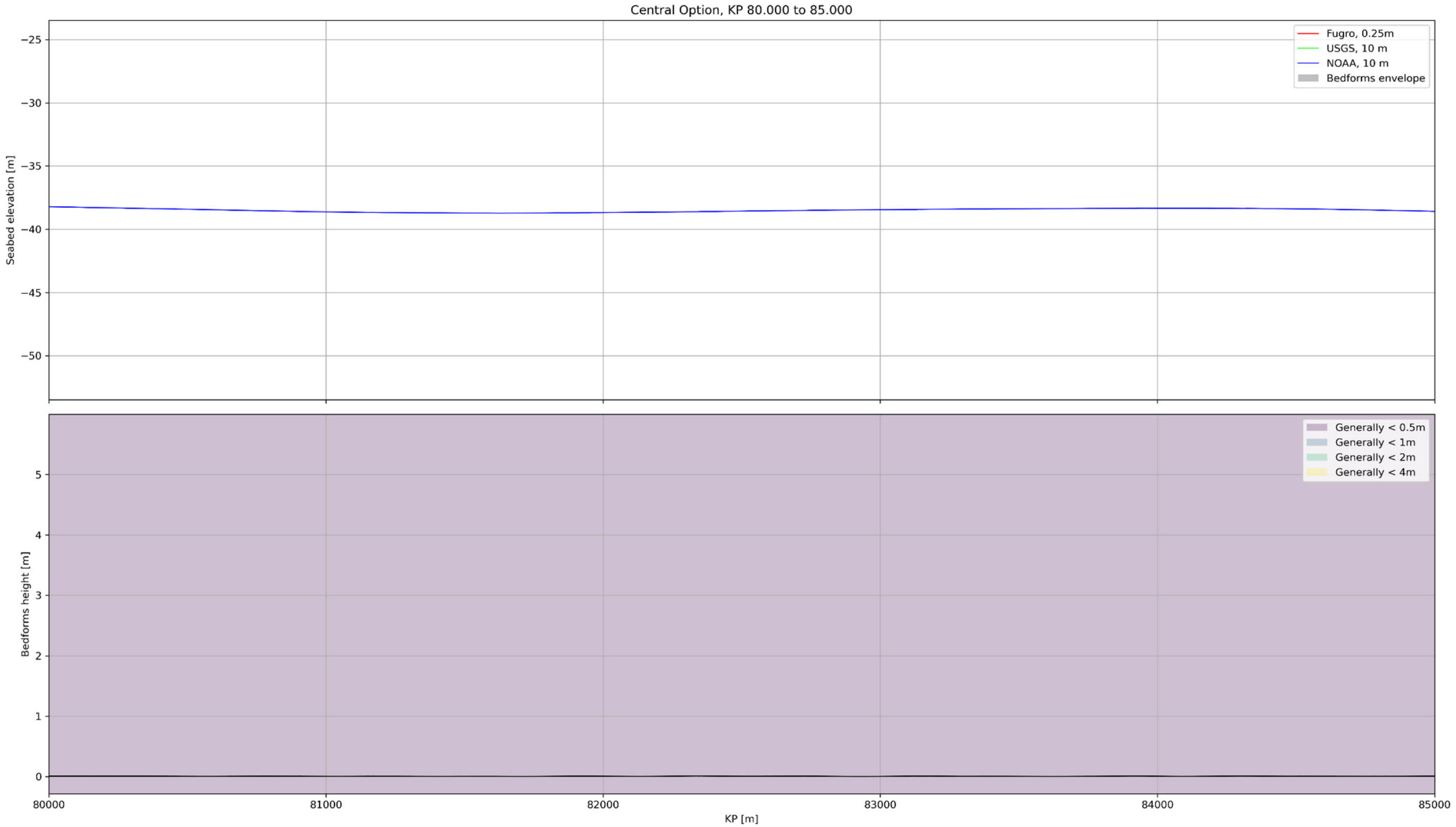
Central Option, KP 80.000 to 85.000
Fugro, 0.25m
USGS, 10 m
NOAA, 10 m
Bedforms envelope
Seabed elevation [m]
−25
−30
−35
−40
−45
−50
Generally < 0.5m
Generally < 1m
Generally < 2m
Generally < 4m
Bedforms height [m]
0
1
2
3
4
5
80000
81000
82000
83000
84000
85000
KP [m]

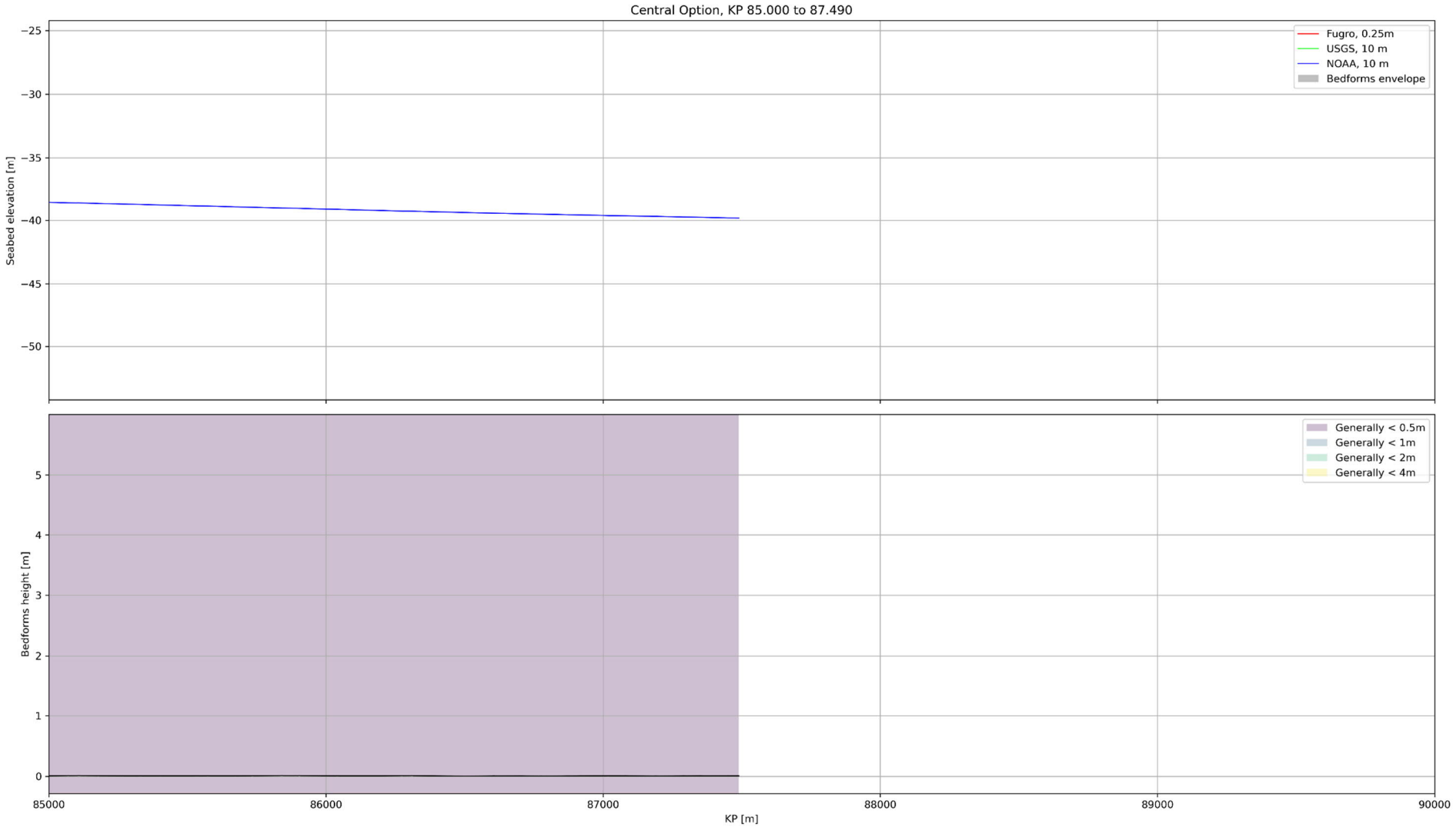
Central Option, KP 85.000 to 87.490
Fugro, 0.25m
USGS, 10 m
NOAA, 10 m
Bedforms envelope
Seabed elevation [m]
−25
−30
−35
−40
−45
−50
Generally < 0.5m
Generally < 1m
Generally < 2m
Generally < 4m
Bedforms height [m]
0
1
2
3
4
5
85000
86000
87000
88000
89000
90000
KP [m]

D.2 Offshore Export Cable Route - Eastern Option

This section shows seabed elevation profiles along the Eastern Option export cable route, including an envelope of lower/higher expected values of local bedforms elevation. Bedform heights are estimated based on this envelope. A morphological zonation is then defined on the route using the bedforms height. Figure D.2 shows the seabed elevation profile, bedforms height, and zonation along the whole route, while the following figures focus on 5-km long sections for improved readability.

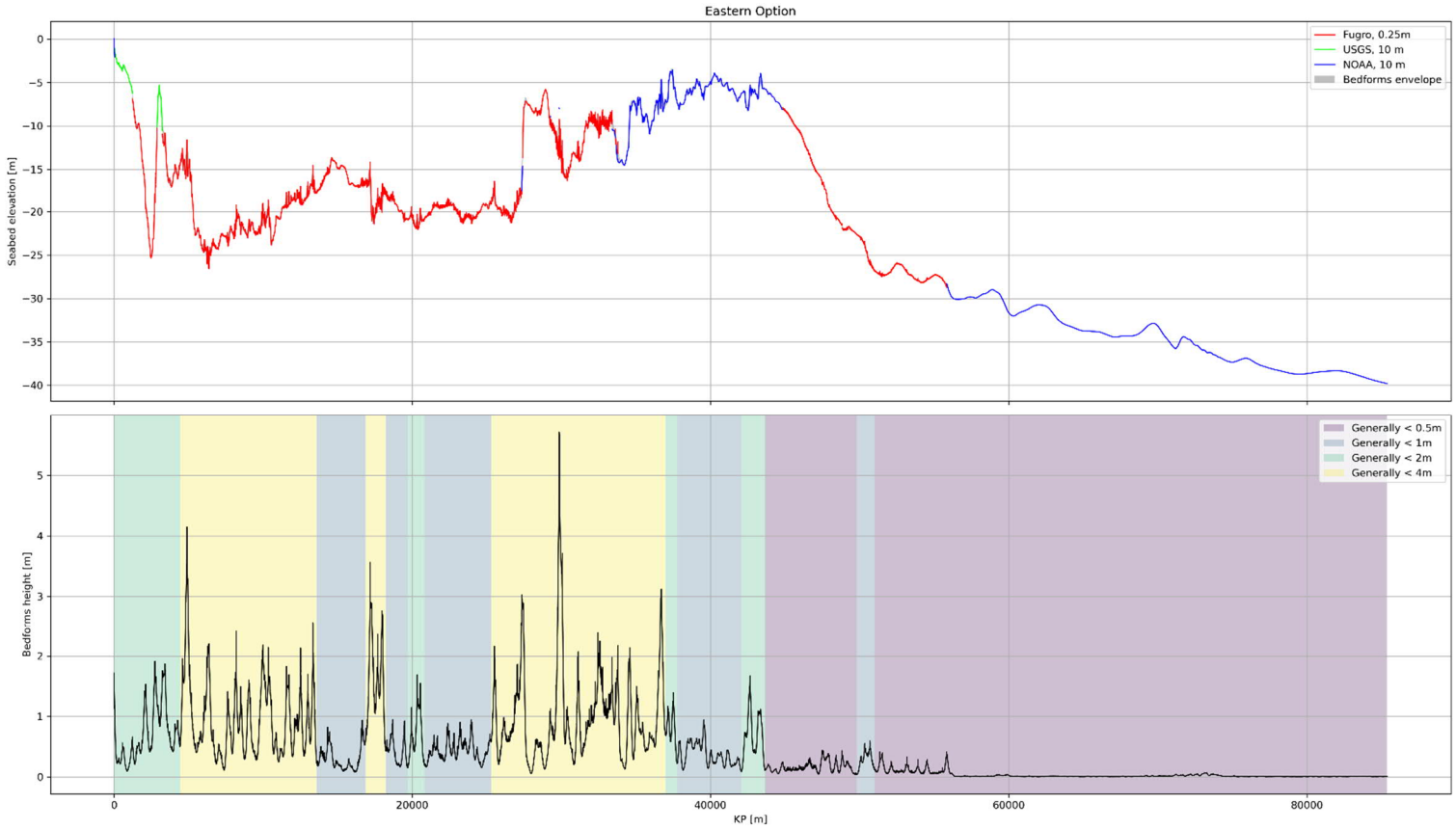

Figure D.2: Seabed elevation profile using the locally most accurate bathymetry (up). Computed bedforms heights and morphological zonation (down).

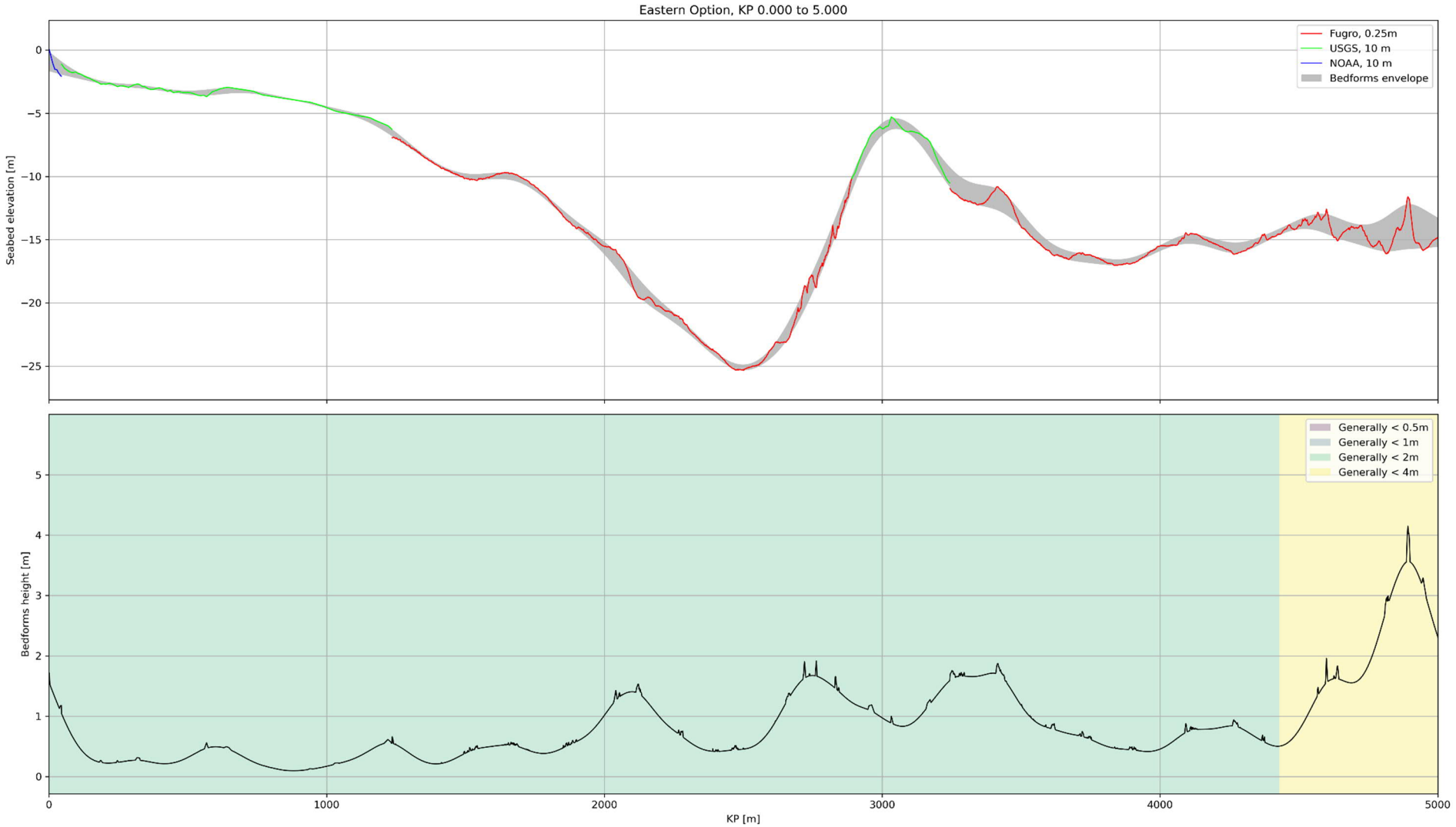
Eastern Option, KP 0.000 to 5.000
Fugro, 0.25m
USGS, 10 m
NOAA, 10 m
Bedforms envelope
Seabed elevation [m]
0
−5
−10
−15
−20
−25
Generally < 0.5m
Generally < 1m
Generally < 2m
Generally < 4m
Bedforms height [m]
0
1
2
3
4
5
0
1000
2000
3000
4000
5000
KP [m]

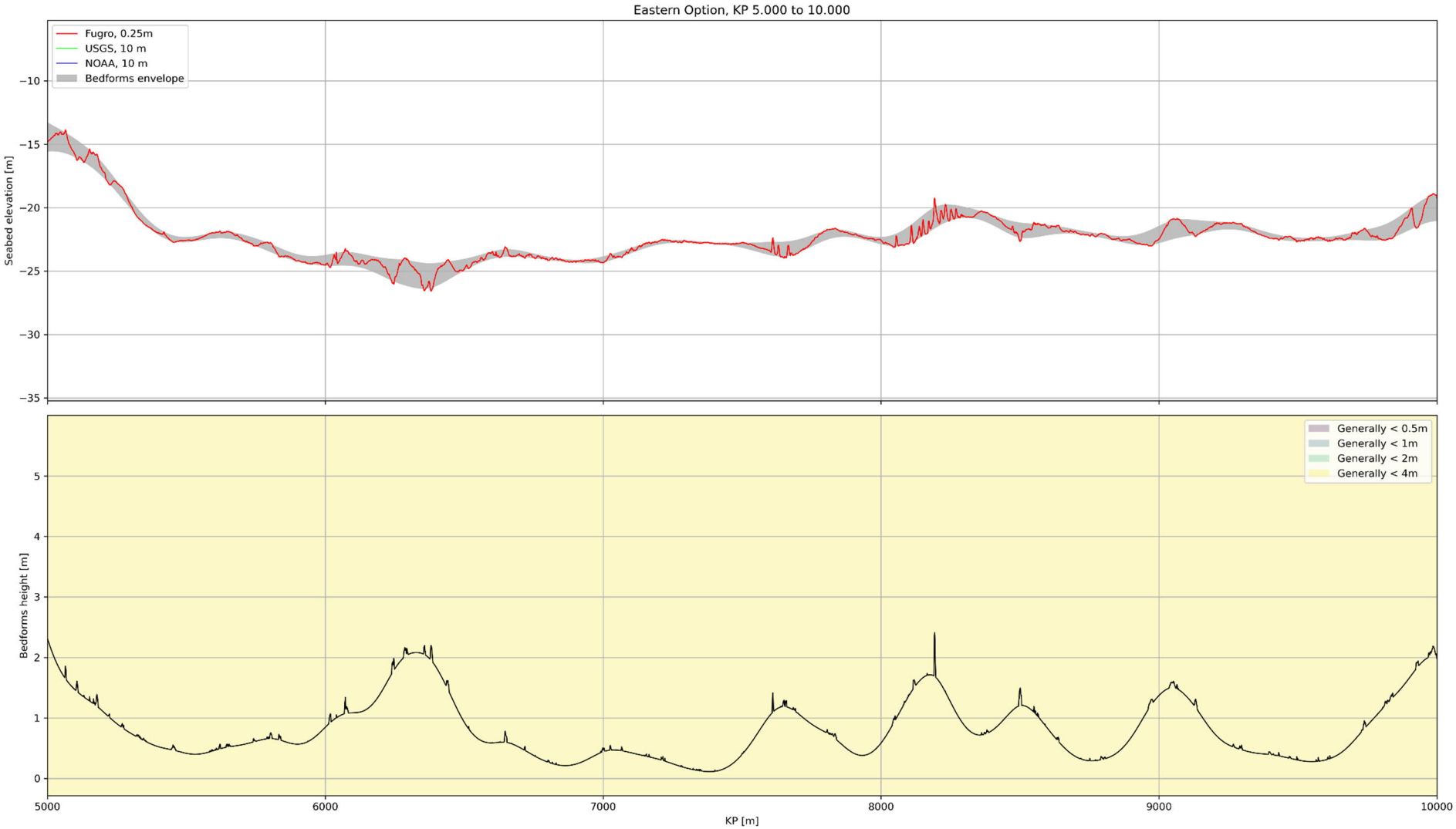
Eastern Option, KP 5.000 to 10.000
Fugro, 0.25m
USGS, 10 m
NOAA, 10 m
Bedforms envelope
Seabed elevation [m]
−10
−15
−20
−25
−30
−35
Generally < 0.5m
Generally < 1m
Generally < 2m
Generally < 4m
Bedforms height [m]
0
1
2
3
4
5
5000
6000
7000
8000
9000
10000
KP [m]

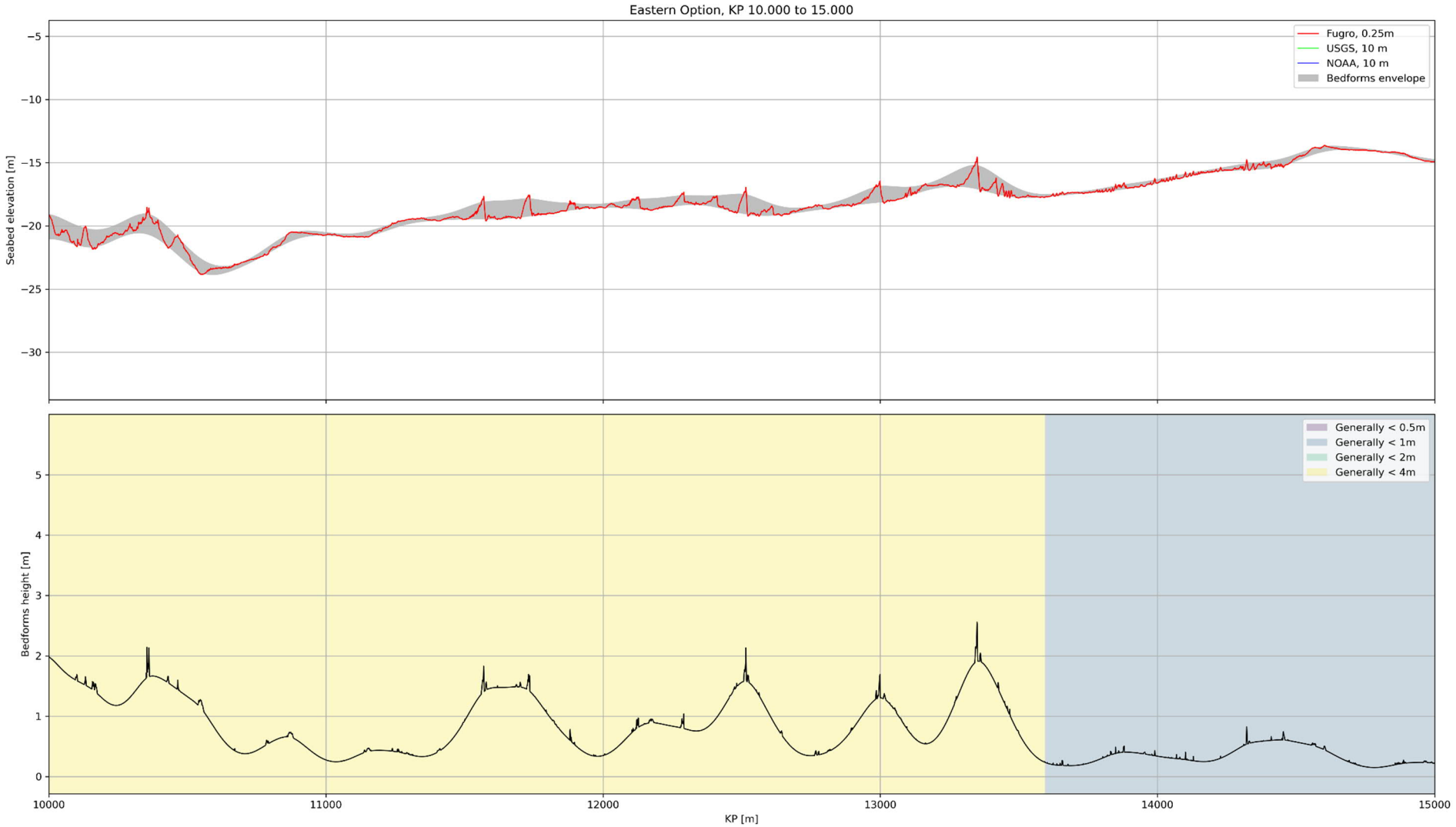
Eastern Option, KP 10.000 to 15.000
Fugro, 0.25m
USGS, 10 m
NOAA, 10 m
Bedforms envelope
Seabed elevation [m]
−5
−10
−15
−20
−25
−30
Generally < 0.5m
Generally < 1m
Generally < 2m
Generally < 4m
Bedforms height [m]
0
1
2
3
4
5
10000
11000
12000
13000
14000
15000
KP [m]

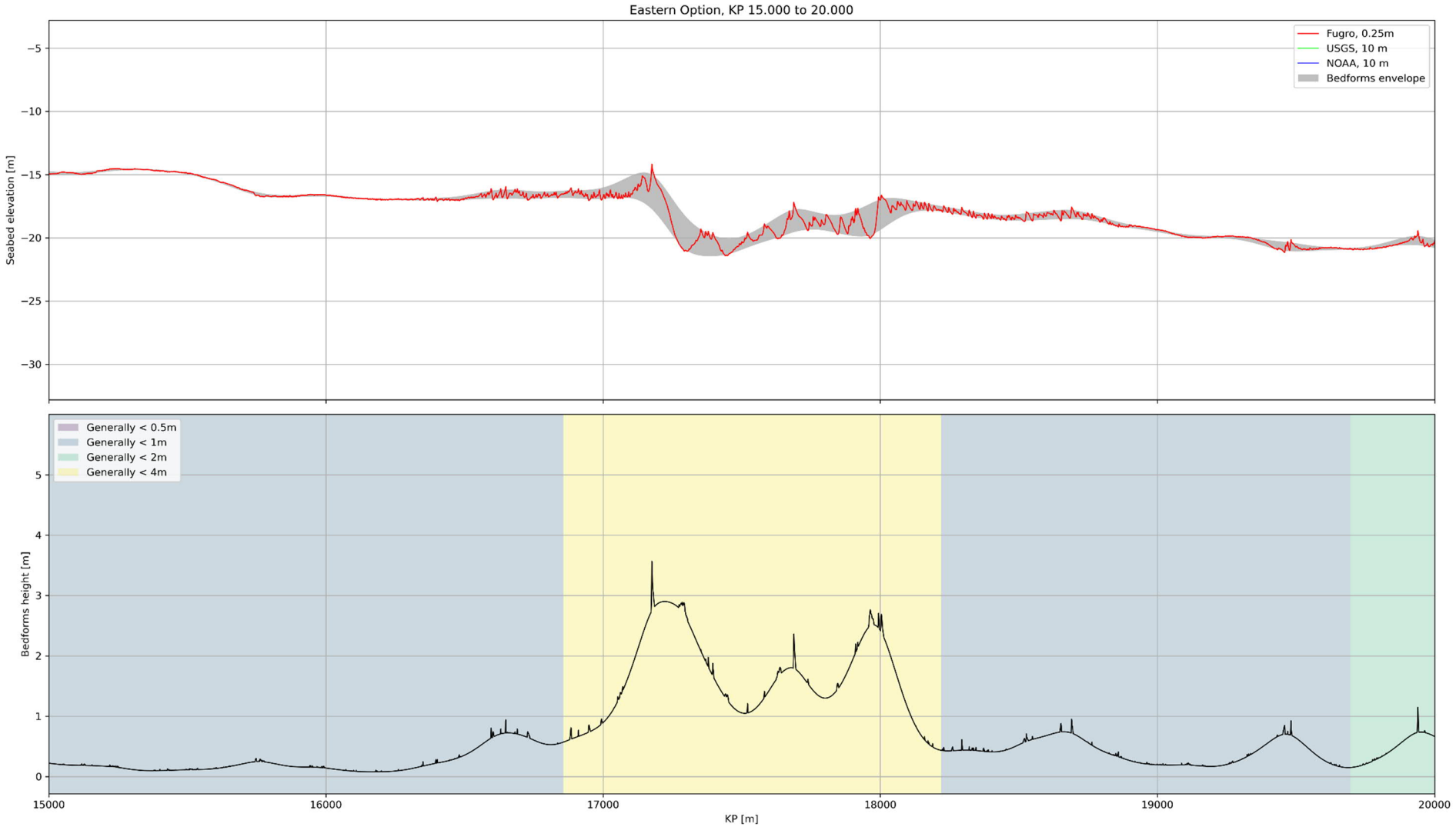
Eastern Option, KP 15.000 to 20.000
Fugro, 0.25m
USGS, 10 m
NOAA, 10 m
Bedforms envelope
Seabed elevation [m]
−5
−10
−15
−20
−25
−30
Generally < 0.5m
Generally < 1m
Generally < 2m
Generally < 4m
Bedforms height [m]
0
1
2
3
4
5
15000
16000
17000
18000
19000
20000
KP [m]

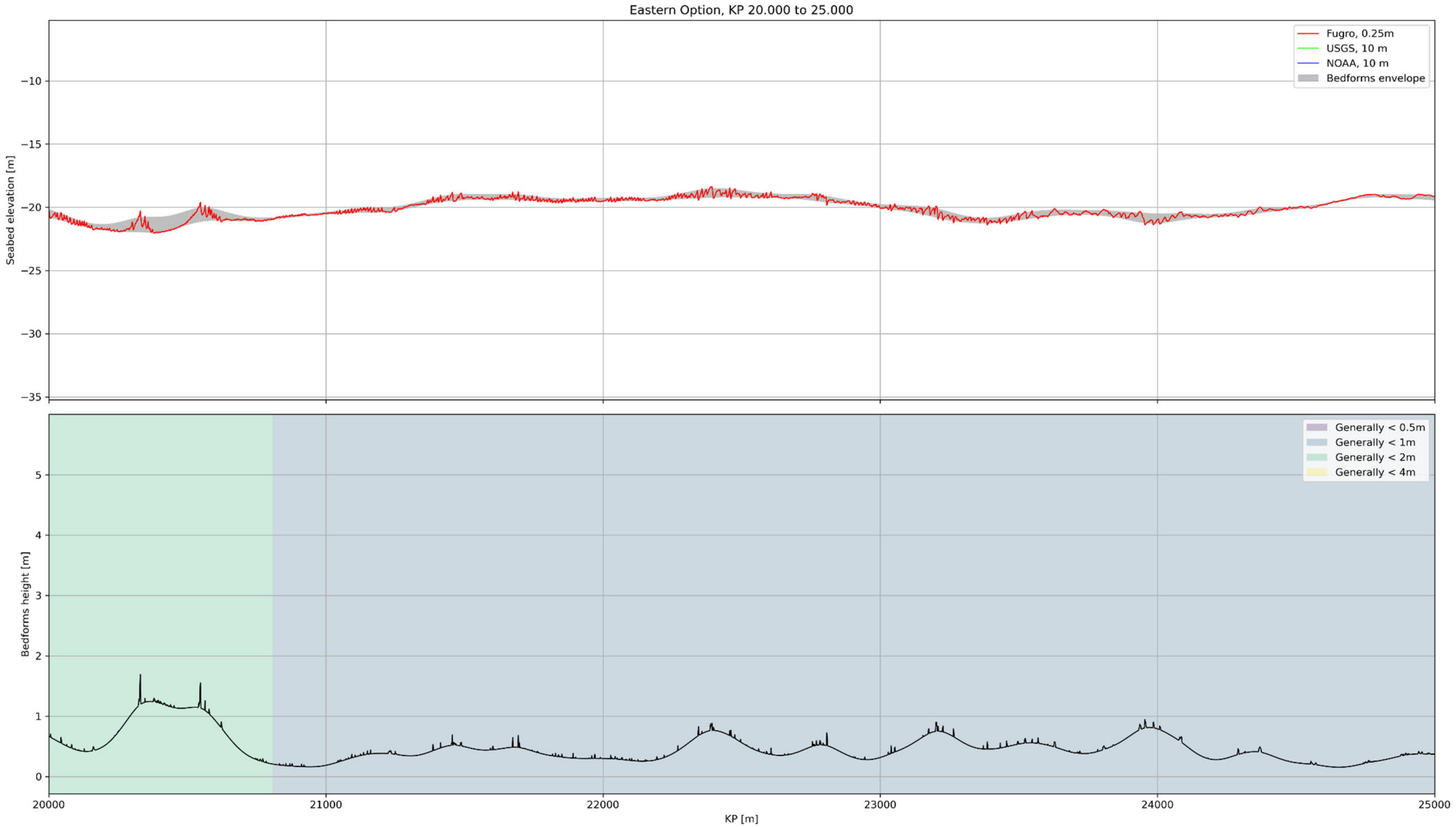
Eastern Option, KP 20.000 to 25.000
Fugro, 0.25m
USGS, 10 m
NOAA, 10 m
Bedforms envelope
Seabed elevation [m]
−10
−15
−20
−25
−30
−35
Generally < 0.5m
Generally < 1m
Generally < 2m
Generally < 4m
Bedforms height [m]
0
1
2
3
4
5
20000
21000
22000
23000
24000
25000
KP [m]

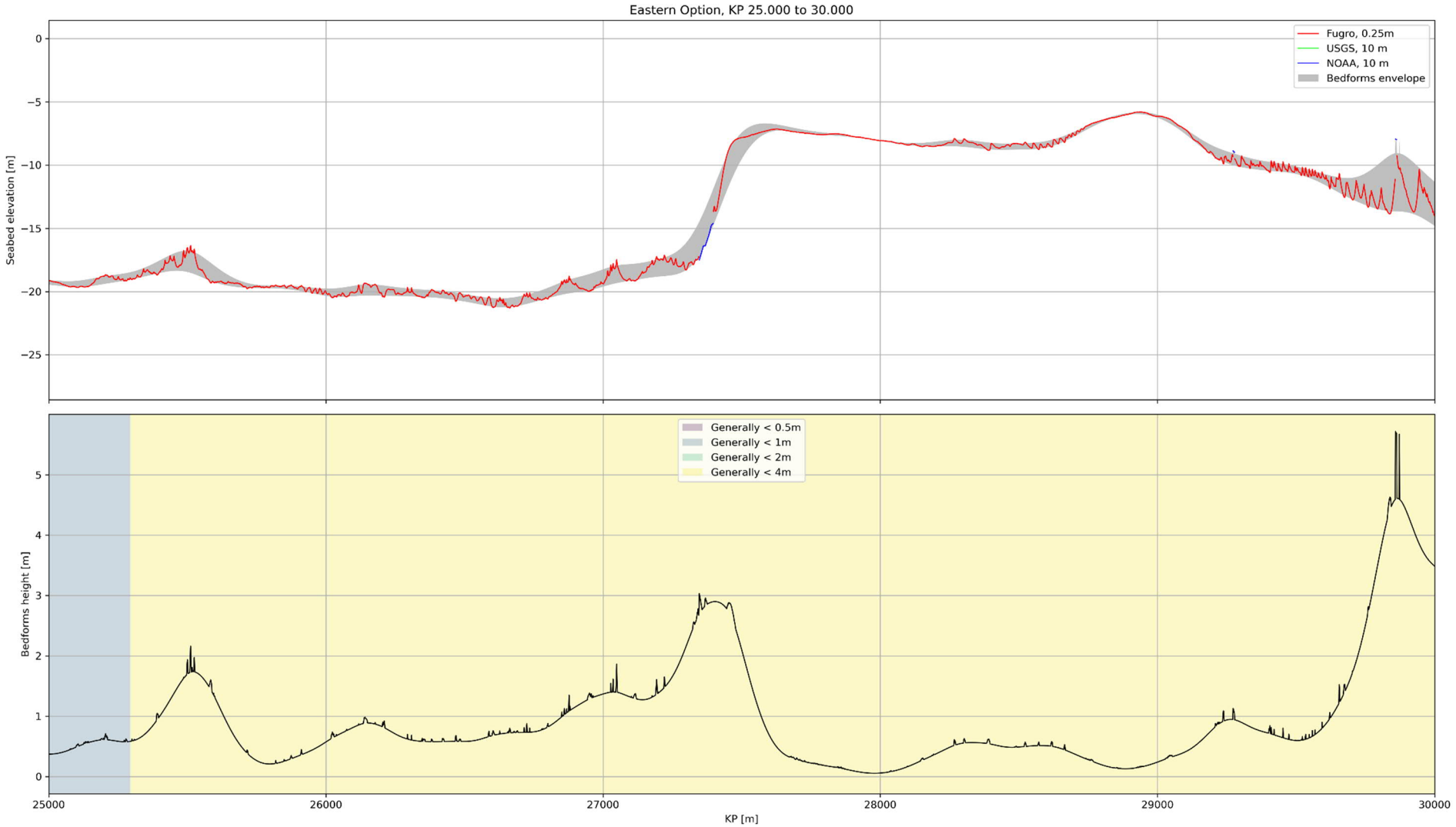
Eastern Option, KP 25.000 to 30.000
Fugro, 0.25m
USGS, 10 m
NOAA, 10 m
Bedforms envelope
Seabed elevation [m]
0
−5
−10
−15
−20
−25
Generally < 0.5m
Generally < 1m
Generally < 2m
Generally < 4m
Bedforms height [m]
0
1
2
3
4
5
25000
26000
27000
28000
29000
30000
KP [m]

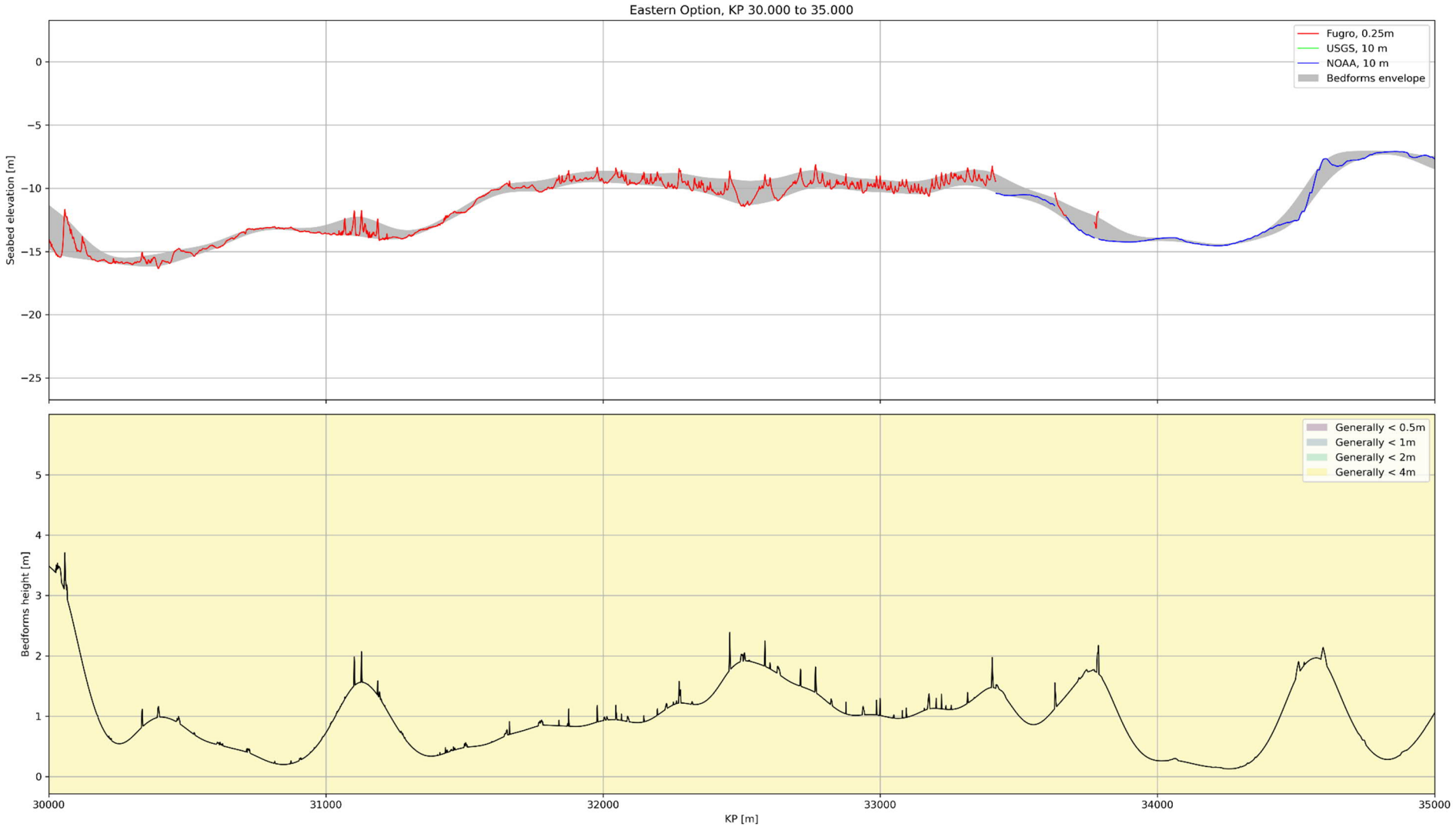
Eastern Option, KP 30.000 to 35.000
Fugro, 0.25m
USGS, 10 m
NOAA, 10 m
Bedforms envelope
Seabed elevation [m]
0
−5
−10
−15
−20
−25
Generally < 0.5m
Generally < 1m
Generally < 2m
Generally < 4m
Bedforms height [m]
0
1
2
3
4
5
30000
31000
32000
33000
34000
35000
KP [m]

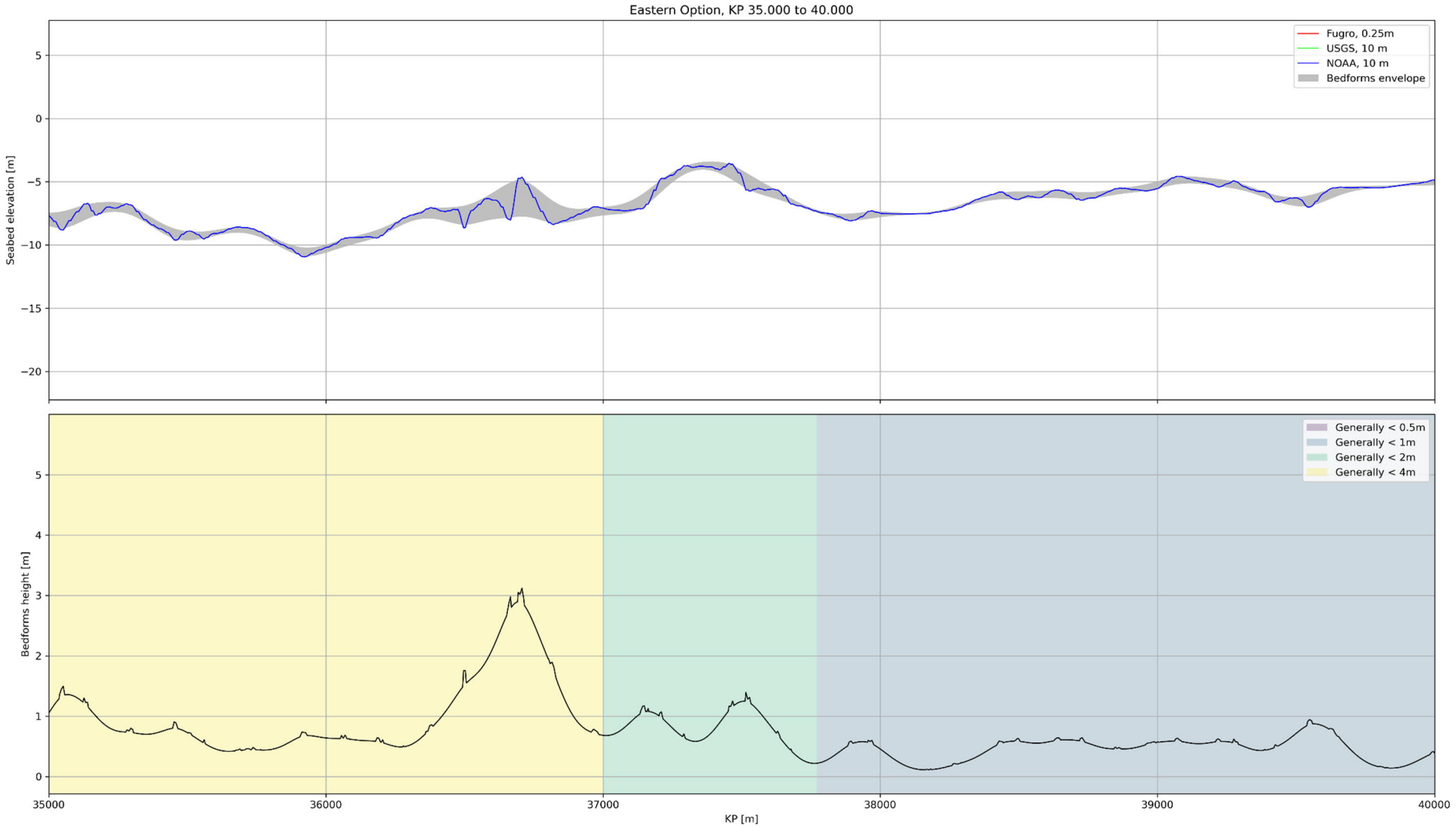
Eastern Option, KP 35.000 to 40.000
Fugro, 0.25m
USGS, 10 m
NOAA, 10 m
Bedforms envelope
Seabed elevation [m]
5
0
−5
−10
−15
−20
Generally < 0.5m
Generally < 1m
Generally < 2m
Generally < 4m
Bedforms height [m]
5
4
3
2
1
0
35000
36000
37000
38000
39000
40000
KP [m]

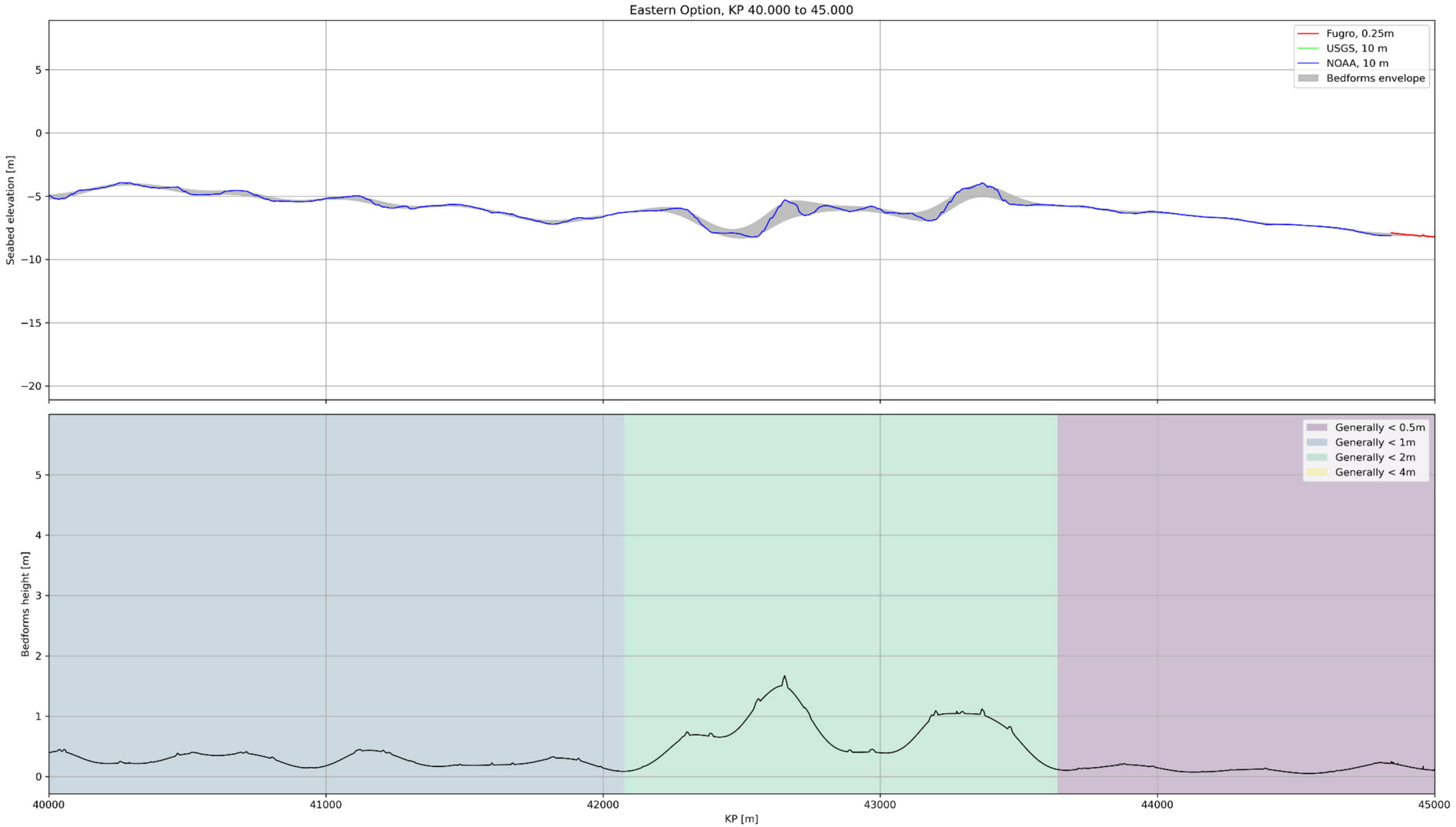
Eastern Option, KP 40.000 to 45.000
Fugro, 0.25m
USGS, 10 m
NOAA, 10 m
Bedforms envelope
Seabed elevation [m]
5
0
−5
−10
−15
−20
Generally < 0.5m
Generally < 1m
Generally < 2m
Generally < 4m
Bedforms height [m]
5
4
3
2
1
0
40000
41000
42000
43000
44000
45000
KP [m]

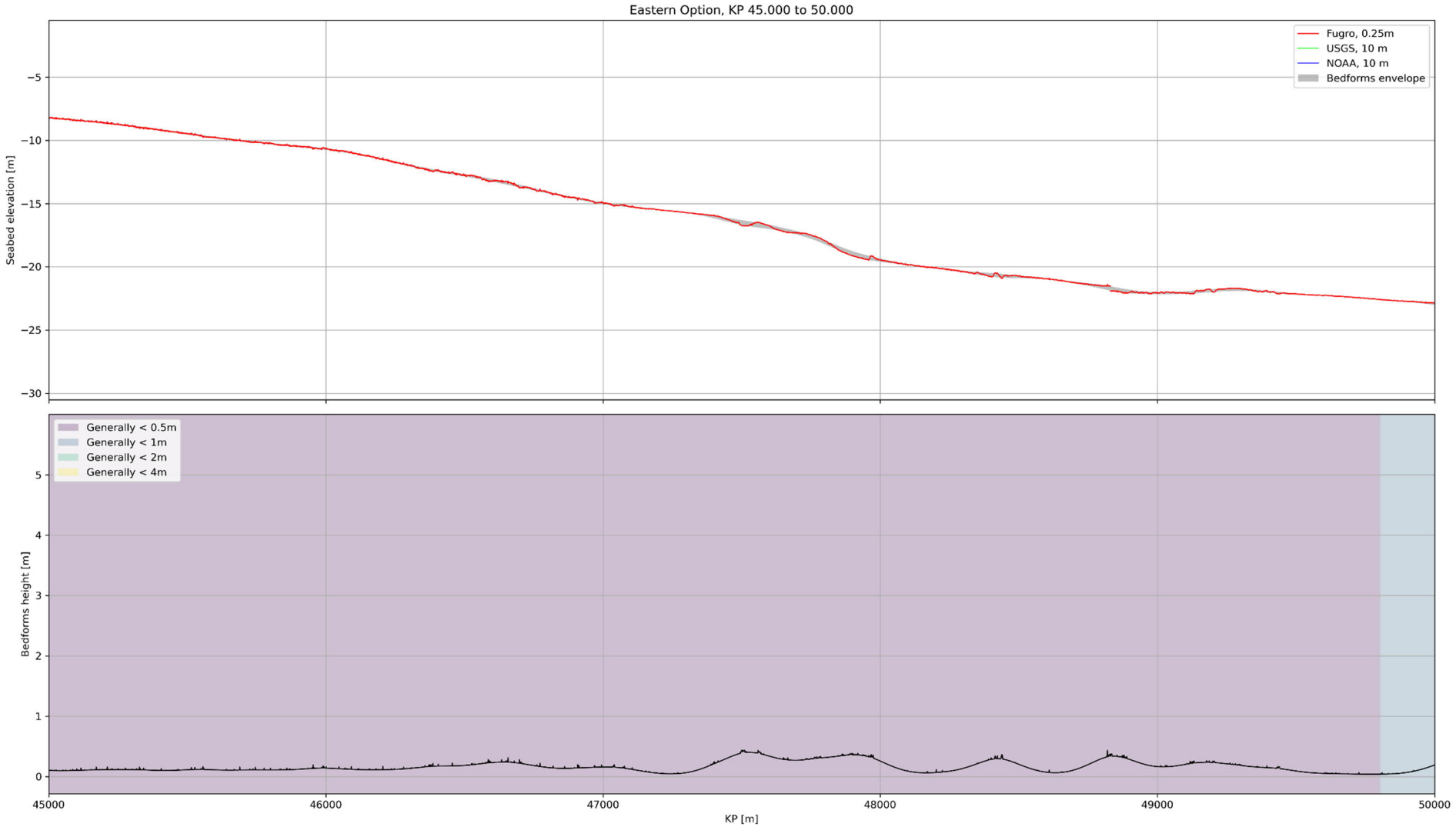
Eastern Option, KP 45.000 to 50.000
Fugro, 0.25m
USGS, 10 m
NOAA, 10 m
Bedforms envelope
Seabed elevation [m]
−5
−10
−15
−20
−25
−30
Generally < 0.5m
Generally < 1m
Generally < 2m
Generally < 4m
Bedforms height [m]
0
1
2
3
4
5
45000
46000
47000
48000
49000
50000
KP [m]

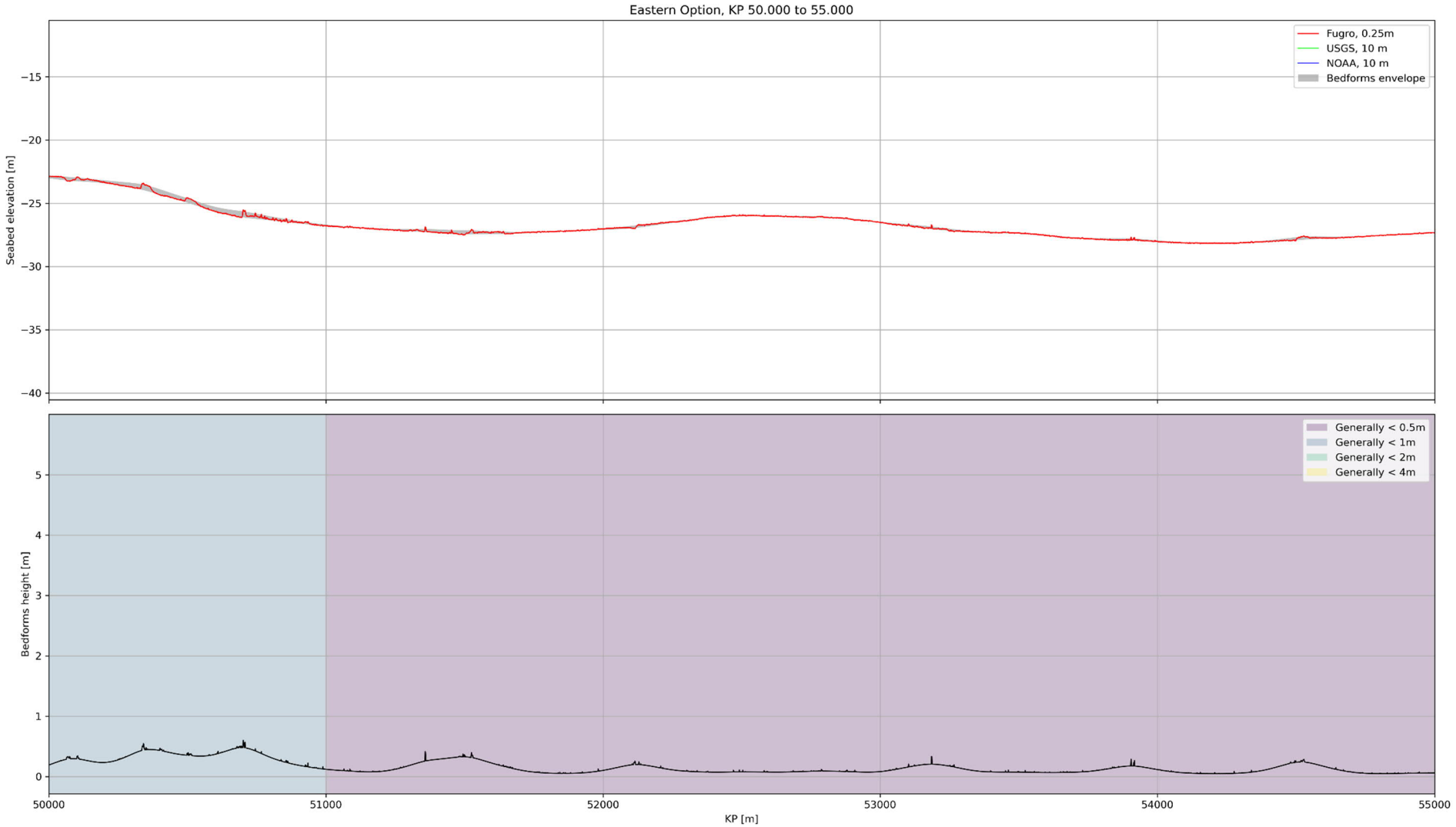
Eastern Option, KP 50.000 to 55.000
Fugro, 0.25m
USGS, 10 m
NOAA, 10 m
Bedforms envelope
Seabed elevation [m]
−15
−20
−25
−30
−35
−40
Generally < 0.5m
Generally < 1m
Generally < 2m
Generally < 4m
Bedforms height [m]
0
1
2
3
4
5
50000
51000
52000
53000
54000
55000
KP [m]

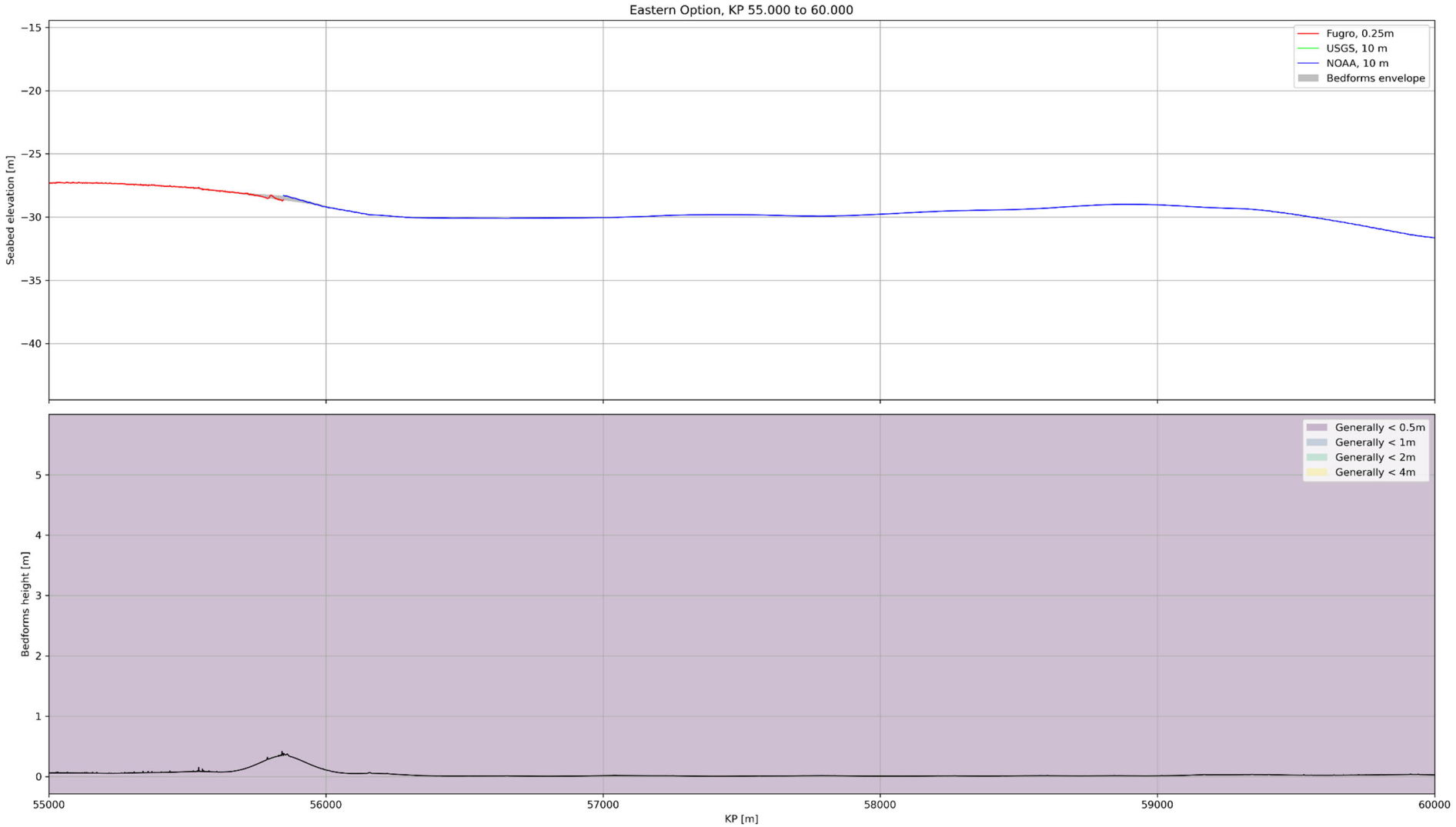
Eastern Option, KP 55.000 to 60.000
Fugro, 0.25m
USGS, 10 m
NOAA, 10 m
Bedforms envelope
Seabed elevation [m]
−15
−20
−25
−30
−35
−40
Generally < 0.5m
Generally < 1m
Generally < 2m
Generally < 4m
Bedforms height [m]
0
1
2
3
4
5
55000
56000
57000
58000
59000
60000
KP [m]

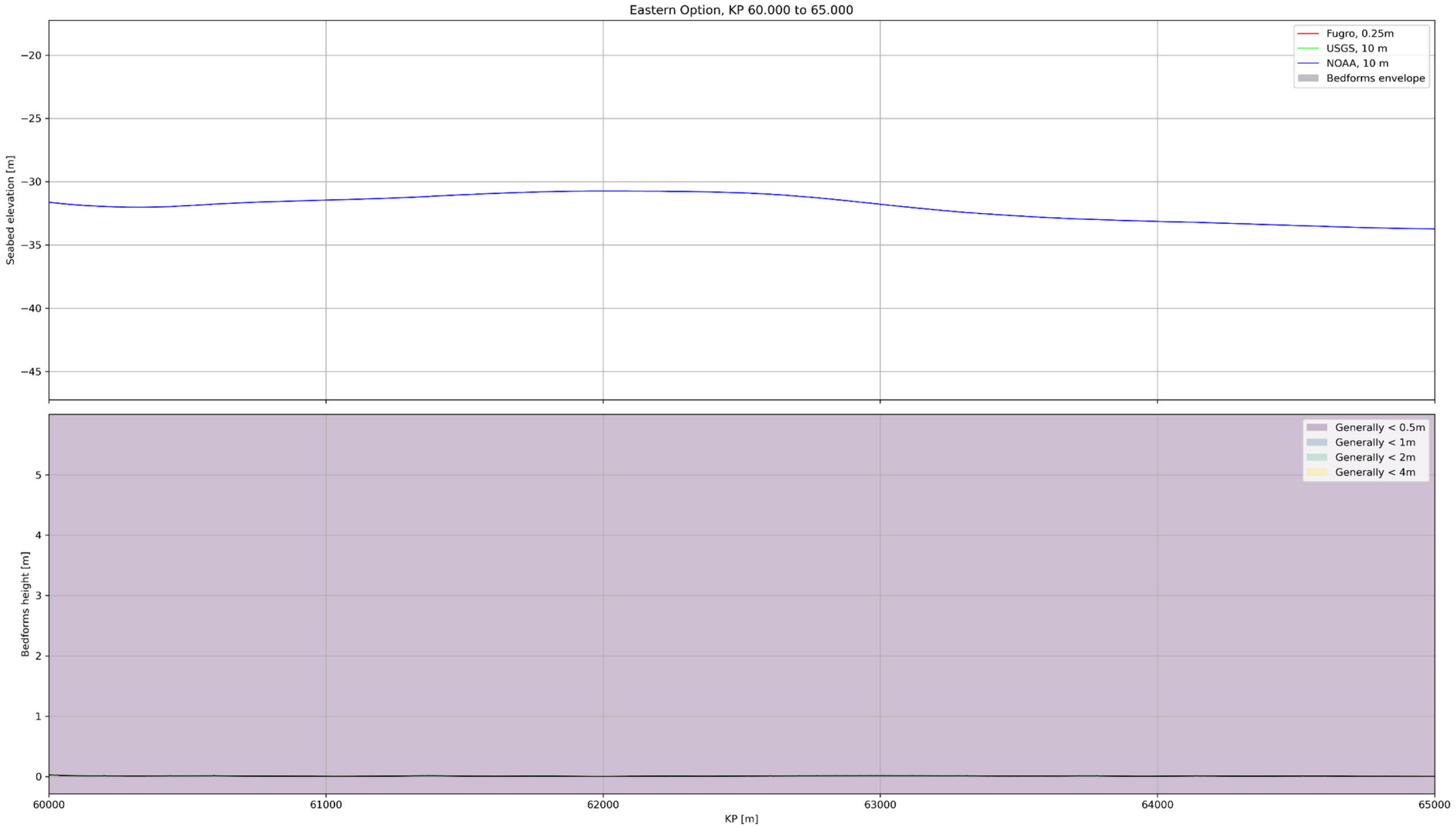
Eastern Option, KP 60.000 to 65.000
Fugro, 0.25m
USGS, 10 m
NOAA, 10 m
Bedforms envelope
Seabed elevation [m]
−20
−25
−30
−35
−40
−45
Generally < 0.5m
Generally < 1m
Generally < 2m
Generally < 4m
Bedforms height [m]
0
1
2
3
4
5
60000
61000
62000
63000
64000
65000
KP [m]

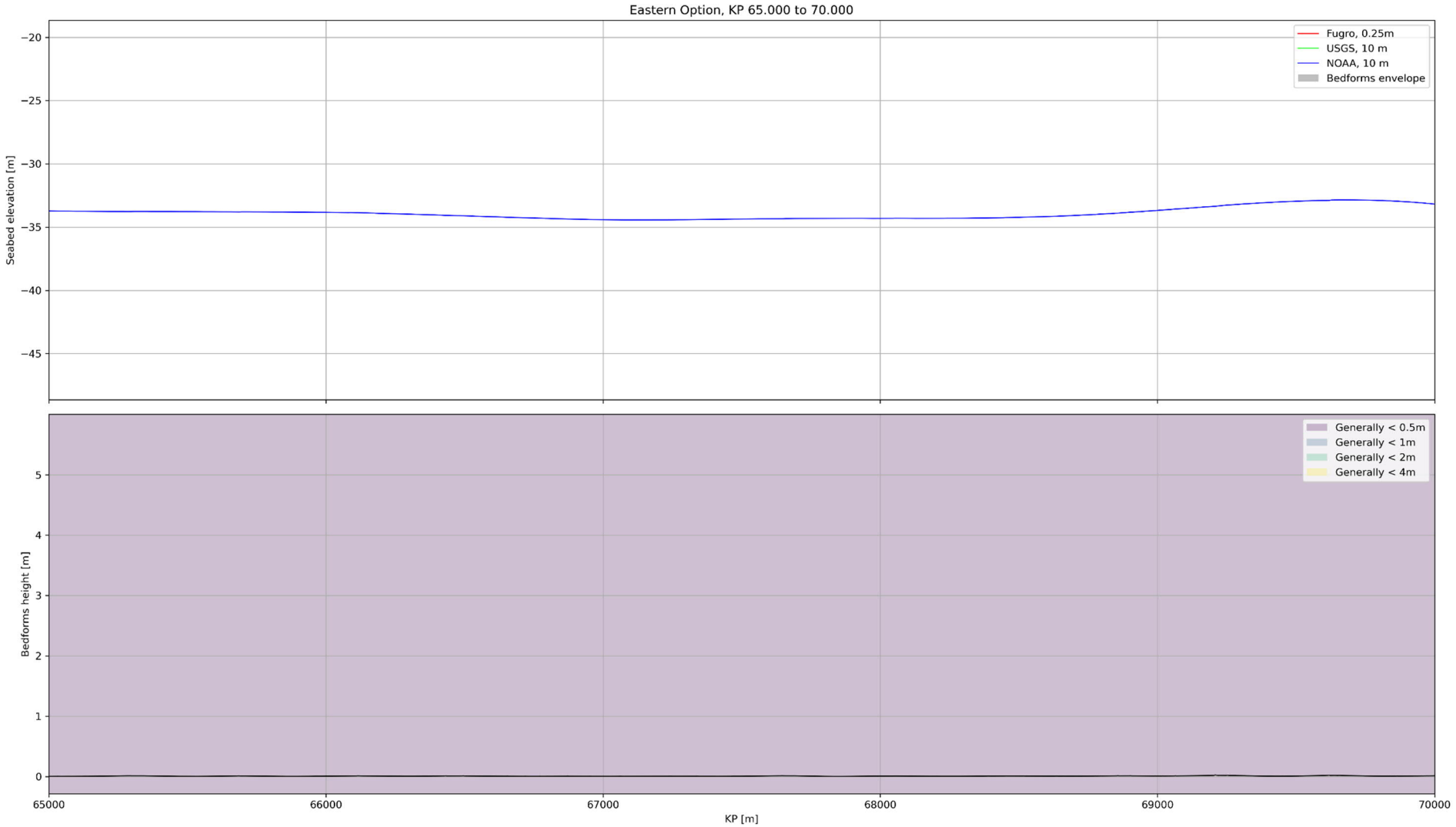
Eastern Option, KP 65.000 to 70.000
Fugro, 0.25m
USGS, 10 m
NOAA, 10 m
Bedforms envelope
Seabed elevation [m]
−20
−25
−30
−35
−40
−45
Generally < 0.5m
Generally < 1m
Generally < 2m
Generally < 4m
Bedforms height [m]
0
1
2
3
4
5
65000
66000
67000
68000
69000
70000
KP [m]

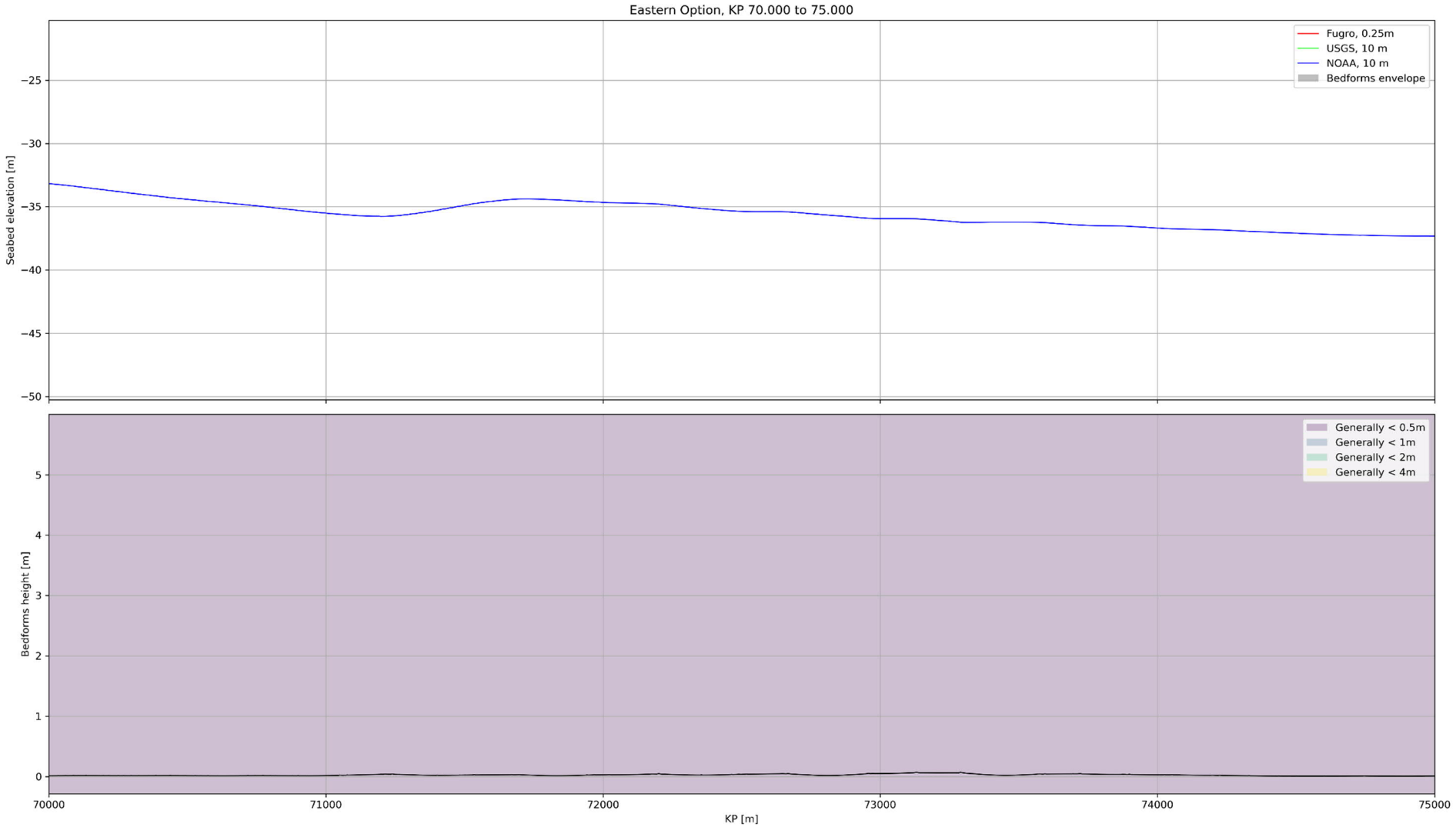
Eastern Option, KP 70.000 to 75.000
Fugro, 0.25m
USGS, 10 m
NOAA, 10 m
Bedforms envelope
Seabed elevation [m]
−25
−30
−35
−40
−45
−50
Generally < 0.5m
Generally < 1m
Generally < 2m
Generally < 4m
Bedforms height [m]
0
1
2
3
4
5
70000
71000
72000
73000
74000
75000
KP [m]


Eastern Option, KP 75.000 to 80.000
Fugro, 0.25m
USGS, 10 m
NOAA, 10 m
Bedforms envelope
Seabed elevation [m]
−25
−30
−35
−40
−45
−50
Generally < 0.5m
Generally < 1m
Generally < 2m
Generally < 4m
Bedforms height [m]
0
1
2
3
4
5
75000
76000
77000
78000
79000
80000
KP [m]


Eastern Option, KP 80.000 to 85.000
Seabed elevation [m]
−25
−30
−35
−40
−45
−50
Fugro, 0.25m
USGS, 10 m
NOAA, 10 m
Bedforms envelope
Bedforms height [m]
0
1
2
3
4
5
Generally < 0.5m
Generally < 1m
Generally < 2m
Generally < 4m
80000
81000
82000
83000
84000
85000
KP [m]


Eastern Option, KP 85.000 to 85.387
Fugro, 0.25m
USGS, 10 m
NOAA, 10 m
Bedforms envelope
Seabed elevation [m]
−25
−30
−35
−40
−45
−50
Generally < 0.5m
Generally < 1m
Generally < 2m
Generally < 4m
Bedforms height [m]
5
4
3
2
1
0
85000
86000
87000
88000
89000
90000
KP [m]

D.3 Offshore Export Cable Route - Western Option

This section shows seabed elevation profiles along the Western Option export cable route, including an envelope of lower/higher expected values of local bedforms elevation. Bedform heights are estimated based on this envelope. A morphological zonation is then defined on the route using the bedforms height. Figure D.3 shows the seabed elevation profile, bedforms height, and zonation along the whole route, while the following figures focus on 5-km long sections for improved readability.

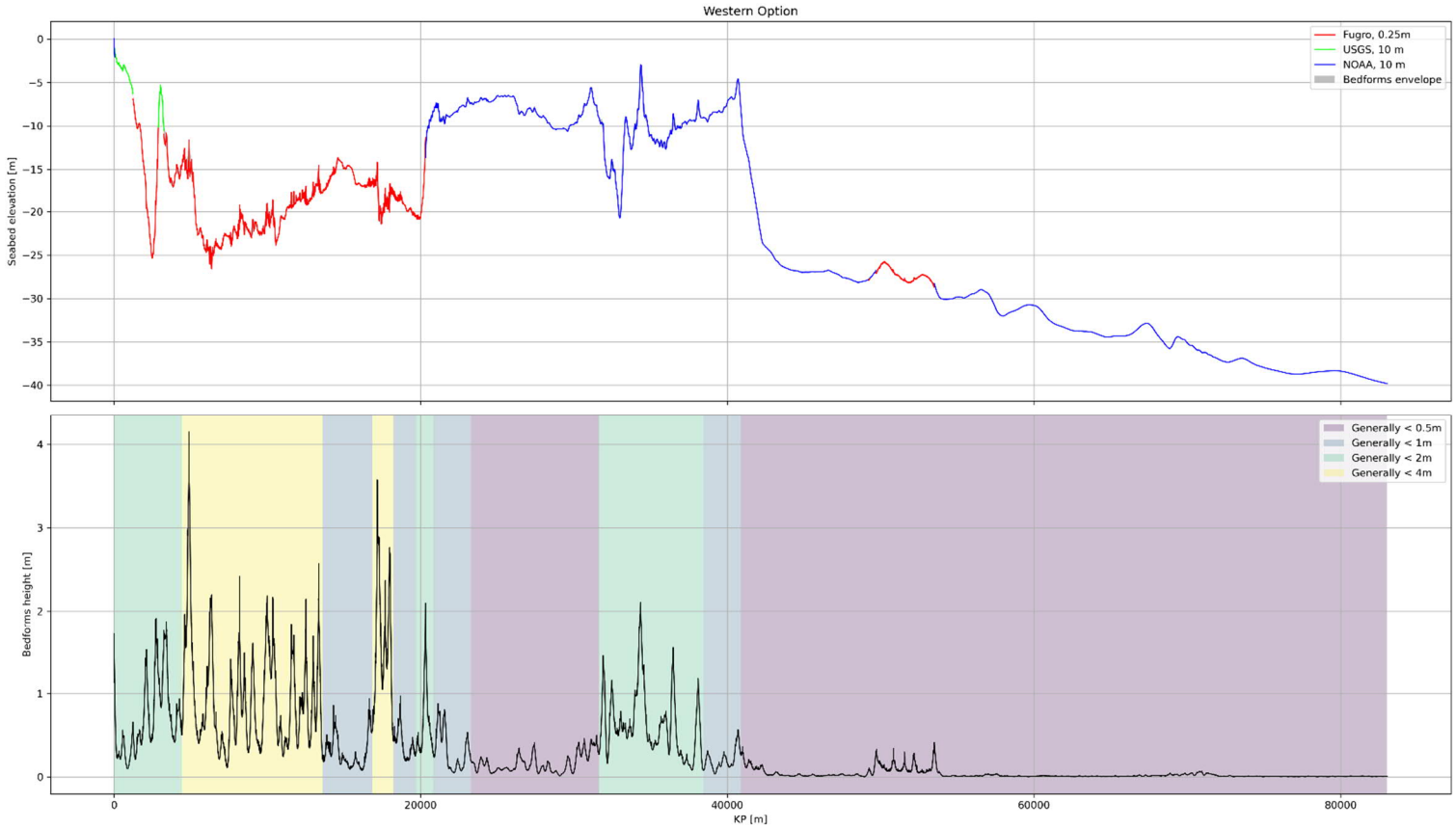

Figure D.3: Seabed elevation profile using the locally most accurate bathymetry (up). Computed bedforms heights and morphological zonation (down).

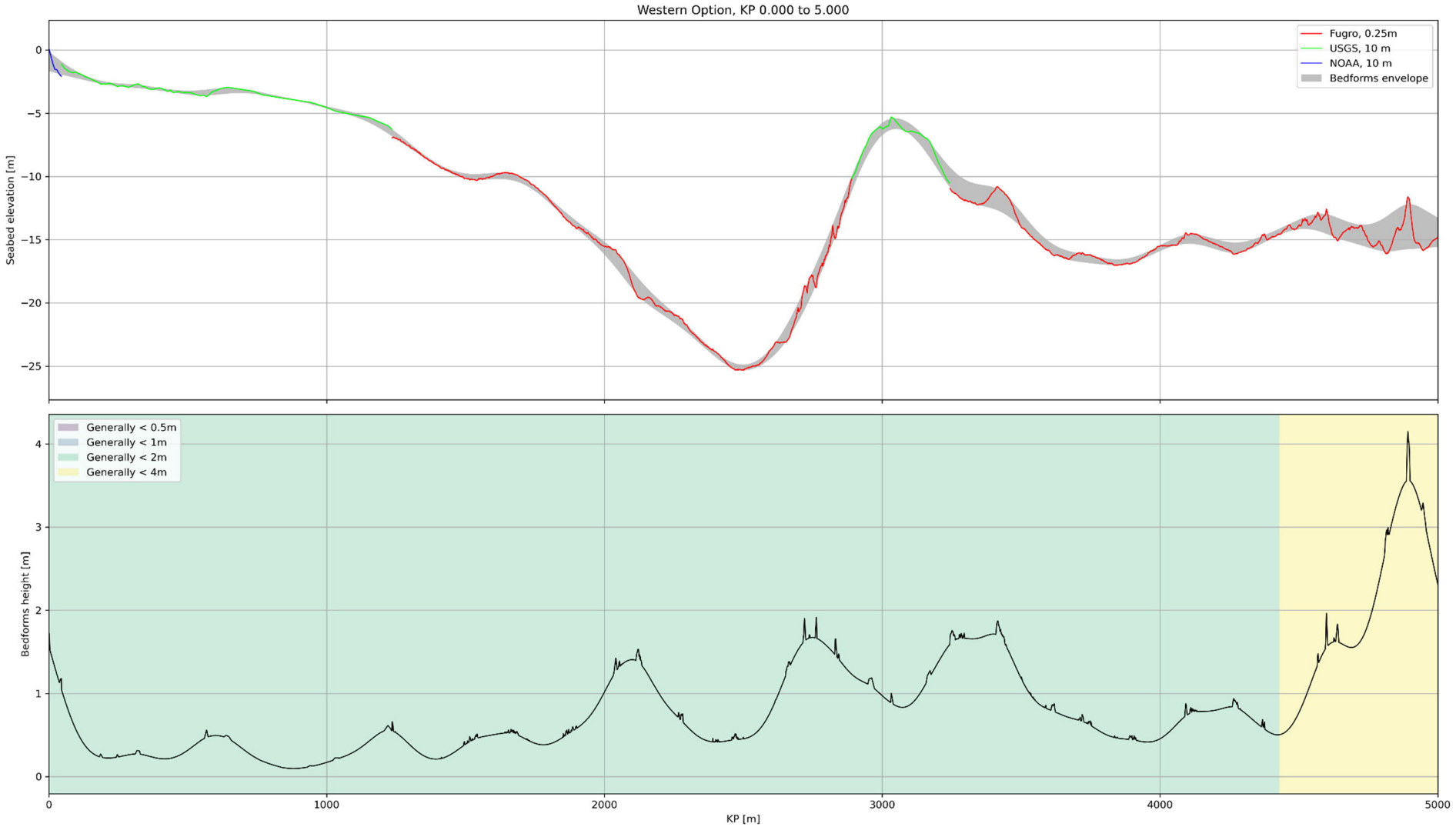
Western Option, KP 0.000 to 5.000
Fugro, 0.25m
USGS, 10 m
NOAA, 10 m
Bedforms envelope
Seabed elevation [m]
0
−5
−10
−15
−20
−25
Generally < 0.5m
Generally < 1m
Generally < 2m
Generally < 4m
Bedforms height [m]
0
1
2
3
4
0
1000
2000
3000
4000
5000
KP [m]

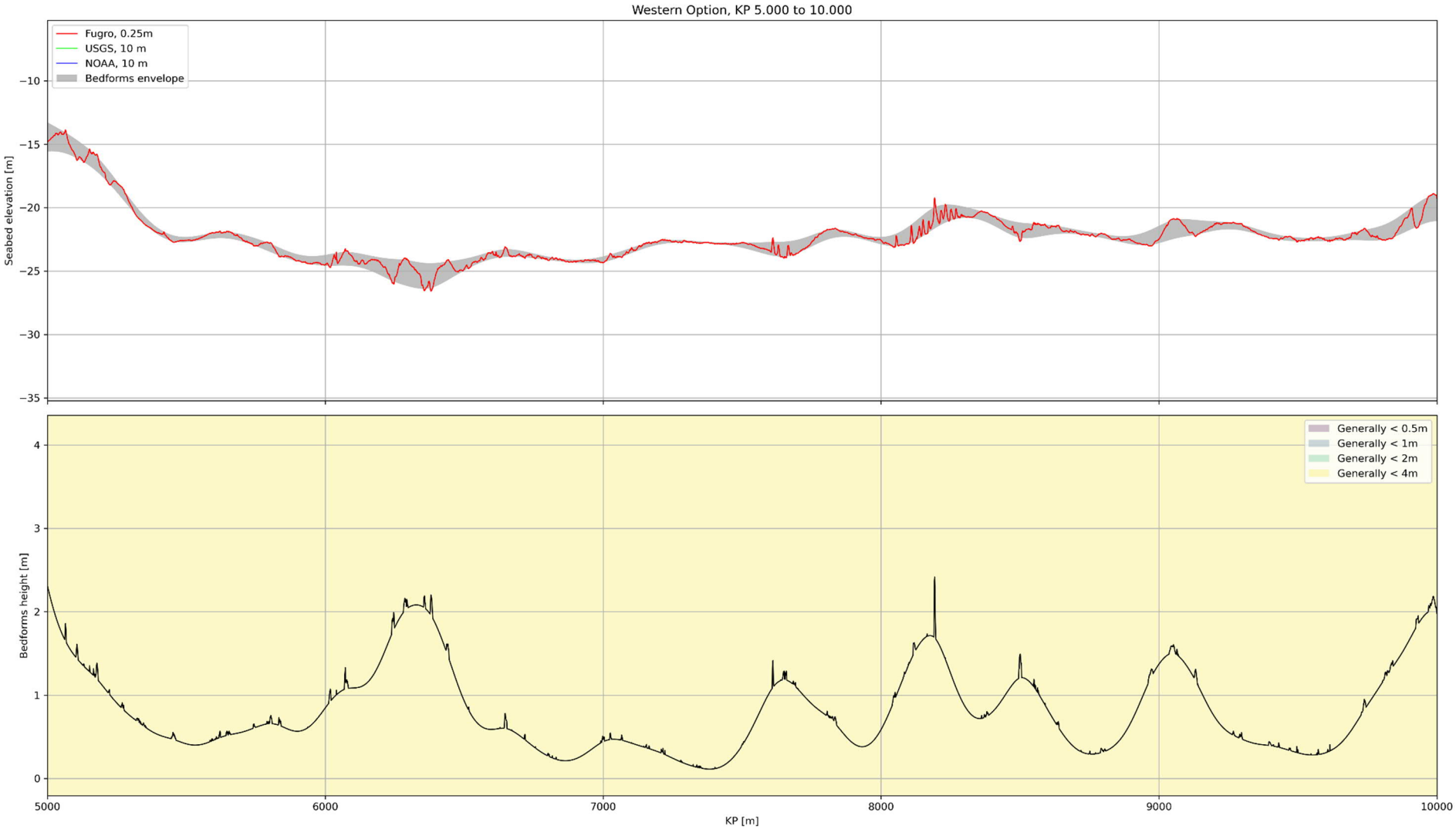
Western Option, KP 5.000 to 10.000
Fugro, 0.25m
USGS, 10 m
NOAA, 10 m
Bedforms envelope
Seabed elevation [m]
−10
−15
−20
−25
−30
−35
Generally < 0.5m
Generally < 1m
Generally < 2m
Generally < 4m
Bedforms height [m]
0
1
2
3
4
5000
6000
7000
8000
9000
10000
KP [m]

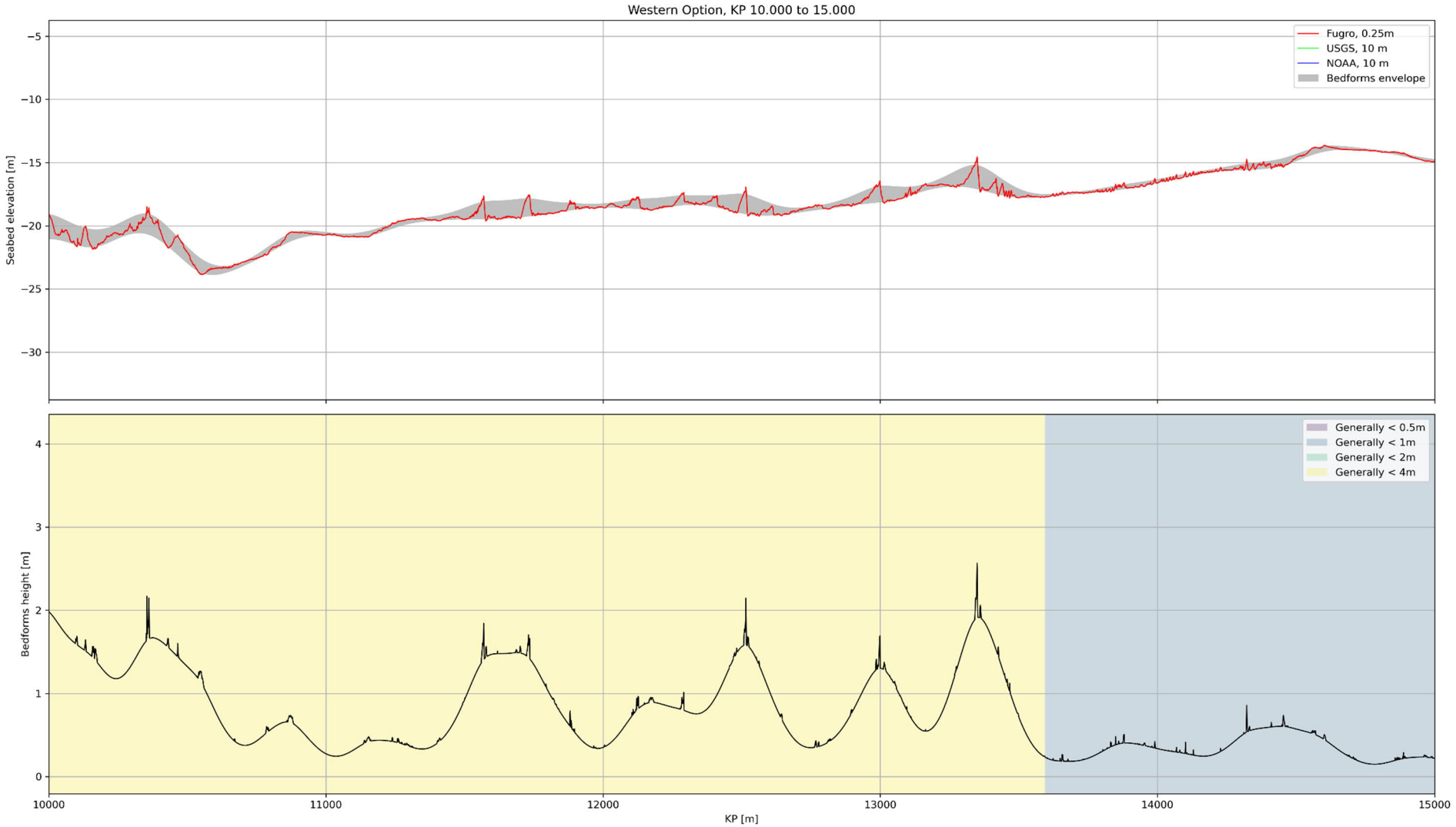
Western Option, KP 10.000 to 15.000
Fugro, 0.25m
USGS, 10 m
NOAA, 10 m
Bedforms envelope
Seabed elevation [m]
−5
−10
−15
−20
−25
−30
Generally < 0.5m
Generally < 1m
Generally < 2m
Generally < 4m
Bedforms height [m]
0
1
2
3
4
10000
11000
12000
13000
14000
15000
KP [m]

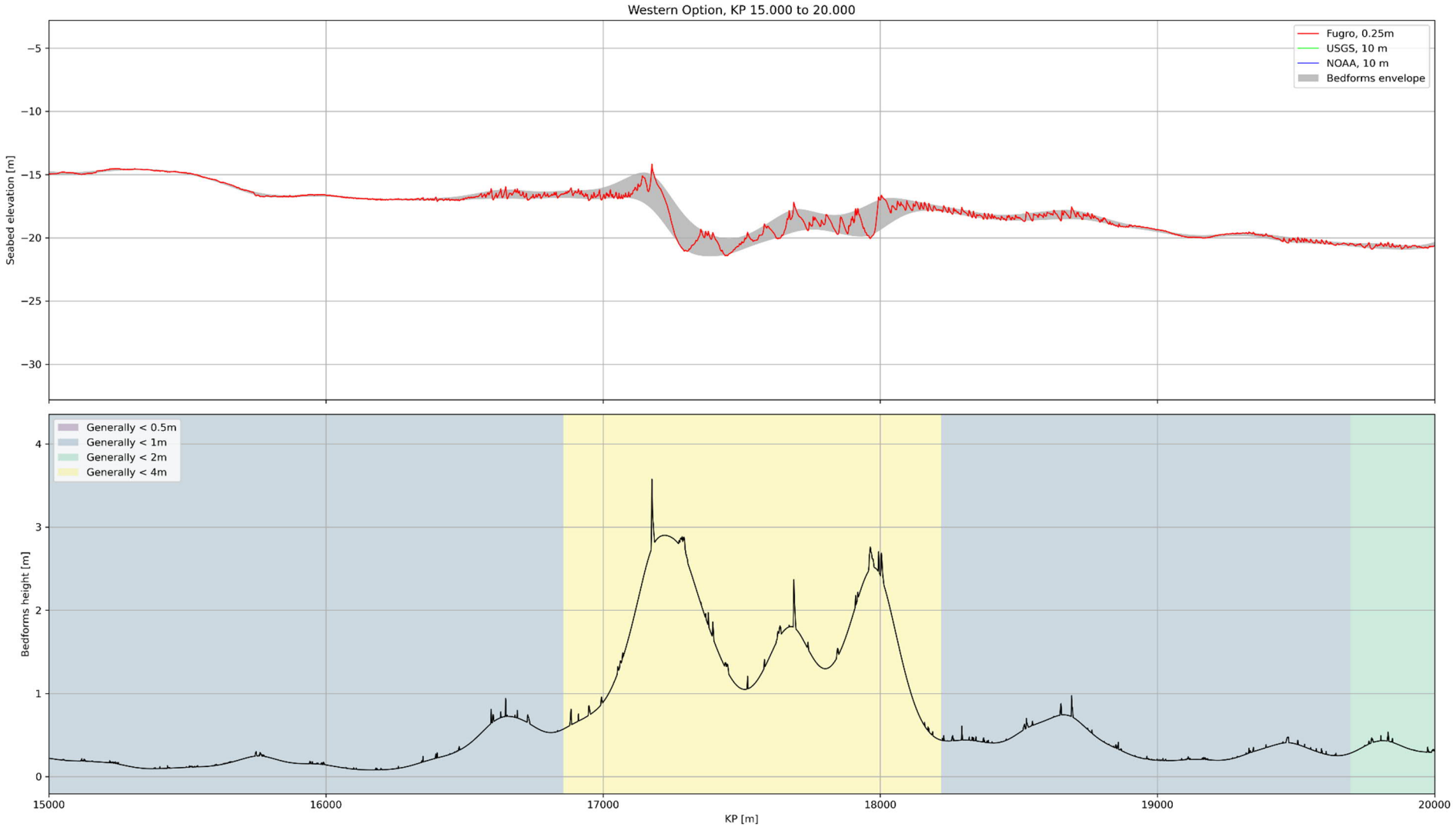
Western Option, KP 15.000 to 20.000
Fugro, 0.25m
USGS, 10 m
NOAA, 10 m
Bedforms envelope
Seabed elevation [m]
−5
−10
−15
−20
−25
−30
Generally < 0.5m
Generally < 1m
Generally < 2m
Generally < 4m
Bedforms height [m]
0
1
2
3
4
15000
16000
17000
18000
19000
20000
KP [m]

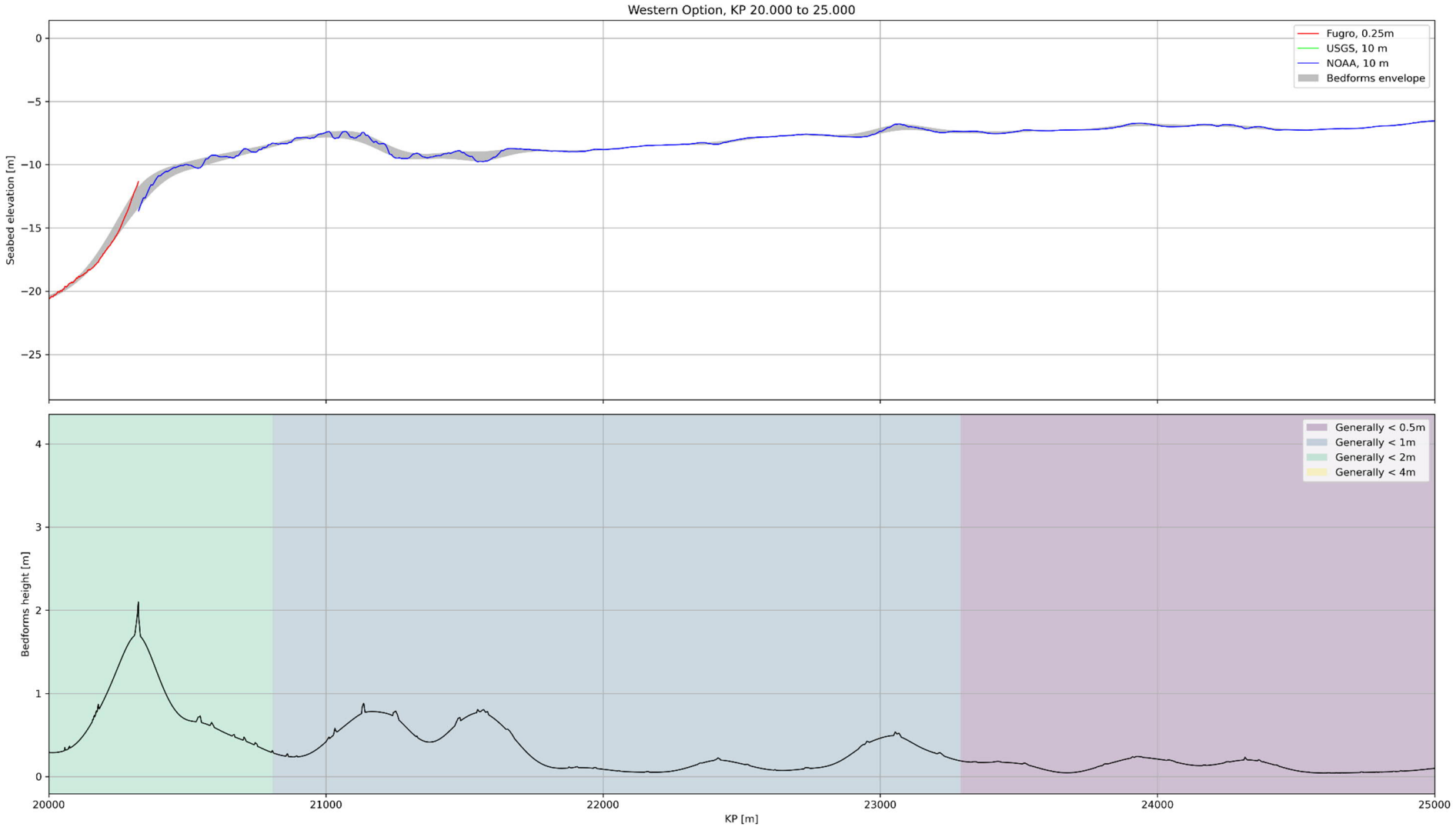
Western Option, KP 20.000 to 25.000
Fugro, 0.25m
USGS, 10 m
NOAA, 10 m
Bedforms envelope
Seabed elevation [m]
0
−5
−10
−15
−20
−25
Generally < 0.5m
Generally < 1m
Generally < 2m
Generally < 4m
Bedforms height [m]
4
3
2
1
0
20000
21000
22000
23000
24000
25000
KP [m]

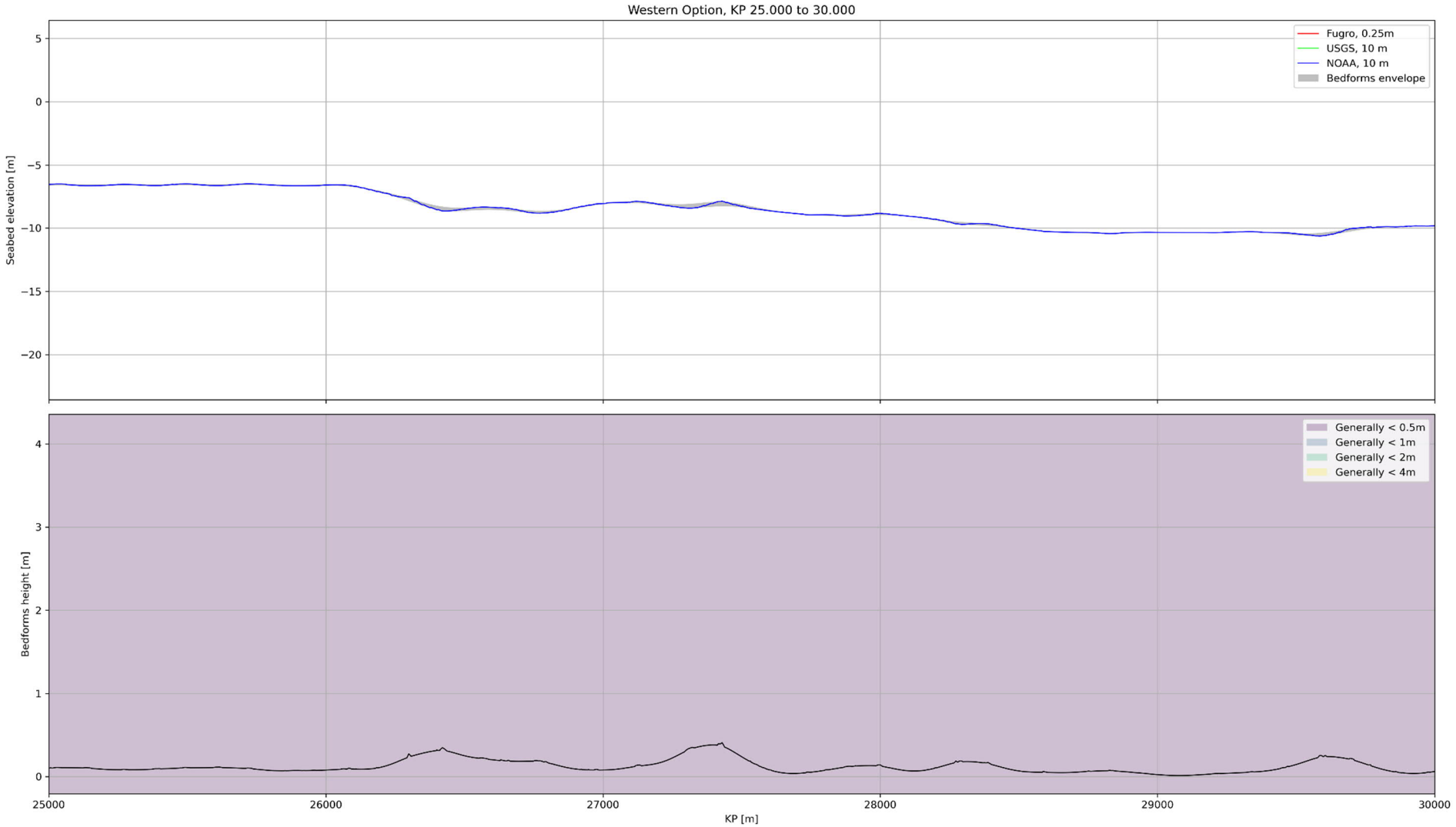
Western Option, KP 25.000 to 30.000
Fugro, 0.25m
USGS, 10 m
NOAA, 10 m
Bedforms envelope
Seabed elevation [m]
5
0
−5
−10
−15
−20
Generally < 0.5m
Generally < 1m
Generally < 2m
Generally < 4m
Bedforms height [m]
4
3
2
1
0
25000
26000
27000
28000
29000
30000
KP [m]

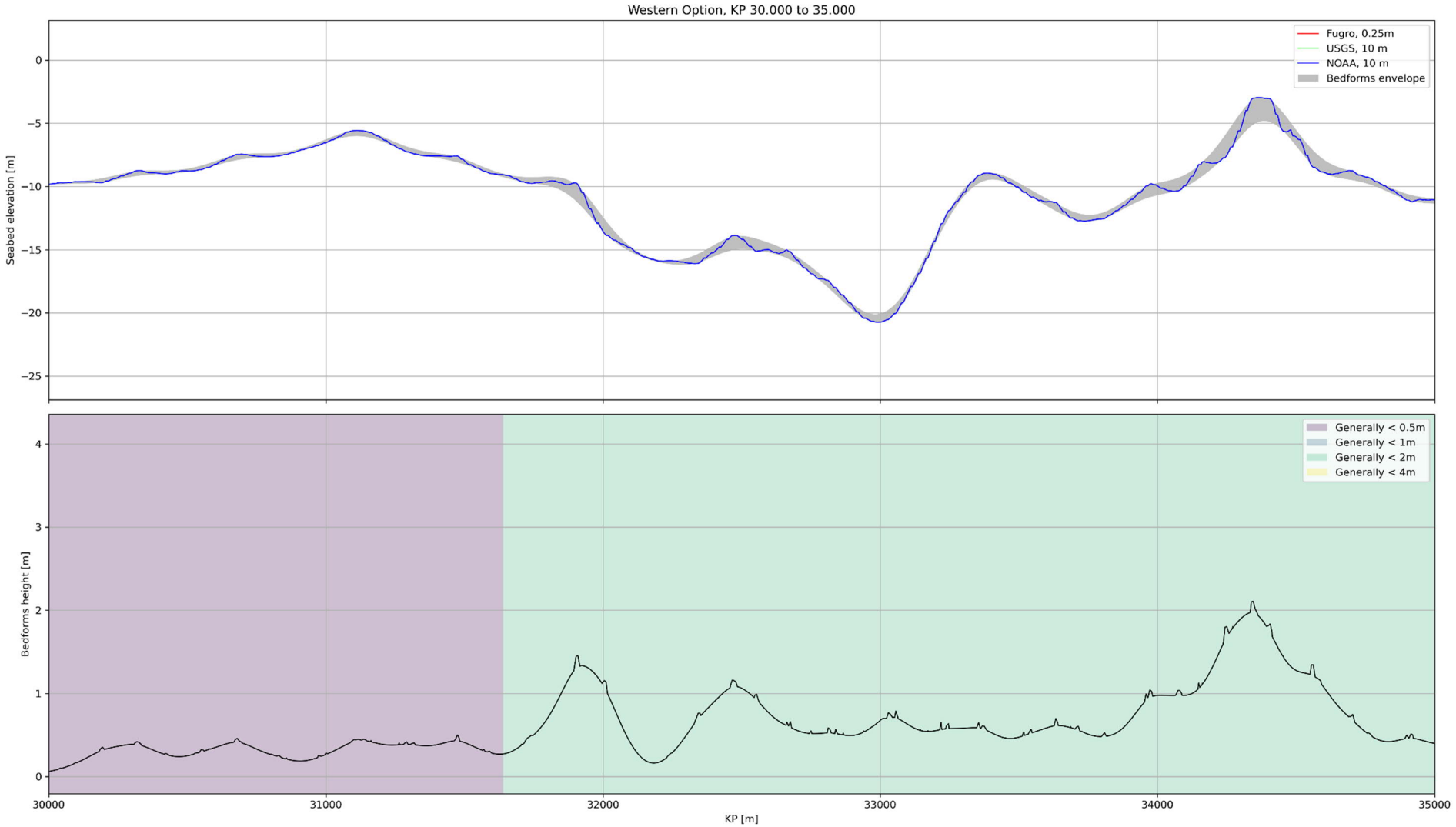
Western Option, KP 30.000 to 35.000
Fugro, 0.25m
USGS, 10 m
NOAA, 10 m
Bedforms envelope
Seabed elevation [m]
0
−5
−10
−15
−20
−25
Generally < 0.5m
Generally < 1m
Generally < 2m
Generally < 4m
Bedforms height [m]
0
1
2
3
4
30000
31000
32000
33000
34000
35000
KP [m]

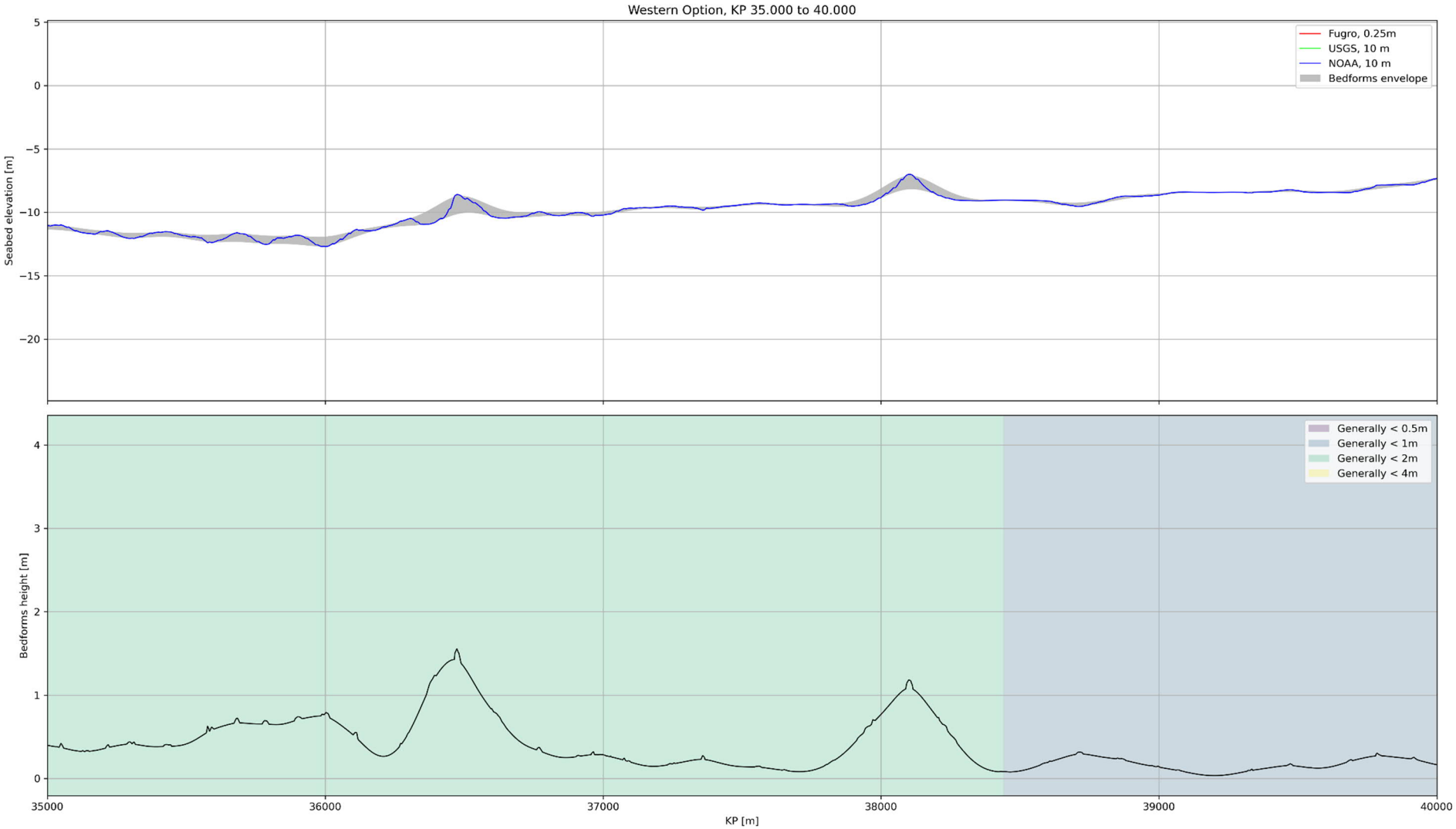
Western Option, KP 35.000 to 40.000
Seabed elevation [m]
Fugro, 0.25m
USGS, 10 m
NOAA, 10 m
Bedforms envelope
Bedforms height [m]
Generally < 0.5m
Generally < 1m
Generally < 2m
Generally < 4m
KP [m]

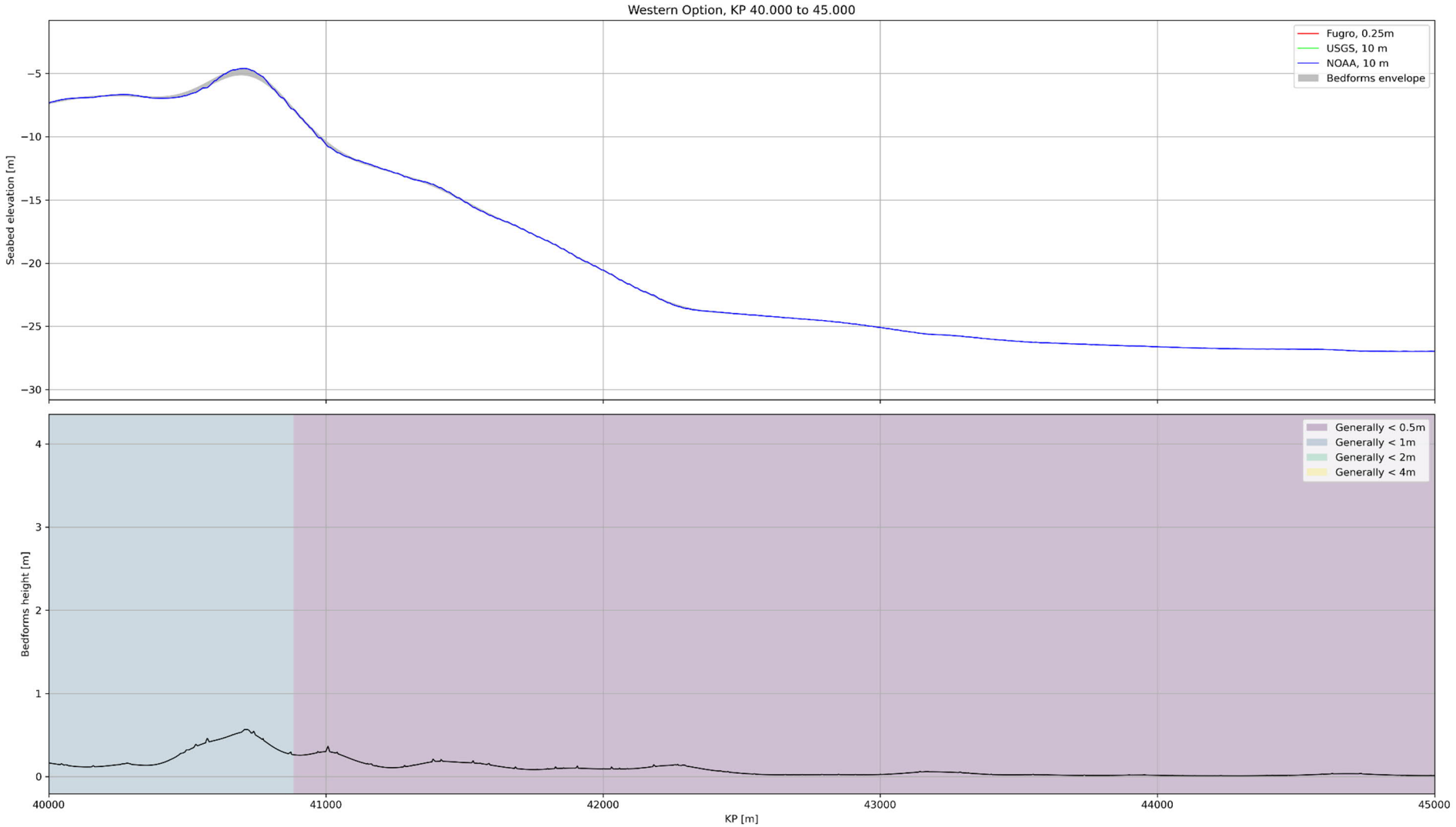
Western Option, KP 40.000 to 45.000
Fugro, 0.25m
USGS, 10 m
NOAA, 10 m
Bedforms envelope
Seabed elevation [m]
−5
−10
−15
−20
−25
−30
Generally < 0.5m
Generally < 1m
Generally < 2m
Generally < 4m
Bedforms height [m]
0
1
2
3
4
40000
41000
42000
43000
44000
45000
KP [m]

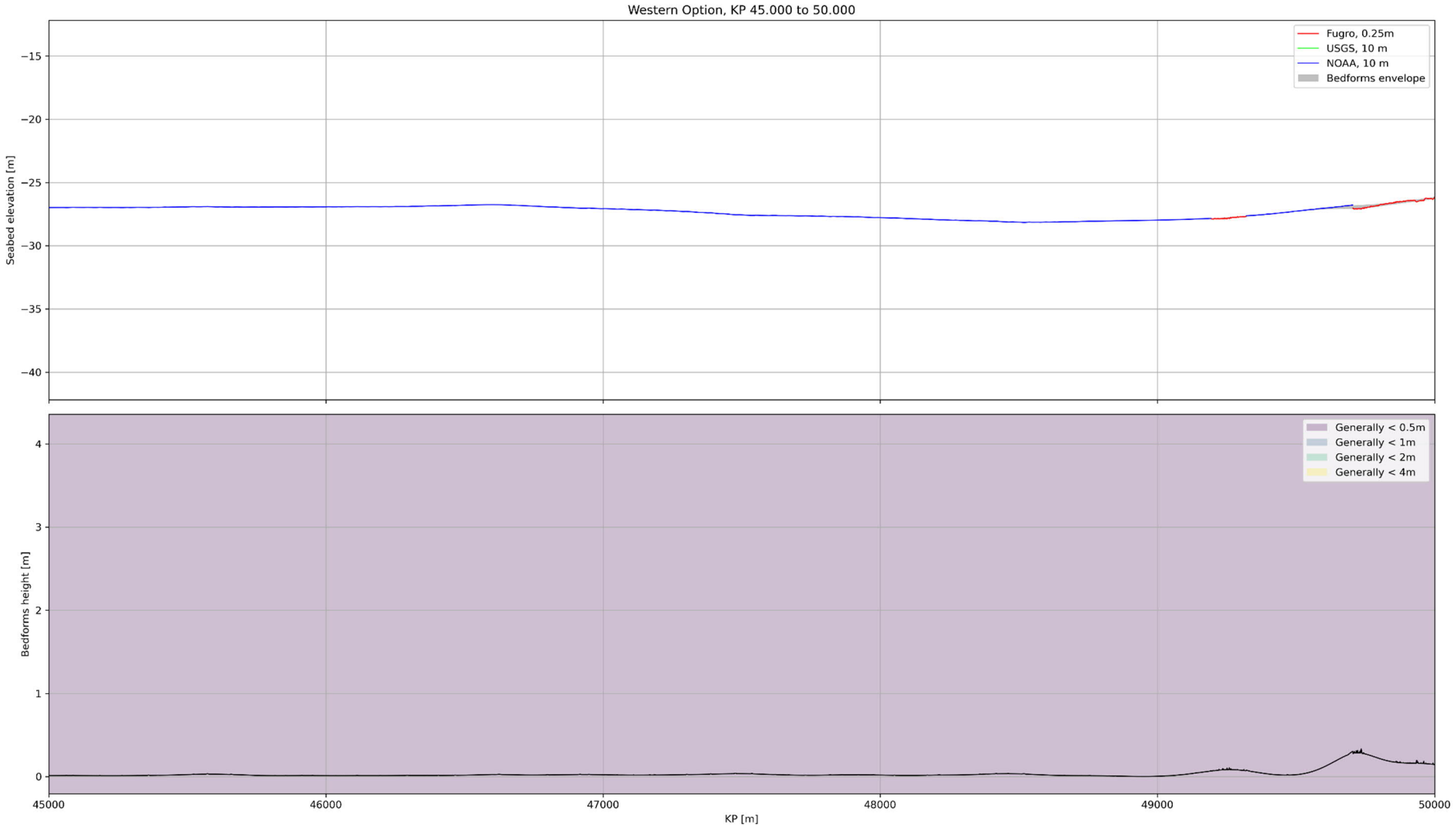
Western Option, KP 45.000 to 50.000
Fugro, 0.25m
USGS, 10 m
NOAA, 10 m
Bedforms envelope
Seabed elevation [m]
−15
−20
−25
−30
−35
−40
Generally < 0.5m
Generally < 1m
Generally < 2m
Generally < 4m
Bedforms height [m]
0
1
2
3
4
45000
46000
47000
48000
49000
50000
KP [m]

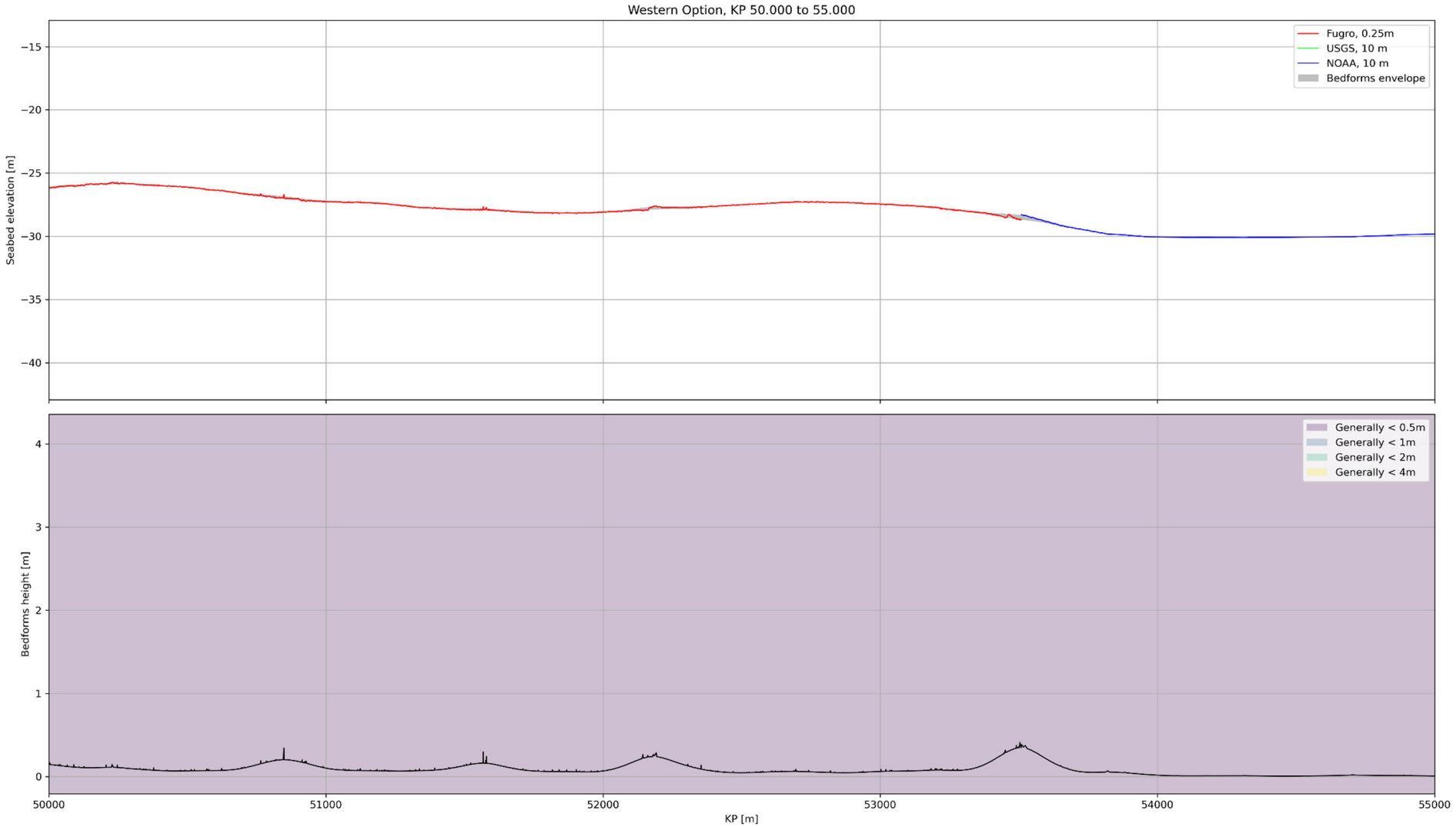
Western Option, KP 50.000 to 55.000
Fugro, 0.25m
USGS, 10 m
NOAA, 10 m
Bedforms envelope
Seabed elevation [m]
−15
−20
−25
−30
−35
−40
Generally < 0.5m
Generally < 1m
Generally < 2m
Generally < 4m
Bedforms height [m]
0
1
2
3
4
50000
51000
52000
53000
54000
55000
KP [m]

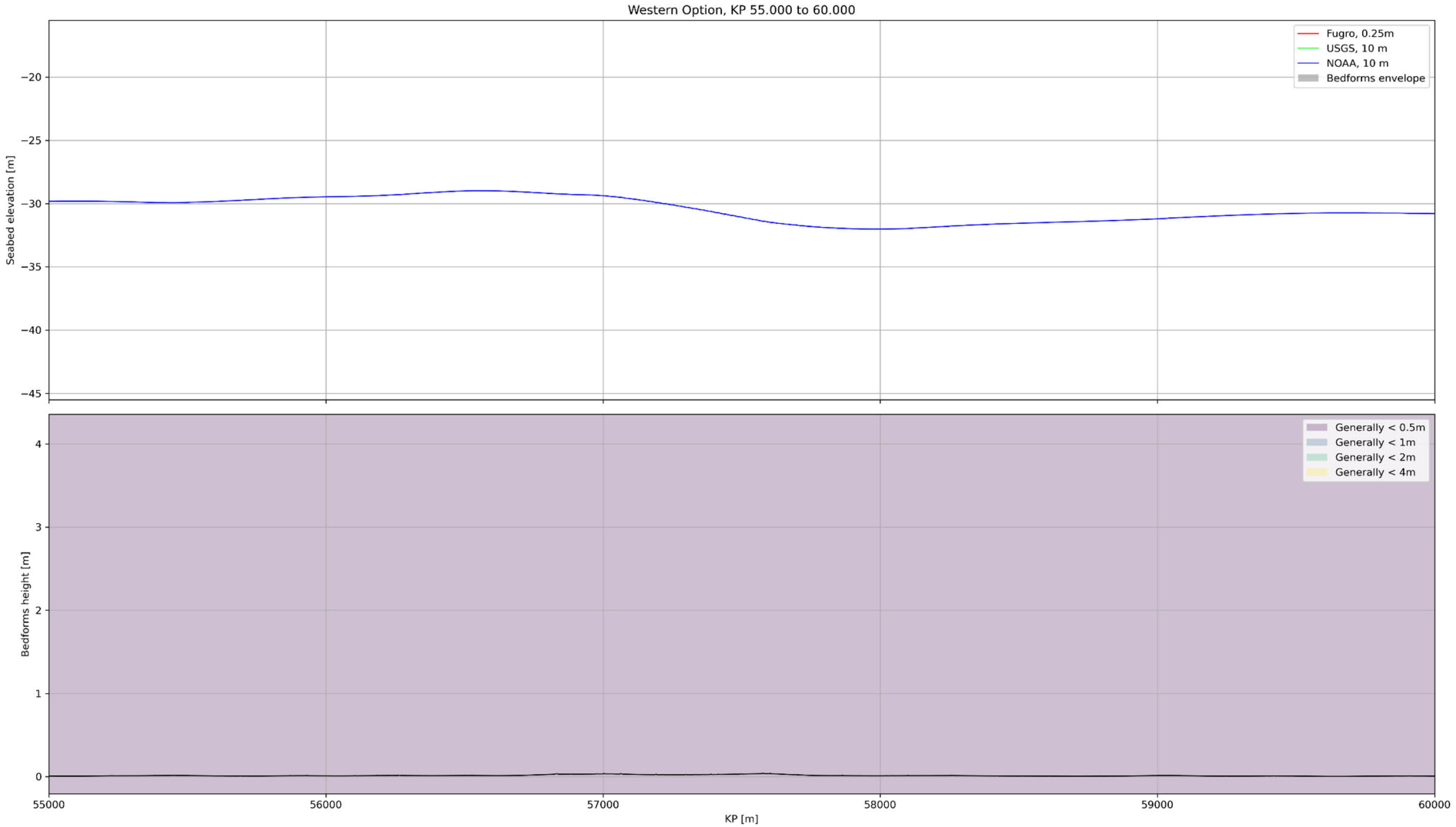
Western Option, KP 55.000 to 60.000
Fugro, 0.25m
USGS, 10 m
NOAA, 10 m
Bedforms envelope
Seabed elevation [m]
−20
−25
−30
−35
−40
−45
Generally < 0.5m
Generally < 1m
Generally < 2m
Generally < 4m
Bedforms height [m]
0
1
2
3
4
55000
56000
57000
58000
59000
60000
KP [m]

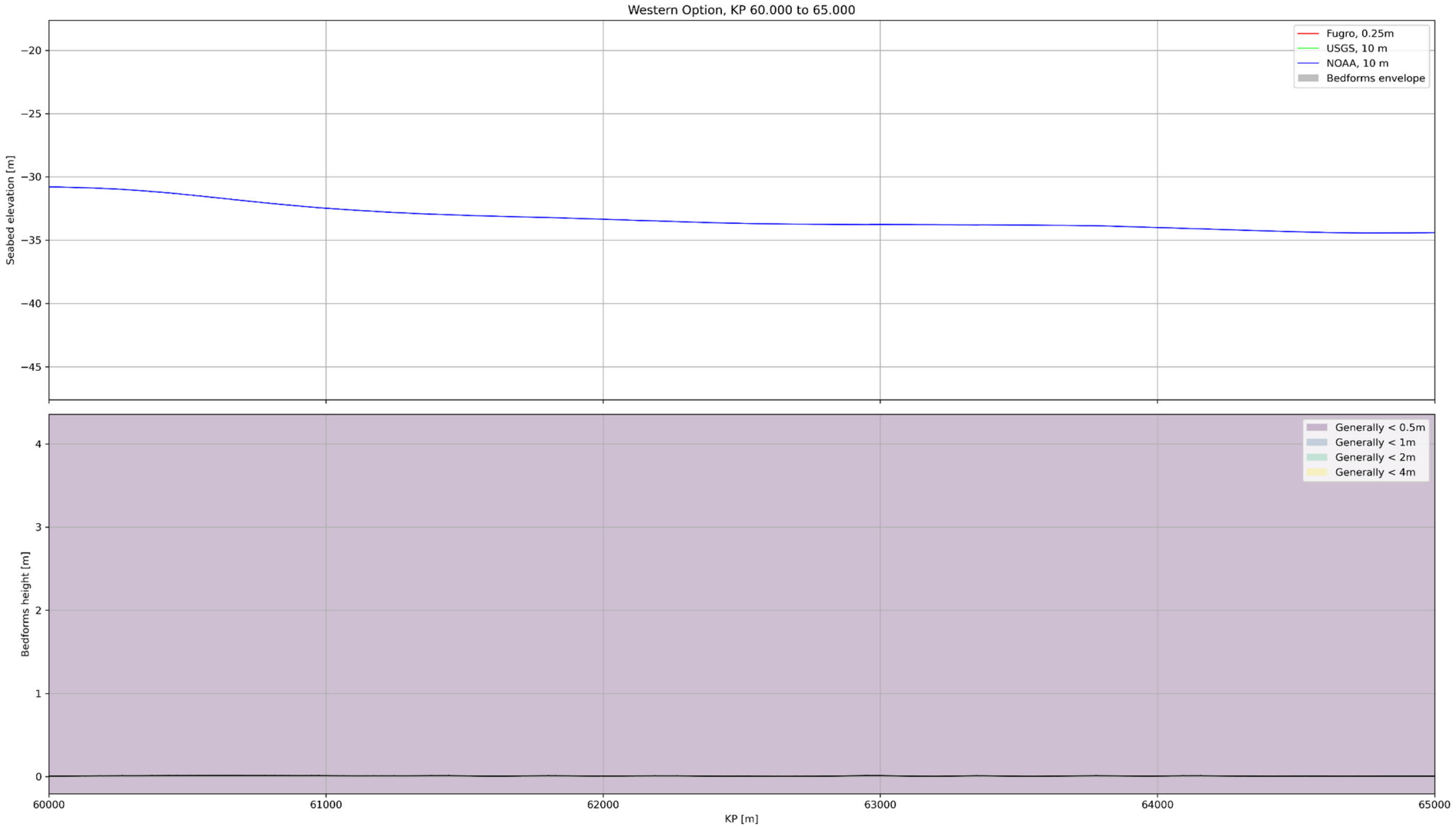
Western Option, KP 60.000 to 65.000
Fugro, 0.25m
USGS, 10 m
NOAA, 10 m
Bedforms envelope
Seabed elevation [m]
−20
−25
−30
−35
−40
−45
Generally < 0.5m
Generally < 1m
Generally < 2m
Generally < 4m
Bedforms height [m]
0
1
2
3
4
60000
61000
62000
63000
64000
65000
KP [m]

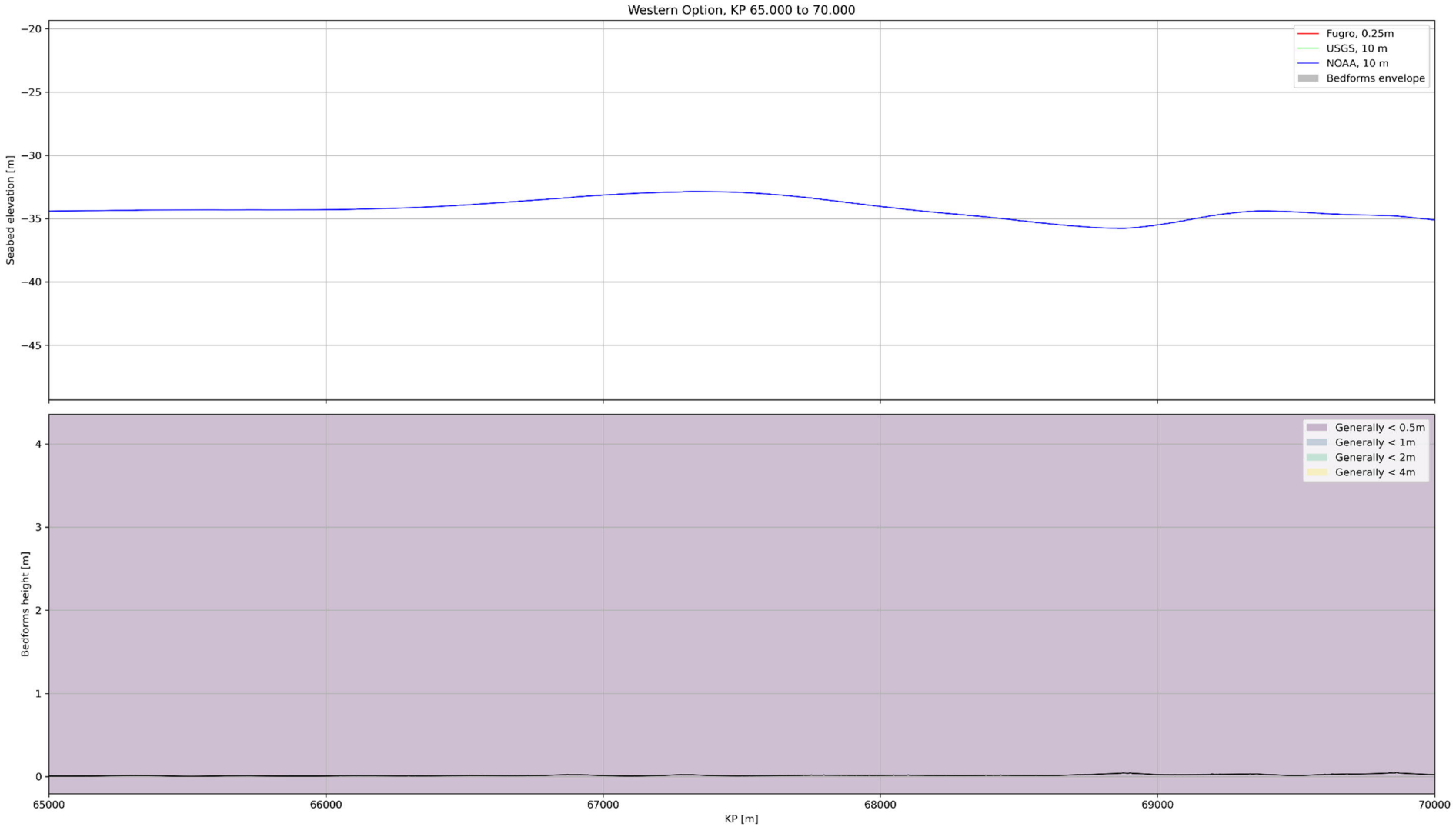
Western Option, KP 65.000 to 70.000
Fugro, 0.25m
USGS, 10 m
NOAA, 10 m
Bedforms envelope
Seabed elevation [m]
−20
−25
−30
−35
−40
−45
Generally < 0.5m
Generally < 1m
Generally < 2m
Generally < 4m
Bedforms height [m]
0
1
2
3
4
65000
66000
67000
68000
69000
70000
KP [m]

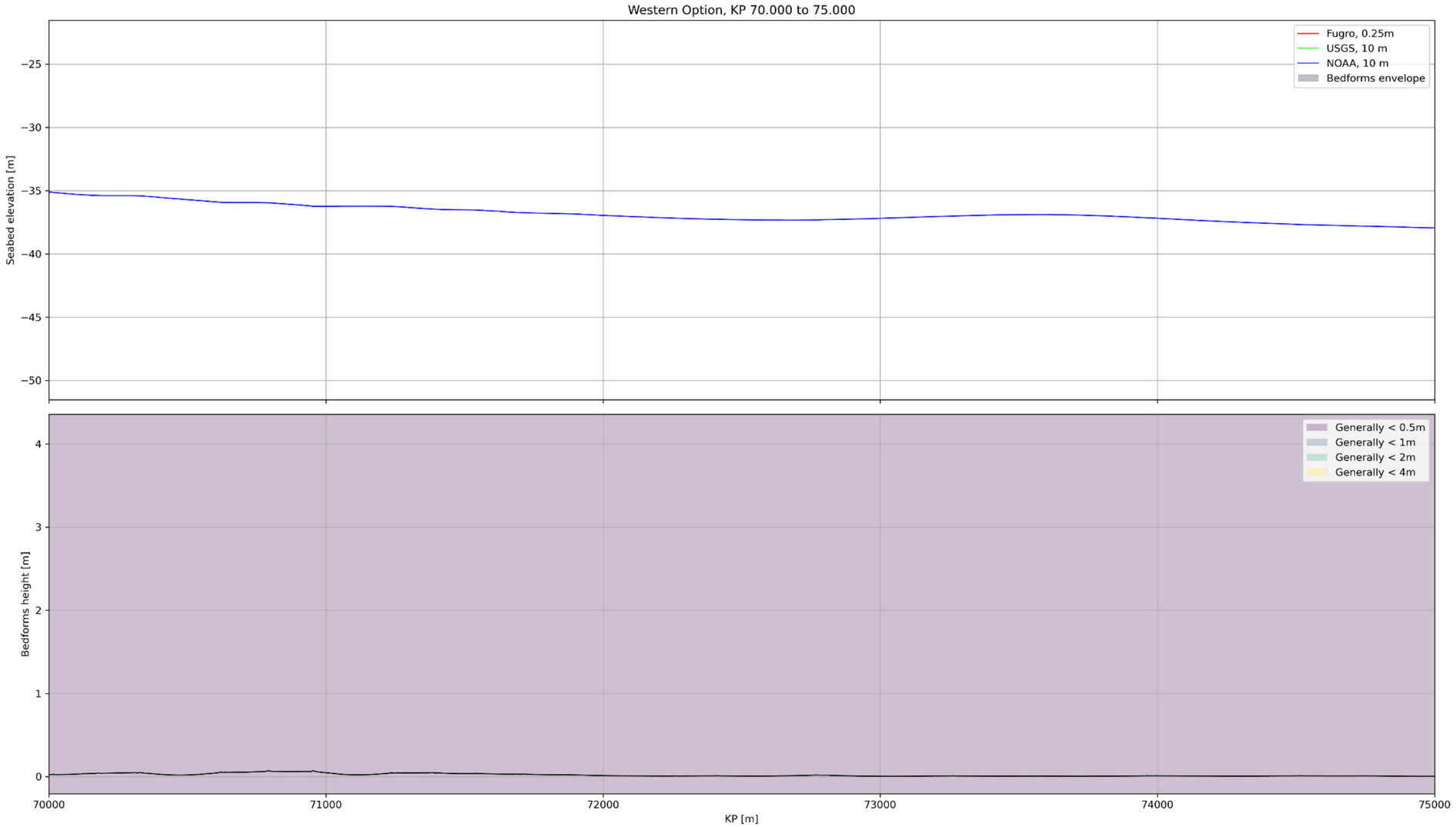
Western Option, KP 70.000 to 75.000
Fugro, 0.25m
USGS, 10 m
NOAA, 10 m
Bedforms envelope
Seabed elevation [m]
−25
−30
−35
−40
−45
−50
Generally < 0.5m
Generally < 1m
Generally < 2m
Generally < 4m
Bedforms height [m]
0
1
2
3
4
70000
71000
72000
73000
74000
75000
KP [m]

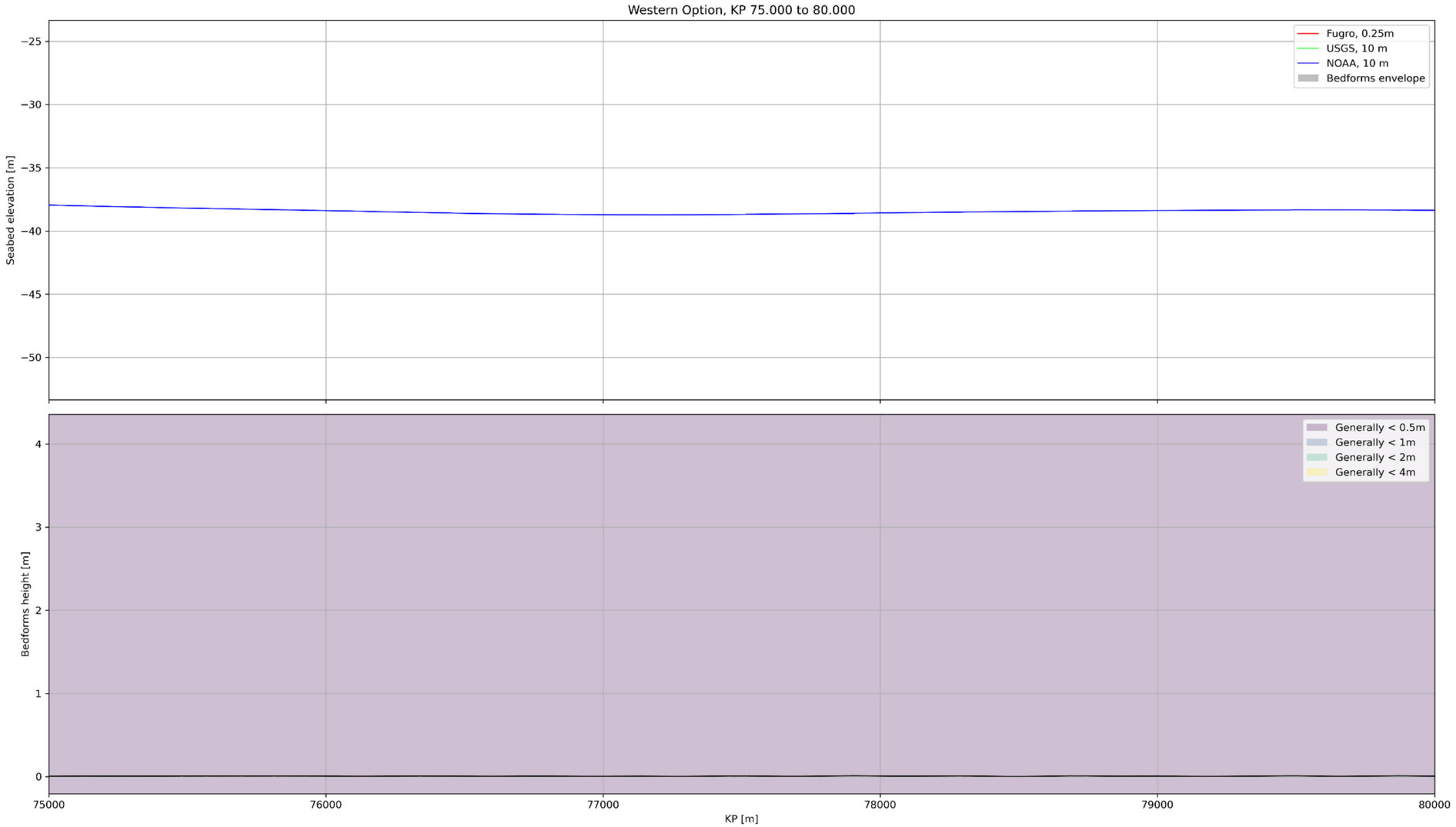
Western Option, KP 75.000 to 80.000
Fugro, 0.25m
USGS, 10 m
NOAA, 10 m
Bedforms envelope
Seabed elevation [m]
−25
−30
−35
−40
−45
−50
Generally < 0.5m
Generally < 1m
Generally < 2m
Generally < 4m
Bedforms height [m]
0
1
2
3
4
75000
76000
77000
78000
79000
80000
KP [m]

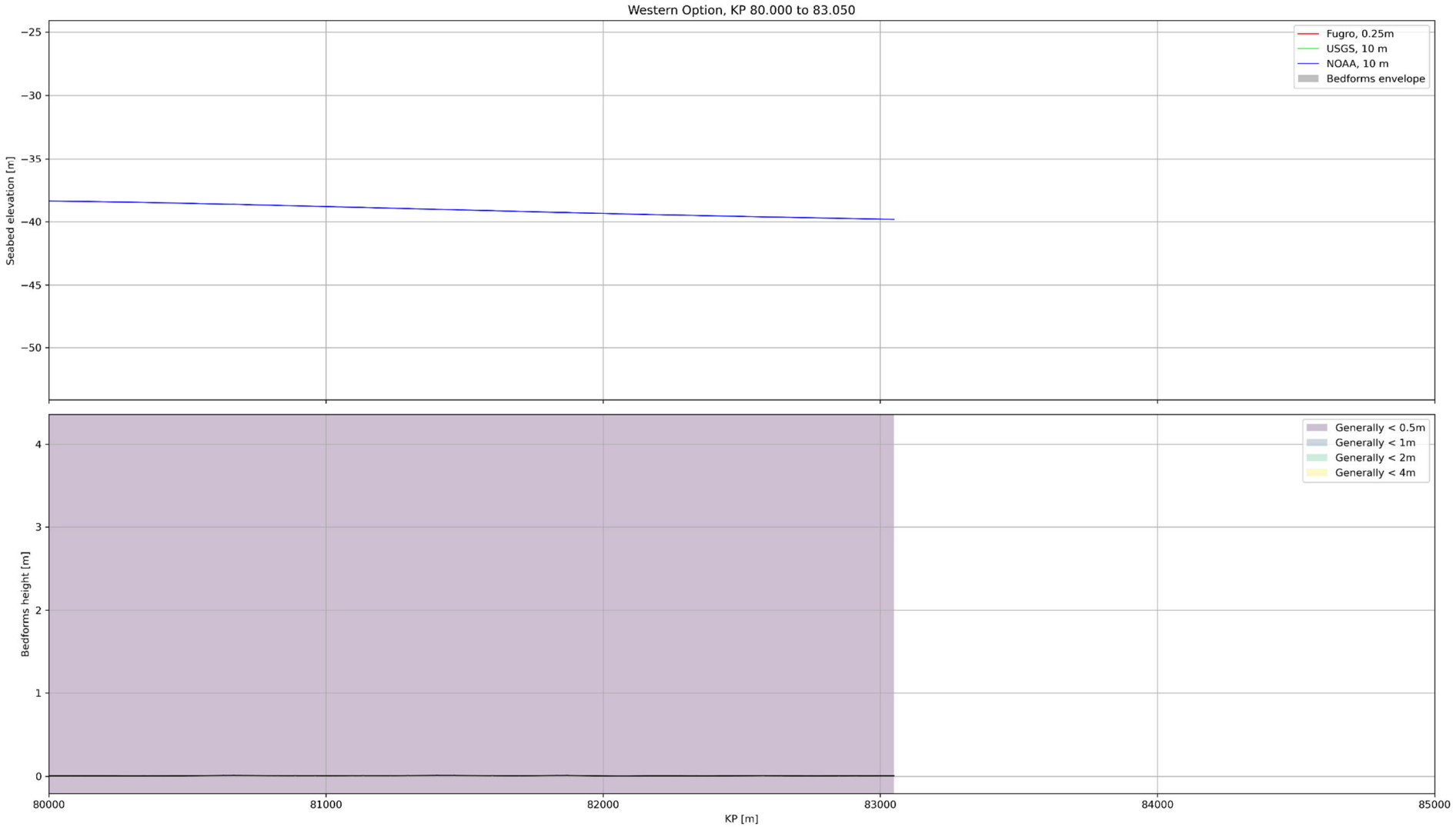
Western Option, KP 80.000 to 83.050
Fugro, 0.25m
USGS, 10 m
NOAA, 10 m
Bedforms envelope
Seabed elevation [m]
−25
−30
−35
−40
−45
−50
Generally < 0.5m
Generally < 1m
Generally < 2m
Generally < 4m
Bedforms height [m]
0
1
2
3
4
80000
81000
82000
83000
84000
85000
KP [m]